UNIVERSITY OF SOUTHAMPTON

Faculty of Engineering, Science and Mathematics

School of Ocean and Earth Science

IMPACTS OF COASTAL REALIGNMENT ON INTERTIDAL SEDIMENT DYNAMICS: FREISTON SHORE, THE WASH

by

Andrew Mark Symonds

Submitted in fulfilment of the requirements for

The degree of Doctor of Philosophy

August 2006

CONTENTS

LIST OF FIGURES

CHAPTER 5:

CHAPTER 6:

LIST OF PLATES

CHAPTER 4:

CHAPTER 5:

CHAPTER 6:

CHAPTER 7:

CHAPTER 9:

LIST OF TABLES

LIST OF ABREVIATIONS

ABR	Autonomous Benthic Recorder
ACD	Admirality Chart Datum
EA	Environment Agency
EMCM	electromagnetic current meter
EPS	extracellular polymeric secretions
HW	high water
LW	low water
MHWL	mean high water level
MHWN	mean high water neap
MHWS	mean high water spring
MLW	mean low water
MLWL	mean low water level
MLWN	mean low water neap
MLWS	mean low water spring
MR	Managed Realignment
MWL	mean water level
OBS	optical backscatter sensor
OD	Ordnance Datum (Newlyn)
RTK-GPS	Real Time Kinematic Global Positioning System
SET	sedimentation erosion table
SSC	suspended sediment concentration
UK	United Kingdom

LIST OF SYMBOLS

A	cross-sectional area of channel (m^2)
A_w	orbital amplitude of wave motion at the bed
C_D	drag coefficient of steady current
d	depth (m)
D_*	dimensionless grain size
D_{50}	mean grain size (mm)
D_{10}	grain size which 10 % was finer than (mm)
E	wave energy ($N.dBar^2.m^{-3}$)
f_{ws}	smooth-bed wave friction factor
f_{wt}	rough-bed wave friction factor
g	acceleration due to gravity
h	hydraulic water depth (m)
h_{mid}	depth of the middle of the breach in the channel (m)
H_s	significant wave height
H_{max}	maximum wave height
L	semi-surface width of the channel (m)
P	plan area of the inundated MR (m^2)
Q	discharge (m^3/s)
Q_s	sediment feed rate
q_{bx}	bedload transport rate in the same direction as the current
q_{by}	bedload transport rate at right angles to the current
R_w	wave Reynolds number
S	channel slope
T_0	adjustment period of channel
T_R	time for channel equilibrium to be reached
T_p	peak wave period (s)
T_z	zero up-crossing wave period (s)
U_{cr}	critical horizontal current velocity (m/s)
U_w	amplitude of the wave orbital velocity
v	vertical velocity (m/s)
V	flow speed (m/s)
W	width of channel (m)
W_s	settling velocity (cm/s)
X	load = solid volume of material transported per second / discharge
y	lateral distance from the centreline of the channel (m)

Ω	tidal prism (m^3)
ρ	density of fluid
υ	kinematic viscosity
γ_s	specific weight of grains in the fluid
υ_{*cr}	velocity necessary for the initiation of sediment transport
v_s	mean terminal velocity of material falling through still water (m/s)
μ	submerged static coefficient of Coulomb friction
τ_w	amplitude of oscillatory bed shear-stress, due to waves
θ_w	skin-friction Shields parameter, due to waves:
ρ	density of fluid
ρ_s	density of sediment
τ_c	current-only bed shear-stress
τ_m	mean bed shear-stress during a wave cycle, under combined waves and currents
θ_m	mean Shield's parameter, over the wave cycle
θ_{cr}	threshold Shield's parameter
Φ_x	dimensionless bedload transport rate in the x component
Φ_y	dimensionless bedload transport rate in the y component
ϕ	angle between current direction and direction of wave travel

Graduate School of the National Oceanography Centre, Southampton

PhD. Dissertation

by Andrew Mark Symonds

Declaration of Authorship

The work presented in this thesis is my own, and was done wholly whilst in candidature for a research degree at this University. Where I have quoted or consulted from the published work of others, the source is always clearly attributed. I have acknowledged all the main sources of help. Where the thesis is based on work done by myself jointly with others, I have made clear exactly what was done by others and what I have contributed myself. Part of this work has been published as:

Symonds, A.M. and Collins, M.B. 2005. Sediment dynamics associated with managed realignment; Freiston Shore, The Wash, UK. In: *Coastal Engineering 2004, Lisbon, Vol 3*, pp. 3173-3185.

Signed: ……

Date: ……...

Graduate School of the National Oceanography Centre, Southampton

This PhD. dissertation by

Andrew Mark Symonds

has been produced under the supervision of the following persons

Supervisors

Prof. Michael Collins

Prof. Graham Evans

Chair of Advisory Panel

Dr. Rachel Mills

ACKNOWLEDGEMENTS

I am very grateful to Professors M.B. Collins and G. Evans for their invaluable supervision and help throughout this study.

I am also highly appreciative of the data provided by the Environment Agency as part of this study, as well as the help received from them; in particular Jane Rawson, Julie Richards and Justin Ridgewell.

Sincere thanks are extended to Dr. Doros Paphitis who assisted during the initial stages of the fieldwork and offered much advice. Special thanks go to Dr. Erwan Garel and Theocharis Plomaritis for their enthusiasm during prolonged periods of fieldwork and their expertise in the laboratory. Ian Townend and Dr. Iris Moeller have both provided valuable comments on parts of the manuscript, which has been much appreciated.

Dr. Urs Neumeier, Isabella Araujo, Julia Addison, Dan Jones and Andy Gates all accompanied me during fieldwork, mainly taking part in the collection of erosion/accretion measurements. Hazel Duckworth undertook part of the laboratory analysis of the sediment collected during the erosion/accretion measurements. Madeline Hodge helped during a week long deployment, and carried out the laboratory analysis of the suspended sediment samples.

The expertise and equipment provided in the RTK-GPS surveying by ABPmer and the CCO (Channel Coast Observatory) was much appreciated. In particular Malcolm Bowdidge, Mark Cluett, Clive Moon, Neil Pittam and Matthew Wadey who all took part in surveys.

Thanks are owed to Andy Gates, Ian Troth, Andy Davies and Dan Jones for their comments on my work and the much needed distractions they provided. Special thanks go to Roz Coggon for offering technical expertise on CorelDraw and the artistic flair that my work lacked.

I am indebted to the people at the Freiston Educational Centre who provided accommodation and, when needed, assisted in the collection of equipment. The manager of the managed realignment site, John Badley of the RSPB, has always been extremely helpful and I am very grateful for everything he has done.

Finally, I am very grateful to all of the support I have received from my family and friends, which has got me through these last 3 years.

CHAPTER 1: INTRODUCTION

1.1 INTRODUCTION

Intertidal flats and saltmarshes occur commonly around the world, fringing large areas of the coastline. These areas are important for coastal defences, as well as being valuable habitats for wildlife. The wide intertidal flats and vegetated saltmarsh offer protection from the sea, for any surrounding low-lying areas; they are becoming ever more important, owing to increased concerns of sea-level rise, combined with an increase in storminess.

It is anticipated that non-intrusive, sustainable forms of coastal protection will be used increasingly in future years. One particular type of coastal defence, which has become popular recently and is being suggested for many sites, is Managed Realignment (MR). This approach is being used presently, despite the lack of a full understanding of the potential impacts, to the MR site and the adjacent intertidal zones. Consequently, it is essential to recognise areas that are suitable for MR and to assess the beneficial and detrimental impacts that a MR could have, on a particular area. To identify the impacts of a MR, it is necessary to understand the natural processes which occur over the intertidal zone. Numerous studies have investigated such environments, but there are still areas where a greater understanding is required; as such, a comprehensive study of the sediment dynamics of intertidal flats and saltmarshes is necessary.

1.2 OBJECTIVES OF THE STUDY

The MR scheme at Freiston Shore was, at the time of its creation, the largest site in the UK; as such, it was designed as an experimental site to study its impacts, prior to the initiation of a larger scheme. The history of the coastal management at Freiston Shore makes it an ideal location to study the affect of anthropogenic changes, over an intertidal zone. Land was reclaimed in 1980; subsequently, the embankment created for land reclamation was breached, as part of the MR scheme, in 2002. Research has been undertaken on the adjacent intertidal flats, over the last 50 years. Data are available from before a land reclamation, since, and following a MR as part of the present study. Following the land reclamation, insufficient width was left in the intertidal zone for the saltmarsh to rejuvenate, or dissipate the incoming wave energy effectively. Consequently, erosion of the 1980 embankment occurred during high wave energy events, associated with winter storms. Such instability, combined with the threat of sea-level rise and an increase in storm events, has indicated that the most viable form of long-term sustainable coastal protection could be provided by managed realignment, as the cost of maintaining the outer seawall would undoubtedly have proven prohibitive and counter intuitive.

The main aims of the present study are outlined below.

(i) To investigate what impacts anthropogenic changes have upon intertidal zones, in relation to both the MR and land reclamation.

(ii) To study the development of a MR site, to establish how it develops in terms of accretion, vegetation colonisation and sediment dynamics, and if this development is as intended in the design of the scheme;

(iii) To understand the evolution of breaches made in an embankment, establishing the necessary dimensions of a breach into an arbitrary area of land, by using empirical equations derived on the basis of the 'Regime Theory'.

(iv) To monitor the development of a creek system over an intertidal flat, adjacent to breaches in an embankment. Likewise, to study the controlling processes, as well as the rates of creek development, before the MR (i.e. under 'natural' conditions), then following anthropogenic changes caused by the MR.

(v) To establish interaction between a creek system and the adjacent intertidal flats, in terms of water and sediment movement.

(vi) To investigate the change in bed level over the intertidal flats, adjacent to a breach in an embankment, in an attempt to identify seasonal patterns and spatial variations, across the intertidal flats. Similarly, to correlate the results obtained, with seasonal variations in wave conditions.

(vii) To study the sediment dynamics over an intertidal zone, to further previous investigations and attempt to improve the overall understanding of these environments.

1.3 THESIS STRUCTURE

The initial 4 chapters of the thesis provide the background to the research: Chapter 1, by means of an Introduction; Chapter 2, in terms of a Literature Review of topics relevant to the research undertaken; Chapter 3, the Regional Background, describing previous work undertaken over the area; and Chapter 4, describing the Methods used in this study. The next section of the text (Chapters 5 to 9) presents the results of the research, together with a discussion of the main observations. Each of the Chapters consists of an introduction summarising the aims, where necessary a section providing additional background, and a

methods section listing which data were used. These Chapters all contain separate sections containing the results, a discussion and, final concluding remarks on this particular aspect of the work, i.e. the part of the investigation described within individual Chapters is 'self-contained'; as such, it is easier to interpret the findings separately. A short discussion of the results and the overall conclusions are given, subsequently, in Chapter 10; this, in turn, includes recommendations for future research.

CHAPTER 2: LITERATURE REVIEW

2.1 INTRODUCTION

This Chapter provides a background to the field of study. Literature is reviewed to highlight the current level of knowledge in the field and to provide examples of relevant studies. A background to the geographical area and previous studies of The Wash and Freiston Shore are provided in Chapter 3.

2.2 INTERTIDAL FLATS

2.2.1 *Introduction*

Intertidal areas fringe many thousands of kilometres of coastline around the world; they exist at all latitudes, within sheltered estuaries and inlets as well as on coasts exposed to wave action, in areas of various tidal ranges (Dyer, 1998). Such flats occupy a zone of transition between terrestrial and marine ecosystems; as such, they play a critical role in sediment exchange between the intertidal flats and the open coastal waters, which is of importance in terms of coastal protection (Davidson-Arnott et al., 2002). A number of classifications have been used for intertidal flats; for this study, it is taken to be the sedimentary body located between mean high water spring tides (MHWS) and mean low water spring tides (MLWS) (Fig. 2.1) (Amos, 1995).

Intertidal flats are generally subject to low wave energies, and often characterised by the accretion of fine-grained sediment, forming mudflats and saltmarshes; these act as sources and sinks for sediment and pollutants, associated with fine-grained particles (Tolhurst et al., 2000a). Intertidal flat deposits occur where vertical and lateral accretion is influenced primarily by waves and tidal currents (Amos, 1995). The sediment composition is related to tidal elevation, with the upper zones (near to high water (HW)) consisting of fine-grained muddy sediments, with the middle to lower zones (near to low water (LW)) being composed of coarser (sandy) sediment (Evans, 1975; Reineck, 1975; Elliott, 1986; and Eisma et al., 1998). The boundaries between these sub-environments are not definite, but can vary depending on variables such as sea-level change and the periodicity of wave events. A detailed investigation into the sub-environments was carried out in The Wash; the sediment properties, degree of reworking of the sediment through wave and tide induced currents, organisms found there and the rate of sedimentation expected were all noted for each sub-environment (Fig. 2.1). However, the geomorphology of intertidal mudflats is highly complex and not fully understood (Pethick, 1996). The cross-sectional shape of intertidal mudflats has been investigated; high, convex profiles indicate accretion-dominated, while low, concave profiles indicate an erosion-dominated mudflat (Kirby, 2000).

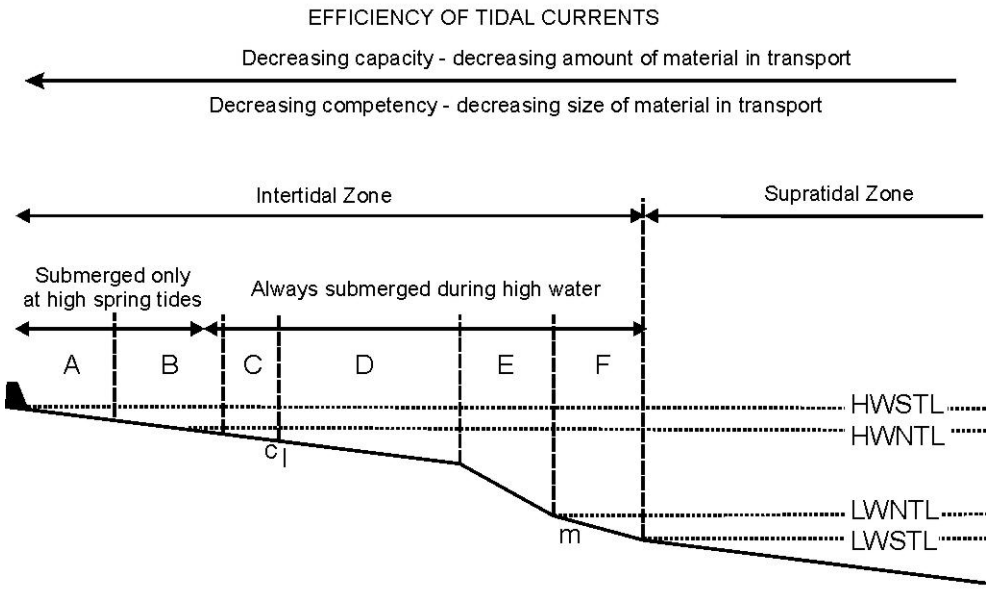

A	Saltmarsh	No reworking by waves or organisms. Fairly slow sedimentation. Sediment bound by plants, which cause a filter effect.
B	Higher mudflats	Very limited reworking be waves and organisms. Fairly rapid sedimentation. Sediment bound by algae.
C	Inner sandflats	Limited reworking by waves, extensive reworking by Corophium. Slow sedimentation.
D	Arenicola sandflats	Extensive reworking by waves and Arenicola. Slow sedimentation.
E	Lower mudflats	Little reworking by waves or organisms. Rapid sedimentation.
F	Lower sandflats	Little or no organic reworking, minor wave-action, strong-tidal currents. Slow sedimentation.
c	Cardium edule	
l	Lutraria elliptica	Organisms extracting suspended clay from seawater.
m	Mytilus edulis	

Figure 2.1: Schematic representation of the dynamics and sedimentation of the intertidal zone of The Wash, with the tidal zones and environments shown (after Evans, 1965).

Despite the fact that intertidal flat areas are some of the most active regions, in terms of sediment transport and deposition, there is still only limited information available on predicting the response of the intertidal flats to changes in external circumstances, i.e. coastal engineering, sea-level change or a change in sediment supply (Ke et al., 1994; and Roberts et al., 2000).

In recent years, there has been an increased interest in intertidal flats and the processes occurring on them. This interest is related to increasing concerns about the effect of environmental change, both natural (sea-level rise) and anthropogenic (embanking, retreating, dredging) (Pye, 1996). Also, the saltmarsh, mudflat and sandflat environments have been recognised as being of ecological significance. Much of the work has been directed at improving the understanding of the functions of intertidal flats and our ability to evaluate the potential impact of human activity (Allen and Pye, 1992; and Allen, 2000b). From recent

work, several approaches to the study of sedimentary dynamics on coastal flats can be recognised, as outlined below.

1) Measurements of the hydrodynamics, sediment dynamics (sediment erosion, deposition and transport) and sediment budgets associated with individual tidal cycles and/or the spring-neap cycle, in tidal creeks (Postma, 1967; Boon, 1975; Evans and Collins, 1975; Bayliss-Smith et al., 1979; Ward, 1979; Pethick, 1980; Ward, 1981; Roman, 1984; Reed, 1987; French and Stoddart, 1992; and Shi, 1995) and over the sediment surface (Letsch and Frey, 1980; Stumpf, 1983; Stevenson et al., 1988; Wolaver et al., 1988; French and Spencer, 1993; French et al., 1995; and Christiansen et al., 2000).
2) Measurements of sediment accumulation, rates of vertical growth and changes in the extent of marshes and tidal creeks, over periods ranging from a year to several thousands of years (Jacobson, 1988; Pringle, 1995; and Orson et al., 1998).
3) The development of simulation models, to investigate the importance of different controls, at a variety of time-scales (Allen, 1990; French, 1993; and Woolnough et al., 1995).

It appears that the scientific areas receiving ever increasing attention are the relationships between shoreline erosion, sediment inputs and sea-level rise (Stevenson and Kearney, 1996). The differing temporal and spatial scales at which processes influence intertidal flats are important; these have been examined by Allen (2000) in the very short (days-years), short (decades), medium (centuries) and the long (millennia) terms. Elsewhere, Pethick (1996) examined different range scales, short-term periodic changes (hours-days), medium-term changes (decades) and long-term changes (since the Holocene). For the present study, the system will be studied at temporal ranges of up to medium term.

The physical processes occurring over intertidal flats are the primary determinants of the configuration and distribution of the environments (Roman and Nordstrom, 1996). For example, as the tide advances over the intertidal flats, the competency and capacity of the tidal wave decreases, reducing the current velocity and leading to a differentiation of material with a distinct gradient in grain size from low to high water (Evans, 1965). These varied environments on the intertidal flats can be divided into a number of sub-environments, based upon: topographic variations, the degree of vegetation cover; bed-form types; and the characteristics of the deposited sediment (Carling, 1978).

2.2.2 *Formation*

Turbid waters flooding the intertidal flats deposit sediment during slack water, then on the ensuing ebb some of this sediment is resuspended (Van Straaten and Kuenen, 1958). This results in sediment accretion, which causes a reduction in the current velocity, thus enhancing future deposition. This is due to a phenomenon, which Postma (1967) referred to as "settling lag". This process occurs as a suspended sediment grain is transported onshore and the tidal current velocity falls below its settling velocity, so the grain starts to settle out of the water column. Due to the presence of a weak tidal current, the grain does not fall vertically, but is transported inland, away from where the critical deposition velocity was reached. As the tide turns (assuming similar current velocities on the flood and ebb) the grain will not be re-entrained until much later in the flow: the grain is located higher within the intertidal zone, compared to where the critical deposition velocity was reached. Consequently, on the ebb, the grain will be suspended for a shorter period, thus not moving as far offshore as it did onshore, during the flood (Fig. 2.2). This occurs throughout most tidal cycles, causing the concentration and deposition of suspended sediment to increase landwards, towards the shoreline.

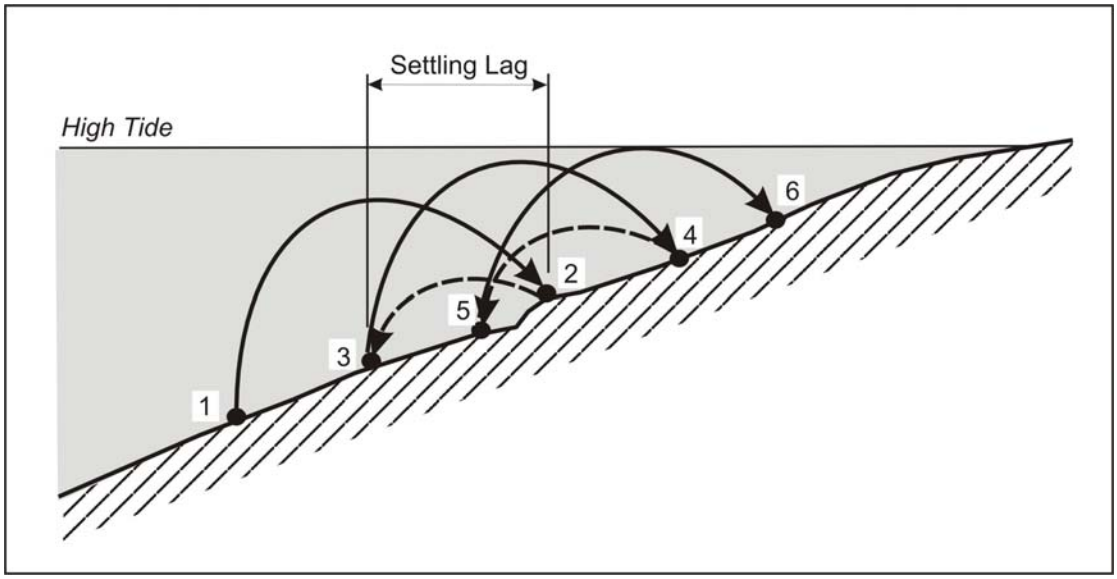

Figure 2.2: Settling Lag of a particle. The numbers next to the grain represent its successive position after the tides, i.e. 1-2 is after a flood tide, 2-3 is following an ebb tide etc (from Postma, 1967).

The most important factor controlling sediment transport on the intertidal flat is the tide. Generally, as the tide starts to rise over the lower areas of the intertidal flats, the tidal current velocities increase; when roughly half of the flats are submerged, the current velocities are at their maximum and, then, they gradually decrease until they reach zero at high water when most if not all of the intertidal flats are covered (Allen, 2000b). It is the horizontal variation in the tidal current velocity, over the intertidal zone, producing high velocities on the middle

and lower areas and low velocities around the upper areas, which causes the variation in grain size shown on intertidal flats. Coarser grain sizes are deposited as soon as the velocities begin to drop at mid-tide, thereafter, the grain sizes become finer to shorewards.

The upper part of the intertidal flats will gradually accrete by deposition of fine-grained sediment and by raising the level of the surface, reducing the frequency and duration of future tidal inundations. Eventually, the mudflat will be exposed for sufficient time to allow vegetation to colonise the area. There are a number of variables, as identified by Pielou and Routledge (1976), which control the elevation at which this occurs:

1) the type of plant species available for colonisation (some species are able to colonise at lower levels than others);
2) the tidal current velocities, which may uproot plant seedlings if too high;
3) the availability of light for the growth of the plant, which is dependent upon the duration of the tidal flooding and the overlying turbidity of the waters; and
4) the salinity of the tidal waters.

Common pioneer species documented for intertidal flats in North America and Western Europe are *Salicornia* spp. (marsh samphire) and *Spartina* spp. (marsh cord grass); these can both withstand high salinities. Such colonisers will gradually spread, forming eventually a complete cover over the upper intertidal flats to form a saltmarsh environment. The presence of the vegetation will increase the rate of deposition on the marsh, which increases its height and reduces the frequency and duration of tidal inundation. Thus, the environment will become habitable for an increasing number of plants, leading to species competition and a succession of plant communities developing (Ranwell, 1972; and Luternauer et al., 1995).

Vegetation changes the depositional processes; the leaves and stems of the plants dissipate tidal currents, allowing deposition to occur throughout all of the tidal inundation (unless prevented by wave conditions). It is unlikely that much deposition would occur if it were not for the vegetation, as only fine-grained sediments are present and the duration of slack water is limited (Pethick, 1984). A number of previous investigations have examined the role of vegetation, by investigating: the enhancement of sedimentation rate and bed accretion (French et al., 1995; Fonseca, 1996; Roman et al., 1997; Brown, 1998; and Cahoon et al., 2000); the reduction in erosion (Boorman et al., 1998); the hydrodynamic impact of the vegetation on the flow (Brampton, 1992; Fonseca, 1996; and Neumeier and Ciavola, 2004); and the long-term evolution of saltmarshes (Allen, 1997).

2.2.3 *Sediment Stability*

The stability of the sediment, following deposition, is enhanced by consolidation and biochemical processes (Janssen-Stelder, 2000). The consolidation of the bed causes an increase in the strength of the bed; thus, an increase in the shear stress threshold for erosion. The mudflat sediment can also be stabilised by hardening, caused by exposure to strong sunlight (Whitehouse and Mitchener, 1998). In the upper area of the intertidal flats, the saltmarsh vegetation acts as a very efficient sediment stabiliser. The soil becomes reinforced through the root mass of the vegetation and, in addition to this plant growth, reduces the shear stresses due to the tidal currents, enhancing sediment deposition (Boorman et al., 1998). The erosion shear stress of the sediment over an intertidal zone shows dependence on the percentage of fine-grained sediment (< 63 μm) and on the benthic diatom concentration present in the upper 1 mm; muddy areas are the most dependent upon the diatom concentration (Riethmuller et al., 1998).

The primary control on sediment stability over the intertidal flats is biological activity. Stability is linked strongly to variations in the benthic biota (Davey and Partridge, 1998; and Widdows et al., 1998). Macro-benthic organisms are capable of stabilising and destabilising the surface sediment (Meadows et al., 1998b; Christie et al., 2000; and Paterson et al., 2000). For example, *Macoma balthica* density has been correlated to long-term changes in sediment erodibility, but no consistent seasonal cycle could be identified (Widdows et al., 2000). The sediment is destabilised through bioturbation, which is a result of burrowing and deposit feeding bivalves. Sediment stability can be enhanced also by the production of extracellular polymeric secretions (EPS), with the primary producer being microphytobenthos (Blanchard et al., 2000; and Underwood, 2000). The EPS is present as a cohesive matrix around the particles of the intertidal sediment, forming a microbial biofilm (Decho, 2000). Areas with the biofilm present have higher sediment stability than similar areas without (Tolhurst et al., 2000b), with the EPS reducing the current-induced shear stress by smoothing the surface (Riethmuller et al., 1998). The biofilm has been found to lack a physically-structured organisation; rather, it is thought to be randomly distributed (van Duyl et al., 2000). The biological productivity of sedimentary environments is extremely varied, with differences in habitats and animal communities occurring over very short distances (Meadows et al., 1998a). Species cluster generally within areas of specific sediment parameters, although it has been found that in many cases the greatest ecological influence is the period of tidal immersion and emersion (Harris, 2000); the tidal phasing, in terms of the time of day at which low water occurs during spring and neap tides, and the duration of the emersion period, control the biomass dynamics (Friend et al., 2003; and Friend et al., 2005).

The biological activity either stabilising or destabilising sediment can enhance or remove any seasonal trends in the erosional/accretional patterns of the sediment; these, in turn, depend upon the correlation of wave activity with strong tidal currents. In the Dollard estuary, The Netherlands, sediment was stabilised by a diatom bloom in April: the sediment consolidated during this time, increasing the surficial sediment stability for when the diatom film disappeared in May. The consolidation of the sediment, in turn, minimises erosion; however, in June, consolidation is reduced by the bioturbation and grazing of *Corophium volutator,* leading to an increase in erosion (Kornman and De Deckere, 1998). It was found also that the lower limit of the saltmarsh (MHWN) coincided with the upper limit of the abundant amphipod *Corophium volutator*, in relation to tidal inundation. Any seedlings planted below this level were disturbed by the activity of this amphipod, with populations of up to about 14,000 m^2 being effectively able to prevent seedling establishment (Davy et al., 2000). Due to the temporal variation in species and density throughout the year, a related variation in the erodability of the sediment can also be expected. These changes can occur rapidly, over a 2 week period; thus, it is important to undertake regular erosion/accretion measurements.

There have been contrasting results concerning the primary control on cohesive sediment stability on intertidal flats (Widdows et al., 2000). For example, it has been suggested that either the biological activity or the physical parameters of the sediment could be the primary control (Wood and Widdows, 2002). Clearly, the sediment stability varies spatially and temporally and there is a clear temporal signal, which can be affected by climatic factors (such as rainfall), which reduce the sediment stability.

2.3 SALTMARSHES

2.3.1 *Introduction*

Coastal saltmarshes are a wetland ecosystem flooded regularly by saline waters; they are vegetated by dense stands of halophytic vegetation and are generally depositional environments (Stevenson et al., 1988; Allen, 1992; Allen and Pye, 1992; Allen, 2000b; Davidson-Arnott et al., 2002; Nielsen and Nielsen, 2002; and Cheng, 2004). Morphologically, saltmarshes consist of a gently sloping vegetated platform, dissected by a network of tidal creeks, these increase in width and depth, to seaward. The location of saltmarshes is controlled predominantly by the coastal geomorphology, with low wave energy conditions being necessary for their formation. Such deposits are found in areas sheltered from high wave action, allowing the deposition of fine-grained sediments and the establishment of vegetation (Pethick, 1996). The vegetation causes a drag on tidally- and wave-driven currents; these prevent the re-erosion of deposited sediment, except under severe

conditions (Neumeier and Ciavola, 2004). Accretion on the saltmarsh surface varies within the marsh area and temporally throughout its development.

Areas for saltmarsh development include back-barrier lagoons and bays, river mouths, estuaries and deltas, natural embayments and zones sheltered by spits or barrier islands (Dijkema, 1987; Allen and Pye, 1992; Kelley et al., 1995; Luternauer et al., 1995; and Pethick, 1996). Marshes develop also on open coasts, but the wave energy needs to be dissipated over a wide, shallow near shore area (Davidson-Arnott et al., 2002). Saltmarshes are higher, in relation to mean tide level, than the surrounding mudflats/sandflats and are flooded only during high spring tides. Several investigators have considered the location of saltmarshes, in relation to tidal levels. In north west Europe, saltmarshes have been considered to occur in the supratidal zone, above the mean high tidal level (Reineck, 1975; and Ke, 1995). Logically, saltmarshes should be taken as being located on the intertidal flats, between mean high water neaps (MHWN) and mean high water springs (MHWS), as they are only flooded during high water spring tides (Evans, 1965) (Fig. 2.1). Such marshes are characterised by fine-grained sediments (silts and clays), formed through a combination of physical (sediment deposition and erosion) and biological (vegetation growth) processes (Reed, 1990).

Saltmarshes act as sinks for fine-grained sediments, carried in by both the tidal waters and by runoff from the adjacent land, in addition to functioning as pollution filters (Gordon et al., 1985; and Hazelden and Boorman, 1999). Generally, marshes are in a continual state of change, often showing evidence of continuous sediment accumulation over their surfaces. Rates of sedimentation vary, alternating between periods of erosion and accretion (Section 2.6.2). An important process in the maintenance and development of the marsh is the entrapment and stabilisation of suspended inorganic sediment, on the marsh surface (Allen, 2000b). The evolution (vegetation succession) of a vegetated marsh is controlled by the changing balance between the tidal regime, wind-wave climate, sediment supply, relative sea-level change and wetland vegetation (Dyer, 1986; Reed, 1990; and Davy et al., 2000). Hence, saltmarshes are subjected to a wide range of physical and biological controls and processes**;** these include climate, shoreline configuration, wave conditions, tidal range, sediment sources, sediment input, sea-level history and vegetation characteristics (Allen and Pye, 1992; Luternauer et al., 1995; Allen, 2000b; and Davidson-Arnott et al., 2002).

Saltmarshes are not isolated features, but form part of a much larger sedimentary system: this incorporates the saltmarsh, unvegetated mudflats and sandflats and the surrounding estuary or embayment. Describing one part, without reference to the others results in severe limitations.

For example, the morphodynamics of the upper vegetated surfaces of the intertidal flats are related so closely to that of the unvegetated mudflats of the intertidal flats, that the two must be regarded as part of the same geomorphological unit (Pethick, 1996). The saltmarsh acts as an area of long-term sediment storage within the system, containing sediments that have built up during low-magnitude high-frequency events. Such sediment is released during these events, producing the short-term morphological response of the profile to storms. Sediment flux within the system, i.e. magnitude and direction, is critical to the understanding of the accretionary budget of individual marshes; as is the role it plays in the larger coastal, or estuarine, system (Stevenson et al., 1988).

2.3.2 *Classification*

Saltmarshes have been classified in various ways, based generally upon their geomorphological characteristics. European marshes have been grouped into five main categories and twelve sub-categories, based upon: (a) the origin of the substrate; (b) the main geological agency; and (c) the morphology, in relation to ecological conditions (Dijkema, 1987). A different approach was adopted by Allen (2000b), who suggested that all saltmarshes could be divided into two fundamental, geomorphological zones: (a) a convex-up, planar, or concave-up vegetated platform, located high in the tidal frame that is habitually flooded by the tide i.e. the high marsh; (b) generally unconnected networks of tidal channels that branch and diminish inland.

A more detailed scheme was developed for a narrower range of marshes, found generally on the Atlantic and Southern North Sea coasts of Northern Europe, by Pye and French (1993). This scheme was related to Dijkema's classification (see above), and recognises seven types of marsh, as outlined below.

1) Open coast marshes, typically sandy systems coupled with relatively exposed sandflats.
2) Open coast back-barrier marshes, sandy-muddy systems found on the sheltered, landward sides of coastal barrier islands and spits.
3) Open embayment marshes, with predominantly sandy sediment, which fringe the edges of large tidal embayments with unobstructed entrances.
4) Restricted entrance embayment marshes with sandy-muddy sediment, partly closed off at the mouth.
5) Marshes within estuaries, of which there are two sub-classes, depending upon the amount of obstruction of the estuary mouth: (a) fringing; and (b) back-barrier. These tend to be muddy if the river discharge is significant or sandy where the sediment source is marine.

6) Ria/loch-head marshes, which are generally muddy and may also include those, which lie in the shelter of a spit.

2.4 MUDFLATS/SANDFLATS

2.4.1 *Introduction*

Based upon the subdivision of the intertidal flats undertaken by Wang and Eisma (1988), mudflats and sandflats are located between MHWN and MLWS (Fig. 2.1). These areas are submerged too frequently for the colonisation of halophytic vegetation; hence, they are present below the level, and seaward, of the saltmarshes, i.e. generally the area between the saltmarsh and the subtidal areas. Mudflats occur adjacent to saltmarshes and can range from MHWN to MLWS, depending on the presence of sandflats; they are composed of predominantly fine-grained silts and clays (Evans, 1965; and Pethick, 1984). Sandflats are widespread between the mean sea level and MLWN; these are composed of fine to very fine sands (Amos, 1995), allowing only small-scale bedforms (such as wave- and current-induced ripples) to develop (Amos and Collins, 1978). In response to settling and scour lag (Section 2.2.2), and horizontal variations in tidal current speeds over the intertidal zone (Evans and Collins, 1975), low velocities are experienced around the upper areas and high velocities on the middle and lower areas of the intertidal zone, which causes a variation in grain size on intertidal flats (Collins et al., 1981). Coarser grain sizes are deposited as soon as the velocities begin to drop at mid-tide and, thereafter, the grain sizes become finer shorewards (Pethick, 1984).

Another difference between the sub-environments (Amos, 1995), is that sandflats are located where the mean inorganic suspended sediment concentration (SSC) of the inundating waters is less than 1 g l^{-1}; mudflats where the SSC is greater than 1 g l^{-1}. A number of landforms and bedforms occur in these areas (Eisma et al., 1998):

1) ridges oblique to the main direction of flow and longitudinal ridges;
2) channels, creeks, gullies and associated features such as levees;
3) outcrops of old deposits or bedrock; and
4) man-made constructions, e.g. embankments for land reclamation.

These areas show large morphological variability, which, in turn, can be enhanced by differences in sediment composition and climate, i.e. these controls cause a variation in the local topography and sediment properties.

The profile shape of an intertidal mudflat/sandflat is controlled by tidal range, wave climate, sediment composition and sediment supply (Whitehouse et al., 2000). The bed level of a mudflat varies over decadal, seasonal, spring-neap and tidal time-scales; with accretion

experienced during spring and summer, then erosion during autumn and winter (O'Brien et al., 2000). Any spring-neap and tidal variations are destroyed frequently by intermittent, locally-generated, wave events. The accretion experienced over spring and summer months have been attributed to a number of interrelated factors:

1) decrease in frequency and intensity of local wave conditions (Kirby et al., 1993);
2) biostabilisation of the sediment surface (Paterson et al., 2000); and
3) an increase in sub-aerial exposure/processes, leading to surface stability (Amos et al., 1988).

2.4.2 *Classification*

In comparison to studies undertaken on saltmarshes, only limited research has been undertaken into mudflats/sandflat classification. A wide range of variables were investigated by Dyer et al. (2000); using statistical tests. The tidal range, degree of wave exposure, slope and the dry density of the sediment (of relevance only in the classification of some mudflats) were found to be the most important variables, in the classification of different mudflats/sandflats.

2.5 HYDRODYNAMICS

2.5.1 *Tides*

The tidal wave is a controlling factor on intertidal flat processes, with high and low tides being the crest and trough of the wave, respectively, with a wavelength of hundreds of kilometres. The influence of wind waves shift, in response to tidal movement, with the tidal currents transporting any suspended sediment entrained by wave action (Pethick, 1996). However, intertidal flats, such as mudflats, sandflats and saltmarshes, are all a response to tidal energy (Pethick, 1984). Tidal wave propagation over the intertidal flats causes currents to develop; these can initiate sediment transport and determine its direction of movement. Tidal current flows over intertidal flats are not uniform; they vary in an offshore direction and throughout the water column (Wood et al., 1998). Peaks in the tidal current velocity over the intertidal flats occur at the start of the flood (first phase flood) and the end of the ebb (last phase ebb). The dominance of these peaks depends upon local conditions. For example, strong ebb dominance was recorded in the Dollard Basin, Wadden Sea, Holland, which was attributed to the extensive intertidal flats (Ridderinkhof et al., 2000). In comparison, at Freiston Shore, The Wash, flood and ebb dominance varied in response to climatic conditions, with maximum tidal current velocities being higher during the flood (Postma, 1967; and Evans and Collins, 1975). Over the mudflat in Wenzhou Bay, China, the tidal current velocity was higher during the flood, but the ebb duration was longer, leading to an accretional environment (Wang and Eisma, 1988). In general, flood-dominant intertidal flats

tend to be net importers of sediment: high rates of accretion occur, in response to a longer slack water period at HW, than at LW. Ebb-dominance tends to be associated with a longer LW slack period, causing increased offshore movement of sediment (Kirby, 1987; and Pethick, 1996). This is due to the timing of the low tidal current speeds, which allow sediment to settle out of suspension and be deposited. The flood or ebb dominance occurs due to differing physical parameters affecting the flats, such as the bathymetry, tides and climatic conditions.

2.5.2 *Wave activity*

An important hydrodynamic process on intertidal flats is that of wave activity and the resultant currents induced (French, 2001). Erosion experienced over the intertidal zone is more likely to be induced by wind waves than tidal flows, with the SSC being predominantly influenced by wind-induced waves (Ridderinkhof et al., 2000). However, erosion mainly occurs under shallow water conditions, as the bed shear stress under waves is inversely related to the water depth (Madsen and Grant, 1976; and Amos and Collins, 1978). The waves cause an oscillatory movement of the water; this weakens the surficial sediment and allows the resuspension of consolidated sediment (Maa and Mehta, 1987; Mehta et al., 1989). The wave exposure over intertidal flats has a control on the intertidal flat sediments and the morphology over a Holocene time scale. In Strangford Lough, Northern Ireland, Ryan and Cooper (1998) found that the characteristics of the intertidal flats are dependent on the extent of wave exposure: mud-dominated tidal flats are created in sheltered areas where tidal currents are the dominant sedimentary agent; an intermittent fetch wave climate causes an erosional platform with a dominantly sandy, thin sedimentary veneer; and the most exposed site was predominantly depositional in character, with sand being the most common deposit.

Intertidal zones with extensive mudflats and landward saltmarshes are important in the dissipation of wave activity (Moeller et al., 1996; Moeller et al., 1999; Moeller and Spencer, 2003; and Cooper, 2005). This dissipation of wave activity has major engineering implications, as it allows a more relaxed coastal defence design for areas fronted by saltmarshes (Brampton, 1992). Due to concerns over the threat of sea level rising, combined with the increased associated cost of coastal defence, research has been undertaken into the wave dissipation by mudflat and saltmarsh surfaces (Moeller et al., 1996). Knowledge of the physical effect of saltmarshes and mudflats on the wave hydrodynamics is necessary to promote and predict the effects of MRs and to help in the restoration of degraded marsh systems or the creation of new marshes in front of threatened defences. Despite the recent increase in work over these areas, there have still been relatively few field-based studies in European intertidal zones. Two similar studies over the Stiffkey Marshes, North Norfolk,

UK, found that the wave energy dissipation rates over the saltmarsh were significantly higher (average of 82 %) than over the sandflat (average of 29 %), with the difference in water depth between the two not being sufficient to account for the differences (Moeller et al., 1996). Similar work, by Cooper (2005), was carried out at 3 sites around The Wash; Wrangle Flats, Butterwick Low (adjacent to Freiston Shore) and Breast Sand; the findings at Butterwick Low showed that on average the wave height was reduced by 23 % and the wave energy dissipated by 36 % over the mudflats, and 64 % and 79 % respectively across the saltmarsh. These studies show that saltmarshes should be maintained in front of existing sea defences, while the creation of new saltmarsh through schemes such as MR should provide better coastal protection than through repairing or creating new embankments.

2.6 SEDIMENT TRANSPORT

The transport, deposition and erosion of sediment are controlled by a variety of physical, biological and chemical processes. The most influential controls on the sediment transport has been widely discussed, with the tidally- and wave-induced currents being found as the primary controls on the transport (Amos and Collins, 1978; Collins et al., 1981; and Eisma et al., 1998).

2.6.1 *Suspended Sediment*

Previous studies into the sediment dynamics of intertidal flats have focused upon relationships between SSC, tidal currents and wave activity. During periods associated with low tidal currents, no correlation was found between the currents and SSC (Janssen-Stelder, 2000); under high tidal currents (during spring tides) the SSC increases, e.g. some 5 times between spring and neap tides, during calm weather conditions (Christie and Dyer, 1998; and Whitehouse and Mitchener, 1998). When the tidal currents are flood dominant, sediment accretion on the upper saltmarsh is enhanced; when ebb dominant, net loss of sediment occurs (Widdows et al., 2000). During calm weather conditions, the tidal current velocity combined with wave activity, influences the bed shear stresses; peaks in shear stress occur at the start of the flood and end of the ebb. In contrast, under rough and stormy conditions, bed shear stresses are dominated by wave-induced stresses; the highest occur around HW (Janssen-Stelder, 2000). For example, on the mudflat at Portishead, Severn Estuary, UK, the SSCs increased 3 times between periods of low and high wave activity (Whitehouse and Mitchener, 1998). Under stormy conditions, a positive correlation has been established between wave height and SSC (Evans and Collins, 1975; and Janssen-Stelder, 2000). SSC is primarily dependent on wave activity; tidal currents drive the resulting fluxes until a specific wave height is reached (dependent on local variables; sediment properties, depth, vegetation and biological activity), then the wave induced currents cause the net sediment transport direction

to switch to offshore (Bassoullet et al., 2000). In more exposed areas of the intertidal flats, wave activity will have a greater impact than on sheltered areas (French et al., 2000). Saltmarsh erosion, in response to high-energy wave events, releases large quantities of sediment; this is deposited on the lower areas of the mudflat/sandflat, creating a flatter profile (Pethick, 1996). This slope reduction means that the mudflat/sandflat profile will attenuate more wave energy than it originally did, thus reducing erosion around the saltmarsh. So a process relationship exists between the unvegetated and vegetated areas of the intertidal flats which creates short-term morphological responses to storm events.

2.6.2 *Sedimentation*

The rates of sedimentation over an intertidal marsh are spatially and temporally variable, even within relatively small areas (Carling, 1982). The whole of the intertidal zone does not react to the same prevailing hydrodynamic conditions, as the impacts will differ at various tidal heights (Bassoullet et al., 2000). It is the start and end of the tide, when the water depth is shallow (< 0.5 m) that the most important contribution to changes in bed level are made. When these periods coincide with high wave activity, erosion is enhanced and the bed level is dramatically reduced (Whitehouse and Mitchener, 1998). This process has a much greater impact on steep intertidal flats, as the tide will rise more slowly (Fig. 2.3), thus enhancing the impact of the waves. Nonetheless, on intertidal flats with shallow gradients it has been found that a rapid flood tide inundation can lead to erosion (Christie and Dyer, 1998; and O'Brien et al., 2000).

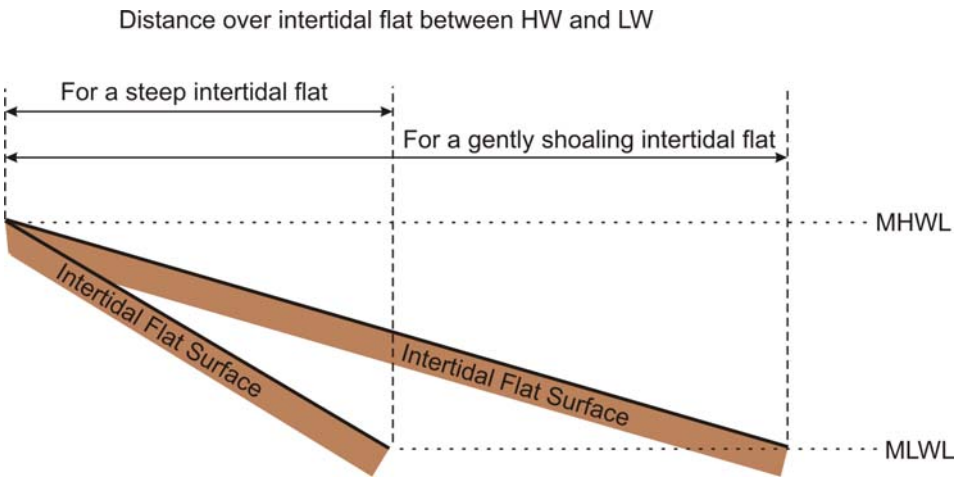

Figure 2.3: The difference in distance the tide has to flow over to reach MHWL, for steep and gently shoaling intertidal flats. The water level (area of strong currents and erosion) will be in contact with the intertidal flat at any given elevation for twice as long on the steep as opposed to the gently shoaling intertidal flat.

A variation in bed level of 10-20 mm has been identified on a tidal time-scale, dependent on the phasing of the tide i.e. the ambient sediment supply, in relation to the local water depth

and wave activity (Whitehouse and Mitchener, 1998). The change from spring to neap tides causes the 'shoreline' to migrate seawards; this, in turn, causes areas of deposition to migrate (Wang and Eisma, 1988). Differing rates of erosion/accretion are to be expected over intertidal flats, dependent upon the stage of the tide. On flood dominant flats, it is possible that sediment deposited during high water neap tides will be re-entrained on the following tide; it will gradually move up the intertidal slope, as the tidal height increases towards spring tides, until reaching the upper zone.

An increase in sediment supply during spring tides, on an accretional intertidal flat, can increase the bed elevation by around 10 mm compared to the previous, or following, neap tides (Whitehouse and Mitchener, 1998). However, this effect could be attributed partially to an increase in the sediment stability, brought about by an increase in the subaerial exposure during spring tides, causing dehydration and compaction (Amos and Mosher, 1985). This variation over a spring/neap tidal cycle is difficult to record, as there is often a frequent modulation present in the bed level, in response to episodic wave events (O'Brien et al., 2000).

There can be significant seasonal variation in the bed level over intertidal flats; with a rise in the bed elevation in the spring and summer; this could be followed by erosion, under short period waves, in winter (Amos and Mosher, 1985; Kirby et al., 1993; Boorman et al., 1998; and O'Brien et al., 2000); however, such seasonal trends are not always present (Widdows et al., 2000).

Over a longer temporal scale, such as a number of years, a mudflat can appear to be in an 'apparent' equilibrium (Bassoullet et al., 2000).

2.6.3 *Settling*

The low settling velocity of discrete particles of fine-grained sediments means that the duration of slack water over an intertidal zone is often insufficient to permit deposition. However, sedimentation can occur due to fine-grained suspended particles aggregating and forming mud floccules; these have higher settling velocities than the individual grains and when deposited they require higher energies to transport (Mehta and Partheniades, 1975; Dyer, 1986; Van der Lee, 2000; Winterwerp, 2002; Winterwerp et al., 2002; and Manning, 2004). Flocculation occurs when individual particles subjected to Brownian Motion are attracted to each other by forces of cohesion and collide repeatedly, eventually forming an aggregate (Vos and van Kesteren, 2000). It is when the SSC exceeds 100-300 mg l^{-1}, that 'free settling' of the sediment particles changes to 'flocculation settling', in response to

increased inter-particle collisions (Mehta, 1989). The process of flocculation is determined by: (a) the collision frequency; and (b) the efficiency of the collisions of floccules, in aggregation. The collision frequency is controlled by the Brownian Motion, differential settling, fluid shear or turbulence intensity and the SSC or number of flocs in suspension (McCave, 1979). The collision efficiency is dependent upon physical, chemical and biological factors (EPS, salinity, surface charge of the clay minerals); therefore, it is assumed to be constant throughout any particular tidal cycle, but variable on a seasonal scale (Van der Lee, 1998). The sizes and the settling velocities of floccules correlate with the SSC over the time scale of a tide, but not on a seasonal basis. Seasonally it has been established that floc size is dependent upon the binding property of the sediment; settling velocities showed little variation (Van der Lee, 2000). As the size of a floc increases, so its overall density decreases; nonetheless, the net effect is that the settling velocity increases (Mikkelsen and Pejrup, 1998). The boundary between cohesive and cohesionless sediment is not clearly defined, as it varies with the type of material and the grain size. Cohesion is more pronounced with clays (< 2 μm), than silts (2 – 63 μm) (Mehta et al., 1989).

2.6.4 *Sediment Fluxes*

On the basis of the derivation of sediment fluxes, the overall budget of an intertidal zone can be established. The flux is calculated by combining SSCs and tidal current velocities (Suk et al., 1999); as such a uniform SSC throughout the water column, together with a logarithmic velocity profile, are assumed (Evans and Collins, 1975; and Bassoullet et al., 2000). These derived fluxes relate to suspended sediment over the intertidal flats; nonetheless, derived bedload transport is of importance; as such, this should be considered in any flux calculations. Bedload transport is dependent on the boundary shear stress and the critical shear stress necessary to induce erosion (Sternberg, 1972).

2.6.5 *Bedforms*

Over intertidal flats it is uncommon to find a planar bed surface: instead, generally, there is a wide range of bedforms of varying sizes, often with high spatial and temporal variability. The formation and impact of bedforms on sandy sediments are well documented; however, the formation of bedforms within cohesive sediments is less well documented and understood (Whitehouse et al., 2000). Bedforms interact with intertidal mudflats and sandflats in a number of ways:

1) shallow water tidal flow/flow-channel interaction;
2) wave propagation/dissipation;
3) sediment strength/erodibility;
4) diffusion of sediment into the flow and sediment flux; and

5) storage of water/sediment.

The most commonly-occurring bedform features are described below.

Ripples are the most common bedform; these are present on non-cohesive and cohesive sediments (Reineck and Singh, 1980). Ripples are small-scale regular features, formed either by waves or currents and conventionally described in terms of their size and shape: this can vary considerably, but generally they range up to 0.2 m in height, with a wavelength of up to 0.3 m (Whitehouse et al., 2000). The crests of the ripples are aligned perpendicular to the direction of the waves or currents (Van Straaten, 1958; and Amos et al., 1988). Such features are not common on mudflat environments, but form when there is a high sand content to the sediment, or a sand veneer has become exposed/created (perhaps after storm activity); although current ripples do form in muddy sediments, but these are always erosive (Reineck and Singh, 1980). A large number of ripple types can form, with two-dimensional, three-dimensional, wave-formed, current-formed, combined wave/current ripples and megaripples (see Reineck and Singh (1980) for detailed description of all ripple forms).

Rill marks are erosional features, which are formed under a thin layer of water flowing on the sediment surface during the falling water level (Le Hir et al., 2000). There are a wide variety of types of rill marks that can form; this is mainly dependent on the local morphology, slope of the sediment (generally low angle slopes of around 2-3°) and grain size (generally better defined in fine sediments compared to coarser) (Reineck and Singh, 1980). Parallel rills, separated by ridges, are commonly found around the mean water level (MWL) on many intertidal flats. Such features range from 0.5 - 1.5 m in width and 0.1 - 0.4 m in depth, with their crestlines orientated perpendicular to the coastline; they are considered to have been caused by wave-induced erosion and deposition (Wang and Eisma, 1988; and O'Brien et al., 2000). The ebb tide flows into the gullies, with a heavy sediment load; these form the only passage of the flow, during the last phase of the ebb. At the same time, a considerable amount of fluid mud is deposited in the rills. Over the upper mudflat, these bedforms are of a reduced amplitude; over the lower mudflat, they become more sinuous, as the along-shore tidal currents become more influential (Whitehouse et al., 2000).

Water flowing over a soft sediment surface may, under certain conditions, erode the sediment to form a tidal creek (Reineck and Singh, 1980). These are present on the majority of intertidal flats. They form a dendritic pattern of creeks of varying sizes (Whitehouse et al., 2000). The creeks perform a drainage function; they can continue to flow when the mudflat is fully exposed. The process of the development of such creeks is described in Section 2.9.

2.7 CLIMATE CHANGE

Primarily it is the predicted rise in sea-level which has led to an increase in research into low energy intertidal zones, as they are perceived as being areas of 'high risk'. In many cases, this is related to anthropogenic changes to the intertidal flats, fixing the landward barrier and preventing the natural response to sea-level rise, i.e. a landward retreat of the intertidal flats to the appropriate elevation relative to the increasing tidal height (Pye, 2000). Within a global context, sea-level rise was the main driving force for coastal evolution during the early Holocene (Vos and van Kesteren, 2000). From research undertaken into the rates of intertidal flat accretion, in comparison to sea-level rise, it has been found that many areas are accreting at a similar (or higher) rate (Allen, 1991; and French et al., 2000). For example, the Kongsmark mudflat in Denmark has derived accumulation rates of 5 – 8 mm yr^{-1}, whilst the local sea-level rise is predicted to be 1.1 mm yr^{-1} (Andersen et al., 2000). In the Dollard area, on the border between Netherlands and Germany, vertical intertidal flat accretion rates of 1.4 – 2.7 mm yr^{-1} have been reported, whilst the sea-level rise has been predicted at 2 mm yr^{-1} (Kornman and De Deckere, 1998). The Skeffling mudflat, in the Humber Estuary UK, is accreting at a rate of 6 – 10 mm yr^{-1} (Paterson et al., 2000), whilst the local sea-level rise over the last 4000 years has been around 1 mm yr^{-1}. However, as in many others areas, the high accumulation rates for the Kongsmark and Skeffling mudflats can be attributed, at least partially, to anthropogenic influences; these cause a morphological change to the system, enhancing erosion/accretion.

2.8 ANTHROPOGENIC IMPACTS

In the past, and continuing today, man has had an important impact upon intertidal flats, in a variety of ways. The most important of these has been land reclamation, which involves the construction of dykes and embankments to prevent the sea from flooding coastal areas. The reclaimed area has been drained, then used for agriculture. This has been undertaken on intertidal areas throughout the world, with large reclamations in east Asia and western Europe (Eisma et al., 1998). Land reclamation has a similar effect to sea-level rise, i.e. extensive shallow water areas are removed, and thus increasing the water depth adjacent to the sea defence (Pethick, 1996). This is the most radical change to intertidal flats caused by anthropogenic activity, but it is not irreversible. For example, some past land reclamations have become inundated, i.e. re-flooded due to the failure of sea walls, and have been transformed back to saltmarsh; such situations provide a unique opportunity to study the possible effects of MR. This approach involves the inland realignment of an earlier embankment, which protects previously reclaimed land (usually in the form of agricultural land) (Macleod et al., 1999). From two such sites in the southeast of England, it was found that smaller areas are more likely to re-colonise with saltmarsh vegetation, whereas larger

sites more commonly revert to mudflat (French et al., 2000). The larger of the sites, (Bulcamp Marshes, Blyth Estuary, UK), after some 55 years of abandonment, is still (on average) only 0.13 m higher than the existing reclaimed land. The area shows no sign of re-establishment of saltmarsh, indicating that the main assumption of MR (i.e. that significant post-retreat regeneration of saltmarsh) is not always correct (French et al., 2000).

There are other more minor anthropogenic impacts to the intertidal flats; these include the extraction of sediment (for aggregate purposes and navigation channels), fishing and mollusc collection (through a variety of methods, including dredging), the grazing of livestock (on the saltmarsh area) and the collection of saltmarsh plants (Eisma et al., 1998). The creation of dams, locks and training works on rivers, leading into these areas, also indirectly affect them; these prevent the natural input of sediment, from the rivers.

When trying to predict the future development of intertidal flats, it must be considered that any development will be dependent upon changes in the rate of sea-level rise, as well as any anthropogenic effects, such as dyke or embankment construction (Vos and van Kesteren, 2000).

2.9 MANAGED REALIGNMENT

2.9.1 *Introduction*

Predicted rises in sea-level, will lead to a significant upgrading of coastal defences, to maintain the current level of protection in certain areas (French, 1999; and Blackwell et al., 2004). Consequently, erosional and accretional rates within the coastal zones, including low energy intertidal flats such as saltmarshes and mudflats, are predicted to increase (Crooks and Pye, 2000; and Pethick, 2001). Owing to this, there has been an increase in evidence suggesting that instead of maintaining the existing line of defence, it may be a better long term solution to allow the sea to flood parts of the coast (French, 2001). MR is a sustainable form of coastal protection, which allows the sea to re-flood parts of the coastline.

Over the past 15 years a number of small-scale MRs have been undertaken across the UK: Abbots Hall, Essex; Northey Island, Essex; Orplands Farm, Essex; Tollesbury, Essex; Medway, Kent; and the River Torridge, Devon (ABP, 1998; French, 1999; Macleod et al., 1999; Underwood, 2000; Chang et al., 2001; Watts et al., 2003; and Blackwell et al., 2004). A wide range of effects and impacts has been investigated, within the MR sites, to attempt to understand the associated processes prior to any large schemes: including; sedimentological; geochemical; biological; and hydrological processes.

2.9.2 *Problems*

The predicted rate of sea-level rise has the potential to cause major problems in many areas around the UK, as coastal defence structures are present, preventing the consequent inland migration of the intertidal flats. Under natural conditions, the mean high water mark would migrate inland, as would the saltmarshes and mudflats so that they remained in the same relative position within the tidal framework, i.e. migrating landwards or seawards, as sea level rises or falls, respectively (French, 1999). Coastal landforms change their location, to maintain the same relative position in relation to marine processes. With an increase in sea level, mudflats will move to areas of lower wave and tidal energy; in turn, they will be replaced by sandflats, which will move inland from more exposed areas associated with high levels of wave energy (Pethick, 2001). In order to manage the coastline effectively, it is important to predict the rates of coastal migration in response to a given rise in sea-level.

In many areas, sea defences were established during land reclamation schemes (to provide protection to land which was previously intertidal); as such they fix the landward barrier of the intertidal flats. These sea defences prevent the mean high tide mark migrating landwards, in response to sea level rise (French, 2001). Such "coastal squeeze" reduces the width and changes the characteristics of the intertidal flats; this, in turn, places important habitats (saltmarshes and mudflats) under threat (Dyer, 1998; French, 1999; and Blackwell et al., 2004). Under such circumstances, water deepening occurs, causing the higher marsh communities to become unstable; this is in relation to the increased frequency and period of flood coverage, leading to the higher marsh to revert eventually to lower marsh communities and, ultimately, mudflats. A reduction in the marsh width increases wave activity at the sea defence, resulting in an increase in erosion of the defences; which will not have been designed originally for such an increase in wave size (Pethick, 2001). Saltmarshes which normally act as highly effective natural 'buffers' for wave activity, dissipating wave energy and protecting the sea defences from erosion are thus destroyed. Recent coastal management approaches aim at re-creating saltmarshes and mudflats (King and Lester, 1995).

The threat of 'coastal squeeze' has caused an increase in the use of soft engineering methods, utilising coastal engineering works to re-create natural processes, rather than stopping them (French, 2001). It has been stated that the "management response must focus on the removal, wherever possible, of flood defences to facilitate the landward transgression of the morphology" (Pethick, 2001). Consequently, an increasingly used approach in tide-dominated coasts, in many countries, is MR; this is the predominant response to mitigate the affects of climatic change and the associated sea level rise (Allen, 2000a; and Blackwell et al.,

2004). The most seaward embankment is either removed or breached, to permit tidal inundation and the creation of mudflat and saltmarsh environments over the former agricultural land of the outermost reclamation. This arrangement is expected to function as an integral part of the flood defence system and create ecological conservation areas (Macleod et al., 1999). However, large areas of the coast have been popular for settlement and industrial growth, with only small areas of the coastline which are not used; hence, in many cases the main limitation is finding areas where MR is allowed, which involves public education and persuasion (French, 2001).

2.9.3 *Planning*

In the planning of a MR, it is important to select a suitable site; otherwise, the effects could be detrimental rather than beneficial to the surrounding areas. This approach is most appropriate in areas with high levels of erosion, or where sea-level rise or land subsidence occurs (Midgley and McGlashan, 2004). In such areas, which require improvements to the present defences to provide satisfactory coastal protection, it can be cost-effective to undertake a MR. Areas where MR has been most successful, have been found to be where the land has previously been claimed from the sea, for agricultural use. The land needs to be at a relatively high elevation in the tidal frame (Cundy et al., 2002), i.e. a continuation of the slope of the existing intertidal flats. However, also of importance are the number of relict creeks present, the use of the land prior to the MR and the prevailing hydrodynamics of the area (Midgley and McGlashan, 2004). The success of a MR scheme depends upon the soil conditions inside the MR site i.e. being resistant to erosion by waves and tidal currents, and thus allow sediment accretion at a similar rate (at least) to sea-level rise (Watts et al., 2003).

Following a successful MR scheme, the costs of maintenance of coastal defences should be reduced: the saltmarsh will provide a natural defence to the inner strengthened embankment, by dissipating wave energy (King and Lester, 1995). Such a process both reduces the risk of flooding to the land protected by sea defences and increases the area of saltmarsh; and results in the establishment of a productive ecosystem both above and below ground level, which is important in the functioning of estuaries and coastal environments (Doody, 1992). In addition, the reflooding of a previous intertidal area helps also to ‘naturalise’ the tidal regime (Midgley and McGlashan, 2004), i.e. reverting back to its original tidal characteristics.

In response to compaction and dewatering due to water loss and the loading by farm machinery, old reclaimed land is likely to have suffered a relative lowering in surface elevation; and it will be in a much lower position in the tidal frame, than the adjacent marshes

to seaward. Such areas may become vulnerable to scour and erosion, with strong flood and ebb currents, as experienced in the Medway Estuary (French, 1999).

2.9.4 *History*

The set-back of sea defences, i.e. abandonment of land to the sea, has been widely practised in Britain since the Medieval times (Allen, 2000a); as such, these should be taken into consideration when examining modern examples, as they provide information on longer-term temporal and spatial effects (Cundy et al., 2002). In the Severn Estuary, historical "set back" has taken place successfully between 1300 and 1590. This has been followed by the recreation of mudflats and marshes with accretion of sediment, with no evidence of any major detrimental effects (Allen, 2000a). Natural storm breaches occurred within the Medway Estuary around 100 years ago (French, 1999). This particular set back location suffered less erosion than the open saltmarsh, over a 70 year period and provided a localised form of coastal defence, which allowed the site to survive natural erosive processes more effectively than the open marsh. The observation that marshes form following storm breaches clearly shows that the contemporary landward retreat of sea defences can benefit from enhanced protection provided by the new marsh formation. However, deep scour holes may form in breaches in the seabank, which gradually grow wider and deeper; while networks of tidal creeks develop within the MR over a short time scale of months, and over decades gradually reach the scale and density of the natural creek systems (Allen, 2000a).

Based on existing MRs, it was found by French (2001) that the most successful schemes occurred where:

1) the elevation of the MR site was within the elevation at which saltmarsh vegetation can grow;
2) the site was adjacent to an existing marsh area which acted as a seed bank for flora and as a migration site for fauna;
3) the breach in the embankment was of sufficient size, a relict/artificial creek network was present and the site was sufficiently sheltered from waves; and
4) the site has been well researched and the details of the hydrological, sedimentological and ecological aspects of the area understood.

2.9.5 *Summary*

MR is being suggested today for many sites, unfortunately often without a full understanding of the implications, neither for the actual MR sites nor the adjacent sedimentary environment (Blackwell et al., 2004). However, experimental sites (such as Freiston Shore) are being utilised, to try to improve the understanding of the processes involved and the practical techniques required (Watts et al., 2003).

2.10 CREEK DEVELOPMENT

2.10.1 *Introduction*

For the purpose of this study, creeks are taken to be features over intertidal zones which run dry, whereas channels always remain partially submerged. The majority of work undertaken about creeks over intertidal zones has been focused on the saltmarsh, so very little background can be provided on the creeks over mudflats and sandflats.

The morphological evolution and development of saltmarsh tidal creek networks, both spatially and temporally, has received only limited attention in comparison to the work undertaken on other aspects of the intertidal zone and similar fluvial systems (Zeff, 1988; and Shi, 1995). The hydrodynamics in these tidal creeks are highly complex, with unsteady flows and well-defined velocity transients occurring close to the bankfull stage, on both the flood and ebb phases of the tide (French and Clifford, 1992). The creeks distribute tidal water and suspended sediment over the channel banks, then return the tidal waters and any undeposited silt to the sea as the tide ebbs (Allen, 2000b). Hence, tidal creeks facilitate the exchange of waters, nutrients and sediments between marshes and open marine environments (Ward, 1981).

Creek networks usually consist of branching, blind-ended channels, with a variety of different plan forms. The boundary surrounding these systems is generally an hydraulic one, but, in some cases where the creeks reach back to the inland side of a marsh or a sea defence, it becomes a topographic boundary. The type of creek network, which develops over an intertidal system is linked to several natural factors: the slope of the intertidal flat; the grade of sediment available; the age of the system; and the tidal characteristics. Anthropogenic impacts can effect the development by impairing the evolution and development of the creeks through the construction of sea defences, or directly affecting the creeks by dredging (Allen, 2000b).

2.10.2 *Hydrodynamic Environment*

When considering channels within the intertidal zone, it is important to remember that they are affected by differing conditions, especially in response to the spring-neap tidal cycle. Most neap tidal volumes of water will merely enter, and remain confined within the banks of the creek, without extending over the saltmarsh (undermarsh tides). In contrast, high spring tides will rise above the banks of the creek and inundate the saltmarsh for a period (overmarsh tides) (Allen, 2000b). At a number of sites the undermarsh tides have been found to be

associated with relatively weak flows, of the order of 0.1 - 0.2 m s^{-1} (Bayliss-Smith et al., 1979; Healey et al., 1981; French and Stoddart, 1992; and Pringle, 1995). The velocity in the creek is low when the water level is below, but not exactly at bankfull stage; it then peaks at around 1 m s^{-1}, as the bankfull stage is exceeded and water flows onto the saltmarsh. The low flow velocity associated with undermarsh tides and during high-water slack allows suspended sediment to settle on the beds and banks. Similarly, erosion and transport of the bed material is possible, whilst the emptying of the intertidal platform causes higher velocities (Allen, 2000b). Another important difference between the two is that overmarsh tides create large amounts of turbulence, whereas undermarsh tides create little disturbance. The overmarsh tides maintain a strong vertical concentration of suspended particles and, during the flood, the velocity-maximum delivers a pulse of suspended fines to the adjoining marsh platform (French and Stoddart, 1992; and Allen, 2000b). The different impacts which the flood and ebb stages of the tide have, on channels in the intertidal zone, can also be important. For example, in North Norfolk, UK, integrated ebb-aligned drainage systems are a feature of the tide-dominated marshes and are regarded as major conduits for material exchange (French and Stoddart, 1992). At this particular site, the flood/ebb duration ratio is not constant; it varies from approximately 0.65 on neaps, to 0.90 on springs. In certain circumstances, such as in this example, it is possible to identify the dominant process involved in marsh development, by examining the morphology of the channels.

2.10.3 *Formation and Development*

The development of creek systems is dependent upon the tidal range, with macrotidal areas consisting generally of straight, steep channels lying perpendicular to the shoreline: microtidal and mesotidal marshes often have more complex creek patterns (Luternauer et al., 1995). Seven different network types have been identified, in relation to British saltmarshes (Pye and French, 1993). The sequence, progressing from linear to meandering-dendritic, is found to be associated with an increase in marsh maturity (Fig. 2.4). However, this sequence is based entirely upon saltmarsh creek systems. Research into creek formation over the intertidal flats has been focused mainly in estuarine environments, which experience only limited creek development on the mudflats and sandflats. Insufficient research has been undertaken over large intertidal zones with extensive mudflats/sandflats, where different processes and formations occur, compared to the estuarine environments.

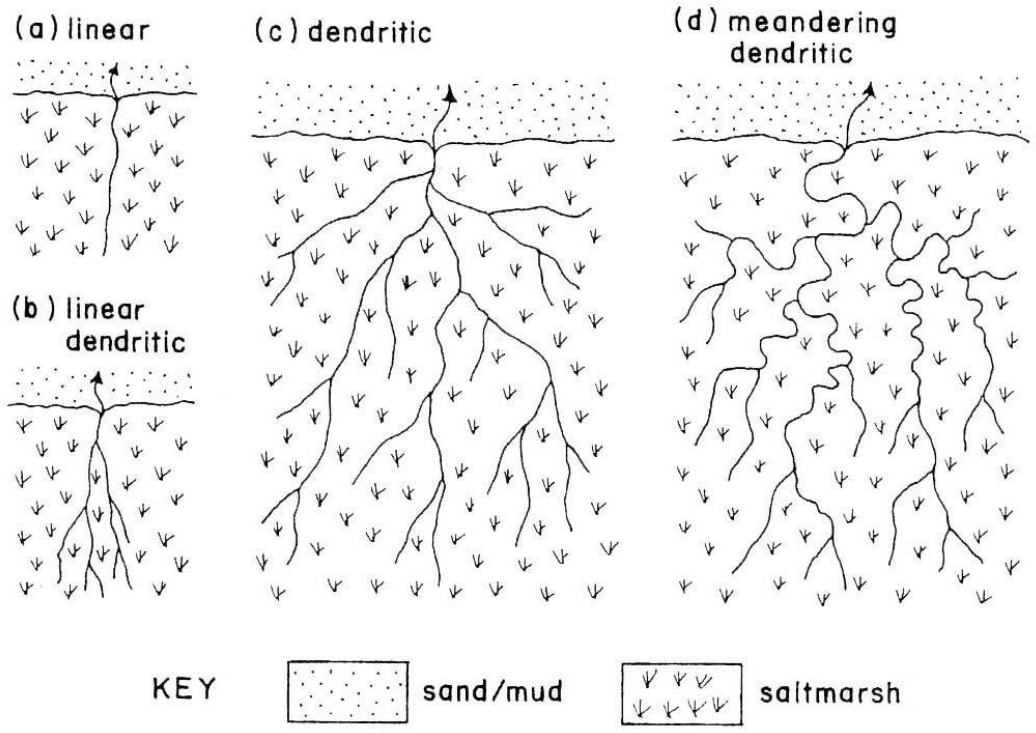

Figure 2.4: A classification of tidal-creek networks in saltmarshes (from Allen, 2000).

The formation of a dendritic creek system over intertidal flats is mainly a result of mudflats not being efficient at carrying surface water away from the flat as the tidal water retreats (Whitehouse et al., 2000). Subtle variations in surface topography focus/dissipate the sheetflow and cause the initial stages of channel development (Horton, 1945, for river systems). The initiation of creek development, as found by Perillo (2003) for the Bahia Blanca Estuary, Argentina, was attributed to the burrowing of crabs. Elsewhere, sheetflow caused by heavy rainfall at low water has been found to impact and disperse cohesive substrate; in comparison, ordinary tidal flows did not exceed the critical shear stress (Mwamba and Torres, 2002). Once a depression is created, then more flow will be attracted to the area, to create a larger bed shear stress and cause an increase in erosion (Whitehouse et al., 2000).

Sheetflow also intermittently controls the headward erosion of low-order intertidal creeks (Mwamba and Torres, 2002). Headward erosion rates, up to a few metres annually, have been noted from youthful back-barrier marshes in North Norfolk, where the ebb-tide probably facilitated the process (Steers, 1939, 1977, cited in Allen, 2000b). The evolution of a tidal creek network was investigated over the coastal plains of the Mary River, northern Australia (Knighton et al., 1992). From aerial photography it was found that, over 50 years, the creeks extended over 30 km inland; a number of the associated tributaries were noted to have had

headward retreat rates over 0.5 km yr^{-1}. These rates have been attributed to the associated large tidal range (6m in nearby macro tidal gulf), relatively flat plains and the availability of pre-existing channel lines (in the form of palaeochannels).

The phases and processes associated with network and channel evolution in fluvial systems can be compared with those of creek evolution on intertidal flats (Glock, 1931; and Horton, 1945). Schumm et al. (1987) identified 3 models of channel evolution that had been described. The first model suggested by Horton (1945), stated that on a steep, newly exposed, surface a series of parallel rills will develop. With time, cross-grading and micro-piracy would occur among the rills, producing an integrated dendritic network (Fig. 2.5(a)). The second model of network growth relies on the action of headward growth of the channel. Quite simply, this involves the channel growing in a headward direction, whilst also bifurcating (Fig. 2.5(b)). With time, this will fill the space available and form a fully developed dendritic network. The third model was based on the findings by Glock (1931), who showed that the drainage area becomes rapidly subdivided by channels, with the addition of tributaries filling any available space (Fig. 2.5(c)). The most common form of natural channel growth was found to be related to this third model (Schumm et al., 1987). As such, the network evolution can be subdivided into various phases: (i) initiation; (ii) extension by headward growth (elongation); (iii) tributary addition (elaboration); (iv) maximum extension; and (v & vi) integration through abstraction and capture.

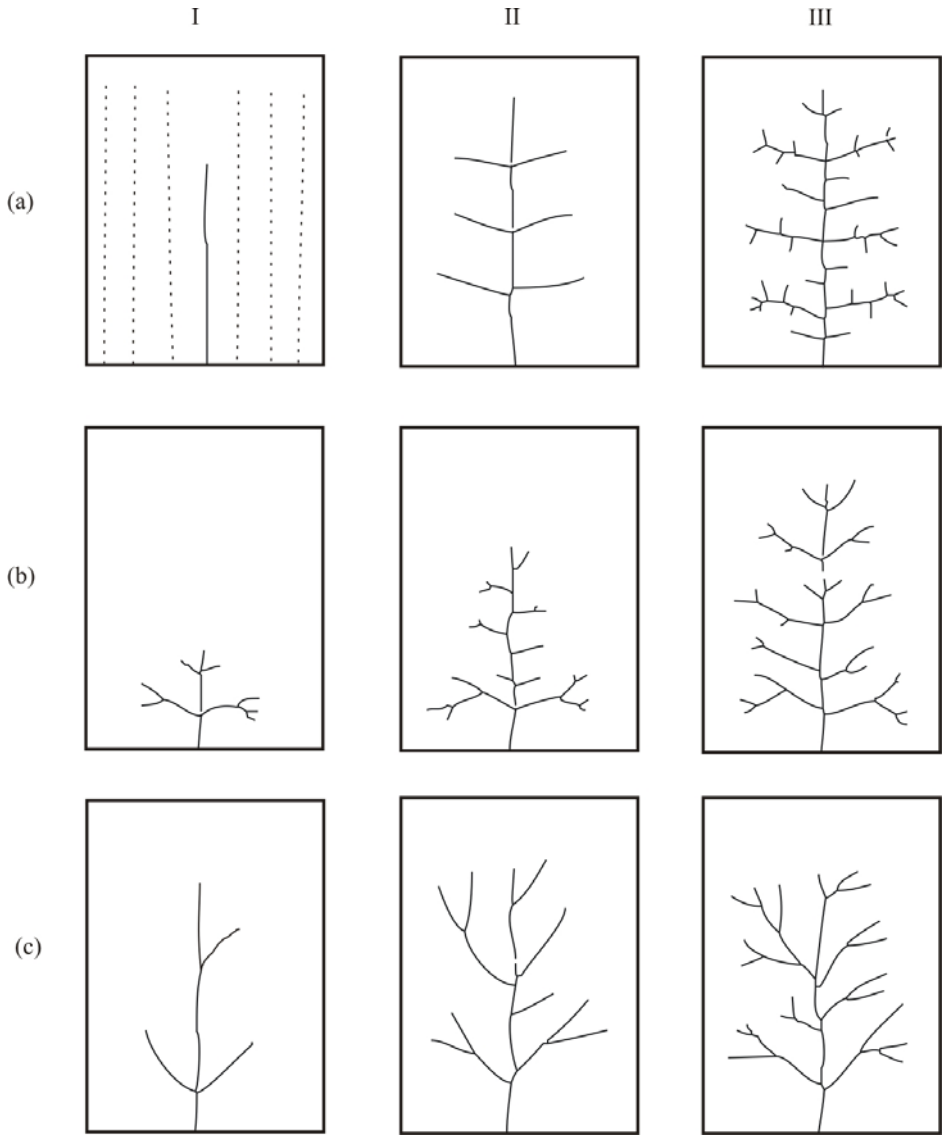

Figure 2.5: Models of the drainage network growth over time (1-3 represent the development of each network over time): (a) replacement of parallel rills by an angular dendritic pattern; (b) expansion by headward growth; and (c) extension of rapidly growing, long channels, with tributaries added subsequently to fill in drainage networks (Schumm et al., 1987).

A number of variables have been identified as being the most important in the development of creek systems: the elevation and slope of the land; the nature of the sediment present; and the water and sediment yield (Leopold et al., 1964; Allen, 1977; Chang, 1985; Richards and Lane, 1997; Werritty, 1997; and Schumm et al., 2000). The direction and magnitude of flow, within the tidal creeks and over the marsh surface, are controlled by the complex interaction of the topography, the tidal stage and the effect of wind and waves (Davidson-Arnott et al., 2002). If these variables undergo a progressive/instantaneous change, then the channel may cross an extrinsic threshold and experience change. If an imposed disturbance causes the system to cross such a threshold, then new landforms may develop (Werritty, 1997). The initial landform assemblages are then deemed to have been "geomorphologically responsive" to the changes. The effectiveness (impact) of a destructive event, such as a flood, depends

upon the force exerted, the return period of the event and the magnitude of constructive or restorative processes that occur in the intervening period (Wolman and Gerson, 1978). When the surrounding area stabilises, then the creek may become adjusted to the new conditions, returning to a dynamic equilibrium (Brookes, 1996).

Once creeks are formed on the intertidal flats, then the movement of the sediment, in terms of erosion and deposition, is important in controlling their evolution. The changes in the channel morphology, due to erosion/deposition, affects the rate of sediment transport and, consequently, the change in channel characteristics; this, in turn, affects the rate of erosion/deposition, creating a feedback relationship between the changes in the process and form (Pickup, 1977). The effect of erosion/deposition in the channel characteristics is likely to vary widely, from creek to creek. Such erosion/deposition is dependent upon factors such as channel size, erosion resistance, angle of repose of the bed and bank sediment, the effects of vegetation, sediment load of the stream and the magnitude and frequency of the water discharge (Pickup, 1977).

Natural changes over intertidal flats need also to be taken into consideration; for example, the response of creeks to sea-level rise is a natural change, which represents a long-term trend towards increased energy dissipation (Pethick, 1992). This pattern occurs because, as sea-level rises, both the tidal prism and tidal energy increases within the creeks. Hence, as the flow moves to landwards, not all of the energy is dissipated. This effect leaves a significant flow velocity still present when the flood tide reaches the landward end of the creek, causing undermining of the creek banks and, eventually, their collapse. For any change in water and/or sediment discharge, channel metamorphosis will occur; this involves an adjustment of the width, depth, slope or planform of the creek (Harvey, 1977; and Petts, 1977). The frequencies of the major discharges and sediment-producing events are important in the channel morphology, as they determine the recovery time. In association with these processes, scour, which occurs in the channels due to flood and ebb currents, is a major process controlling the depth of the creeks and their overall hydraulic geometry; this is through its effect in initiating bank undercutting and collapse (Pye, 1992).

2.10.4 *Fluxes in the Channels*

Tidal creeks are one of the main routes along which silt and very fine sand are transported to the upper foreshore. In The Wash, eastern England, the supply of silt and very fine sand through the creeks has been identified as the principal way in which fine-grained material travels to the upper foreshore, to cause accretion (Amos, 1974; and Kestner, 1975). In the study of sediment transport through intertidal creek systems, it is mainly the quantity and

direction of sediment in the channel which has been investigated. Within this context, the temporal sampling intervals of the measurements of velocity and suspended sediment are critical. Sampling at 30 minute intervals can underestimate the discharge, with the optimum sampling interval being every 5 minutes (Reed, 1988). From the available data, it would appear that there is a need for more attention to be given to the velocity and discharge variability, in estimating the fluxes of water or sediment (Bayliss-Smith et al., 1979; and Reed, 1987).

A major emphasis of many of the studies undertaken into intertidal sediment dynamics has been related to the input and output provided by the marsh creek system (Odum et al., 1979); as the creeks facilitate sediment transport, by acting as conduits between the intertidal flats and the adjacent body of water. However, there are only a limited number of studies on the role of the sediment circulation and temporary storage, in relation to inorganic and organic material (Reed, 1988). Studies that have been undertaken, on fluxes in the intertidal zone, have examined the dissolved and particulate material fluxes and the net sediment balance. Sediment flux studies in tidal creeks have yielded varying results; in part, due to the fact that the suspended material transport depends upon the season and the physical characteristics of the tidal cycle being monitored. Only one or two continuous tidal cycle measurements were carried out, for most of the sediment flux studies undertaken previously. Hence, the seasonal fluctuations in suspended loads have been determined, but the large, short-term variability between tidal cycles has been missed (Ward, 1981). The majority of flux studies have focused primarily upon the tidal exchange via the creek system, without giving consideration to either the complexity of channelised tidal flows, or the possibility of a more complex transport pathway (French and Stoddart, 1992). In some cases it has been found that a large proportion of the total marsh tidal prism enters and exits across the broad front of marsh margin, rather than through the creek network (Davidson-Arnott et al., 2002). Clearly, such a pattern of water movement means that input and output measurements solely in the creeks are not sufficient to fully quantify the sediment budget. Hence, computations of channel fluxes may be conceptually inappropriate, owing to the fact that large proportions of the total tidal exchange occur across the intertidal flat. Few investigations have determined both the hydrodynamic processes and the resultant sediment fluxes associated with tidal creeks (Ward, 1981).

An investigation into the fluxes of a tidal creek was undertaken on Kiawah Island, South Carolina, over a saltmarsh (Ward, 1981); this showed that, on the basis of 15 tidal cycles monitored in March, there was an export of organic matter and a balance of inorganic matter. At the same location, during 8 tidal cycles investigated in July-August, there was a net export

of both organic and inorganic matter. The export of the suspended material was attributed to the time-velocity asymmetry of the tidal currents. The peak ebb velocity in the creek was 20 – 30 % stronger than the peak flood velocity, meaning that higher concentrations of suspended material are transported for longer periods of time on the ebb tide, creating the seaward movement of the material. In Dipper Harbour Creek, New Brunswick, Canada, the current velocities within the creek were strongly flood-dominant, with a consistent low-stage peak in the flood velocity, followed by a secondary high stage flood surge, then a weaker ebb peak occurring around bankfull stage (Ayles and Lapointe, 1996). These overall patterns show that the tidal asymmetry affecting the ebb and the flood velocities is highly variable; likewise, it is dependent mainly upon local factors, such as the morphology of the intertidal flats and the tidal cycle. The spring-neap tidal cycle is important in the fluxes of sediment, as sediment fluxes decrease as the tidal range and the tidal prism decreases.

Sediment transport was found to be a non-linear function of the mean velocity in the estuarine channel in The Wash (Kestner, 1975); a peak ebb velocity was around 1 m s^{-1}, with a corresponding sediment flux of around 2000 g s^{-1} m^{-1} (grams per second, per metre width), whilst the peak flood velocities were around 2 m s^{-1}; however, the corresponding sediment flux varied non-linearly and was 4 times higher, at 8000 g s^{-1} m^{-1}. Such a relationship means that even moderate changes in current velocities have a very marked effect on the sediment balance. Further, the functional relationship between sediment flux and mean velocity may differ for each grain size fraction, especially for the silt and very fine sand-sized sediment (Kestner, 1975).

Meteorological conditions can cause flux differences, on effectively similar tides. For example, in South Carolina winds which gusted up to 40 km hr^{-1} from the northeast and east were found to cause a slight water level set-up, a higher discharge and an increase in wave activity within the tidal channels (Ward, 1981). The wave activity eroded the material from the channel banks, increasing the SSC and sediment flux. During the succeeding tidal cycle, the winds remained strong but blew from the south; this led to a reduction in the suspended material flux, despite the winds gusting up to 35 km hr^{-1}.

2.10.5 *Interaction with the intertidal flats*

Studies have been undertaken into the formation of levees on the banks of major creeks; likewise, on how these affect the drainage of the intertidal flats (Amos, 1974; Kestner, 1975; and Pye, 1992). However, interaction between the creeks and the surrounding intertidal flats is not well understood. A number of measurements using a vertical array were undertaken by Schostak et al. (2000), in a saltmarsh tidal creek in Cumberland Basin, Bay of Fundy, Canada,

to investigate: (a) the vertical velocity profile; (b) the changing bed shear stress over a tidal cycle; and (c) an estimate of the net sediment flux through the cross-section. Near bed, maximum velocities < 0.1 m s^{-1} were measured; this is below the erosion threshold for transport for mud and sand. The low velocities were explained by the small tidal prism in the creek, related to the short channel length, steep gradient and simple pattern of the creek network. In contrast, with a channel, with a shallow gradient, levee formation and the development of a more complex creek network are likely to be associated with high levels of suspended sediment.

2.10.6 *The Regime Theory*

Drainage canals tend to develop a particular section and slope, irrespective of their original geometrical configuration, i.e. wide and shallow with steep slopes, or narrow and deep with flat slopes. This characteristic forms the basis of the Regime Theory: water discharge, charge (load), size and specific gravity of the material in movement (independent variables) determine the regime dimensions and slope (dependent variables) (Inglis and Allen, 1957). The basic principle of the Regime Theory was initially derived from engineers creating irrigation canals in India; it was found that the canals tended to develop the same natural section and slope whether they were originally constructed wide and shallow with steep slopes or narrow and wide with flat slopes. For an intertidal zone in regime, accretion and erosion balance. However, generally a very low frequency change is taking place; in estuaries and embayments, this is usually accretional. If land reclamation occurs, the tidal prism is reduced: this, in turn, increases the rate of accretion (Evans and Collins, 1987). The regime of intertidal flats is dependent upon tidal range, the local currents, and the quantity of material in transport (Inglis and Allen, 1957).

Creeks on intertidal flats are associated with a particular ‘catchment area’; they transport nutrients and sediment, from within the network itself (seaward) and from the more distant estuary or sea (landward) (Allen, 1997). If erosion was experienced or the sea-level rose, there would be an increase in the tidal prism, which each network must carry to and from its catchment during overmarsh tides. The Regime Theory requires changes in hydraulic duty (the work that must be done to lift water, expressed as hydraulic energy), to effect corresponding changes in the network hydraulic geometry. Channels are said to be ‘in regime’ (in dynamic equilibrium) when, on a time-scale of months to years, the space-time average flow velocity or shear stress acting on it is steady; thus, neither net erosion or accretion is occurring (Allen, 1997). In theory, the effect of an increase in the duty would be an increase in the channel cross-sectional area, due to the increased discharge; this would not occur instantaneously, but would usually be associated with a time-lag. Further, the

topography of the intertidal flats may undergo changes; the network may become denser and more elaborate topologically, due to headward growth of first order creeks and channel initiation (Glock, 1931). The opposite would occur if there was a decrease in duty, with the channel cross-sectional area reducing in response to accretion (Allen, 1997). This has been overlooked in many cases of engineering over the past century.

The deliberate abandonment of artificial flood defences is presently becoming an increasing practice, which re-exposes areas to tidal siltation. This newly inundated area creates a potentially influential hydraulic duty (Allen, 1997). On the basis of the Regime Theory, any new creeks initiated together with existing ones, should undergo rapid erosion. Such erosion would be in the form of widening, deepening and associated topological elaboration of the creeks, by extension and densification of the system (Glock, 1931). In the absence of any channels, network initiation and rapid growth are likely to occur. Thus, as the marsh ages, an increasing proportion of the (declining) tidal prism is transported through the channels, as opposed to over the marsh. In time, with the continuation of a fall in hydraulic duty, channel expansion and elaboration should be replaced by abandonment, infilling and simplification of the network.

2.10.7 *Summary*

The main function of creeks located within intertidal flats, is to act as a link to exchange nutrients and sediments between the intertidal zone and the open marine environment. The creeks are one of the primary pathways along which silt and very fine sand are transported to the intertidal flats. Therefore, the areas surrounding the creeks on the upper intertidal flats and saltmarsh are associated with high rates of sediment deposition. This deposition can lead to the formation of levees on the banks of the creeks on the saltmarsh and upper intertidal flats (Evans, 1965).

Initiation of tidal creeks is considered to be in response to subtle variations in the surface topography, which may channel any sheetflow across the intertidal flats. Within these areas of concentrated flow, “nick-points” are created, causing the initiation of a tidal creek; subsequently, headward erosion creates the entire creek network. Rates of headward erosion are commonly found up to 3 m yr^{-1} but, on the coastal plains of the Mary River, these were up to 0.5 km yr^{-1} (Knighton et al., 1992). Creek development is dependent upon: the slope of the intertidal flats; the sediment characteristics; the age of the system; and the tidal range. If any of these variables undergo a change, then the creek will be affected directly and change; likewise, the flows on the surrounding intertidal area and over the marsh are controlled by complex interactions between the topography, tidal stage and wind/wave effects. Finally,

tidal creeks are affected differently in terms of tidal ranges and height, in relation to overmarsh and undermarsh tides.

CHAPTER 3: REGIONAL BACKGROUND

3.1 INTRODUCTION

The area under investigation is an intertidal zone at Freiston Shore, located within a tidal embayment on the east coast of England, The Wash (Fig. 3.1). The conditions experienced over the intertidal flats within The Wash can be influenced by the prevailing conditions in the adjacent southern North Sea; hence this area will be considered (Evans and Collins, 1975).

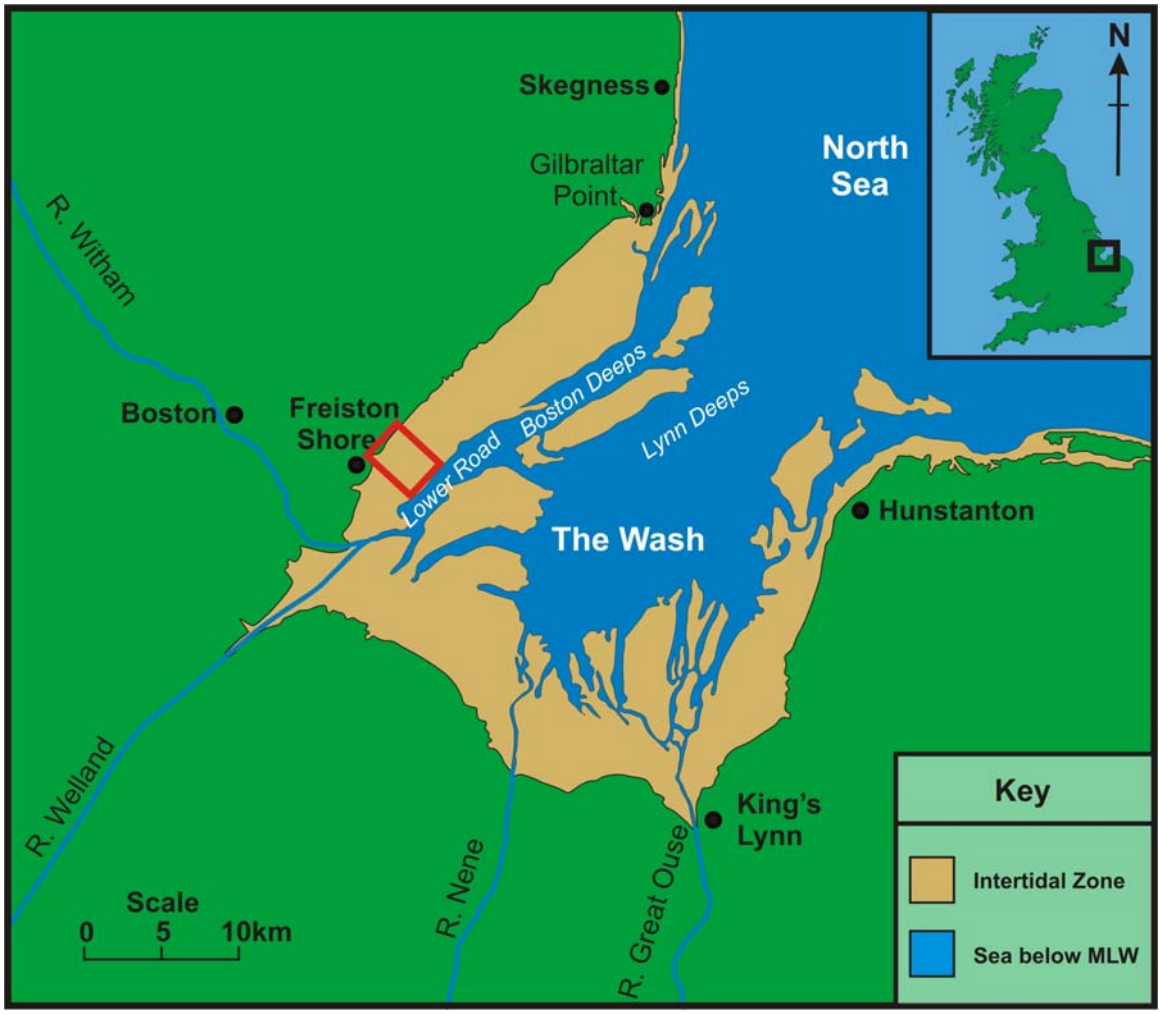

Figure 3.1: Map of The Wash, showing the intertidal zone and highlighting the location of Freiston Shore.

3.1.1 *Southern North Sea*

Sediment transport in the southern North Sea can influence the surrounding coastlines, by supplying and removing beach material. The area of the southern North Sea surrounding The Wash is predominantly less than 20 m deep, except for a deeper gully (Fig. 3.2); this runs from the Lynn Deeps (Fig. 3.1) in The Wash to the offshore area to the east of Grimsby, where the deepest point is located (> 80 m). Water circulation in the North Sea demonstrates

a general anticlockwise tidal pattern, with the residual water flow in the area adjacent to The Wash being towards the south-east (Eisma, 1981). A study, combining much of the past research carried out in the North Sea, found that the onshore transport of sediment dominates the Lincolnshire and north Norfolk coasts (Chang and Evans, 1992).

Strong winds dominate generally the North Sea between November and March, with a dominant wind direction from the south-west. These strong winds cause intense wave activity through the winter months, with mean wave heights in the North Sea reaching up to 2 m (Ke et al., 1996). The SSC in the offshore North Sea waters are low (< 2 mg l^{-1}); these increase inshore (> 10 mg l^{-1}) and become much higher over the intertidal areas (50 to 100 mg l^{-1}) (Eisma, 1981; and Evans and Collins, 1975). During storm conditions, waves and tidal currents, both in the southern North Sea and within The Wash, suspend sediment from the bed; this causes SSCs which are many times greater than those experienced during calm weather conditions (Evans and Collins, 1975; and Collins et al., 1981).

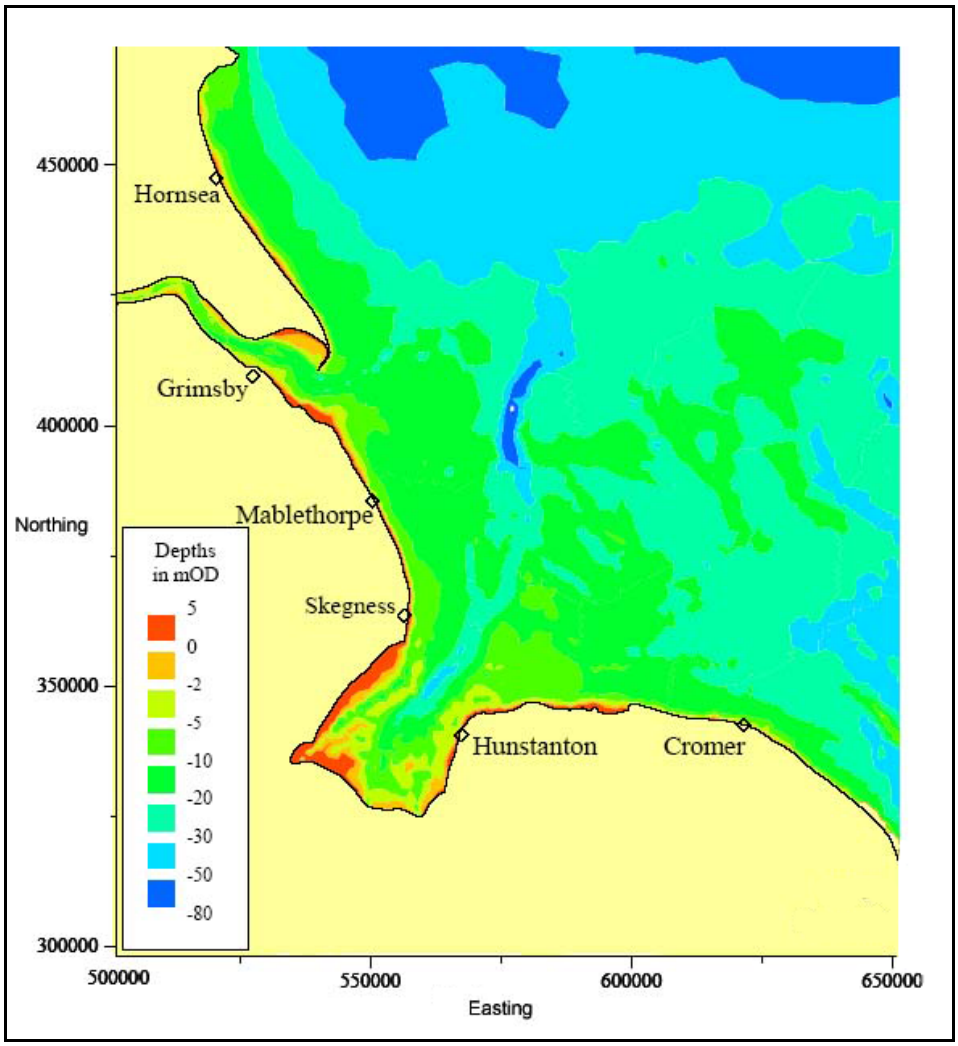

Figure 3.2: Bathymetry of The Wash and the surrounding area of the southern North Sea (from HR Wallingford et al., 2002).

In the North Sea region, the longest tide gauge mean sea-level records show no record of recent increases in sea-level trends, although the regional rate of change of eustatic sea-level rise is approximately 1.0 ± 0.15 mm yr^{-1} (Shennan and Woodworth, 1992)).

3.1.2 *The Wash*

A number of rivers (the Ouse, Nene, Welland, and Witham) flow through trained outfalls, into The Wash (Darby, 1940; Evans, 1965; and Brew and Williams, 2002). Past studies have shown the fluvial supply of water and sediment to be negligible, within this area of active sediment dynamics, compared to that from the adjacent North Sea (Wilmot and Collins, 1981; and Dugdale et al., 1987). In such a coastal embayment subjected to these conditions, sedimentary processes are controlled predominantly by tidally-induced water and sediment transport (Ke, 1995).

The embayment is approximately 20 km wide at the mouth and 30 km in length, with an area of 615 km^2 (below High Water); of this, some 325 km^2 lie below the Lowest Astronomical Tidal Level (Ke et al., 1996). The maximum water depth is around 40 m in the Lynn Deeps, at the entrance to The Wash. The intertidal zone occurs, typically, in two forms: a marginal strip around most of the embayment, which varies in width; and a series of large offshore sandbanks, which are separated throughout the tidal cycle by deep channels and are, in many cases, linked to the coastal intertidal strip. Tides in the Wash are macrotidal and semi-diurnal in character; with a mean tidal range of approximately 5 m, and mean neap and spring ranges of 3.5 and 6.5 m, respectively.

The Wash has been the subject of a wide range of studies; many of these have been focused upon the intertidal zones and the effects of land reclamation. In particular, there have been detailed studies undertaken on the intertidal zone at Freiston Shore; these commenced in the 1950s, and have continued to the present day. Since the studies began, a relatively recent land reclamation was undertaken in 1980; interestingly a subsequent managed realignment was undertaken on this particular reclamation in 2002. Consequently, such activities have provided a unique data set. Hydrodynamic and sediment dynamic measurements are available over the intertidal flat: before the land reclamation, since its establishment and following the breaching of the embankment, as part of the MR. As such, the intertidal zone at Freiston Shore, in The Wash, is an ideal location for a study of this particular nature.

The Wash and the surrounding Fenland were formed initially during the Tertiary (Evans, 1959). During this time, the area was uplifted to leave an east-south-east tilt, to the land surface; on the resulting surface, many river systems were formed. These rivers carved deep

valleys in the uplifted, chalk-covered, land mass. Such erosion by rivers, combined with marine erosion, formed the depression known as the Fenland. During the Pleistocene epoch, glaciers crossed this area, with the most recent being from a north-easterly direction, extending just into The Wash. These glaciers caused more erosion and deposited till, and there are also marine deposits known from this age. Since the last glaciation, deposition has prevailed up to the present day, with peat being deposited within the freshwater areas (on the inner side of the Fenland depression), together with silts and clays on the seaward side. The inner parts of the Fenland are, in many cases, below sea-level, owing to the creation of embankments for land reclamation, preventing the natural flooding of the Fenlands. In addition, since the 17th Century a number of drainage schemes have been implemented; an unforeseen effect of this was the rapid lowering of the peat surface (Darby, 1940; and Steers, 1946).

3.2 SEDIMENT SOURCES

Various researchers have investigated the supply of sediment to The Wash, as summarised in Figure 3.3 (Evans and Collins, 1987). An early interpretation of these mechanisms was that the floors of the North Sea and The Wash, together with the eroding boulder-clay cliffs and adjacent sea-floors of Lincolnshire to the north and Norfolk to the east, were the main source of the sediment (Evans, 1965; and Pye, 1995). A bedload parting zone was identified on the north Norfolk coast (around the area where the furthest arrow to the east on the north Norfolk coast is located on Figure 3.3) through examination of the heavy mineral composition in the sediment (Chang and Evans, 1992). Through analysis of the clay mineral composition, it was found that a further important source of clay-sized sediment was from the erosion and redeposition of the intertidal flat sediment (Shaw, 1973).

As the principal rivers, which discharge into The Wash, cross the Fenland they have extremely low gradients and are unable to carry appreciable sediment loads (Wilmot and Collins, 1981). This is proven clearly when the sluice-gates at the river mouths are closed for long periods. Limited deposition occurs on the landward side, whereas dredging is necessary on the seaward side (Evans, 1965; and Kestner, 1975). Such an observation is consistent with later findings, where the total annual sediment loads of the rivers were established to range between 43,000 and 173,000 tonnes; in comparison, a minimum of 30,000 and 120,000 tonnes of suspended sediment was found to be carried, in the overlying waters, over the intertidal flats of The Wash, during each neap and spring tide, respectively (Evans and Collins, 1975). On the basis of these quantities, at least 6.5 m of sediment had been deposited over the intertidal zone over the last 2000 years. Despite various inaccuracies in the computation, the average deposition of coastal sedimentation, over this time, was 8×10^6

tonnes yr^{-1} (Evans and Collins, 1975). Hence, it would take approximately 50 years of river supply to produce enough material to maintain the derived annual rate of coastal accretion.

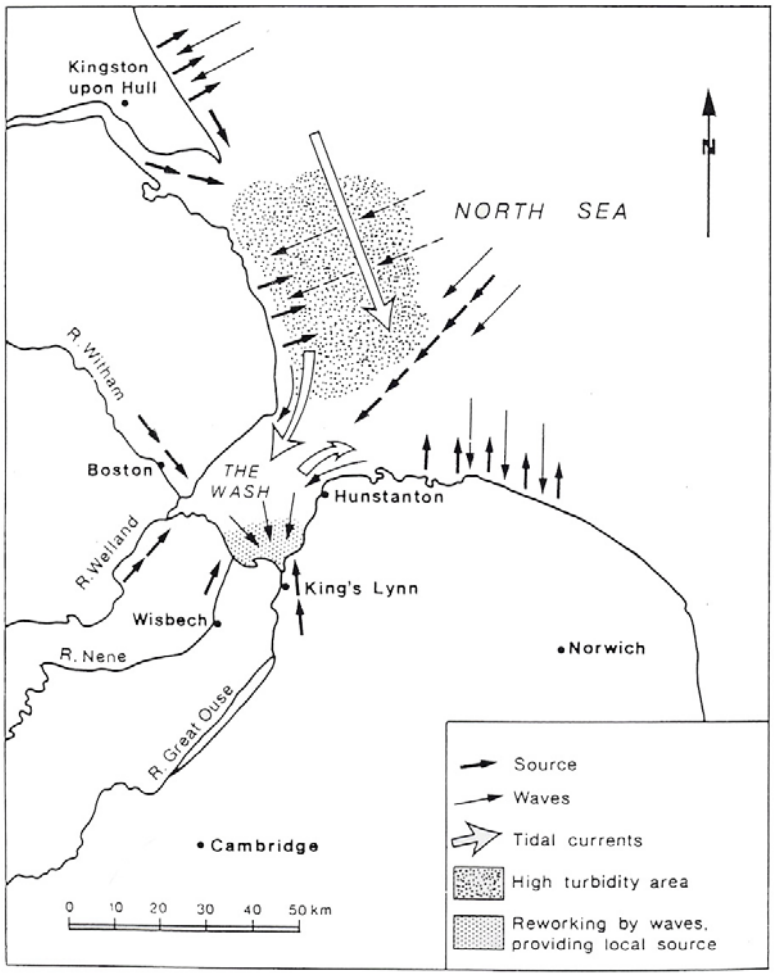

Figure 3.3: Summary of sediment sources and transport paths in The Wash and neighbouring areas. Note: dashed arrows represent the more intermittent processes (from Evans and Collins, 1987).

The main and most immediate sources of sediment supply to The Wash are the adjacent marine areas and, possibly, the eroding coastlines to the north (McCave, 1987). It is interesting to note that studies by the Hydraulics Research Station show an apparent deepening of The Wash since the earliest surveys in 1828 (Inglis and Kestner, 1958), indicating that erosion of the adjacent bed may also be an important source of sedimentary material. Subsequent findings appear to agree with this earlier statement (Evans and Collins, 1987), with the major part of the sediment supply to The Wash originating from the North Sea floor, together with the coastlines of Lincolnshire, Yorkshire and Norfolk. Residual hydrodynamics and sediment dynamics have been investigated on the basis of a detailed re-analysis (Ke et al., 1996) of an extensive data set obtained in relation to the *Wash Water Storage Scheme* (Hydraulics Research Station, 1972, 1974a, 1974b, and 1975). Predominantly suspended sediment was supplied from the north, the suspended sediment

pathways coincided with the spring tidal water movements and the subtidal areas acted as the main conduits. Suspended sediment transport was the dominant mode of transport within The Wash, with bedload transport only reforming the seabed into bedforms. During spring tides, the main areas of bedload transport were along both flanks of the entrance to The Wash and at the landward end of Lynn Deeps; throughout the rest of The Wash, the tidal currents were capable of transporting the sediment in suspension (Ke et al., 1996).

3.3 SEDIMENT DYNAMICS

Extensive coastal progradation has occurred over approximately the last 2000 years and has been enhanced by land reclamation. Such a supply of sediment has caused the shoreline to build seawards, despite the inexorable rise in sea-level (Evans and Collins, 1987). Accretion of the intertidal flats shows that flood-tidal deposition has been dominant, over ebb-tidal erosion; this is as a result of the mechanism described as "settling lag" (Section 2.2.2) (Postma, 1967). This mechanism has caused the development of a broad coastal fringe, consisting of intertidal sands, silts and clays. As the tidal current speed decreases gradually landward over the intertidal flats, there is a reduction in competency (the largest size of material in transport) and capacity (the amount of material in transport) (Evans, 1965); this results, in turn, in a gradual differentiation of the load. Such differentiation has resulted in the formation of seven sub-environments (Fig. 3.3): (a) saltmarsh (well-laminated silty clays and clayey silts, with small amounts of sand); (b) higher mudflats (laminated or thinly-laminated silty sands and sandy silts); (c) inner sandflats (sands and silty sands); (d) *Arenicola* sandflats (sands and silty sands, median diameter slightly larger than inner sand flats); (e) lower mudflats[1] (poorly-sorted laminated sands and silty sands, consisting of a "…soft, smooth, muddier surface….with large, shallow scours." (Evans, 1965); (f) lower sandflats (sands with minor amounts of fine-grained material); and creeks and bordering areas (from low- to high-water, sediments change from sands through silty to clayey sediments). Each of these sub-environments is characterised by distinctive surface features, associations of organisms and sediments with differing composition, texture, and sedimentary structures. Deposits from creeks and their bordering sub-environments form as belts, which cross the boundaries of other sub-environments in The Wash. These creek belts have been noted to narrow in a shoreward direction (Evans, 1965), as the creeks tend to decrease their zone of lateral migration, progressively inland (Fig. 3.4). Hence, a relatively "stable" upper part of the system gives way to a relatively "unstable" lower part, towards LW. This is shown by the

[1] Note: the origin of this sub-environment is not fully understood, because: (a) it can be likened to depositional processes which relate to creek systems within the higher mudflat; and (b) it has been found to be a mud deposit present within an area of net erosion and increased tidal currents (Ke et al., 1996).

appearance and disappearance of the lower mudflat sub-environment over the various studies at Freiston Shore (Collins et al., 1981).

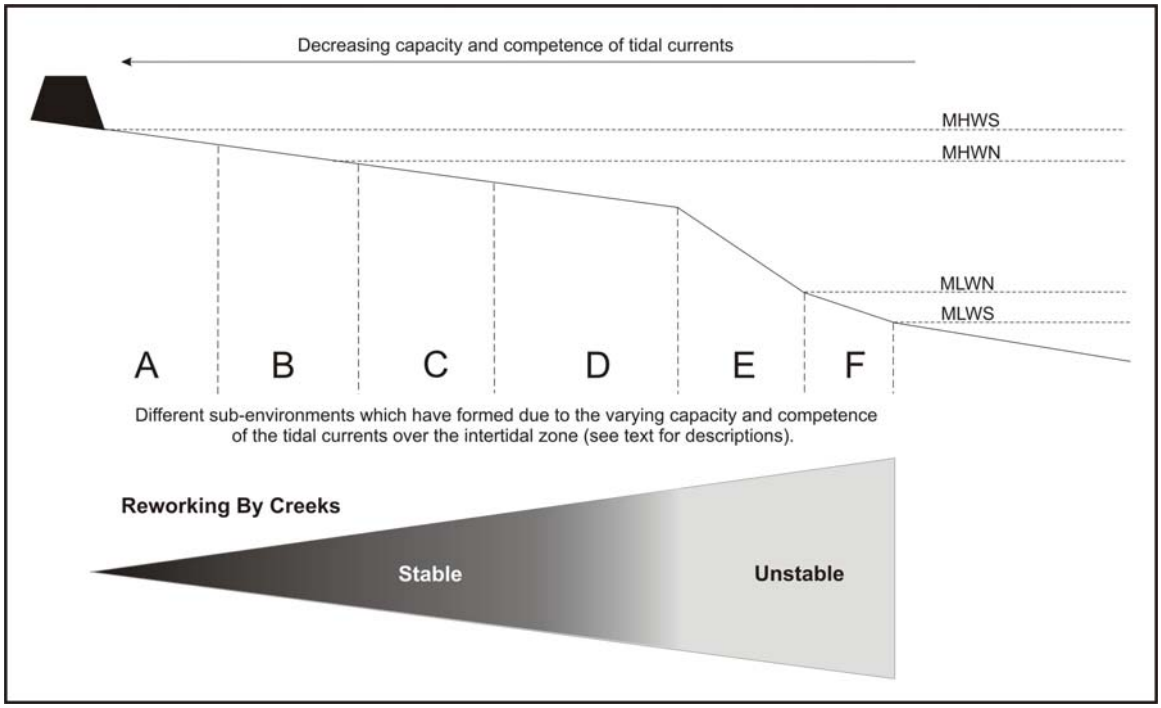

Figure 3.4: Profile of the intertidal zone of The Wash, with a schematic representation of the dynamics of sedimentation and the resulting sub-environments (from Evans, 1965).

Tides within The Wash are characterised by a standing wave; their velocity maxima occur at mid-flood and mid-ebb (Pugh, 1987). However, across the intertidal flats, the maxima occur during the first phase of the flood and the final stage of the ebb (Evans and Collins, 1975). Such a pattern influences sediment transport processes, as it means that sediment will be eroded at the start and end of the tide. This pattern means that sediment will be deposited at slack water but, after the ebb peak in flow, any sediment suspended will be removed from the intertidal flats to the deeper channels in The Wash.

Tidal current velocities over the intertidal flats of The Wash have been recorded over a range of temporal and spatial scales. Flood currents were found to be higher than those during the ebb, whilst the near-surface currents are greater than the mid-depth and near-bed flows (Ke et al., 1996). Measured tidal currents vary, in relation to their location within The Wash: (a) around 1.2 m s^{-1} in the offshore channels; (b) between 0.5 and 0.7 m s^{-1} over the exposed intertidal flats; and (c) less than 0.2 m s^{-1}, over the saltmarshes (Ke and Collins, 2000).

At the beginning of the flood phase of the tide, waters on the intertidal flat move perpendicular to the coast but, as the mid-tidal stage is reached, those over the lower intertidal

flats begin to move parallel to the coastline. On the ebb, this alongshore movement is again dominant at the mid-tide stage, over the intertidal flats; it then gradually diminishes and the dominant movement over the lower intertidal flats becomes perpendicular to the coastline (Evans, 1965). On the basis of field measurements, the alongshore component of the tidal velocity was found to be of equal magnitude to the onshore-offshore component and was relatively consistent in strength throughout the tidal cycle. Thus, the tidal waters do not simply advance and retreat over the intertidal zone, but there is a marked clockwise rotation in the waters, throughout a tidal cycle (Collins et al., 1981).

Wave heights have been found to decrease rapidly over the more sheltered parts of the intertidal flats, typically to 0.3 to 0.5 m (Amos and Collins, 1978; and Ke et al., 1996). Waves in The Wash can be classified into two types: (a) locally-generated wind waves, having their origin within the embayment (with a maximum fetch of around 30 km); and (b) swell waves originating from outside the immediate area of interest, i.e. the adjacent North Sea. The influence of these waves in The Wash is relatively limited. However, the combined influence of wave- and tidally-induced currents is the most important entrainment and transport mechanism over the intertidal flats; as only over approximately 40% of a tidal cycle, within the intertidal flats of The Wash, is the tidally-induced current sufficient to cause sediment motion, independently (Collins and Amos, 1975). Therefore, the combination of waves and tidal currents can enhance significantly, the erosion and transportation of sediments (McCave, 1971; and Ke, 1995). Wave heights of around 0.6 m have been found to occur commonly over the intertidal flats, on windy days (Ke et al., 1994). However, in areas where the SSC is high (> 100 mg l^{-1}), fine-grained sediment will be deposited irrespective of the wave activity, while under conditions of high current speeds (0.4 to 0.5 m s^{-1}) and low SSC, the deposition of fine-grained sediment may be inhibited (McCave, 1971).

Suspended sediment movement appears to be the dominant mode of transport throughout the embayment, whilst bedload transport is important in reforming the sea bed into a variety of bedforms; these are particularly well developed on the margins of channels and shoals. Approximately 6.8×10^6 tonnes yr^{-1} of suspended sediment is supplied to the embayment from offshore areas, whilst the bedload sediment supply was of lesser importance, i.e. approximately $\approx 1.4 \times 10^4$ tonnes yr^{-1} (Ke et al., 1996). Bedload transport rates are both higher and longer in duration during the flood, than during the ebb (Collins et al., 1981); this means that the bedload transport (of sediment) is onshore and alongshore. However, bedforms preserved on the intertidal flats, following high water, provide indications of water movements during the last phase of the ebbing tide (Collins et al., 1981); although the bedforms measured over a tidal cycle and at LW did not differ greatly (Ke et al., 1994).

However, bedforms can be used generally to identify the hydrodynamic conditions which prevail over the flats, as they indicate whether tidally- or wave-induced currents, or both, are responsible for their formation (Amos and Collins, 1978).

Detailed measurements have revealed that the mean content of sediment carried in suspension over the intertidal flats is usually about 200 mg l^{-1}; however, it varied from around 2 mg l^{-1} to 2,000 mg l^{-1}, with the later corresponding to storms in the adjacent North Sea (Evans and Collins, 1975). As such, sediment in suspension over the intertidal flats has been found to be controlled by stormy conditions outside The Wash, i.e. not necessarily within the embayment. Maximum silt and clay contents in the overlying tidal waters, under such conditions, have been observed to increase ten-fold (with sand being three-fold), in comparison to calm water conditions associated with a similar tidal range in the North Sea (Collins et al., 1981).

3.4 ANTHROPOGENIC IMPACTS

Land reclamation has been ongoing in The Wash over a considerable period of time, with large areas of agricultural land being reclaimed by the construction of artificial embankments, commencing with the so-called "Roman Bank", during the 13th Century (Steers, 1946; Evans, 1965; Collins et al., 1981; and Brew and Williams, 2002). The most significant changes due to land reclamation have occurred since the 17th Century, when a vast programme of reclamation and river engineering was initiated (Darby, 1940). The reclamations were achieved by a standard method, involving the construction of an embankment on the saltmarsh; this confines an area, preventing subsequent intertidal deposition (Pethick, 1996). The material used in the construction of these banks was removed from 'borrow' pits, excavated to seaward of the embankment. The high rate of siltation, often observed within these pits, depends upon the frequency the tide floods the area and the sediment supply.

Presently, much of The Wash is bounded by artificial embankments, with the most recent having been completed at Freiston Shore in 1982 (with a pilot-bank in 1980) (Fig. 3.5). Such embankments rise some 3 to 4 m above the inner parts of the intertidal zone, acting now as a front line of defence for 80,000 ha of low-lying Fenland; this includes urban areas and prime agricultural land. In total, 1,245 km^2 have been reclaimed, with this area now being used for agricultural purposes (Collins et al., 1981). The embankments initiated rapid accretion on their seaward side following their construction, with saltmarsh often developing within a few years of the embankments being built (Wheeler, 1876). Such a mechanism is considered to relate to a reduction in (tidally-induced) velocities, across the intertidal zone (Fig. 3.6). Likewise, to the seaward displacement of the location at which the low hydrodynamic conditions lead to deposition of silt and clay. Such a depositional process makes it possible to

construct new seawalls to seaward of these original constructions, after sufficient accretion has taken place for the saltmarsh to redevelop. On the basis of pre- and post-constructional (embankment) measurements, accretional/erosional characteristics of the intertidal zone can be extrapolated.

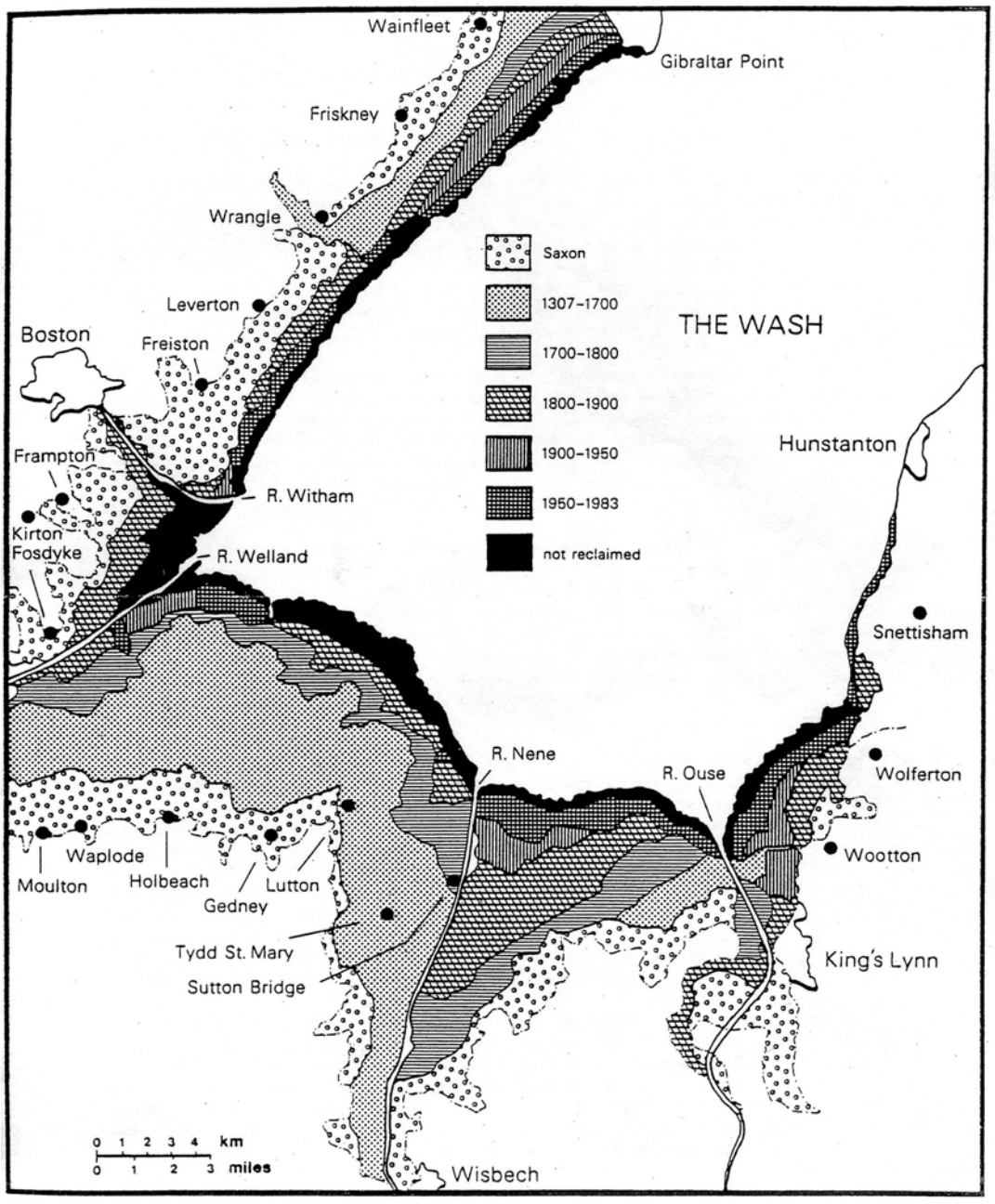

Figure 3.5: A map of The Wash showing the areas and periods when land reclamation has been undertaken (abstracted from Doody and Barnett (1987)).

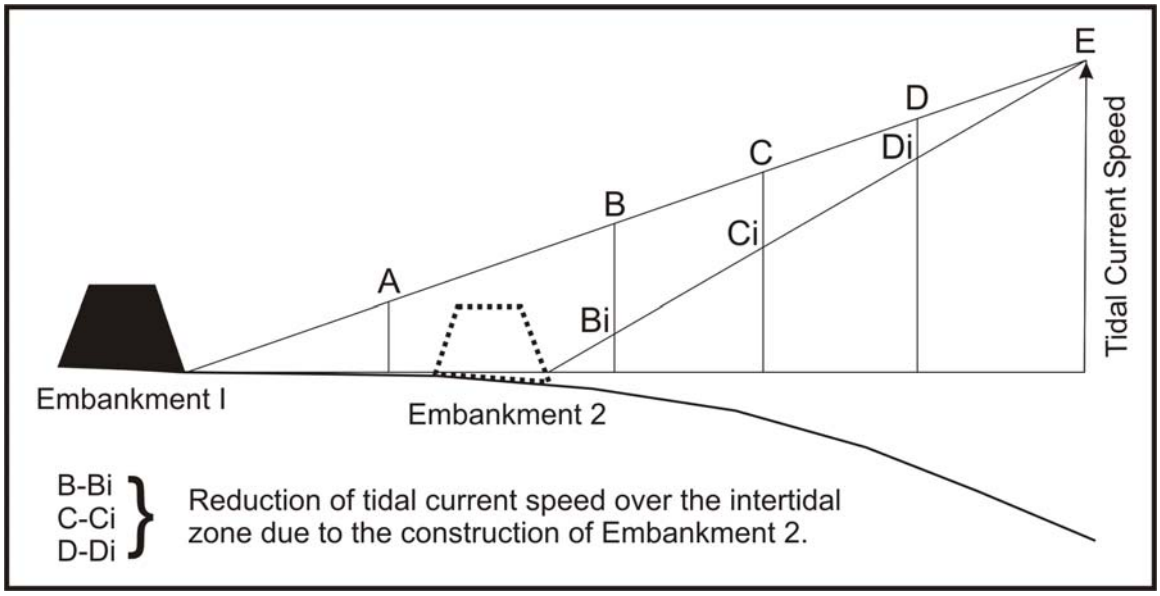

Figure 3.6: Profile of a typical intertidal zone, showing the changes in tidal current speed following land reclamation (from Evans and Collins, 1987).

3.5 FREISTON SHORE

3.5.1 *Background*

In contrast to the remainder of The Wash, the saltmarshes around Freiston Shore retreated by up to 15 m per year following the land reclamation undertaken in 1980 (Brew and Williams, 2002). This effect was attributed to an insufficient intertidal mudflat elevation, at the time the embankment was constructed, preventing vegetation from colonising (Pye, 1995). Insufficient width was left within the intertidal zone, for the saltmarsh to rejuvenate or to dissipate effectively the incoming wave energy. Erosion of the 1980 embankment was experienced during high wave energy events associated with winter storms. As a result of this erosion, the responsible body for the coastal protection, the Environment Agency (EA), carried out a cost-benefit analysis to assess the most suitable form of coastal management for the future.

3.5.2 *Past Studies*

Various process-orientated studies have been undertaken throughout The Wash in general and, specifically, Freiston Shore, by a number of investigators. The different types of data available for comparison (predominantly) over the past 50 years are listed in Table 3.1. Such intermittent data sets include sedimentological, morphological and hydrodynamical observations.

Table 3.1: Data available for comparative purposes, predominantly over the past 30 years.

Publication	**Data Available**
Inglis and Kestner (1958)	Accretion/erosion
Evans (1965)	Surveying Cores Surface samples-granulometric analyses
Amos (1974)	Tidal current velocities Wave conditions Accretion/erosion Bedforms (observed and measured) Surface samples-granulometric analyses Radiographic analysis of unconsolidated sediments Coring Creek cross-section surveying
Evans and Collins (1975)	Tidal current velocities SSCs Local hydrodynamic/meteorological conditions
Kestner (1975)	Accretion/erosion [In the Great Ouse, near King's Lynn: Tidal current velocity SSCs]
Collins, Amos and Evans (1981)	SSCs Tidal elevations Tidal current velocities Wave heights and periods Accretion/erosion Grain size distributions Surface bedform morphology
Van Smirren and Collins (1982)	Accretion/erosion Tidal current velocities
Evans and Collins (1987)	SSCs Sediment supply: river input and from offshore
Ke, Collins and Poulos (1994)	Tidal current velocities Wave heights and periods Bedform profiles
Ke, Evans and Collins (1996)	Tidal current velocities SSCs Bed samples
Ke and Collins (2000)	Tidal current velocities
Tsompanoglou (2003)	Cores
Cooper (2005)	Wave dissipation

3.5.3 *Tides and Currents*

The tidal curve at Freiston Shore is asymmetrical over the lower part of the intertidal zone; it becomes gradually more symmetrical across the intertidal flats, towards the saltmarsh (Ke and Collins, 2000). Furthermore, tidal height symmetries change in response to tidal range, seasons and local control mechanisms that require more research to be fully understood. Tidal currents over the intertidal flats are asymmetrical in character. The flood currents are dominant, in terms of both the mean and maximum velocities, being generally higher than those on the ebb (Ke and Collins, 2000). Throughout an individual tidal cycle, there is a velocity gradient across the intertidal flats (Collins et al., 1981).

Observations of tidal characteristics are available from 1972, 1980 and 1991-1993; with the latter two occasions being post-reclamation. The early observations (Evans and Collins, 1975) showed: (a) that the tidal waters did not advance and retreat over the intertidal flat, normal to the shoreline – rather, they rotated clockwise, throughout the tidal cycle; and (b) the tidal current velocities, in onshore-offshore and alongshore directions, were of equal magnitude (of up to 0.4 m s^{-1}) and were present throughout the tidal cycle.

The measurements repeated in 1980, at the stations studied earlier in 1972, revealed an increase in the tidal current speeds and an enhancement in the longshore component. For example, at a particular location and for tides of similar heights, the maximum U_{10} speed increased from 0.3 m s^{-1} to 0.5 m s^{-1}, between 1972 and 1980. Such an increase, it was suggested, could have been attributed to hydraulic readjustment to the land reclamation, involving the (preliminary) construction of the embankment in 1979-1980; this, in turn, could have explained an observed erosional phase on the lower area of the intertidal zone. A trend towards a more logarithmic velocity distribution, throughout the water column, was observed in 1982. However, current patterns measured across the intertidal flats (saltmarsh, mudflat and sandflats), in 1991-93, were similar to these documented in the 1970s; these showed, on both occasions, strong alongshore components, at ca. a 25º oblique angle to the shoreline (Ke and Collins, 2000). This study also showed that mechanisms for the deposition of sediments over the tidally-dominated intertidal (accretional) environments, of The Wash, to include: (i) flood tidal current dominance; (ii) a "step-like" shoreward hydrodynamic energy gradient; and (iii) the occurrence of strong tidal currents, especially during the first phase of the flood, and the last phase of the ebb.

There is an order of magnitude difference between suspended sediment fluxes over the intertidal flats on spring and neap tides in The Wash, as noted by a number of investigators (Evans and Collins, 1975; and Ke et al., 1996).

3.5.4 *Accretion/Erosion*

The long-term evolution of the saltmarshes and intertidal flats of The Wash is accretional; however, short-term erosion of the intertidal flats occurs. Long-term accretion/erosion has been studied on the intertidal flats using silica plugs; these have indicated a general accretional trend (Inglis and Kestner, 1958). Between September 1957 and July 1958, accretion of 1.3 cm, 1.3 cm and 1.25 cm was observed on the higher mudflats. Experiments undertaken on the *Arenicola* sandflats showed reworking of the upper 1.4 cm, but no overall accretion. Measurements on the lower mudflats showed alternating phases of accretion and erosion (Evans, 1965). Silica plugs were used also to measure the rates of accretion/erosion, over a 12 month period, between October 1972 and November 1973 (Amos, 1974). The rate of accretion of the saltmarsh was consistently low (0.2 cm yr^{-1}); it increased on the higher mudflat (1.8 cm yr^{-1}) and the cuspate deposits associated with the upper parts of the creeks (5 cm yr^{-1}). However, within the context of an overall accretional trend, short-term erosional phases in the intertidal zone were observed. The intertidal zone was separated into 6 sub-environments by Evans (1965) (Fig. 2.1); however, from field observations in 2002 it was found that there were no obvious differences between some of these, with the saltmarsh and mudflat[2] being the dominant environments. Throughout the thesis the mudflat will be described in terms of its elevation along the intertidal profile (upper, middle and lower).

In 1971, a number of bases were installed on the intertidal zone, for supporting sampling towers, for the measurement of tidal currents and suspended sediments in the water column (Evans and Collins, 1975; and Collins, 1976). Using the surface of the bases as a reference level, it was noted that erosion (approximately 25 cm) had taken place, between 1972 and 1980, on the lower intertidal zone (Van Smirren and Collins, 1982). Such erosion was attributed to possible hydraulic readjustments (Section 3.5.3) and/or storm activity. However, this period has been recorded elsewhere as being stormy and erosional, in other parts of the North Sea. Within this pattern of increasing tidal current speeds and overall erosion of the outer section of the sand flats, a lower mudflat type deposit developed towards the seaward end of the sampling line (Van Smirren and Collins, 1982). At present, some 30 years after their installation, some of the bases are still visible and indicate: (1) similar bed levels nowadays, as in 1971, over the upper part of the intertidal zone; and (2) accretion of around 40 cm on the lower exposed part of the intertidal zone. The rise in the reclaimed saltmarsh surface, to seawards, shows that accretion of the saltmarshes is keeping pace with sea-level rise (Ke and Collins, 2000).

[2] Note: large surficial sandy deposits were occasionally witnessed over the mudflats, but these were scarce and non-permanent.

3.5.5 *Managed Realignment*

The land reclamation undertaken in 1980 at Freiston Shore was found to have been located too far to seaward, not leaving sufficient width of the intertidal zone for the saltmarsh to rejuvenate and, thus, dissipate wave energy effectively. Such a limitation was considered to be the cause of erosion of the bank; this was experienced under high wave energy events, during winter storms. Such instability, combined with the possibility of sea-level rise, has meant that, in terms of coastal protection, the most viable option was to retreat the sea defences back to an old inner bank. This approach is referred to as managed realignment (MR), as it attempts to restore previously reclaimed land back to an intertidal habitat, to reduce flooding and other hazards of the coastal system (Townend and Pethick, 2002).

The MR is a 78-hectare site (Fig. 3.7), which has been modelled hydrodynamically, prior to its design (Symonds and Collins, 2005). The subsequent scheme was based upon the findings of the modelling and the guidelines highlighted by French (2001) (Section 2.10.4), with the preparation of the site involving: 1) strengthening of the old bank, some 2 years prior to the breaching; 2) the creation of an artificial creek system, which joined with already existing creeks on the saltmarsh (an attempt was made to simulate the natural creeks, in terms of their general characteristics, i.e. size, length, sinuosity); 3) breaching the embankment at 3 locations, with a width of 50 m (decided on the basis of the modelling (Halcrow, 1999)). Breaching of the embankment was undertaken towards the end of August 2002, immediately prior to the highest spring tides of the year.

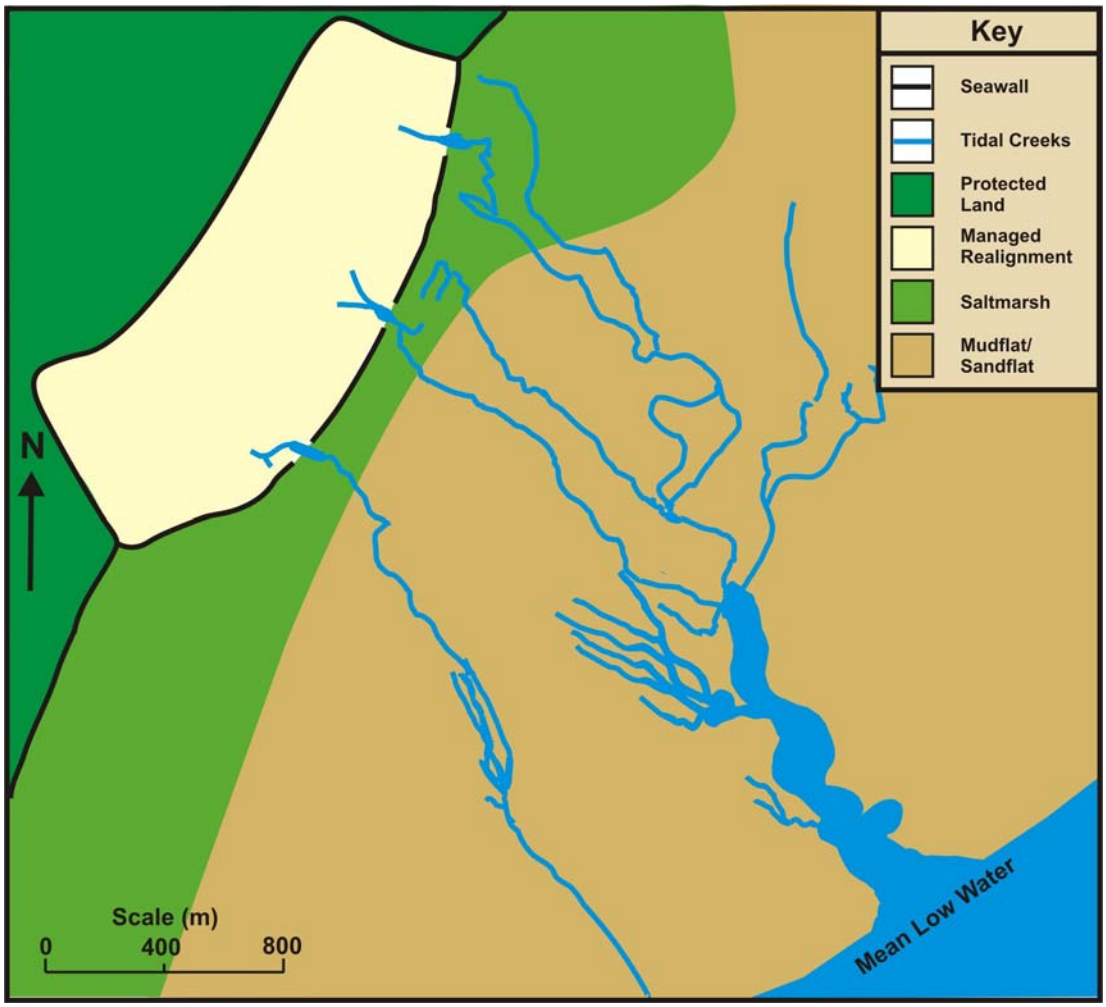

Figure 3.7: Plan view of the intertidal zone at Freiston Shore, highlighting the MR site and the local creek network, which was connected to the channels within the breaches in the embankment (28/01/2003).

CHAPTER 4: METHODS

4.1 INTRODUCTION

This Chapter provides a detailed description of the methods used in the collection of data as part of the present study. The hydrodynamic and sediment dynamic measurements were collected during 4 deployments of equipment. First the equipment is described and then the measurements made during each deployment are outlined. Other data were collected aside from the deployments; these have been separated into relevant sections and explained. Following this, details of supplementary data not collected by the author, but provided from various sources, are given.

4.2 EQUIPMENT USED

4.2.1 *Autonomous Benthic Recorders*

To obtain measurements of the hydrodynamic and sediment dynamic characteristics of the intertidal flat area, Autonomous Benthic Recorders (ABRs) were used. The instruments were manufactured by Valeport UK, and are self-logging recorders, incorporating: an electro-magnetic current meter (EMCM) (Accuracy $\pm$ 0.02 m s^{-1}), with an integrated Seapoint sensor (Model 808); a directional wave and tide recorder (Model 730D) (Accuracy: direction $\pm$ 1°; pressure $\pm$ 0.01 %); and an Optical Backscatter Sensor (OBS). The instruments can be set-up in a number of ways depending on the type of measurements required and the length of deployment; they were all set to record at 4 Hz, to enable spectral analysis of the wave climate to be undertaken.

The same method of deploying the ABRs on the intertidal zone has been used throughout this study. Scaffold poles, 2.5 m in length, were driven vertically into the sediment where the ABRs were to be deployed, leaving approx. 1 m of the scaffold pole above the surface. The ABRs were attached to a solid steel pole, which was also driven vertically into the ground (Note: if the ABR was more than 5º off vertical, the EMCM would not output accurate tidal current information); this was positioned adjacent to the scaffold pole and was driven in until the pressure sensor on the ABRs were 0.5 m above the intertidal surface. To ensure that the ABRs were retained upright and did not move throughout the deployments, the steel pole to which they were attached was fixed to the scaffold pole using metal clasps (Plate 4.1). This instrument set-up meant that the EMCM was located at 0.25 m above the sediment – water interface, whilst the pressure sensor and OBS were located at 0.5 m. It should be noted that the ABRs can only measure in water depths greater than 0.5 m, so over an intertidal environment this means that the very first phase flood and last phase ebb of the tide could not be recorded.

The rate at which the measurements were obtained varied, depending upon the length of the deployment. Throughout all the measurements, the tidal burst was fixed at 60 seconds, whilst the wave burst was 512 seconds; high frequency data were output, as well as the averaged conditions, over these periods. Due to the time taken for this process, together with instrument sorting and saving the data, the shortest period between bursts was 15 minutes. This was the burst length used during the short deployments, with a period of 40 minutes between bursts for the longer deployments. The repetition of the wave burst could be changed to be every other tidal burst, in order to save memory on the ABRs, allowing for a longer deployment.

4.2.2 *Bedload Traps*

In order to measure bedload transport over the intertidal flats, up to 8 bedload traps have been used simultaneously. The traps consist of a container for the sediment collected, with an opening (in the form of a flap, 15 cm wide and 5 cm high) on the top, through which only sediment travelling towards it will be trapped (Plate 4.2). The traps were positioned such that their tops were level with the sediment surface. The opening protruded above the surface and, as such, collected any sediment transported within 5 cm of the bed (i.e. bedload). This approach helped to minimise flow disturbance, optimising the efficiency of the samplers. Elsewhere, such samplers have been found to record, at best, 70 % of the actual bedload transport (Novak, 1959; and Graf, 1971). When deployed, 4 bedload traps were positioned at right angles, to measure the alongshore and cross-shore transport.

4.2.3 *Suspended Sediment Samplers*

In addition to the turbidity measurements collected by the ABRs, suspended sediments were collected from waters over the intertidal zone. The samplers consisted of cylindrical bottles, with a diameter of 75 mm and a volume capacity of 700 ml. These were attached to vertical scaffold poles, at varying depths (Plate 4.3); their orientation was such that, if sediment settled out of suspension at slack water, the higher samplers would not interfere with those lower in the water column. The samplers were designed to obtain samples of sediment in suspension and to provide comparison, throughout the water column, of settling during periods of slack water.

4.3 DEPLOYMENTS

A maximum of 3 ABRs were installed, in varying configurations, at 4 sites over the intertidal zone and two sites inside the MR. Throughout all deployments, an ABR was installed at site

3, on the lower intertidal zone near a station used in previous studies known as Base 4 (Amos, 1974; Evans and Collins, 1975; Collins et al., 1981; and Van Smirren and Collins, 1982) (Fig. 4.1(a)); this was to provide continuity throughout the measurements. In *Deployments 1, 2* and *4*, an ABR was installed at site 1, on the upper intertidal zone adjacent to another old station used in the same previous studies, called Base 3. These sites were chosen as the past measurements provide background information and they represent two environments of the intertidal flat (higher/upper mudflats and lower mudflats) and are located on a seaward transect from Breach 1[1]. During *Deployment 1*, an ABR was positioned in the channel within Breach 1, to investigate the fluxes of water and sediment entering and leaving the MR site. Breach 1 was chosen, as it was the most easily accessible of the 3 breaches, and was thought to be representative of the other 2. Following *Deployment 1*, the channel in Breach 1 had eroded significantly, preventing any further ABR deployments in this channel. Instead, during *Deployment 4*, an ABR was installed 100 m inside the MR site adjacent to Breach 1, so the wave and tidal conditions inside the site could be monitored.

4.3.1 *Deployment 1*

Three ABRs were deployed between 04/09/2002 and 11/09/2002, over the intertidal zone: in the channel within Breach 1; at site 1, on the upper intertidal zone, adjacent to Base 3; and at site 3, on the lower intertidal zone, near Base 5 (Fig. 4.1(a)). The instruments were set to record tidal and wave conditions every 40 minutes, allowing them to be deployed over a 7 day period. This deployment was undertaken during spring tides, with the peak tidal height on 09/09/2002 (am) (with a HW of 4.6 m Ordnance Datum (OD)); this permitted the affects of the highest tides, on the channel within Breach 1 and the intertidal flats, to be investigated.

Unfortunately, due to higher current speeds than predicted (from the numerical model output (Section 3.6.2)), rapid erosion was experienced in the channel; this resulted in the ABR being displaced due to scour (on 07/09/2002). When originally deployed, the instrument was attached to a steel scaffold pole, which was driven into the channel bed to a depth of 1.5 m. As such, the bed must have been eroded by at least 0.5 to 1 m, over a 3 day period; this would have caused the scaffold pole to be removed. Unfortunately, this has meant that the peak spring tides were not recorded; the highest complete tidal cycle recorded was 1 m lower than the peak. Owing to the flow strength and the associated rapid erosion rates, it was deemed unsafe to deploy any further instruments at this particular location, in the absence of a larger-scale operation.

[1] Note: if the MR impacts the intertidal flats, it is thought that the area in front of a breach, where the 'natural' conditions have been previously recorded, would be the best place to identify them.

4.3.2 *Deployment 2*

Two ABRs were deployed, between 16/05/2003 and 19/05/2003, at site 1, on the upper intertidal zone; and at site 3, on the lower intertidal zone (Fig. 4.1(a)). The instruments were set to record tidal and wave conditions every 15 and 30 minutes, respectively. This deployment coincided with a period of spring tides, where the peak spring tide was on 17/05/2003 (pm) and was 4.3 m OD.

4.3.3 *Deployment 3*

The 3 ABRs were deployed at site 3, on the lower intertidal zone: at the same location as the ABR deployed on the lower intertidal zone, during *Deployments 1* & *2*; in the thalweg of the adjacent creek; and on the opposite bank of the creek (Fig. 4.1(b)). The configuration of the ABRs allowed the interaction between the creek and the lower intertidal flats to be studied. The instruments were deployed between 23/11/2003 and 26/11/2003, during spring tides, with a peak tidal height of 4.4 m OD on 25/11/2003 (am). The ABRs were set to record tidal and wave conditions, every 15 minutes.

In addition to the ABRs, 4 bedload traps were installed on each bank, approximately 10 m to landward of the ABRs on the creek banks (Fig. 4.1(b)). These were set up to measure bedload transport in both longshore and cross-shore directions (Plate 4.2).

4.3.4 *Deployment 4*

Between 31/08/2004 - 03/09/2004, 3 ABRs were deployed on the intertidal zone: inside the MR site, opposite Breach 1, on the newly created intertidal surface; at site 1, on the upper intertidal zone; and at site 3, on the lower intertidal zone (Fig. 4.1(a)). The ABRs were set to record tidal and wave conditions every 15 and 30 minutes, respectively.

The bedload traps were deployed, with 4 located at site 1 and site 3. As no bedload transport was recorded over the first 2 days, and the wave height was predicted to drop, the bedload samplers were moved (on 02/09/2004). Consequently, 4 were positioned, in the same longshore and cross-shore arrangement as before, on the saltmarsh, midway between site 1 and the embankment; 2 were moved to face the flow coming into and going out of the MR (located on the bank of the channel within Breach 1); and 2 were moved to a few metres north of the ABR in the MR, with one facing to seaward and one to landward.

Suspended sediment was collected from the waters over the intertidal zone, using the samplers described previously; these were set up at depths of 0.25, 0.5, 0.75, 1 and 1.25 m above the bed at site 3, and at 0.25, 0.5 and 0.75 m at site 1. The sediment samplers were

emptied after they had been inundated by 2 tides; the LW time prevented them from being emptied every tide. Suspended sediment samples were collected at midday on 01/09/04, 02/09/04 and 03/09/04.

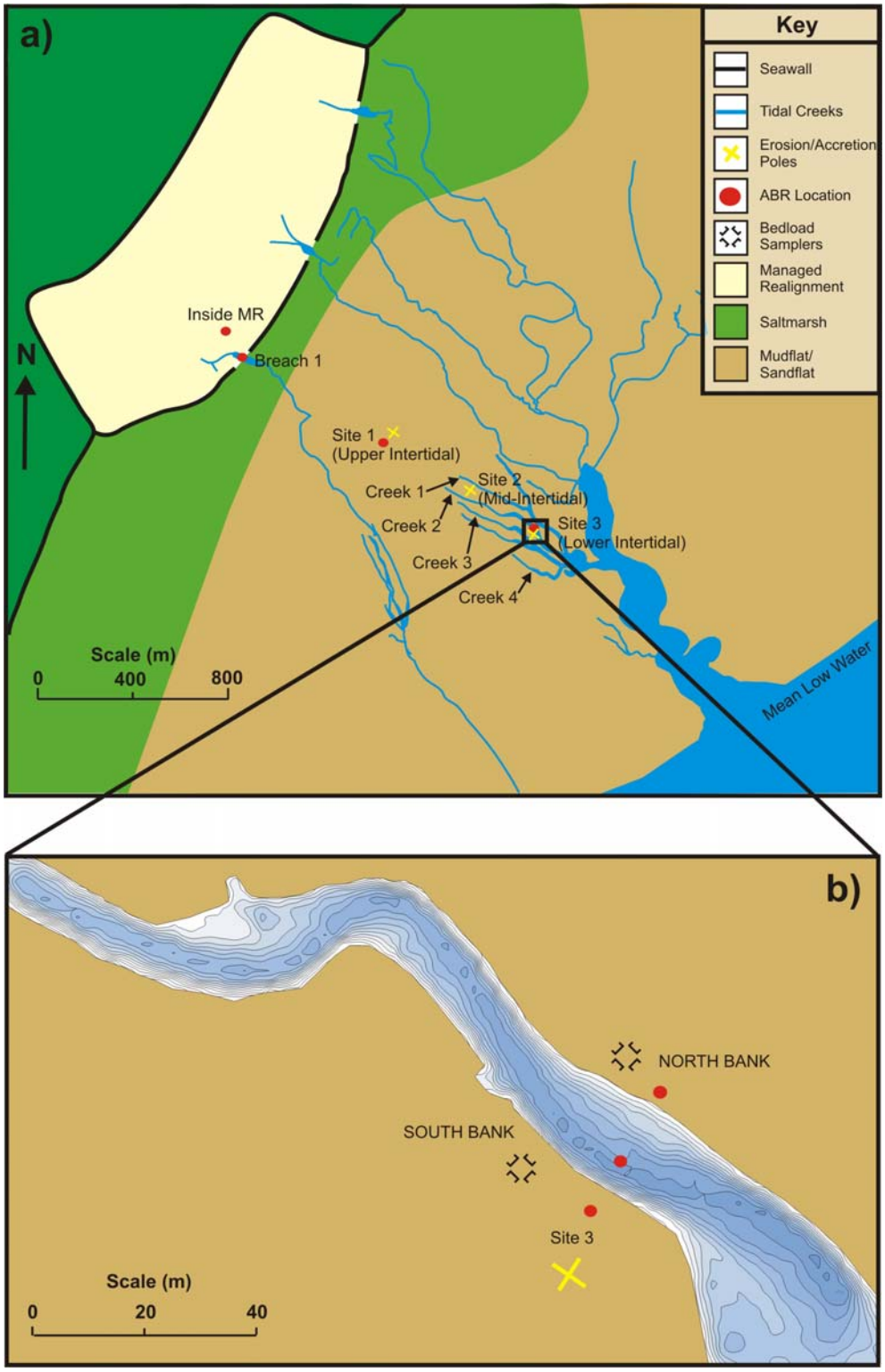

Figure 4.1: a) the intertidal zone at Freiston Shore, showing the locations of the ABR deployment sites and the erosion/accretion poles; and b) a detailed view of site 3, during *Deployment 3*, with the creek bathymetry surveyed using RTK-GPS on 09/06/2003 (Section 4.5).

4.4 MONTHLY SAMPLING

Measurements of bed level change were obtained using erosion/accretion poles at 3 locations over the intertidal flats, every month, over an 18-month period. These have been shown to provide accurate long-term measurements of intertidal flat erosion/accretion rates (Kirby et al., 1993; Boorman et al., 1998; Brown, 1998; Cahoon et al., 2000; de Brouwer et al., 2000; and O'Brien et al., 2000). The sites were positioned away from tidal creeks, as previous studies have shown that these influence conditions over the adjacent intertidal zone (Evans, 1965; Collins et al., 1981; and Ke and Collins, 2000). The erosion/accretion stations were located near sites 1 and 3[2], where the ABRs were deployed, with one station midway between them, site 2 (Fig. 4.1(a)). The stations were set up in an identical manner, with each station consisting of 13 steel poles, 1 m long and 12 mm diameter, arranged in a cross (Plate 4.4). The poles were positioned 1 m apart, with one side of the cross lying parallel to the shoreline and the other perpendicular. As such, erosion/accretion measurements were obtained in a cross-shore and long shore direction at each site.

The poles were installed on 14/04/2003; this involved the poles being driven into the sediment, leaving some 0.2 m exposed. Their surfaces were then levelled, so that all of the poles were at the same elevation. Erosion/accretion measurements were obtained on a monthly basis, between 28/04/2003 and 12/10/2004. To measure the erosion/accretion rates, an aluminium bar was positioned between 2 adjacent poles. Subsequently, the distance between the bar and the sediment surface was measured, using a calliper, through holes in the bar; these were positioned every 10 cm, along the bar (Plate 4.5). These measurements were obtained between each pair of adjacent bars, to provide high-resolution and easily repeatable surveys. Through repeating a survey, the relative accuracy of the method was found to be ± 3 mm. A surficial (to a depth of 1 cm) sediment sample was collected at each site, for each set of erosion/accretion measurements.

Unfortunately, on 28/07/2003, the erosion/accretion poles at site 3 were destroyed by a cockle dredger (Note: the site is not used normally for cockle dredging but, due to pollution elsewhere, it was opened up during the summer of 2003). Consequently, a number of months of data were lost. The poles over the intertidal zone were re-installed on 24/11/2003, when the cockle dredging had finished.

[2] Due to rapid erosion of the creek system over the lower intertidal zone, this site became located near to 2 developing creeks.

4.5 SURVEYING

A Real Time Kinematic Global Positioning System (RTK-GPS) package was used to collect accurate positional data; ± 10 mm in the horizontal (Easting and Northing) and ± 20 mm in the vertical (Elevation) (Dail et al., 2000; and Haxel and Holman, 2004). The package included: a backpack positioning and logging device (Plate 4.6) and a base station, which was installed over a point of known location (a reference point surveyed for the Environment Agency). This method was used to collect a range of data sets; the location of creeks over the intertidal flats; profiles across the intertidal zone; and the bank edge of the channel within Breach 1. Due to the overall complex nature of the creek system, combined with limitations to the method (the length of time the creeks were exposed around LW), only the main creeks were measured. Creeks 1 to 4 (Fig. 4.1(a)) were measured on 6 occasions, over a 3 year period (15/11/2002, 29/01/2003, 09/06/2003, 17/10/2003, 27/04/2004 and 05/09/2005). During the surveys, the location of the "nickpoints" and thalweg, for each of the creeks, were surveyed. Creek size was established by surveying a transect across the creeks (parallel with the shoreline), during each of the surveys. A detailed bathymetry of Creek 2 (studied in detail during *Deployment 3*) was made over a 150 m length (Fig. 4.1(b)) by the RTK-GPS, on 09/06/2003.

The channel profile in Breach 1 was surveyed using a number of methods. Initially (05/09/2002), when the channel was small (only a few metres deep and wide) the profile of the channel was established every 0.1 m, by measuring the distance down from a tight metal wire (fixed at the top of each channel bank), to the channel bed. When the channel became wider, this method became impractical. Instead an approximate profile was obtained (on 15/10/2002), using a fishing line to measure the depth at set distances from the channel bank. An echosounder was used on 14/04/2003; this was floated from one bank to the other, whilst a number of transects across the channel were surveyed. Owing to the time consuming nature of this method and the difficultly in undertaking the measurements they were not repeated.

4.6 FIELD VISITS

In addition to the quantitative data collected, as outlined above, during each site visit numerous observations were made and photographs taken. These help to build up a picture of the changes that have occurred around the MR site and the intertidal zone, and will be used to help interpret the results and visualise changes.

4.7 LABORATORY WORK

All the sediment samples collected were analysed in the laboratory to obtain the grain size distributions, similarly the sediment collected in the suspended sediment samplers and

bedload traps were analysed in the same way. Initially, wet sieving, using a 63 μm sieve, was used to separate the sand from the silt and clay, in accordance with Buller and McManus (1979). As such, the proportion of fine-grained sediment (< 63 μm) to sand-sized sediment (> 63 μm) was calculated, on the basis of the dry weight. The sand-sized sediment was dried and weighed; the dry weight of fine-grained sediment was calculated using the pipette method. The concentration of fine-grained sediment within a 1000 ml measuring cylinder was obtained by collecting a 20 ml sample, from a depth of 20 cm, 20 s after vigorous stirring of the sample and the solution was ceased; this ensured that the 20 ml sample reflected the entire grain population before effective settling (Folk, 1974). The sample was then dried and weighed, allowing the total dry weight of fine-grained sediment to be calculated (Galehouse, 1971; and Poppe et al., 2000).

The grain size distribution of the fine-grained sediment was established using the Coulter Laser Analyser, LS130. The LS130 utilises a laser light source, directed through the sample; this diffracts the light to two Fourier lenses and to three sets of photodiode detectors. This arrangement permits the device to measure the relative number, surface area or volume of particles, between 0.4 – 900 μm. The LS130 incorporates also a Polarization Intensity Differential Scattering; using polarised light and an additional six photodiode detectors, this permits the measurement of grains within the 0.1 to 0.4 μm range. A limitation with this method is that it utilises only a small amount of the sample (~ 0.5 g dry weight); this, in turn, may cause the determination of the grain size to be unrepresentative (Fig. 4.2). Although, the variability between the samples was found to be < 5 %, causing a possible difference between sub-samples of ± 5 μm. This error was minimised by measuring 3 sub samples for each sediment sample and averaging the results.

Following the wet sieving, only a small amount of sand-sized sediment remained, i.e. insufficient for dry sieving (100 g is necessary); consequently a settling tower technique was used to establish the grain size distribution. The settling tower was 2 m high, with an internal diameter of 0.2 m; it was maintained under a controlled laboratory temperature, of 20 °C (± 1 °C). The density of the sand-sized samples was taken to be 2.65 g cm^{-3} (Paphitis and Collins, 2005). For a more detailed description of the settling tower method, refer to Rigler et al. (1981).

The turbidity measured by the ABRs was calibrated, to provide a suspended sediment concentration in mg l^{-1} (Fig. 4.3), as these units are used in most studies. An OBS from an ABR was submerged in distilled water and set to record, whilst varying suspended sediment concentrations were added (the sediment used was a surface sample, from the mid-intertidal

zone at Freiston Shore). Using a syringe, 50 ml samples of the water, containing the suspended sediment, were taken at each concentration level; these were dried and weighed. Suspended sediment concentrations were calibrated then with the turbidity values, obtained from the OBS. The ABRs were equipped with identical OBSs and they were all set-up with the same gain, so it was only necessary to carry out one calibration for each gain setting used (2 gain settings, so 2 calibrations were carried out). This method provides an approximate conversion of the turbidity (volts) to SSC (mg l^{-1}) ($F_{1,12} = 61.3$, $P < 0.001$), allowing the suspended sediment measurements from this study to be related to other studies. A possible error was present in this method; the stirring device used to keep the sediment in suspension may have affected the OBS during the turbidity recording. This has caused a degree of scatter on the calibration, but the measurements only need to provide an approximate SSC for comparison with previous work and so this level of accuracy is sufficient.

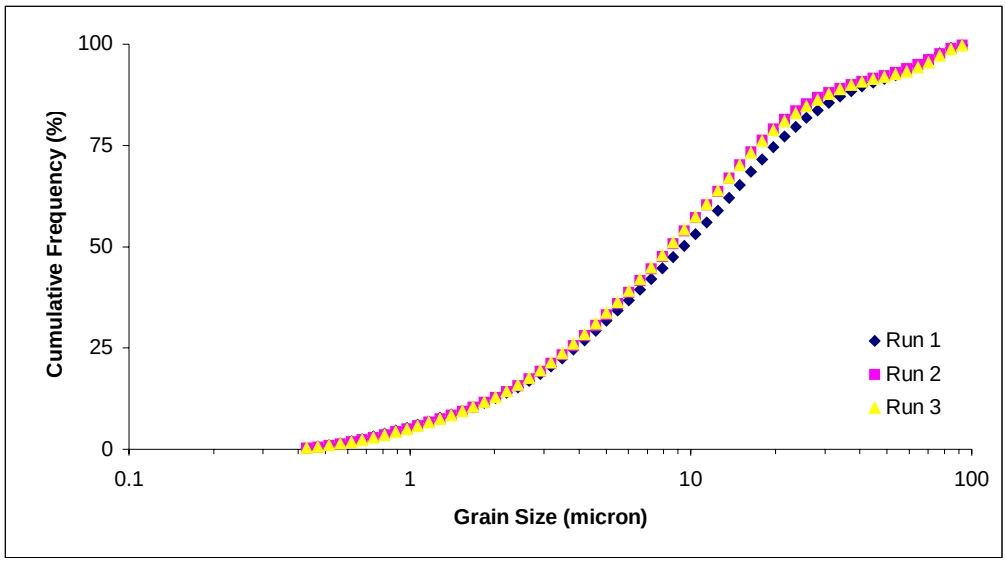

Figure 4.2: A representative cumulative grain size distribution of the fine-grained sediment from a bedload sample (Section 8.3.3). The results of 3 separate runs are shown, using different 0.5 g sub-samples from the original sediment sample, on the Coulter LS130.

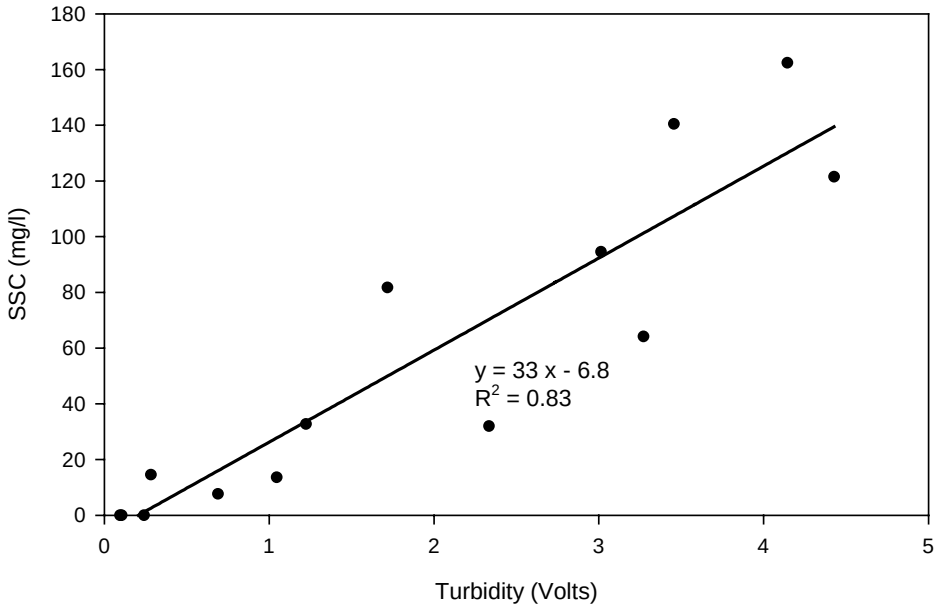

Figure 4.3: Calibration for the OBS on the ABRs, from turbidity (volts) to suspended sediment concentration (mg l^{-1}).

4.8 SUPPLEMENTARY DATA

In order to complement the data described above, supplementary data (obtained from various sources) have been made available to the study. These data were collected as part of the Environment Agency's (EA) investigation into the development of the MR and the general shoreline management of the whole of The Wash (Halcrow, 2001).

4.8.1 *Aerial Photography*

Aerial photography of the intertidal zone has been collected, by the EA, every 6 months since 1991; these were at a scale of 1:5000, covering the whole of the intertidal zone. The photographs were taken at low tide, during spring tides; so much of the intertidal zone was visible. Such aerial photography represents only a "snapshot" of the system, not how the system may have changed. Hence, care must be taken in inferring the changes, between dates, and in generalising the rates of change (Hooke, 1997).

Oblique aerial photographs over the intertidal zone and the MR site have been taken twice since the initiation of the MR scheme. These provide a permanent record of the landscape and its temporal state and provide a reference for monitoring changes.

4.8.2 *GPS Profiles*

At set positions across the intertidal zone, RTK-GPS transects have been surveyed (on behalf of the EA) every 6 months since 1993. These profiles were collected over the entire intertidal

zone of The Wash, with a spacing between the transect lines of 500 m. Since 2001, transect lines 100 m apart have been surveyed along the MR site and adjacent intertidal zone every, 6 months (Fig. 4.4).

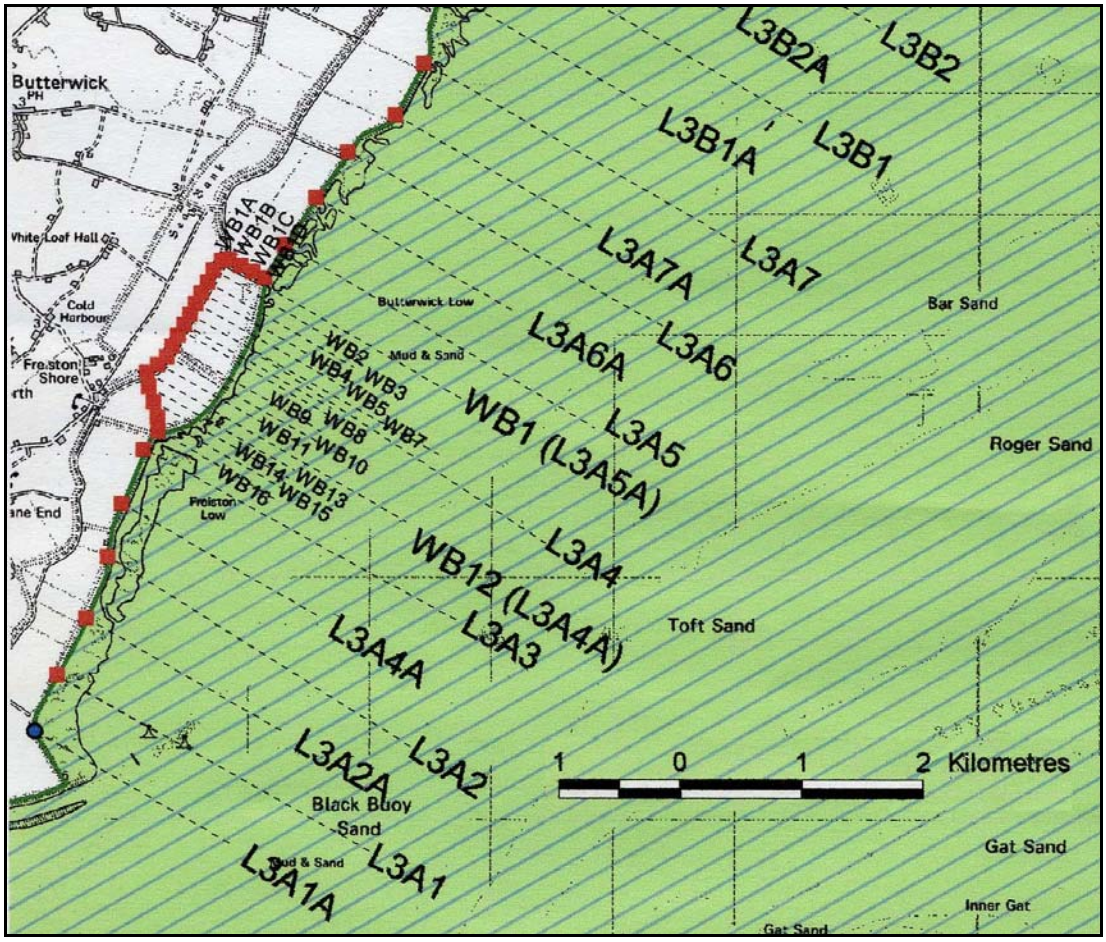

Figure 4.4: Location of the EA intertidal flat profiles across a section of The Wash (labelled L3A…) and, specifically, the Freiston Shore MR site (labelled WB…). (from Environment Agency, 2000)

4.8.3 *Erosion/Accretion*

Measurements of erosion/accretion and the surface elevation have been collected by the Centre for Ecology and Hydrology (CEH) and the Cambridge Coastal Research Unit (CCRU), at locations over the saltmarsh and inside the MR, every 6 months since the initiation of the scheme; these are set to continue over a 5 year monitoring period. The measurements on the saltmarsh were obtained along a transect to the south of the MR site, perpendicular to the embankment (Fig. 4.5). Two methods of measurement were applied along the transect: using buried expanded metal plates; and using canes (Brown, 1998). Each of the sites had 5 replicate metal plates, buried to a depth of 6 to 10 cm; 5 measurements were taken at each plate (relative error to ± 1 mm). At the seaward end of the saltmarsh, where ridges and runnels were present, the topography was not suitable for the use of the plates. Instead, 5 pairs of 1.3 to 1.5 m canes were pushed into the substrate 1.15 m apart, to a depth

of 1 to 1.2 m. Measurements of erosion/accretion were obtained by placing a level on the canes, then measuring down to the sediment surface at 5 locations, with a ruler (relative error to ± 3 mm).

Sedimentation Erosion Tables (SETs) were used to measure changes in the surface elevation; 6 were positioned outside the MR (in October 2001), and 5 inside the MR site (in November/December 2002) (Fig. 4.5). The SETs are non-intrusive, portable and mechanical levelling devices, which provide a horizontal reference level; from this, a distance to the sediment surface is measured, by a grid of 9 pins (Plate 4.7). This approach provides a valuable addition to the erosion/accretion measurements, as the SET measures the surface elevation change. The SET provides a non-destructive method for making highly accurate (± 1.9 mm) measurements of sediment elevation of intertidal and subtidal wetlands over long periods of time relative to a fixed subsurface datum. These measurements take into account the fact that subsurface processes can influence the sediment elevation in intertidal systems (Cahoon et al., 2000).

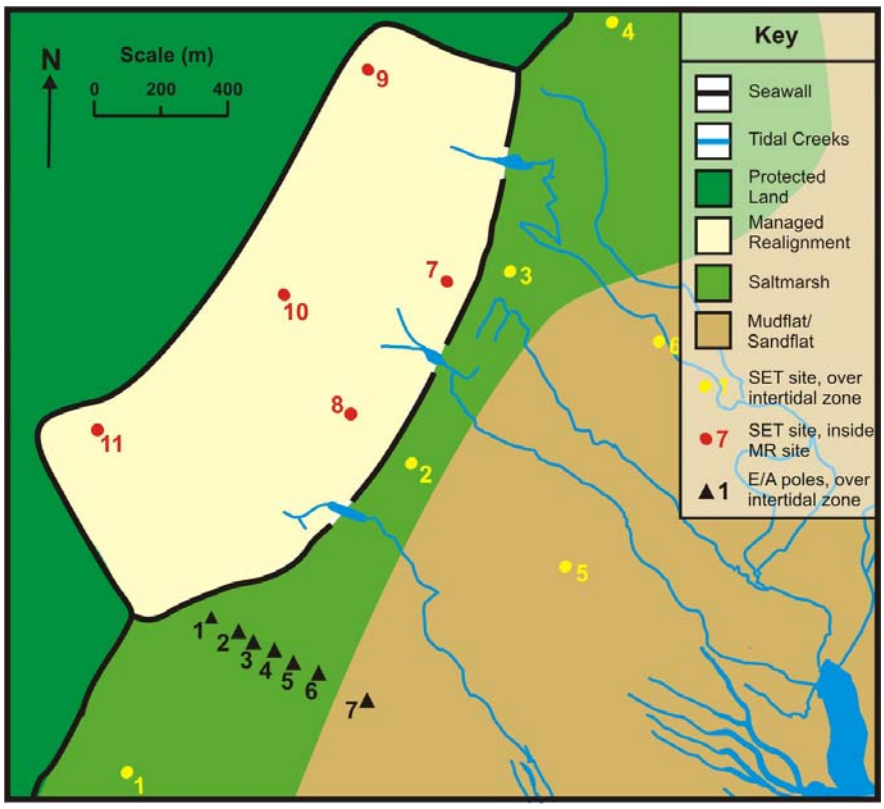

Figure 4.5: The EA erosion/accretion measurement sites, inside and outside the MR.

4.8.4 *Ecological Monitoring*

Ecological monitoring was undertaken by CEH and CCRU, along the same transect lines as the erosion/accretion measurements (see above). The vegetation type and density was

measured, as well as obtaining a sample of the invertebrates. These measurements were carried out annually; once again they are due to continue for a 5 year period.

4.8.5 *Wave and Tide Data*

A directional waverider buoy was deployed at the entrance to The Wash, in a water depth of 24 m, from June 1999 until May 2000 (by Gardline Surveys, UK, on behalf of the EA). The instrument was set to record at 1 Hz for 20 minute bursts every 3 hours. However, due to technical problems, it was unable to record a continuous data set. Nevertheless, the available data have been used to show the monthly averaged wave conditions over a year.

Measurements were taken at 3 locations over the intertidal zone at Butterwick Low (adjacent to Freiston Shore, 1 km north of the MR site), over the same period as the waverider measurements. Directional wave/tide recorders (Valeport 730D) were used at the mid- and lower intertidal sites, and a non-directional wave/tide recorder (WS Ocean Systems WTS-1) was deployed at the upper intertidal site (Fig. 4.6). The directional recorders measured at 1 Hz for 17 minute sample bursts every 30 minutes, and the non-directional recorder measured at 1 Hz for 15 minute bursts every 30 minutes.

Two wave and tide recorders were deployed outside the MR site, by Gardline Surveys (UK), on 15/10/2001, for 12 months before the MR was initiated; following the MR (25/08/2002), one of these was moved to inside the MR site (Fig. 4.7). Data were provided from these instruments until the end of 2004. WTS-1 non-directional wave/tide recorders with precision pressure sensors were used (manufactured by WS Ocean Systems, now WS Envirotech). The instrument pressure sensors were established level with the surrounding terrain. They were set to record tidal conditions every 10 minutes; each tidal record was based upon 1 Hz samples, collected over 1 minute, to eliminate any variation in pressure at (surface) wave frequencies. The wave part of the measuring device was set to record for a 20 minute period, every 30 minutes; as such, every third tidal record was missed, as the instrument was already occupied recording the waves.

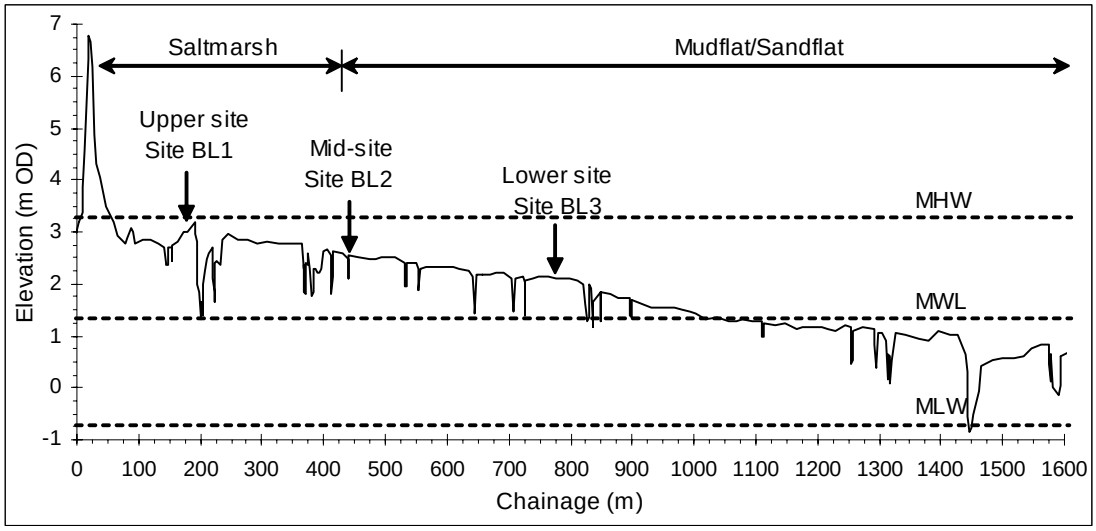

Figure 4.6: The location of the wave/tide recorders, at Butterwick Low, along a profile of the intertidal zone.

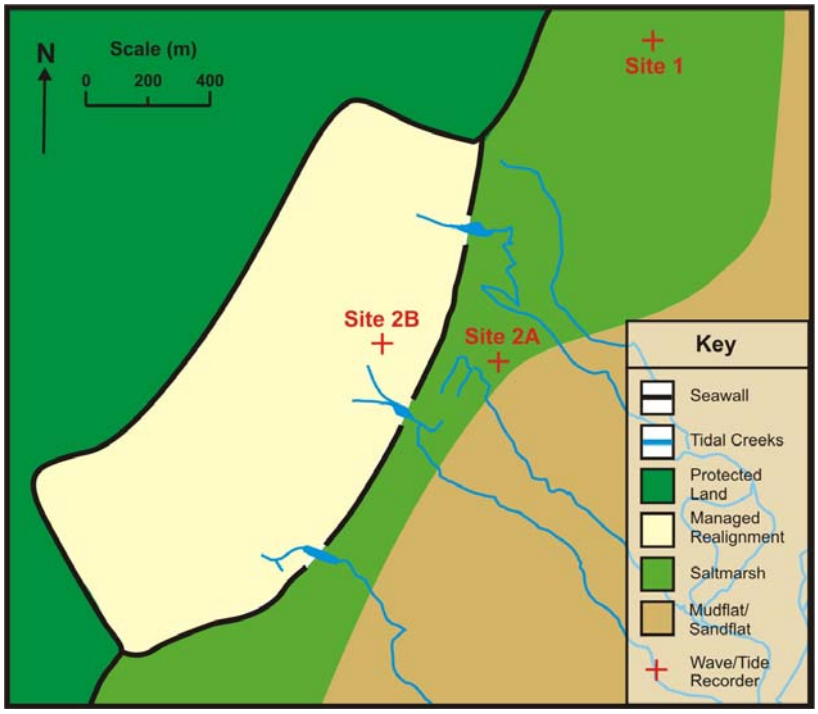

Figure 4.7: Locations of the wave and tide recorders deployed by Gardline Surveys before (Site 1 & Site 2A) and after (Site 1 & Site 2B) the MR was initiated (Gardline Surveys, 2003).

4.8.6 *Bathymetric Surveys*

The Boston Harbour authorities have undertaken bathymetric surveys of the Lower Road Channel, to seaward of Freiston Shore (Fig 3.1). It is an important navigation channel, connecting up with the Rivers Welland and Witham. Six of these surveys have been made available to the present study; these were collected in June 2000, May 2002, April 2003, September 2003, May 2004 and June 2005. Survey lines 25 m apart were used to obtain detailed bathymetry of the area, from the end of the river channel to the Boston Deeps Channel.

4.9 PLATES

Plate 4.1: The ABR deployed in the channel within Breach 1 (05/09/2002).

Plate 4.2: A set of 4 bedload traps during *Deployment* 3, to collect bedload transport from all directions (Note: the entrance to the trap is 15 cm wide and 5 cm high).

Plate 4.3: A series of (5) suspended sediment samplers attached to a scaffold pole at site 3 during *Deployment 4*, at various depths above the bed.

Plate 4.4: The erosion/accretion poles arranged in their 'cross formation' at site 2. The bar used for measuring the levels is in measurement position (Note: the bar is 1 m long).

Plate 4.5: The bar used to measure the erosion/accretion rates, positioned between 2 of the poles. Holes in the bar are visible, for the calliper measurements to the bed.

Plate 4.6: The backpack positioning and logging device of the RTK-GPS, recording the location of Base 3, adjacent to the upper intertidal site, site 1 (05/09/2005).

Plate 4.7: Surface elevation measurements of an intertidal mudflat, taken using an SET (from http://www.pwrc.usgs.gov/set/).

CHAPTER 5: SPATIAL AND TEMPORAL CHANGES WITHIN A BREACHED RECLAMATION

5.1 INTRODUCTION

The MR site has been studied intensively, since the embankment was breached on the 24th of August 2002. Data have been collected to monitor the impact of an anthropogenically-induced marine transgression, on the MR site. The aim of this Chapter is to study how the MR site has developed following its breaching in August 2002; to see if it is fulfilling the initial aims of the MR, these were:

(i) to create a sustainable flood defence scheme through the establishment of saltmarsh; and
(ii) to avoid adverse impacts to existing habitat and the adjacent saltmarsh/mudflat.

In order to create a sustainable defence scheme, the MR site needs to be a suitable area for sediment accretion and vegetation colonisation; this requires low wave energy and low tidal current speeds, i.e. for it to behave as a 'natural' saltmarsh. The flooding and draining of the MR site are important in its development, as halophytic vegetation must remain submerged for a certain length of time to survive; if the site does not flood frequently enough, or remains submerged for too long, vegetation will not colonise. The development of the MR was studied by measuring: the flows into and out of the site; the prevailing wave conditions; erosion/accretion rates; and the colonisation of vegetation.

5.2 BACKGROUND

On the basis of numerous site visits, incorporating various measurements, a major impact of the MR was identified. During HW spring tides, water flowed at high current speeds into the MR site; this was created by the tidal waters discharging into the channels within the breaches of the seaward embankment (Fig. 4.1(a)). Such flows were in response to the high water level, combined with a gravity flow; this, in turn, was related to the difference in height between the outer and inner parts of the system. This difference was of the order of 0.5 to 1 m, with the outer saltmarsh being higher than the MR site, just inside the embankment (Fig. 5.1). Such a difference is partially related to compaction and dewatering of the reclaimed land, following the initial reclamation and drainage for agricultural use (in 1980) (Collins et al., 1981; and Crooks and Pye, 2000) but, in this case, predominantly owing to accretion on the seaward side of the embankment raising the elevation of the adjacent saltmarsh surface. Following HW on spring tides, the MR site became fully submerged; throughout the ensuing LW, the waters overlying the site drained through 3 channels within the breaches.

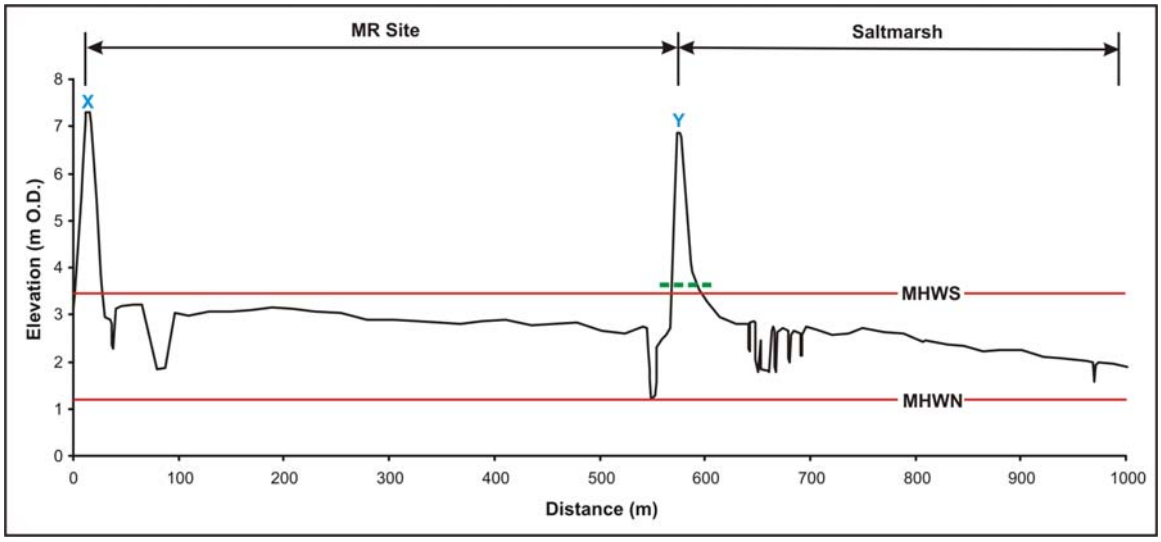

Figure 5.1: A profile (WB12 (L3A4A) on Figure 4.4) across the MR site, Breach 1 and the saltmarsh, obtained by RTK-GPS. The newly strengthened landward embankment (X) is at the start of the profile. The breached embankment (Y) is 600 m along the profile, with the saltmarsh beyond. The dashed green line represents the elevation at which the embankment was breached.

5.3 METHODS

The hydrodynamic data used were from the ABR located inside the MR site, during *Deployment 4* (Fig. 4.1(a)). In addition, a range of supplementary data have been utilised: (a) wave and tide measurements, from inside the MR site and on the adjacent saltmarsh (Sites 1 & 2B, Figure 4.7); (b) erosion/accretion measurements inside the MR site (Fig. 4.5); and (c) ecological monitoring of the vegetation type and cover (Section 4.8.4).

5.4 RESULTS

5.4.1 *Hydrodynamics*

During the initial set of spring tides to flood the MR site, Site 2B failed to drain completely during the ebb tide period, before being flooded again (Fig. 5.2). During these spring tides, Site 2B took longer and longer to drain as the height of the spring tides flooding the MR site increased. Water was still draining from the MR site as the tide started to re-flood it; as such, Site 2B remained submerged for over 12 hours after each HW. The maximum water depth inside the MR site at Site 2B occurred after the maximum water depth over the saltmarsh. It took 1 hour 40 minutes to flood this part of the MR site, from when the first flows entered the site. However, following the flooding of these first spring tides (07/09/2002 – 13/09/2002) the drainage of the site changed dramatically, with the MR site draining more rapidly (Figs. 5.2 & 5.3). Over the subsequent high spring tides, the maximum water depth at Site 2B within the MR, coincided with that at Site 1 on the saltmarsh. During the following spring tidal cycles, it consistently took only 1 hour 10 minutes for the MR site to flood. Towards the end of 2003 and the beginning of 2004, the drainage of the site became more rapid; the tidal curve in the MR site was similar to that over the saltmarsh, with only small

variations during the ebb. The major change in the drainage of the MR site occurred during the first cycle of high spring tides (peak height > 4.0 m OD), as the period the site remained submerged dropped from 12 hours during these tides to 6 hours in the following spring tidal cycle (Fig. 5.4). After 8 months of flooding, the drainage of the MR site appeared to reach a stable rate, with the drainage lasting for 3.5 to 4 hours, while the predicted tidal curve took 3 hours.

Some 2 years following the initiation of the MR, drainage of the site was considered to have stabilised; as such, tidal conditions inside a more 'stable' MR site were studied. On the basis of the results relating to a tidal height of 4.3 m OD, it can be observed that flow into and out of the MR site was asymmetrical; the ebb drainage (measured up to 0.5 m depth) lasted for 2 hours 15 minutes, whilst the flood tide (from 0.5 m depth) lasted only 1 hour 30 minutes (Figs. 5.5 & 5.6). As such, the flood tidal currents were stronger, with speeds of up to 0.8 m s^{-1}; during the ebb the peak flow was 0.2 m s^{-1}. Throughout the 6 tide deployment, the largest peaks in SSC were experienced during the flood tide (Fig. 5.6), with the a peak SSC of 270 mg l^{-1}, experienced during the flood tide on 02/09/2004 am (4.3 m OD tidal height). During the subsequent tide, with a height of 3.5 m OD, hydrodynamic conditions under lower water depths were investigated (Figs. 5.7 & 5.8). The peak current speed, during the flood stage of the tide, dropped to 0.3 m s^{-1}; the peak ebb current speed was 0.15 m s^{-1}. Thus the peak flood current speed was twice that on the ebb; during the previous tide, the flood was some 4 times higher than the ebb. The SSC was lower during the second tide, with concentrations below 100 mg l^{-1}. The SSC peaked at the start of the flood, then reduced gradually to the end of the ebb; this was similar to the previous tide (Fig. 5.8). The corresponding tidal curve inside the site was nearly symmetrical, with both the flood and the ebb stages lasting for 1 hour 15 minutes.

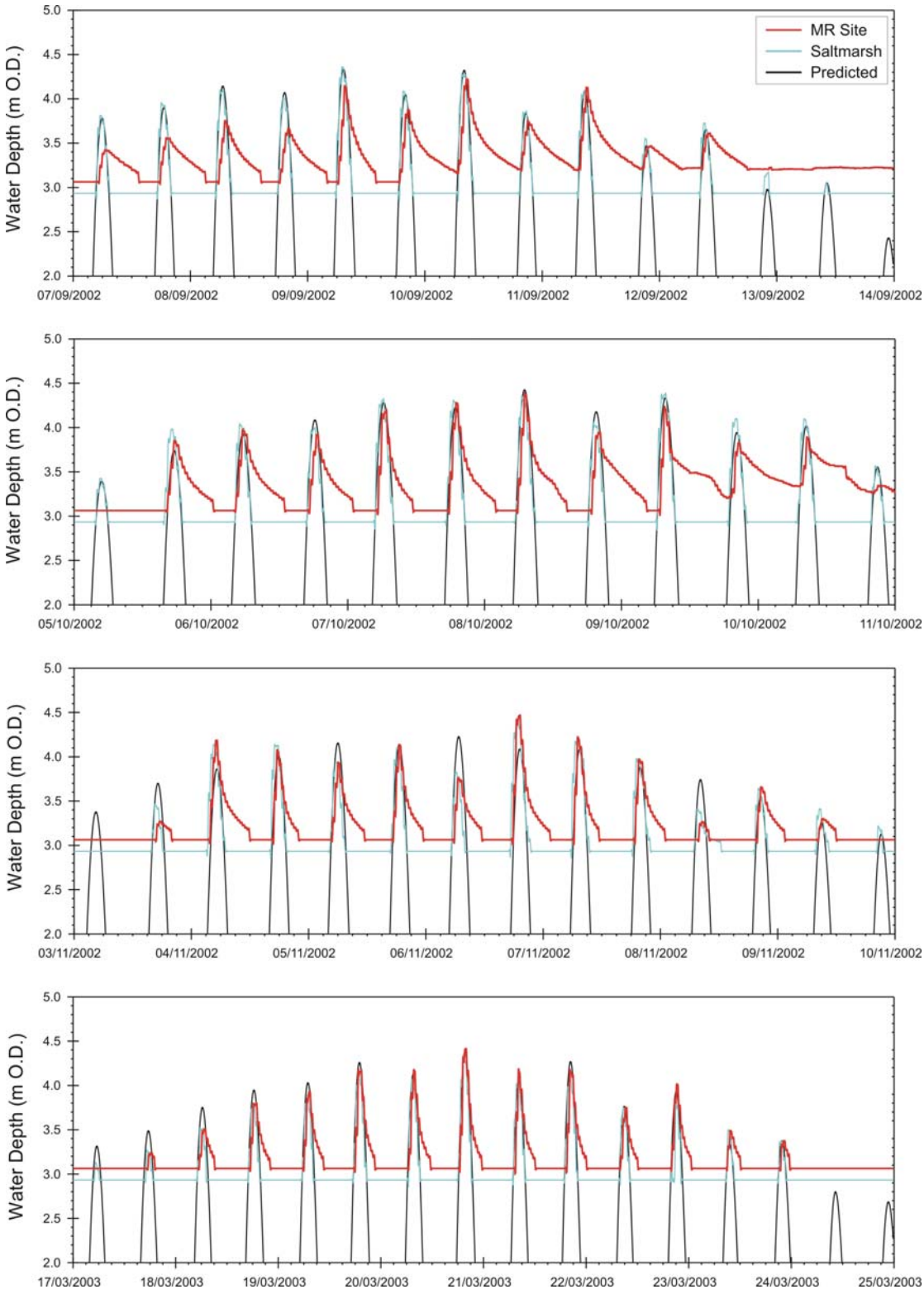

Figure 5.2: Measured water depth inside the MR site and on the saltmarsh, over a series of high spring tides, with the predicted tidal curve (based on the Admiralty Charts) shown (see Sites 1 & 2B in Figure 4.7 for location). These data were provided by the EA and collected by Gardline Surveys.

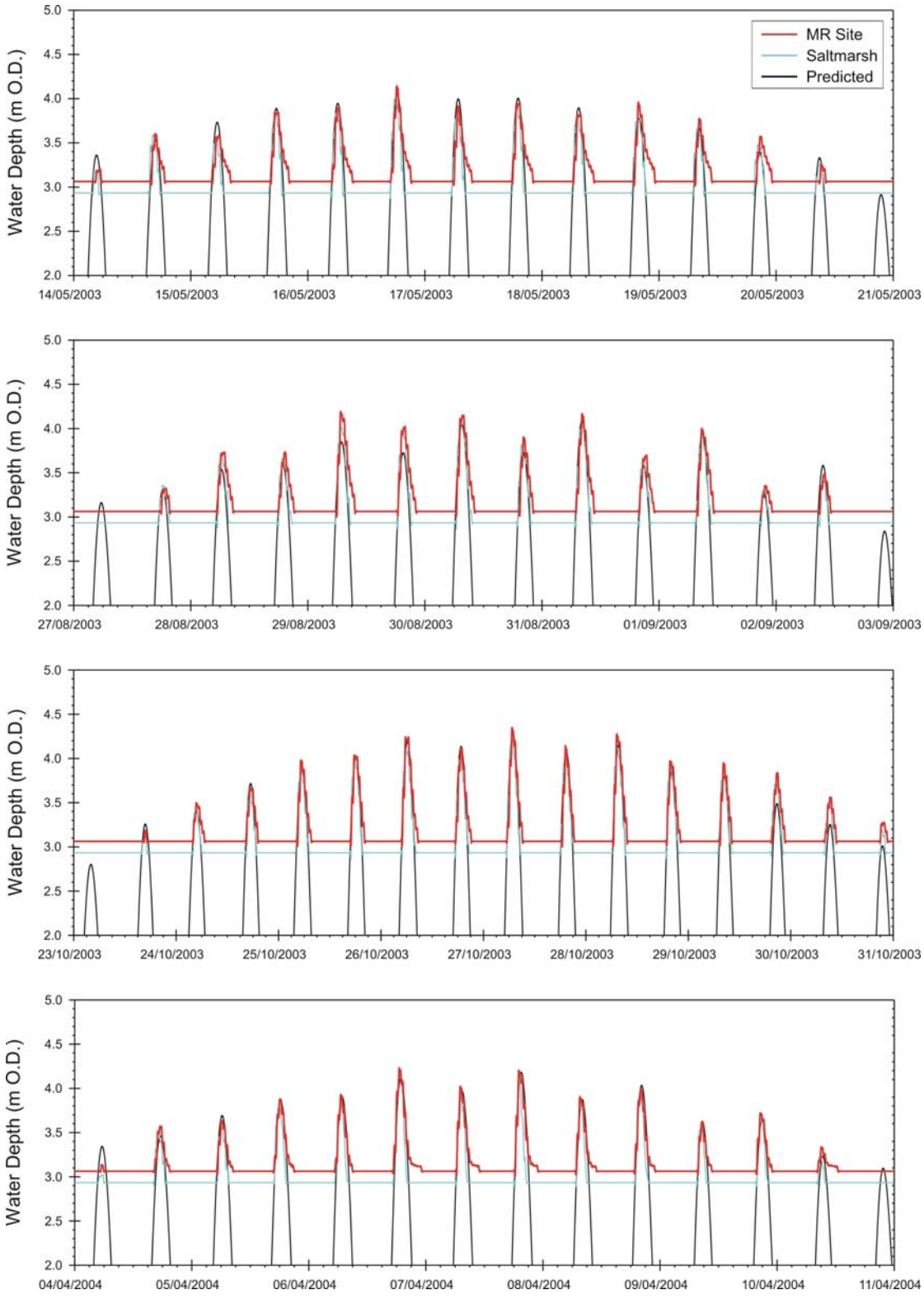

Figure 5.3: Measured water depth inside the MR site and on the saltmarsh, over a series of high spring tides, with the predicted (based on the Admiralty Charts) tidal curve shown (see Sites 1 & 2B in Figure 4.7 for location). These data were provided by the EA and collected by Gardline Surveys.

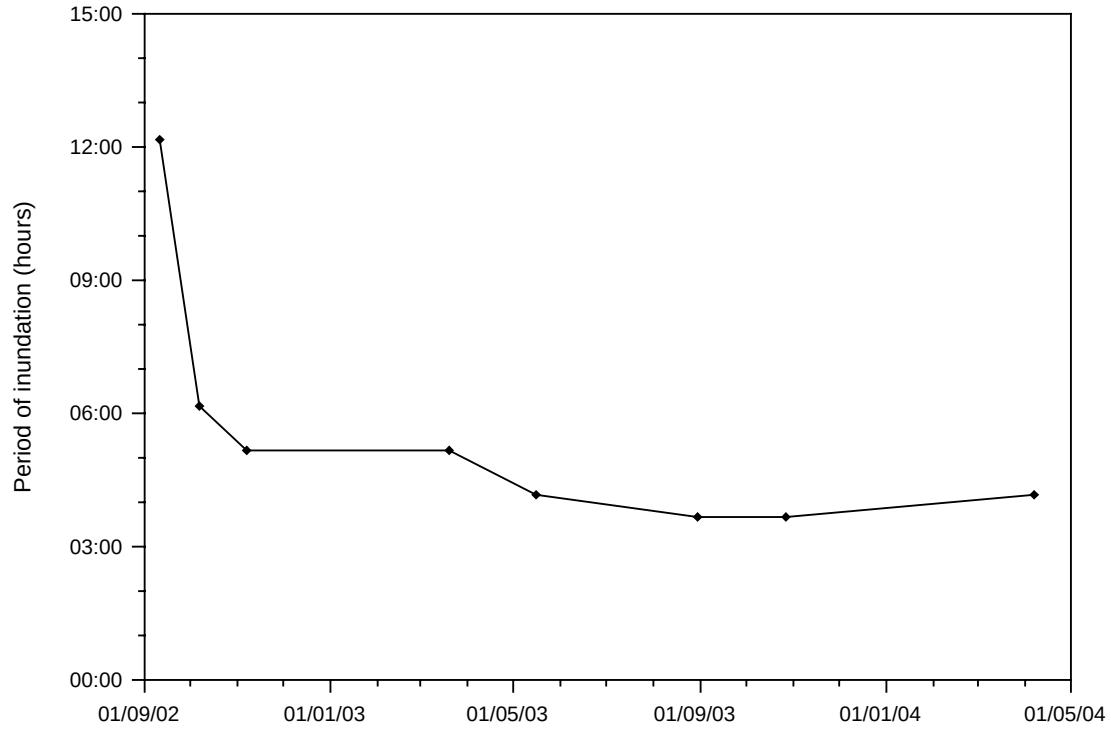

Figure 5.4: The length of time Site 2B within the MR site remained submerged, following high spring tides over an 18-month period.

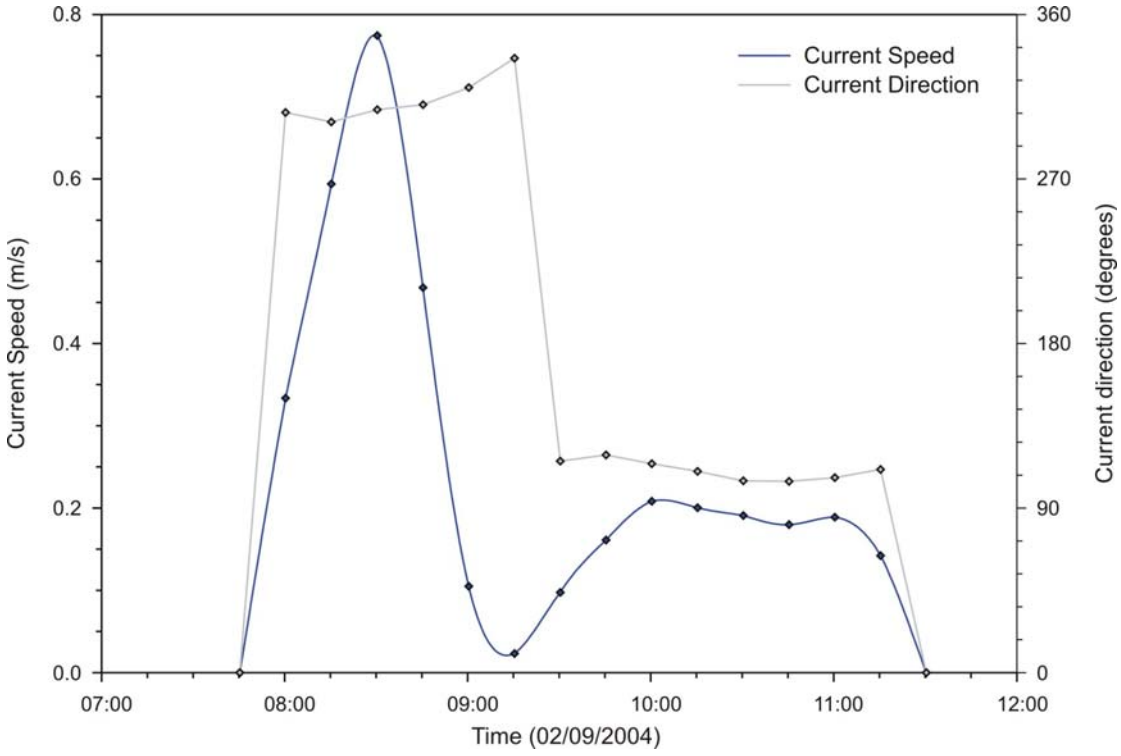

Figure 5.5: Tidal current speed and direction inside the MR site, throughout a tidal cycle. Measured using the ABR during *Deployment 4*, for location see Figure 4.1(a).

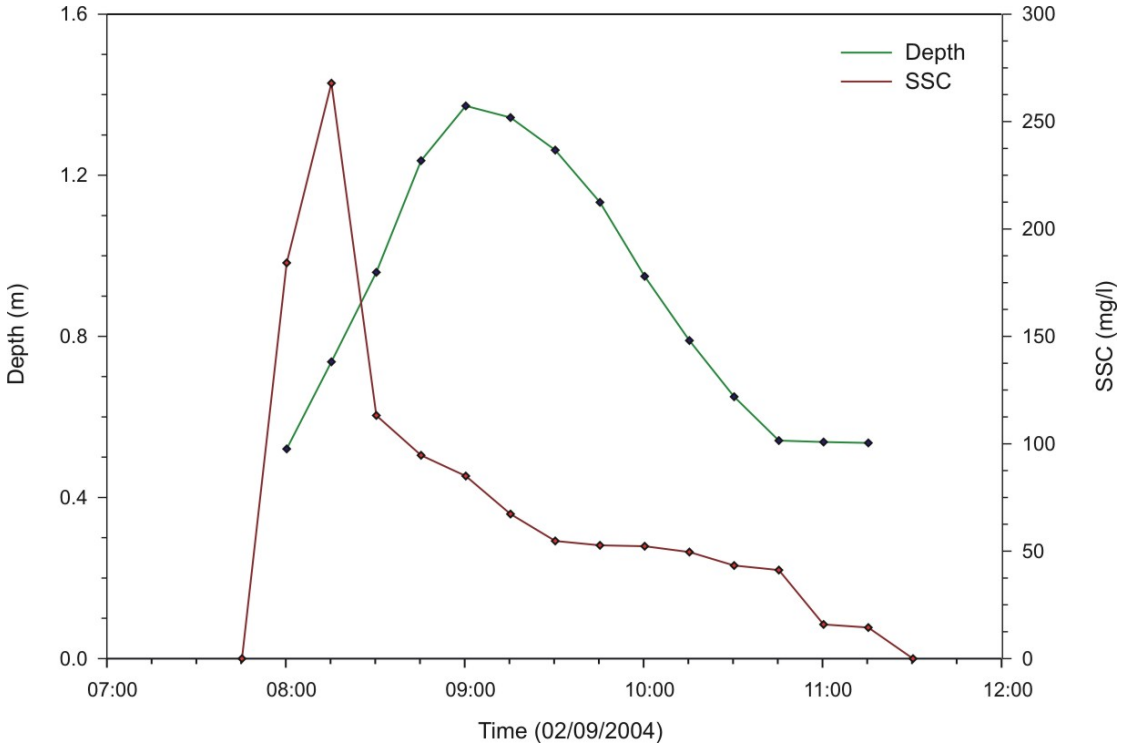

Figure 5.6: The water depth and SSC inside the MR site, throughout a tidal cycle.

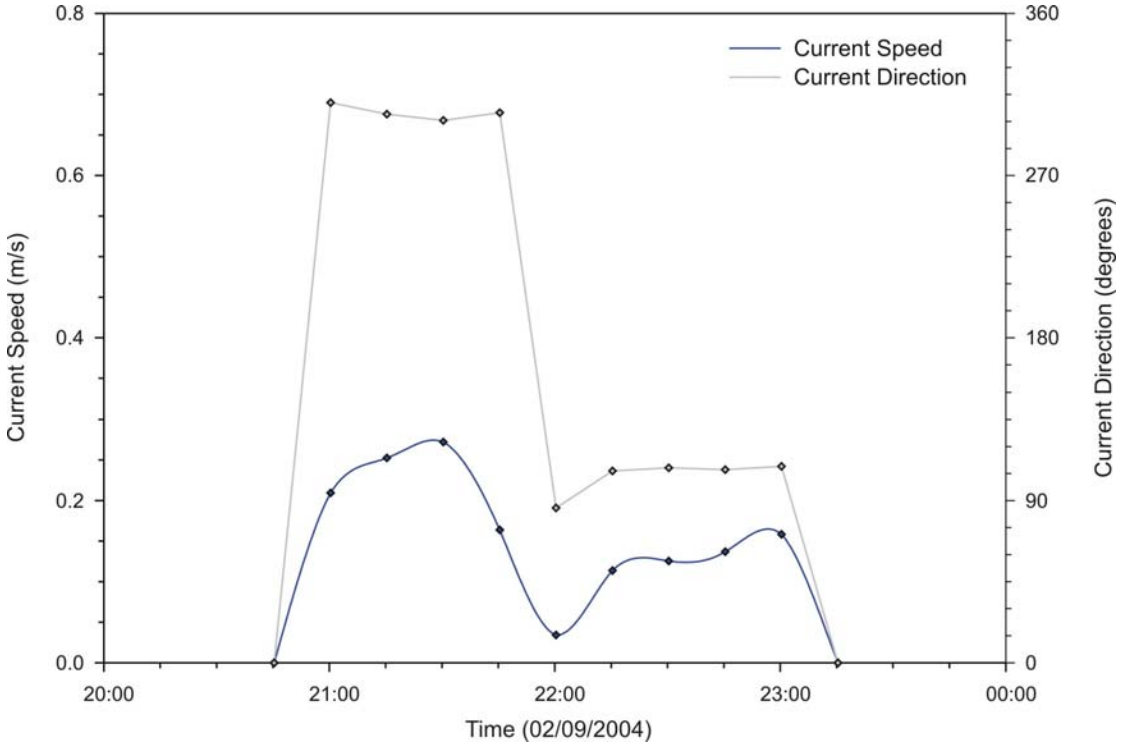

Figure 5.7: The tidal current speed and direction inside the MR site, throughout a tidal cycle.

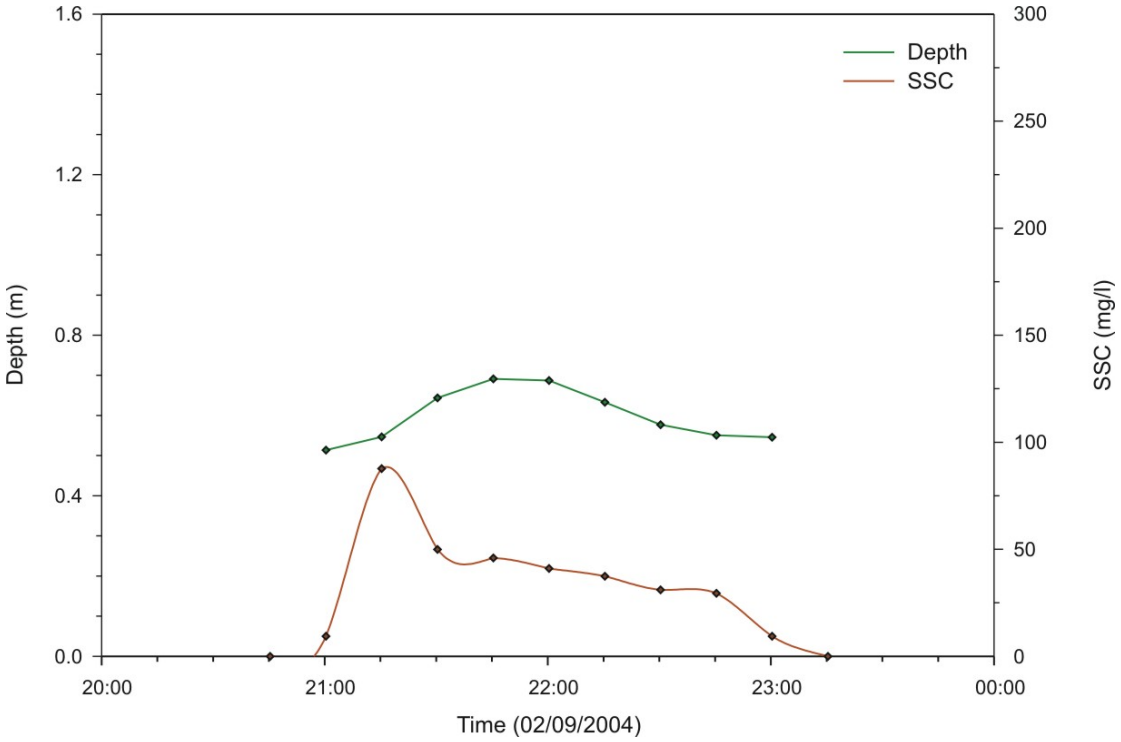

Figure 5.8: Water depth and SSC inside the MR site, throughout a tidal cycle.

Wave conditions inside the MR site have been minimal since the breaching. Maximum and significant wave heights were small within the MR site, compared to those on the adjacent saltmarsh (Figs. 5.9 & 5.10). Significant wave heights (*Hs*) inside the MR site have only reached 2.7 cm on a single occasion, over an 18-month period (Fig. 5.9); comparative *Hs* over the adjacent saltmarsh were small, with occasional peaks extending up to 15 – 20 cm. The MR site was sheltered from these peak wave conditions. Peaks in maximum wave height were experienced concurrently inside the MR site (15 cm) and on the saltmarsh (55 cm); this was the only occasion when higher wave activity over the saltmarsh resulted in a notable difference in the wave height inside the MR site, over the 18-months of measurements (Fig. 5.10).

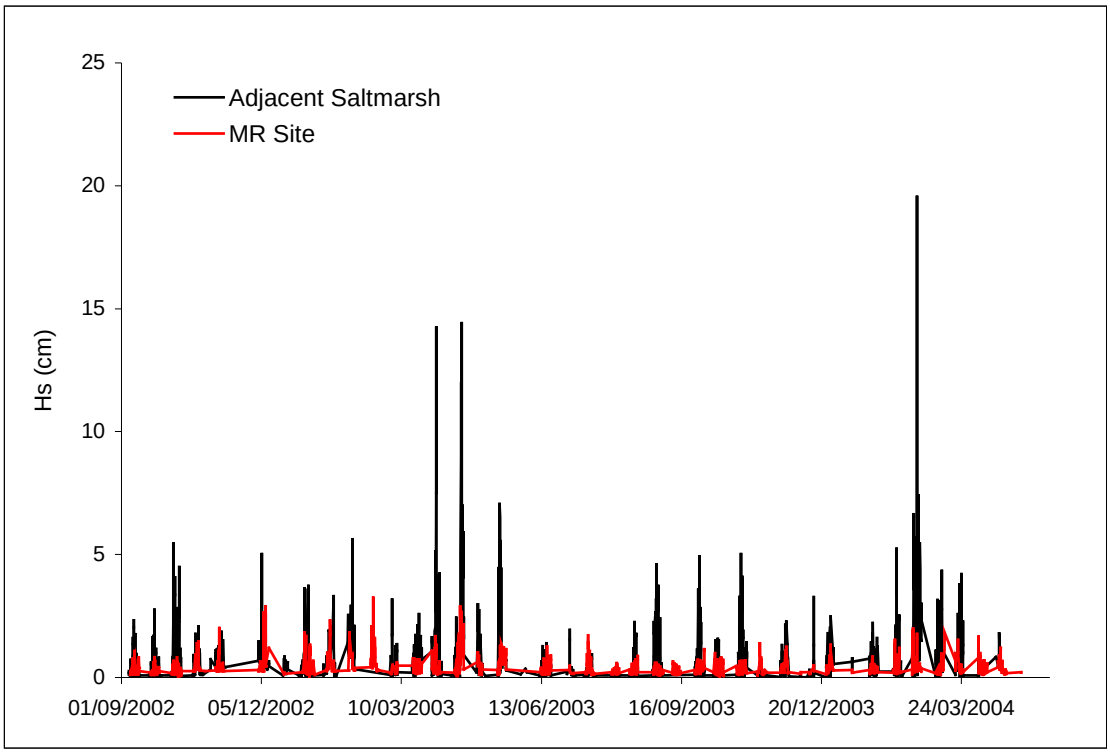

Figure 5.9: The significant wave heights recorded inside the MR site and on the adjacent saltmarsh, over an 18-month period following breaching of the embankment. These data were provided by the EA and collected by Gardline Surveys.

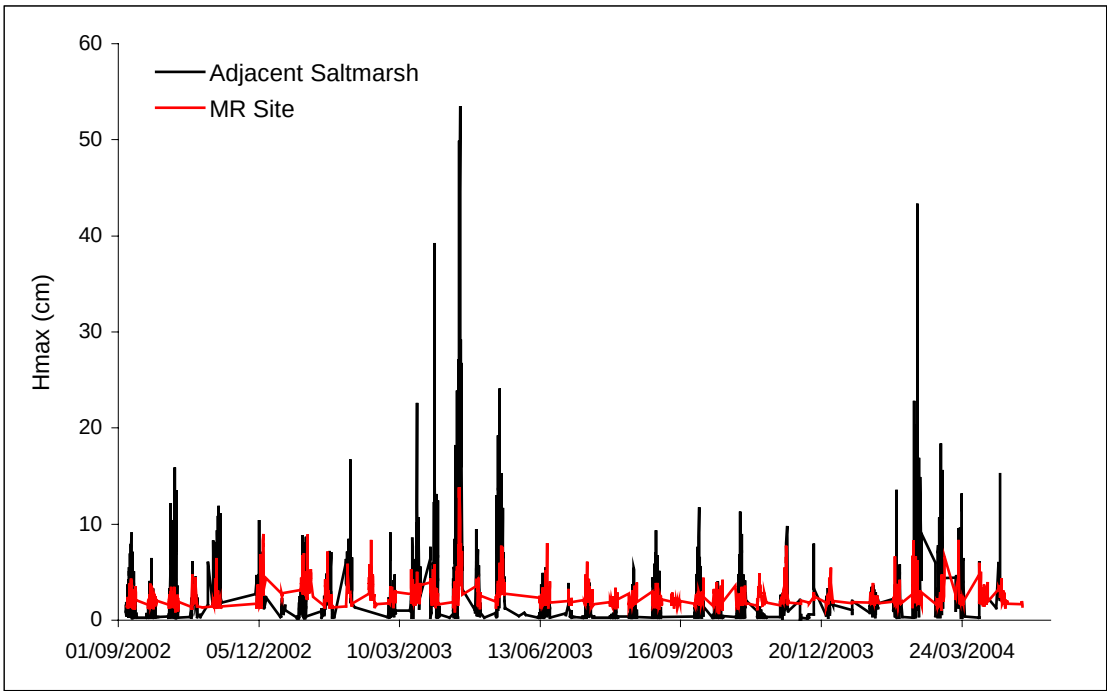

Figure 5.10: The maximum wave heights recorded inside the MR site and on the adjacent saltmarsh, over an 18-month period following breaching of the embankment. These data were provided by the EA and collected by Gardline Surveys.

5.4.2 *Erosion/Accretion*

The highest surface elevation increases, during both winter (Fig. 5.11) and summer (Fig. 5.12), were at Site 7, which was located adjacent to the embankment between Breaches 2 and 3 (Fig. 4.5). The surface elevation increase here was higher during winter, than in summer. The bedlevel variability at Site 7 was also twice as high in the winter. Site 8, located between Breaches 1 and 2, was also subjected to surface elevation increase; however, the mean rate was only half that of Site 7 (Fig. 5.13). At this location the mean surface elevation increase was relatively constant through the summer and winter, with a slightly greater variability in the rates during the winter. The sites at the landward end of the MR site (Sites 9 – 11) did not experience any extensive surface elevation change, during either summer or winter months.

The surface elevation changes inside the MR site were similar to the rates of accretion recorded in 1973 by Amos (1974), when the area was saltmarsh, before the creation of the embankment as part of the land reclamation. These measurements were taken along a transect near to where Breach 1 is now located, so Stations 8 and 11 were nearest to where the previous recordings were made (Fig. 5.13). Station 8 experienced a surface elevation increase of 2 cm over a year, the same rate was also measured on the saltmarsh in 1973; Station 11 increased in elevation by 0.1 cm over the year and the same area accreted by 0.2 cm over a year in 1973. The surface elevation changes measured inside the MR site were similar to the rates of sediment accretion over the natural saltmarsh in 1973.

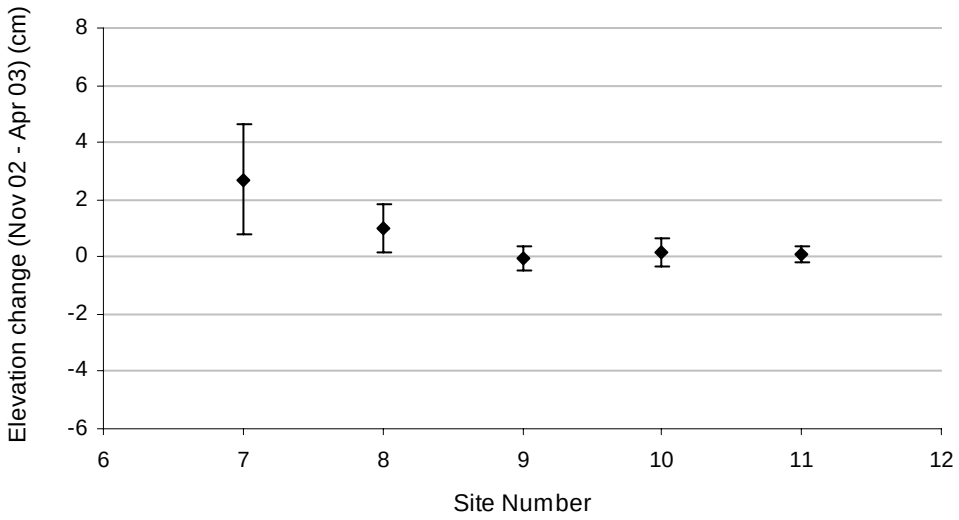

Figure 5.11: The change in elevation over the SET sites inside the MR site, over a 6-month period between November 2002 and April 2003 (Winter). For site locations, see Figure 5.13. These data were provided by the EA and collected by CEH and CCRU.

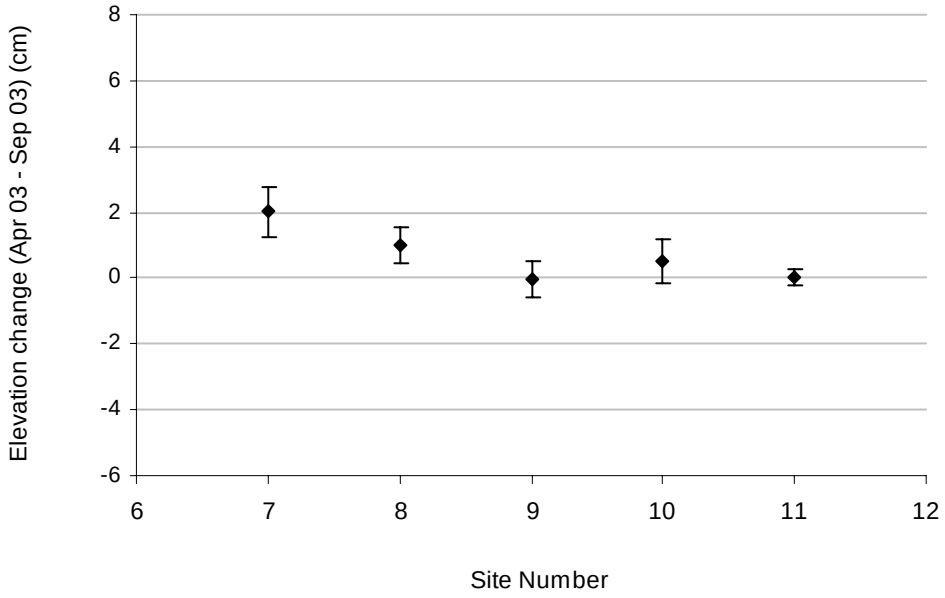

Figure 5.12: The change in elevation over the SET sites inside the MR site, over a 6-month period between April 2003 and September 2003 (Summer). For site locations, see Figure 5.13. These data were provided by the EA and collected by CEH and CCRU.

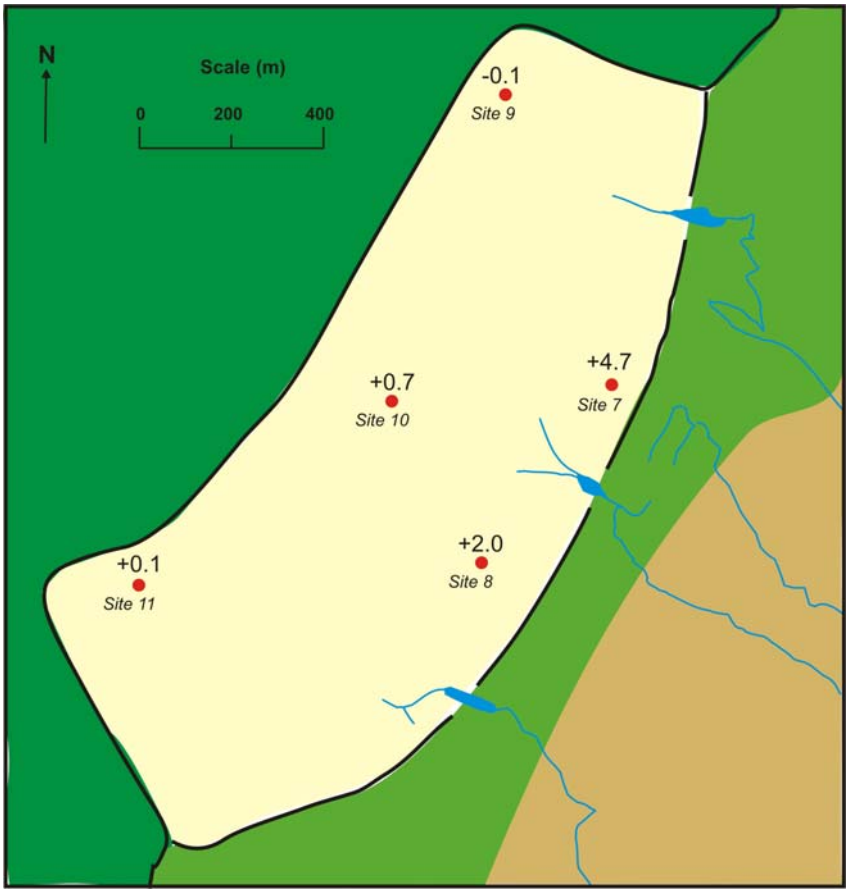

Figure 5.13: The total change in elevation in centimetres at the 5 sites inside the MR, over an 11-month period between November 2002 and September 2003. These data were provided by the EA and collected by CEH and CCRU.

5.4.3 *Vegetation Development*

Following the survey undertaken in September 2003, it was found that vegetation had colonised the majority of the MR site (Fig. 5.14). The density of halophytic vegetation varied across the site, with both high and low percentages present adjacent to the breached seawall (Plate 5.1) and the strengthened landward embankment. There was a pattern in the vegetation cover, with the maximum amount of vegetation cover from each profile revealing that around to Breach 2, the highest percentage cover was adjacent to the landward embankment; while on the profiles at the north and south ends of the site, the maximum cover was adjacent to the breached embankment. Areas of low vegetation cover were often associated with waterlogged areas; here, poor drainage has caused areas to remain submerged for long periods. The main species found to have colonised the site were *Salicornia* spp. and *Suaeda* spp.; these were found in relatively even numbers, with the average percentage of the site covered by *Salicornia* spp. being 18 %, while 19 % of the site was covered by *Suaeda* spp.. A site visit made in September 2005, revealed that most of the site had been colonised by dense vegetation, with only limited areas of bare mudflat remaining (Plate 5.2).

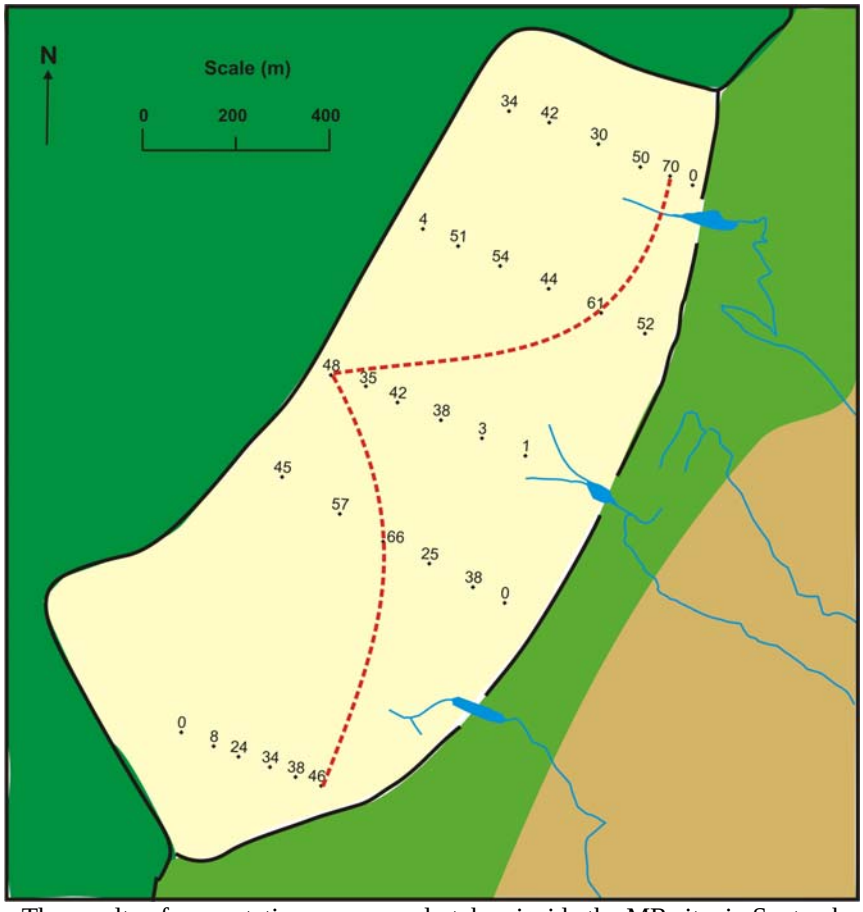

Figure 5.14: The results of a vegetation survey undertaken inside the MR site, in September 2003. Key: the numbers represent the average percentage of the ground covered by vegetation, with a dashed red line connecting up the peak values from each profile line. These data were provided by the EA and collected by CEH and CCRU.

5.5 DISCUSSION

The most dramatic change associated with the MR site is related to its drainage pattern. Over the first month following the breaching of the embankment, there was a marked reduction in the length of time the site remained submerged. During the ebb phase of the tide (especially initially) the drainage, within the natural creeks connected to the channels in the breaches, resulted in discharge throughout LW; under natural conditions they would have been empty. In response to these anthropogenically-induced flow conditions, overbank flow occurred at particular locations along the creeks. This process caused overland flow over the adjacent intertidal flats; this, in turn, has led to the increased development of a creek system (this is described in more detail, in Chapter 7).

The MR site became infilled with water more rapidly, following the first month of inundations. At this time, the flood phase started to mimic closely the tidal curve over the adjacent saltmarsh. After some 20 months, the ebb phase became similar to that on the saltmarsh. The initial dimensions (1 m deep, 2 m wide) of the artificial channels, within the breaches, were insufficient to accommodate the volume of water entering and leaving the MR site. As such, the channel bed within Breach 1 experienced erosion during *Deployment 1*, to a depth of 0.5 – 1 m over 3 tides; these were some 1 m lower in elevation than the maximum spring tide. During these first tides, severe erosion occurred in all of the channels, to permit larger quantities of water to flow in and out of the site. Elsewhere, in the UK and Europe, similar erosion has been experienced at other sites; (a) at Tollesbury, Essex, UK, a 1 m wide breach eroded, over a few days, to a pre-determined (modelled) width of 60 m (Alsop et al., 2004); (b) at Pagham Harbour, southern England, UK, following a natural breach in an embankment, a 160 m wide channel developed, causing significant erosion and reworking of the sediment around the harbour entrance (Cundy et al., 2002); and (c) in the Westerschelde, Holland, within 85 years of the re-flooding of a series of enclosures, a creek network developed that reached back some 12 km from a main channel - this had grown at its mouth to a width of ~ 750 m (Allen, 2000b). The development of the channels, within the breaches will be discussed in more detail in Chapter 6.

The tidal currents inside the MR site flowed landward during the flood phase of the tide; this switched, just after HW, to flow out of the site in the opposite direction. The tidal current speed peaked during the first phase flood; it then remained relatively stable throughout much of the ebb phase of the tide. During high spring tides, the current speed was higher and the flood tide was shorter than the ebb. During lower spring tides, the tidal currents were more symmetrical, with a flood current speed only slightly higher than that on the ebb. This difference was related to the topography of the MR site and the adjacent saltmarsh. During

high spring tides, the water level was higher than the base of the breached embankment, and this caused the water to flow both through the channels within the breaches as well as over the banks of the channels. The difference in levels between the channel banks and the MR site caused flow acceleration inside the MR site, creating high tidal current speeds and a rapid rise in water level. Subsequently, drainage of the site was restricted to the channels within the breaches; this caused the emptying of the site to last for longer than the filling. During the lower spring tides, flood and ebb flows were restricted to the channels within the breaches, and were of the same duration.

Wave activity inside the MR site was found to be minimal; this was due to the site itself having a fetch for locally wind-generated waves, whilst the adjacent saltmarsh dissipated much of the wave activity, approaching from different parts of The Wash (Section 9.3.2). The relationship $h < 10H_s$ shows, when satisfied, that the oscillatory motion of the waves is felt at the seabed (Soulsby, 1997). Only during the first and last phases of the tide did the measurements satisfy this relationship; so when the water depth was less than 0.25 m, the wave conditions were capable of eroding the bed. As such, the modified and prevailing wave climate is not deemed to have been an important factor in the development of the site. In contrast, the internal embankment at the MR site at Northey Island, Blackwater Estuary, UK, suffered erosion from wind waves generated within the 0.8 hectare site (ABP, 1998); in the absence of vegetation, small locally generated wind waves can cause noticeable erosion within the MR site.

Since the initiation of the MR scheme, the site has accreted at a similar rate to the natural saltmarsh prior to the land reclamation in 1980. The rates were highest near the breaches in the seaward embankment; they were lower around the strengthened landward embankment. Areas adjacent to the breaches are likely to have experienced higher rates of accretion, as they were submerged during most of the tides which entered the MR site; this, in turn, provides a greater opportunity for suspended sediment to settle, during slack water. Consequently, the rates appeared highly dependent upon the frequency of submergence; this is in agreement with the findings from Tollesbury (Chang et al., 2001). For example, the peak rate of accretion (5 cm yr^{-1}) in The Wash was located between Breaches 2 and 3, whilst the area between Breaches 1 and 2 experienced only 2 cm yr^{-1} (Fig. 5.13); this indicates that the local topography was important and the sediment inputs from each breach may have varied and affected the accretion rates. These measured rates of accretion were high compared with those observed over other sites: (a) at the historical set-back sites in the Severn Estuary, UK, the annual accretion rates varied from 2.8 to 15 mm yr^{-1} (Allen, 2000a); (b) within the

Crouch, Medway and Blackwater Estuaries, UK, maximum rates extended up to 80 cm, over a 100 year period (Crooks and Pye, 2000; and Pethick, 2001); (c) for the Blyth Estuary, Suffolk, UK, the most exposed area eroded at an average rate of 10 mm yr^{-1}, accreting in the more sheltered areas at rates of between 7 and 16 mm yr^{-1} (French et al., 2000); and, finally (d) at Pagham Harbour, southern England, UK, the rates of accretion were 8 to 10 mm yr^{-1}, since a natural breach in the embankment in 1910 (Cundy et al., 2002).

Vegetation had naturally colonised much of the site, some 12 months after the breaching of the embankment, with the main pioneer species being *Salicornia* spp. and *Suaeda* spp.; rapid natural colonisation of vegetation was also witnessed at the MRs at Northey Island and Orplands Marsh, Blackwater Estuary, UK (ABP, 1998). The vegetation cover varied around the site; it was found to be predominantly dependent upon the frequency of inundation, with the maximum rates of vegetation cover along each profile located at the zone where the duration of submergence was most suited to vegetation colonisation. The vegetation cover has become denser, based upon observations during sequential field visits; this will enhance the entrapment of suspended sediment, causing the MR site to accrete more rapidly (French et al., 1995; Roman et al., 1997; Brown, 1998; and Cahoon et al., 2000). As the vegetation causes frictional deceleration of the tidal currents (Neumeier and Ciavola, 2004), the rate of accretion will increase; the properties of the surficial sediment will change to become similar to the saltmarsh, and this will enable more species to colonise (Pethick, 1984).

5.6 CONCLUDING REMARKS

The initial design of the channels within the breaches of the MR site was such that they were not of sufficient size to transport the volume of water flowing into and out of the MR site. Consequently, the channels were eroded. Hence, after some 18 months (i.e. in February 2004) the flooding and ebbing of the tide over the site were nearly synchronous with the tidal curve experienced over the adjacent saltmarsh. The wave activity over the MR site and saltmarsh were comparable, with the possibility of erosion only present when the water depth was less than 0.25 m[1]. The site has been predominantly accretional, with the highest rates of accretion around the breaches. Some 12 months after the initiation of the project, the site had become colonised by saltmarsh vegetation; this has since been increasing, in terms of the density and coverage.

Generally, the MR site has behaved as designed, i.e. accreting sediment, allowing vegetation to colonise and being subjected to minimal wave activity; as such, it appears to have been

[1] Note: there are no measurements when the water depth was this low, so it is unknown if the waves were still present or if the presence of saltmarsh vegetation had dissipated them.

successful in terms of its main objective, that of coastal protection (Watts et al., 2003). Not all MR sites within the UK have been as successful in terms of coastal protection. In some cases (for example, in the SE of England and around the Severn Estuary), low rates of sediment consolidation and shear stress gain have increased the likelihood of erosion by tidal currents and waves; this has led to a high ratio of bare mud to vegetated surfaces, reducing the flood defence value of the newly-created marsh (Crooks and Pye, 2000).

The impacts of erosion experienced around the breaches at Freiston Shore, together with enhanced flow over the adjacent intertidal zone (resulting in enhanced creek development) are looked at in more detail in Chapters 6 and 7.

5.7 PLATES

Plate 5.1: The MR site adjacent to Breach 3, where an area of sparse vegetation can be seen in the foreground, with more dense vegetation in the distance (September 2003).

Plate 5.2: The MR site adjacent to Breach 1, where predominantly dense vegetation can be seen, with areas of poor drainage and no vegetation visible (September 2005).

CHAPTER 6: STABILITY AND DEVELOPMENT OF A BREACH IN AN EMBANKMENT, USING THE REGIME THEORY

6.1 INTRODUCTION

Artificially-created channels in 3 breaches in an embankment, at Freiston Shore, have been scoured out since the initiation of a MR scheme (Symonds and Collins, 2005). The channels were designed initially to act as a landward continuation of the natural creeks on the saltmarsh; as such, they were of a similar size and shape (1 m deep, 2 m wide) (Plate 6.1). However, some 2 months after the seawall was breached, 50 to 100 m axial lengths of the channels, within the breaches, were eroded to a width of 15 to 20 m, and a maximum depth of ~ 4 m (Plate 6.2). Following this period, the channels have continued to erode, at variable rates (Plate 6.3). Against this background, the Regime Theory will be used to predict the eventual equilibrium size of the channels, to assist in future predictive capabilities for such schemes. Such theories have been used for channels within intertidal zones (Lawrence et al., 2004), but have not been used previously in this type (MR) of investigation. Hence, measurements were made at the site following the initiation of the MR, with the intention of validating and verifying a regime model; as recommended by Dearnaley et al. (1994).

The Regime Theory will predict the size of the equilibrium channel, which will eventually form. Either by using these predictions and the measured rate of change of the channels at the MR site, or from using a separate relationship, it should be possible to predict how long it will take for the channels to reach a dynamic equilibrium. The validity of the Regime Theory will be examined in terms of its applicability to this type of study; if it proves suitable, then a number of differing methods will be analysed, to identify which is the most accurate for this particular environmental setting. If realistic predictions could be attained, then these could be of use in the design of future MR schemes. Within such schemes, the prediction of discharge would be necessary, to predict the size of any artificial channels or breaches based upon their equilibrium channel size.

6.2 BACKGROUND

The Regime Theory has been used elsewhere for the prediction of the size of the entrances of estuaries and tidal inlets. A simple correlation between the tidal volume and inlet cross-sectional area was derived originally, with a relationship proposed by O'Brien (1931):

$$A = 1000\Omega^{0.85} \quad (6.1)$$

A = cross-sectional area of channel (m^2)

Ω = tidal prism (m^3)

Interestingly, this approach was applied to the entrance of The Wash by Evans and Collins (1975); it was noted that despite the tidal prism, flowing into and out of The Wash, having been reduced by land reclamation, it was still in an apparent state of equilibrium according to Equation 6.1. Since this relationship was presented, other similar equations have been suggested (HR Wallingford, in press); however, the majority of these have been shown to be specific to the sites for which they were derived. This limitation has been clearly shown by Gao and Collins (1994), wherein a plot of tidal prism against cross-sectional area of the entrance, for a number of tidal inlets, shows a high degree of scatter (Fig. 6.1). From such findings, it has been deduced that other important controlling factors must also be taken into consideration, such as: the nature of the sediment; sediment supply; geomorphological type; wave activity; and any geological constraints (Townend, 2005).

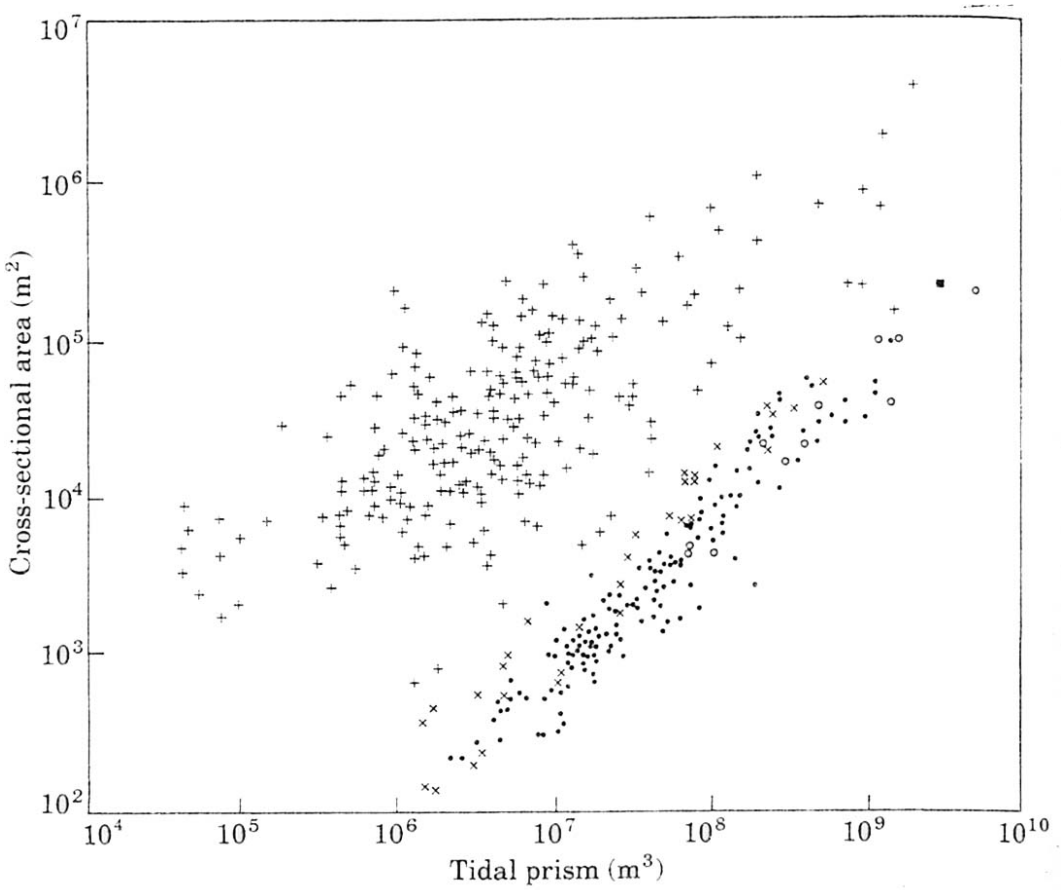

Figure 6.1: Inlet cross-sectional area related to the tidal prism, for tidal inlets in the U.K. (■), the U.S.A. (●), Japan (+) and China (×) (from Gao and Collins (1994)).

A similar approach was adopted for the calculation of the required width of the breaches in the embankment at Freiston Shore, for stability. Here, an empirical approach (derived by Burd et al (1994)) was adopted, where only the breach width was related to the tidal prism (Halcrow, 1999):

$$W = 37.9e^{1.8\times10^{-6}\Omega} \quad (6.2)$$

W = breach width (m)

Ω = tidal prism (m^3)

This computation confirmed that 3 breaches, with widths of 50 m each, i.e. 150 m in total, would be satisfactory for the scheme (Table 6.1). In addition to the breaches in the embankment, small artificial channels were dug into the breaches, to connect up with natural creeks on the saltmarsh; these did not form any part of the numerical modelling.

Table 6.1: Results of the Tidal Prism method used in the prediction of the breach width, at Freiston Shore (Halcrow, 1999).

Assumed Land Level in Calculations (m OD)	Total Tidal Prism (based on MHWS water level) (m^3)	Predicted overall Breach Width (m)
+2.75	771,653	152
+2.85	703,153	134
+3.0	600,403	112

6.3 METHODS

This component of the investigation involved the collection of wide-ranging data over a 30-month period, following the initiation of the MR scheme. The data used in this analysis were: aerial photography; RTK-GPS measurements; echosounding depth recordings; and hydrodynamic measurements, from *Deployments 1* and *4*. These observations were used to monitor any change of the channels in the breaches; likewise to provide the measured data utilised in the prediction of an 'equilibrium regime channel'. The aerial photography available to the study covered all three of the channels within the breaches. However, the other measurements have concentrated upon the channel within Breach 1; this has been assumed to be representative of the other channels[1]. The hydrodynamic measurements used were from: (a) the ABR deployed in the channel within Breach 1 during *Deployment 1*; and (b) inside the MR site during *Deployment 4* (Fig. 4.1(a)).

[1] Note: on the basis of aerial photography, the 3 channels within the breaches developed similarly.

Aerial photographs taken since the MR have been digitised and used here to calculate the length and maximum width of the channels in the breaches (Fig. 6.2), together with the area of these sections of the channels. This procedure has been achieved with accuracy, by identifying reference points on the aerial photographs; validating them with RTK-GPS measurements, recorded simultaneously[2]. The RTK-GPS system was used to survey the position of the edge of the channel, within Breach 1 on two occasions (10/06/2003 and 17/10/2003). Further, an echosounder was used, in conjunction with RTK-GPS, such that the depths of the channel at a number of cross-sections, were obtained.

Finally, a cross-sectional profile of the channel in Breach 1, concurrent (05/09/2002 (pm)) with the hydrodynamic measurements was obtained. Utilising the water depth recorded by the ABR, together with the cross-sectional profile of the channel, the cross-sectional area of the submerged channel was calculated throughout the measured tidal cycles. A homogenous tidal current structure and SSC were assumed throughout the channel, as an approximation, allowing the discharge and load within the channel to be calculated.

Two methods have been used in the calculation of the equilibrium channel: (i) a theoretical method derived by Yalin and Ferriera da Silva (2001) (referred to herein as the Yalin Method); and (ii) an empirical method described by Inglis and Allen (1957) (referred to herein as the Inglis Method). The different methods were utilised for comparative purposes, to investigate which is most applicable to the present type of investigation. Both approaches provide values for the mean width and depth of the equilibrium channel. As an additional approach to the prediction of channel width, a more simplistic method based upon the continuity equation, was used to predict the channel width. Subsequently, channel shape has been predicted using part of the Regime Theory method, adopted by Cao and Knight (1997).

[2] This is known as geo-referencing.

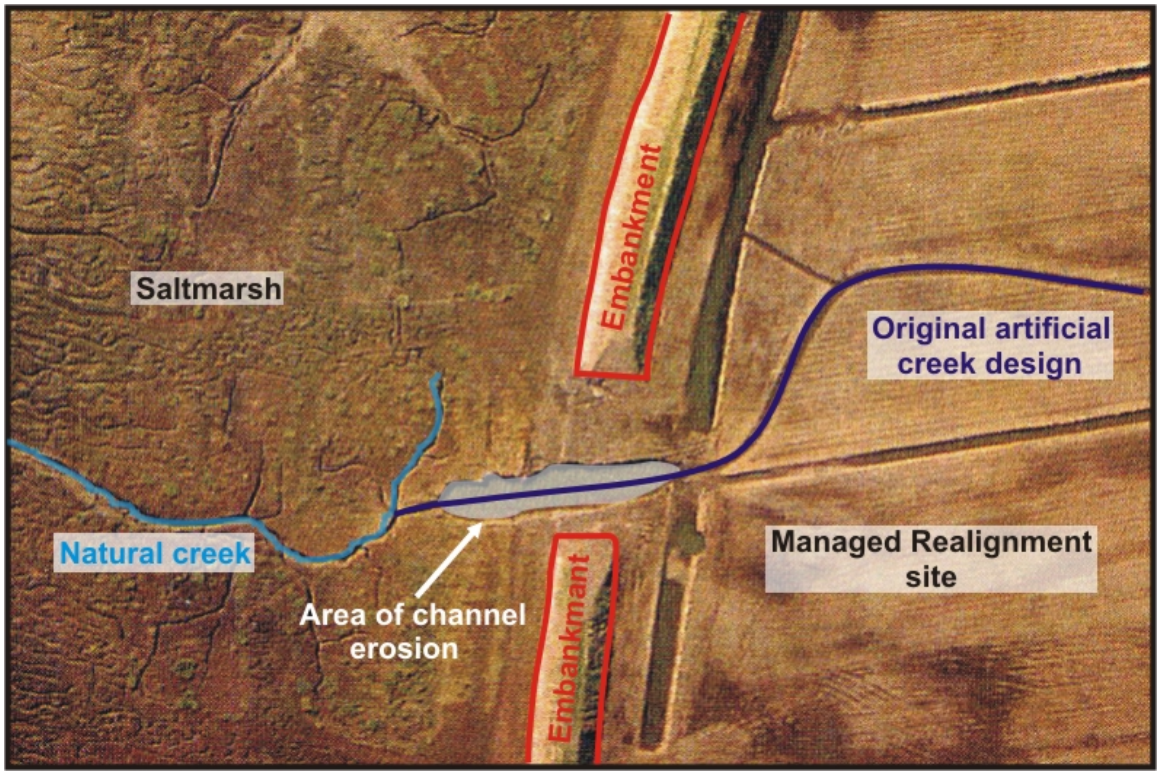

Figure 6.2: Aerial photograph (03/11/2002) of the area around Breach 1, with the area of channel erosion highlighted. The initial artificial channel size and location, together with that of the natural creek, are also shown. Note: for scale, the embankment is 20 m wide.

6.3.1 *Yalin Method:* Yalin and Ferreira da Silva (2001)

This theoretical/rational method, based upon mathematical and physical arguments, utilised laboratory and field data to derive the best expressions. It relies on the channel acquiring its regime state, in response to one of its energy-related characteristics. The flow rate is assumed constant and turbulent, whilst the sediment is cohesionless.

At the entrance to a channel, a constant flow rate (V) and sediment supply (Q_s) is fed into the channel. Following a certain period of time (T_{R1}), the initial channel [W_0, h_0, S_0] will deform into an equilibrium channel [W_{R1}, h_{R1}, S_{R1}]; which is referred to then as the Regime Channel, R_1. Seven parameters control R_1:

V = flow rate (constant);
Q_s = sediment feed rate (constant);
ρ = density of fluid;
υ = kinematic viscosity;
γ_s / v_{*cr} = specific weight of grains in the fluid / velocity necessary for the initiation of sediment transport;
D_{50} = mean grain size; and
g = acceleration due to gravity.

The regime development takes place only after an adjustment period, T_0. Only after this does the width (W), hydraulic depth (h) and slope (S) of the channel, vary gradually with time. Experiments have shown that $T_0 < \sim 0.01 T_R$. Thus, the initial rapid change occurs over a very short period of time, when compared to the total time-scale necessary for regime to occur (Shimizu ,1991; as cited in Yalin and Ferreira da Silva, 2001). The width of the Regime Channel is proportional to $\sqrt{Q}$. (Note: for a full description of the method used, see Yalin and Ferreira da Silva (2001), p95)

6.3.2 ***Inglis Method:*** Inglis and Allen (1957)

This approach is empirical and was derived for irrigation canals in India, for flow in channels with mobile sandy beds. The formulae can only be applied directly to uniform flow, with discharge and load representing the dominant conditions (as the conditions can vary widely in a channel). The expressions used in this method are outlined below.

$$W = 17.8 Q^{\frac{1}{2}} \left(\frac{X v_s}{D_{50}} \right)^{\frac{1}{4}} \tag{6.3}$$

$$h = \frac{0.012 Q^{\frac{1}{3}} D_{50}^{\frac{1}{6}}}{(X v_s)^{\frac{1}{3}}} \tag{6.4}$$

Where:

W = width of channel at water surface (m);

h = hydraulic depth of channel (m);

Q = discharge of channel (m^3/s);

X = load = solid volume of material transported per second (kg m^{-1} s^{-1}) / discharge in channel (m^3 s^{-1}) (taken as 0.0000755);

D_{50} = mean diameter of sediment (m); and

v_s = mean terminal velocity of material falling through still water (m/s).

6.3.3 ***Continuity Method:***

By applying the mass continuity equation to changes in the horizontal and vertical over a fixed domain, as defined by the boundaries of the MR site, a simple equation was derived to predict the channel dimensions. The friction/resistance equation is in effect introduced by limiting the continuity method to the erosion threshold (U_{cr}). Water slope and, hence, the momentum effects are ignored:

$$W = \frac{P.v}{U_{cr}.h_{mid}} \tag{6.5}$$

W = width of the channel in the breach (m);

P = plan area of the inundated MR (m^2);

v = vertical velocity ($m\ s^{-1}$);

U_{cr} = critical horizontal current velocity ($m\ s^{-1}$); and

h_{mid} = depth of the middle of the breach in the channel (m).

6.3.4 *Channel Shape:* Cao and Knight (1997)

The method outlined by Cao and Knight (1997) incorporates variables which are very difficult to measure accurately; instead it has been used to predict the channel shape of the final regime channel, using the predictions of the channel width from the other methods (see above):

$$d(y) = \frac{\mu L}{2}\left[1 - \left(\frac{y}{L}\right)^2\right] \tag{6.6}$$

Where:

d = depth (m);

μ = submerged static coefficient of Coulomb friction (taken to be 0.5);

L = semi-surface width of the channel (m); and

y = lateral distance from the centreline of the channel (m).

6.4 RESULTS

During the 6 days that the ABR was deployed, the channel within Breach 1 suffered severe erosion; the cross-sectional profile was measured at the ABR location at the start of the deployment (05/09/2002). Regrettably, as a result of the strong flows and scouring of the channel, it was not possible to measure the profile again during the deployment. Consequently, the cross-section used in the discharge calculations was that surveyed the day before the hydrodynamic measurements, during a period of channel erosion. The cross-sectional area of the channel was eroded during each tidal inundation during this time, so the impact of a variation in channel size on the discharge (used in the calculation of the channel regime equilibrium), is shown in Table 6.2.

Table 6.2: Discharge variation over the flood period of a tidal cycle (05/09/02 (am)) (the first was at the start of the flood and the last at the end of the flood, the measurements were recorded every 40 minutes), in relation to the date the cross-section of the channel was recorded.

Flow Speed (m/s)	Discharge (m^3/s)
(a) Using cross-section measured on 17/10/03	
0.25	15.1
1.94	121
2.57	181.6
1.09	84.5
(b) Using cross-section measured on 05/09/02	
0.25	3.5
1.94	32.4
2.57	69.9
1.09	38.3

As the water depth varied throughout the tidal cycle, the current speed in the channel within Breach 1 fluctuated; it peaked during high water, causing a simultaneous peak in discharge. On the basis of the field observations, the flow was highly turbulent during this period, and this caused erosion of the channel banks.

6.4.1 *Flow out of MR site*

During a tidal cycle, the ebb flow lasted for ~2.5 times the length of the flood (Fig. 6.3). However, the peak current speed during the flood (2.5 m s^{-1}) was up to 5 times greater than the ebb (0.5 m s^{-1}). This caused the MR site to become submerged during the short flood period, draining at a relatively low steady rate, throughout the following LW; it flooded again, on the next HW. For a detailed explanation into the reason for this see Chapter 7.

In order to compare the relative importance of the flood into the MR site (around HW) and the ebb draining the site (throughout the remainder of the tidal cycle), the discharge was calculated for both of these periods. Owing to the higher current speeds during the flood, the discharge was much higher than during the ebb (Fig. 6.4). The total flood and ebb discharges approximately balanced over a tidal cycle, as expected.

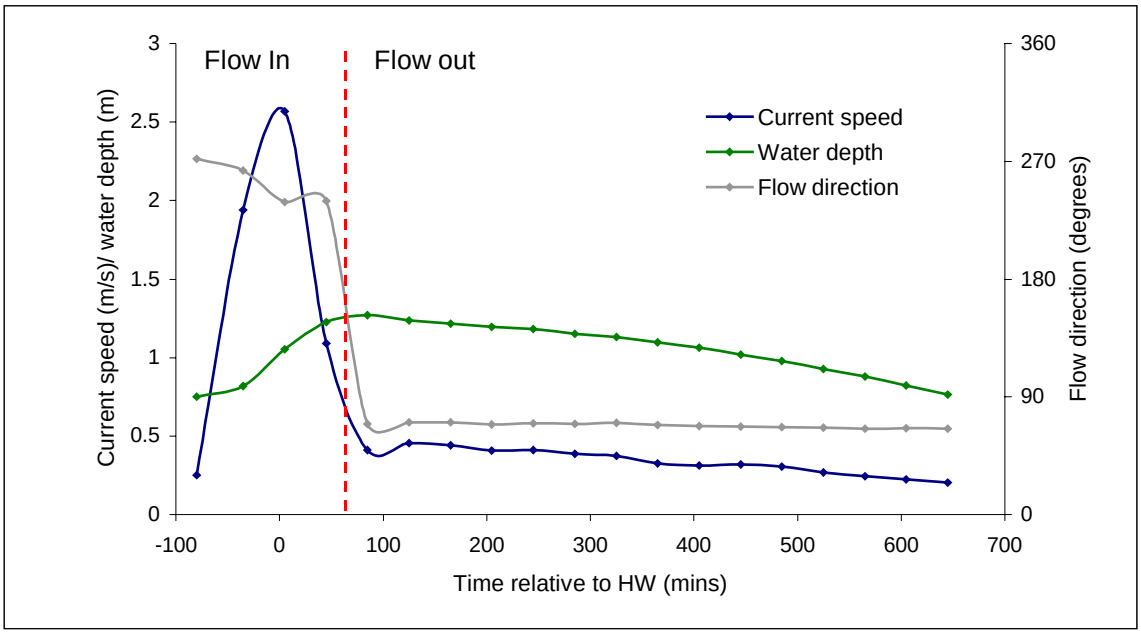

Figure 6.3: Hydrodynamic conditions in the channel within Breach 1, over a tidal cycle (06/09/2002, am). Periods of flow into and out of the MR site are shown.

The water discharge was used to predict variability in the calculated regime equilibrium channel size, throughout the tidal cycle, using both the Yalin and Inglis methods (Figs. 6.4 & 6.5). These approaches show similar patterns, the Yalin method predicted a wider channel, whilst the Inglis method predicted a deeper channel. The predicted channel widths and depths for the ebb flow (draining the MR site) were lower than those predicted for the flood (entering the site). During the period of peak discharge (during the flood, near HW); the channel was more susceptible to erosion; hence, it must be under these conditions that the Regime equations should be used to predict the equilibrium channel. However, the draining of the MR site did impact the intertidal zone (Chapter 7). Nonetheless, its significance for the regime of the channels within the breaches was that in draining the MR site, it allowed high gravity flows to refill the site, during the subsequent HW (Chapter 5).

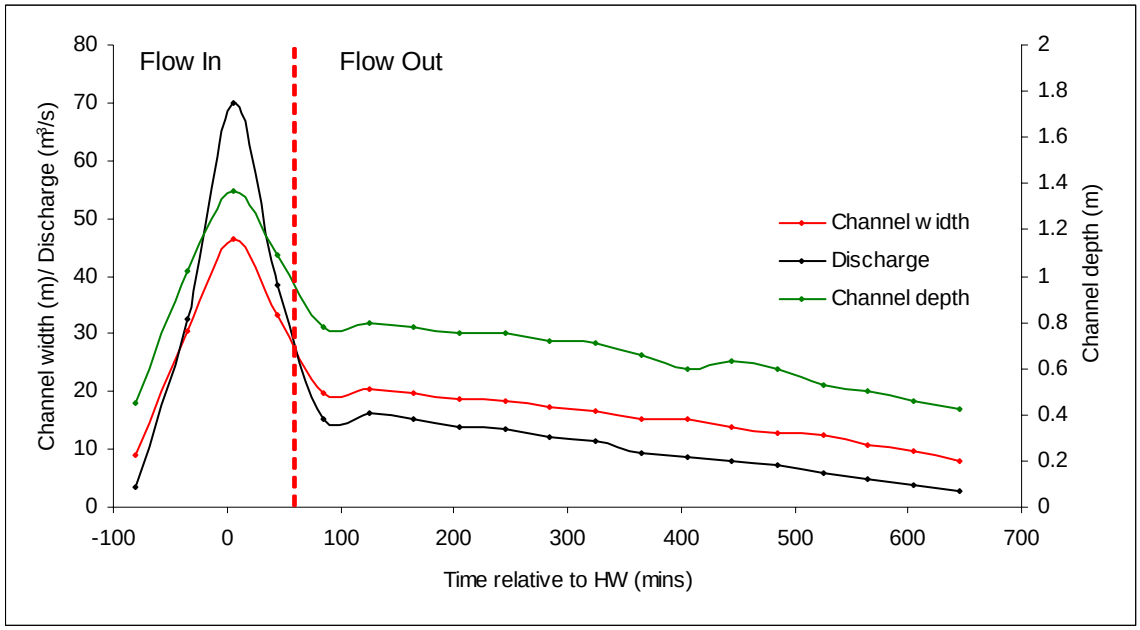

Figure 6.4: The discharge flowing into and out of the MR over a measured tidal cycle (06/09/2002, am). The resulting channel width and hydraulic depth have been calculated using the Yalin method, with a mean grain size of 0.15 mm (see text).

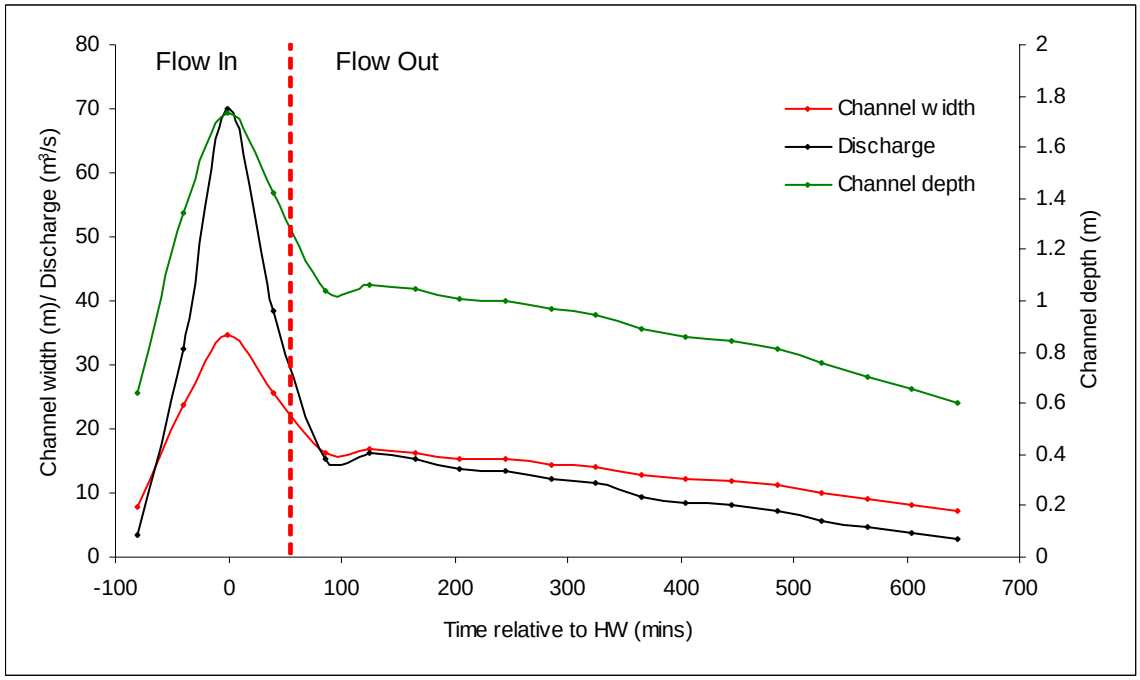

Figure 6.5: The discharge flowing into and out of the MR over a measured tidal cycle (06/09/2002, am). The channel width and hydraulic depth have been calculated using the Inglis method, with the measured mean grain size of 0.06 mm (see text).

6.4.2 *Yalin Method*

Using this approach, both the regime equilibrium channel width and depth increase with discharge (Fig. 6.6); they increase at a similar rate, whilst the discharge increases at a higher

rate. When the sediment feed rate and grain size are kept constant and the current speed is increased, the predicted channel width and hydraulic depth increase in a linear fashion.

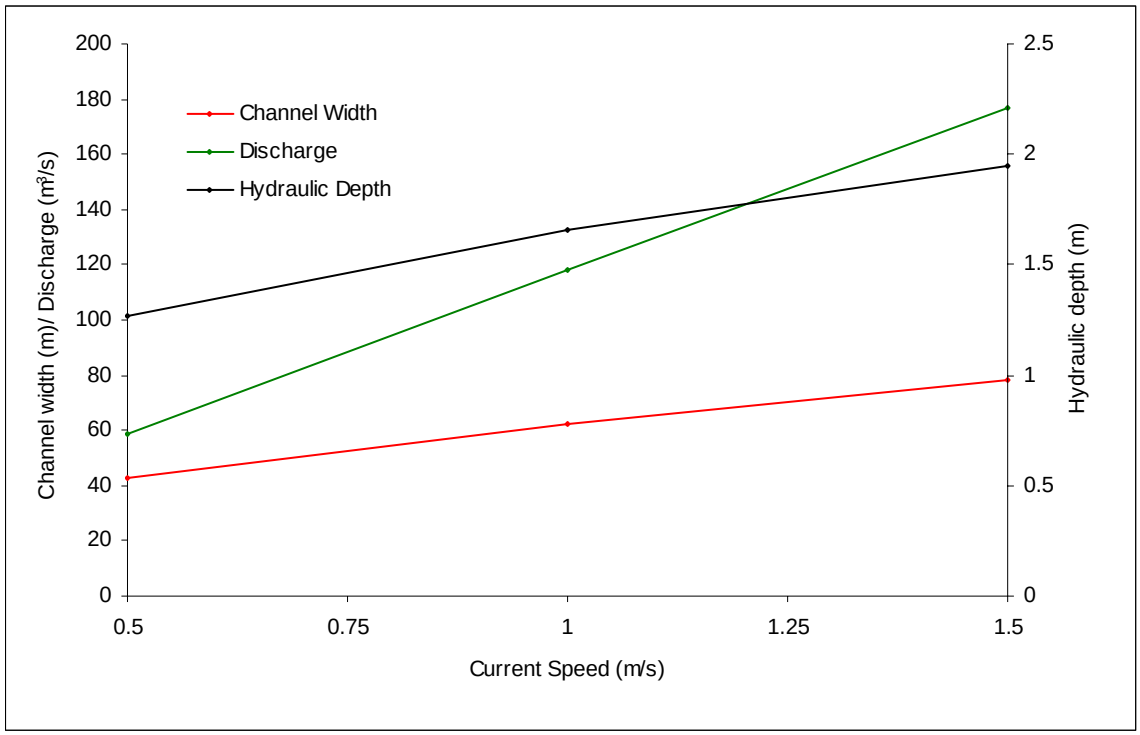

Figure 6.6: The effect of variation in current speed on the predicted channel width and hydraulic depth, using the Yalin method (assuming a grain size of 0.15 mm).

In order to investigate the effect of grain size variation on the output of the Yalin method, a range of grain sizes was used, whilst all other variables were maintained as constant (Fig. 6.7). For grain sizes > 0.3 mm the predicted channel width and depth show little variation. For grain sizes < 0.3 mm, but > 0.12 mm, the channel width increases gradually, whilst the hydraulic depth decreases. However, for grain sizes < 0.12 mm the depth becomes very sensitive to grain size, increasing dramatically with a reduction in grain size; there is a corresponding 'step profile' in the channel width. Finally, this method is incapable of calculating the channel regime for a mean grain size < 0.06 mm. Overall, on the basis of these findings, it appears that this method should not be used for grain sizes < 0.12 mm (fine sand), as the results become unreliable. It was recommended by Yalin and Ferreira da Silva (2001) that the method should not be used with cohesive sediment.

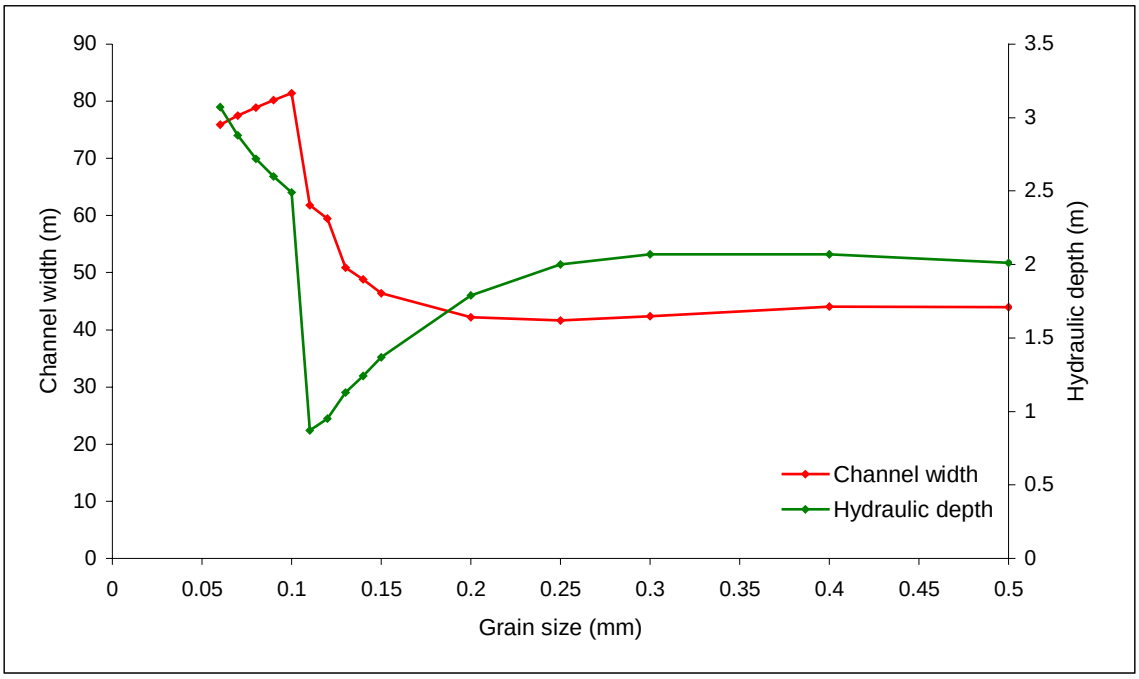

Figure 6.7: The impact of grain size variation on the predicted channel width and hydraulic depth, calculated using the Yalin method.

Assuming a grain size of 0.15 mm (compared with an actual D_{50} of 0.06 mm), utilising the cross-section determined at the start of the deployment (see above), the regime channel size was calculated (using the Yalin method) over the flooding period of the tidal cycle (Fig. 6.8). The discharge values were calculated, using data recorded every 40 minutes by the ABR, this commenced when the flow first entered the channel (80 minutes before HW), finishing when the flow ceased flooding into the MR site (with the last measurement obtained some 40 minutes after HW).

The predicted equilibrium channel width and hydraulic depth increased with discharge, leading to a peak at High Water; here, the current speed and discharge were at their maxima. The calculations of the equilibrium channel using the Yalin method output a channel width of 46 m and hydraulic depth of 1.4 m, giving a cross-sectional area of 64.4 m^2 (the measured cross-sectional area, 6 months after breaching, was 60.3 m^2). These were calculated using the maximum discharge and mean grain size, as thought to be most appropriate.

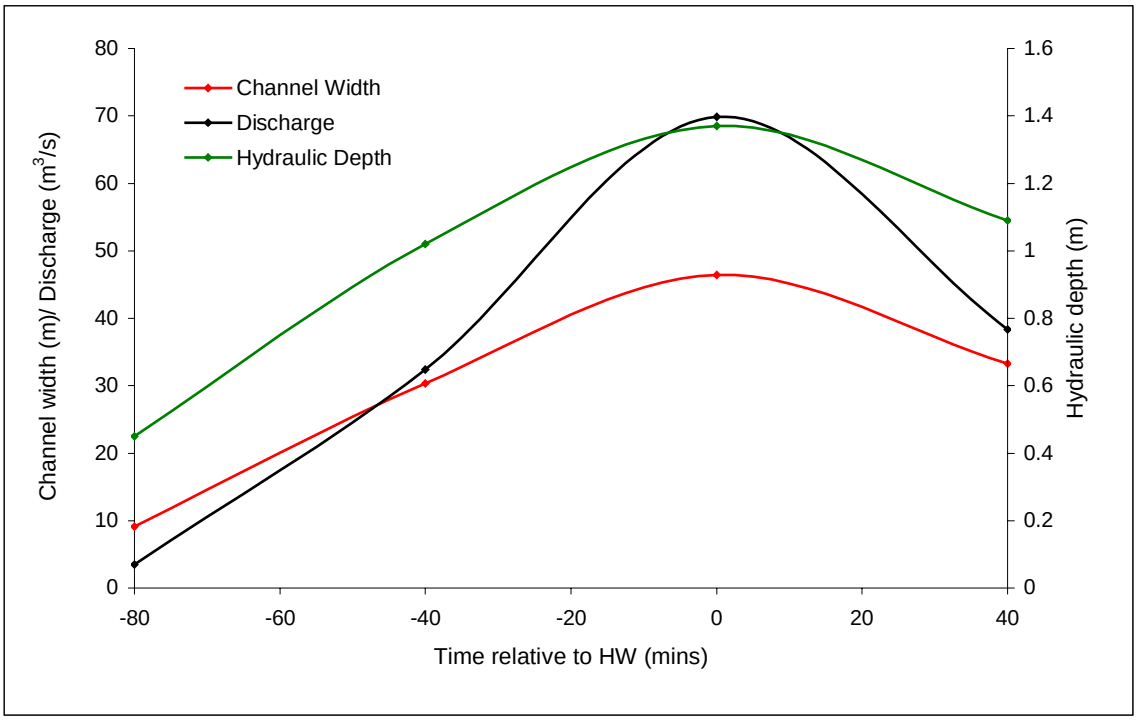

Figure 6.8: The variation in discharge flowing into the MR, over the flood of a measured tidal cycle (06/09/2002, am), together with the calculated resulting variation in channel width and hydraulic depth (calculated using the Yalin method, assuming a mean grain size of 0.15 mm).

6.4.3 *Inglis method*

Using this approach to calculate the equilibrium channel characteristics, the discharge and predicted channel width and hydraulic depth had a positive linear relationship with current speed. There is a correspondence to the predictions using the Yalin method, with channel width and depth showing the same relative increase with current speed (Fig. 6.9). The predicted channel sizes derived from this method are lower than those derived from the Yalin method, using the same input values. The rate of increase in channel width and hydraulic depth are lower using the Inglis method, compared to the Yalin approach. With a 115 m^3/s increase in discharge, the Yalin method predicted an increase in channel width of 40 m and hydraulic depth of 0.7 m: for comparison, the Inglis method provided an increase in channel width of 30 m and hydraulic depth of 0.45 m.

Mean grain size is an important variable in the calculation of the regime channel using the Inglis method (Fig. 6.10), as was the case with the Yalin method. Once again, grain size has been varied whilst the other variables were retained constant. A grain size variation from 0.01 to 0.5 mm changed the predicted channel width and hydraulic depth by ~ 40 m and 3.5 m, respectively. The channel depth follows an exponential decay, in relation to an increasing mean grain size; this causes a change in hydraulic depth of 2.35 m, between grain sizes of 0.01 and 0.05 mm. The channel width was related logarithmically and does not increase so

dramatically. No restriction is applied to the grain size used in the calculations; however, as stated in the method description, it should be used only for non-cohesive alluvium.

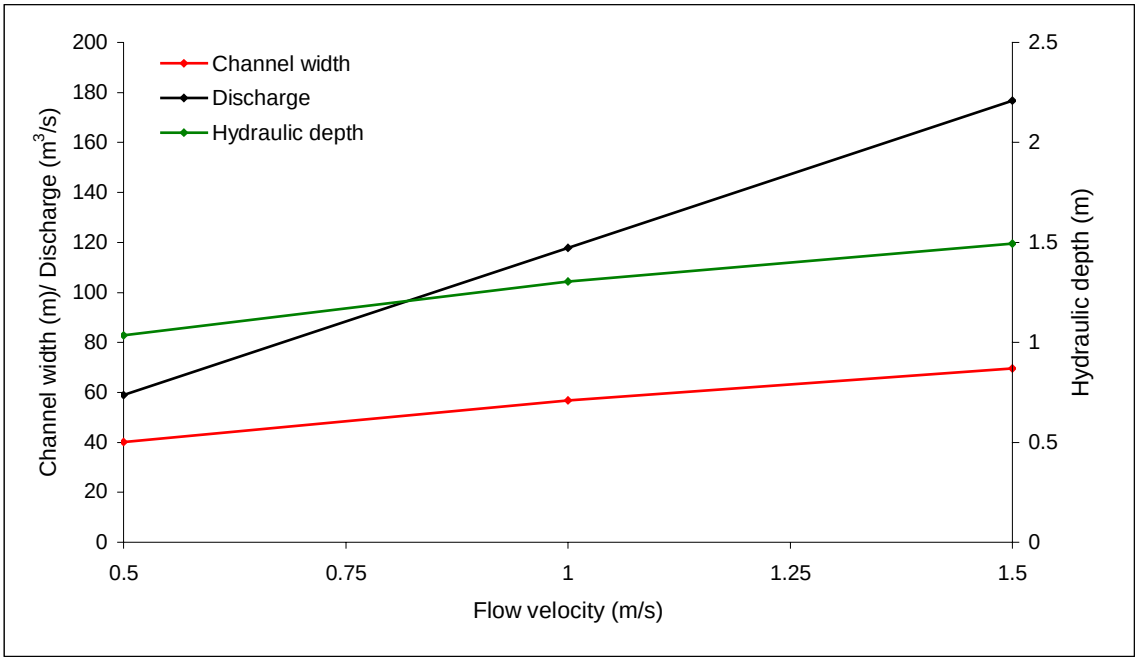

Figure 6.9: The effect of variation in flow velocity, on the predicted channel width and hydraulic depth, using the Inglis method (assuming a grain size of 0.15mm).

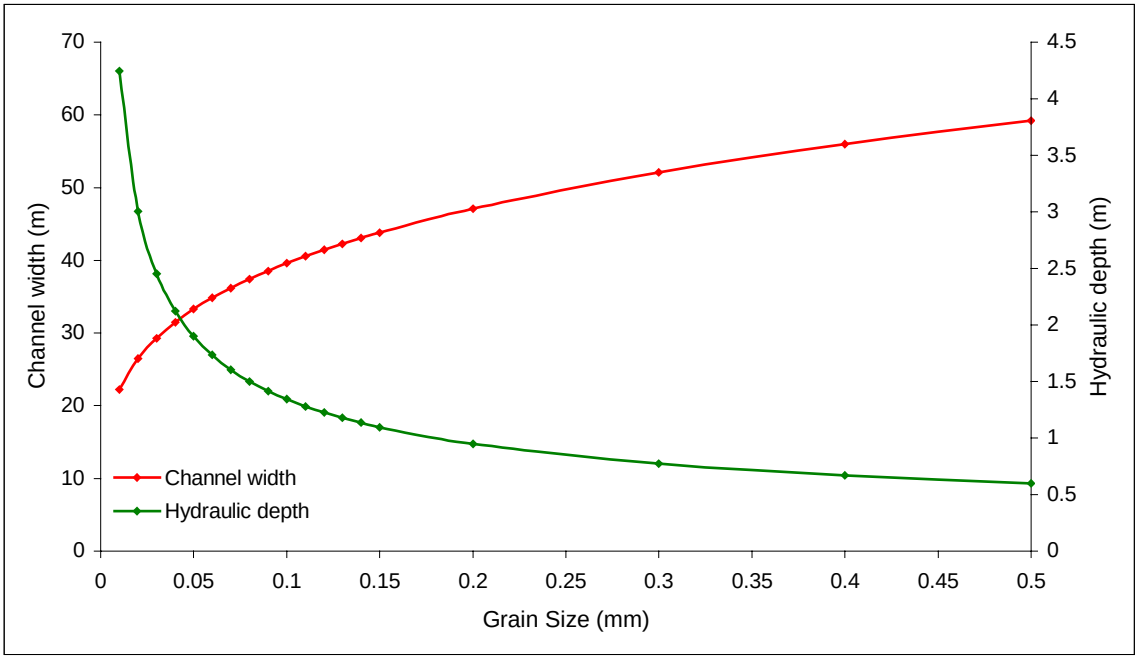

Figure 6.10: The influence of grain size variation on predicted channel width and hydraulic depth, calculated using the Inglis method.

Variable discharge throughout a tidal cycle caused a variation in the predicted channel sizes, relative to the stage of the tide (Fig. 6.11). The predicted channel width and hydraulic depth increased, as the discharge increased, resulting in a peak at HW when the discharge reached a

maximum. The predicted channel width (assuming D_{50} = 0.15 mm), using the Inglis method (from 10 to 44 m), was similar to that of the Yalin method (from 10 to 46 m), over a tidal cycle. There was more variability between the two approaches in terms of hydraulic depth, with the Inglis method ranging from 0.4 to 1.1 m, and the Yalin method being from 0.45 to 1.35 m. When the D_{50} was modified from 0.15 mm to 0.06 mm (the recorded mean grain diameter), the Inglis method predicts a notable change in the channel size (Figs. 6.11 & 6.12): the predicted maximum channel width decreased from 44 to 35 m, whilst the hydraulic depth increased from 1.10 to 1.75 m. The predicted final equilibrium channel using the Inglis method during the maximum discharge with the measured mean grain size, was a channel width of 34.8 m and a hydraulic depth of 1.74 m, giving a cross-sectional area for the channel of 60.6 m^2 (the measured cross-sectional area, 6 months after breaching, was 60.3 m^2).

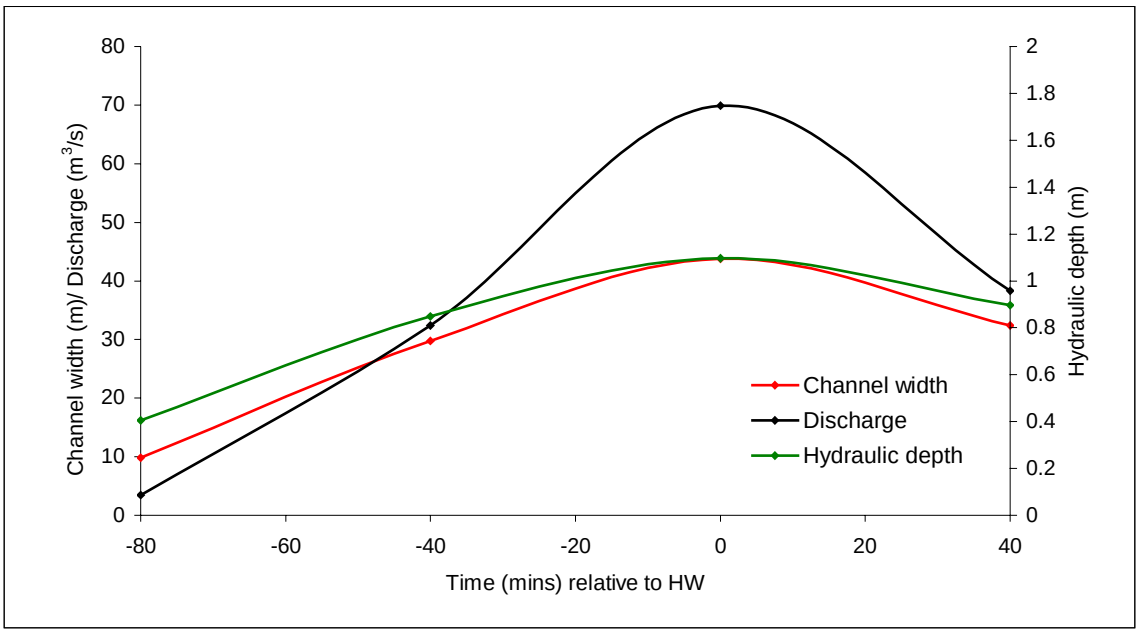

Figure 6.11: The variation in discharge flowing into the MR, over the flood of a measured tidal cycle (06/09/2002, am), with the calculated resulting variation in channel width and hydraulic depth calculated using the Inglis method (assuming a mean grain size of 0.15 mm).

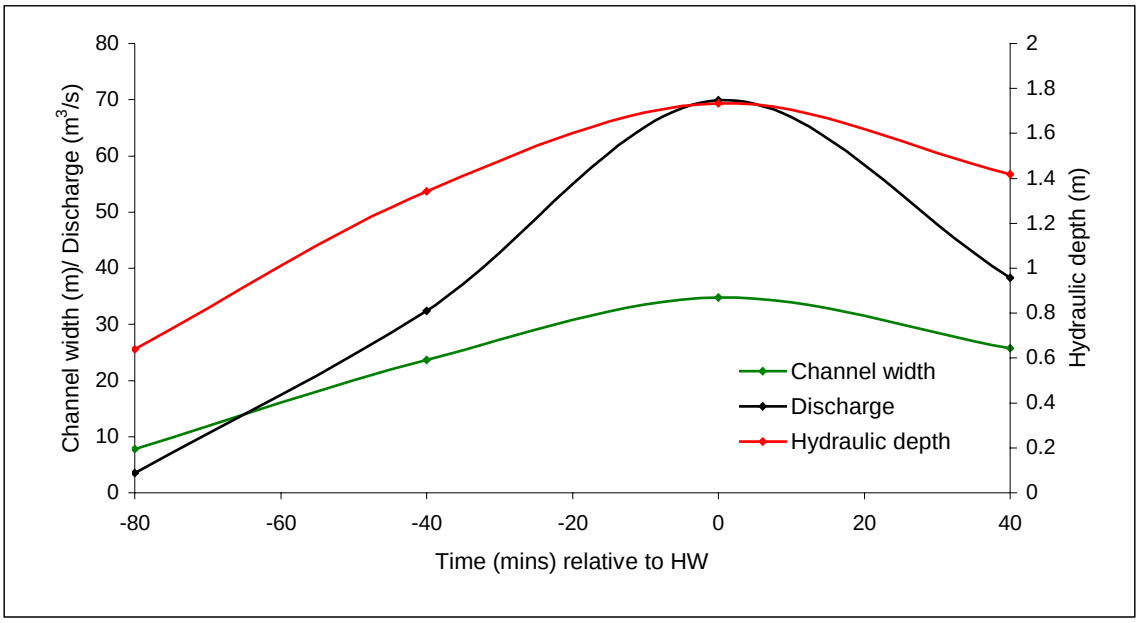

Figure 6.12: The variation in discharge flowing into the MR, over a measured tidal cycle (06/09/2002, am), using the measured mean grain size (0.06 mm). The resulting variation in channel width and hydraulic depth has been calculated using the Inglis method.

6.4.4 *Continuity Method*

On the basis of field observations, it was found that by high water during spring tides, the majority of the MR was submerged; as such, the value used for *P* was 780,000 m^2 (78 Ha). The site became flooded rapidly, because the area of the MR adjacent to the inner strengthened embankment was only 0.4 m higher than the area of the MR adjacent to the breached embankment, whilst the breaches were the same elevation as these highest points (Fig. 5.1), i.e. once the tidal height was sufficient to flow into the MR, it rapidly became fully submerged. From the ABR deployed inside the MR site, the highest recorded water level rise was 0.0003 m s^{-1}. The peak tidal current speed, measured in the channel within Breach 1, was 2.56 m s^{-1}; this was in a water depth of 1.25 m. On the basis of these measurements, it was predicted that an equilibrium channel width of 73.1 m would develop. However, 3 breaches were created in the seawall; thus, the equilibrium width of each of the channels would be 24.4 m. If the critical current speed is used (0.972 m s^{-1} from Eq. A7, in Townend, in press-a), then the width of the 3 breaches would be 192.6 m.

6.4.5 *Channel Shape*

The prediction of channel width, using the Inglis method and the most recent RTK-GPS measurement of the channel width, reveal that an equilibrium width of 30 m is appropriate to use for the prediction of the channel shape. The measured channel is used as an indication of the regime channel and is not the 'equilibrium' channel size or shape, but an approximation of it, as it was measured 3 years after the initial breaching of the embankment. The aerial

photography shows that the channels have widened since the measurements of the channel cross-section; however, it has not been possible to re-measure accurately the cross-section. The shape predicted by the Cao and Knight (1997) method was similar to that of the measured channel; as such, it appears to be capable of predicting the shape of the channel, in this particular example (Fig. 6.13). Nonetheless, this method is dependent strongly upon channel width and, if the prediction of the equilibrium channel width is inaccurate, then the channel shape will be derived inadequately. Figure 6.14 shows clearly that the channel shape did not vary with width; however, the maximum depth was dependent upon the predicted width.

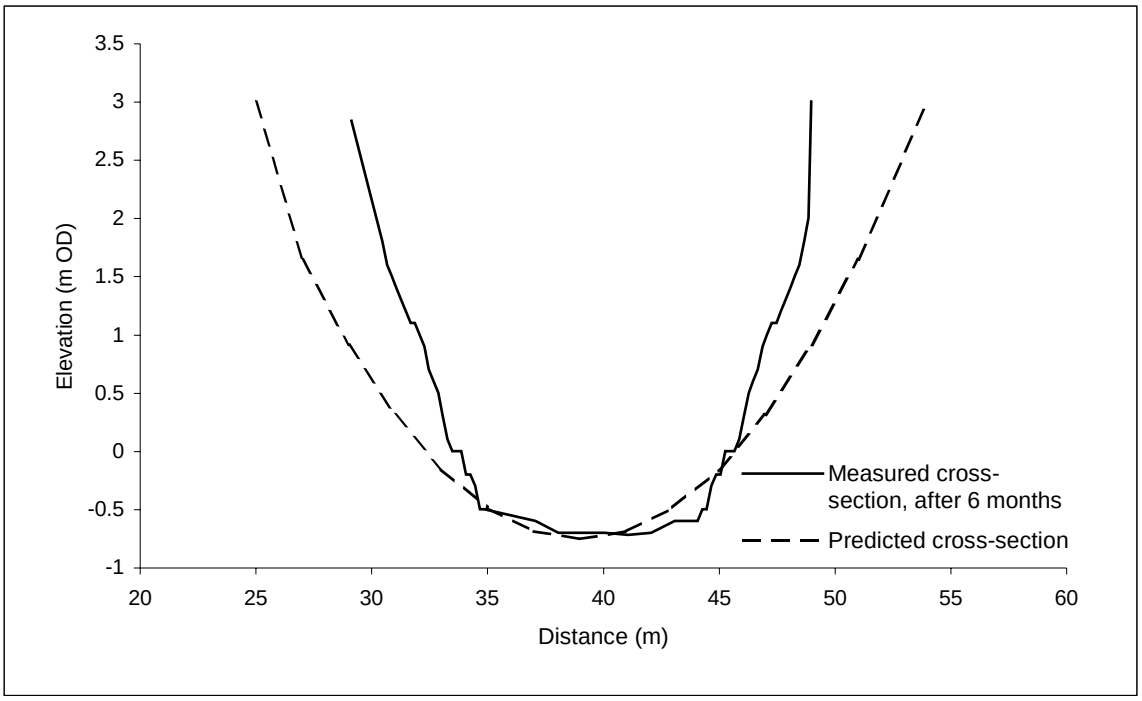

Figure 6.13: A comparison of the measured channel cross-section and the cross-section predicted using the width from the Inglis and Allen (1957) method and the shape from the Cao and Knight (1997) method.

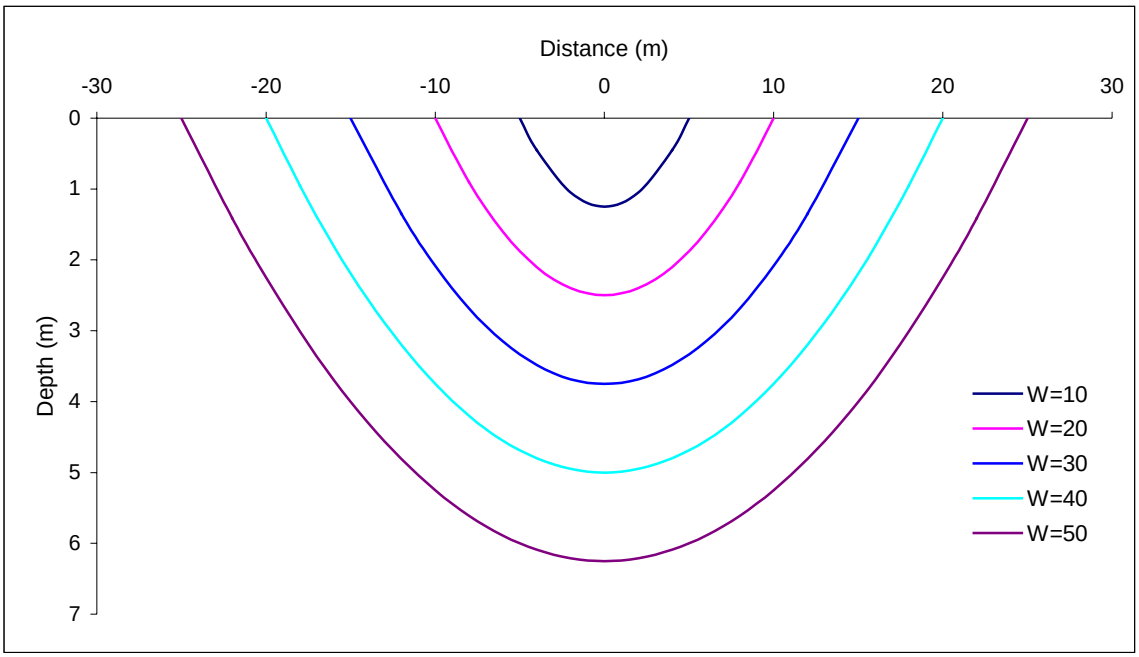

Figure 6.14: Showing how the Cao and Knight (1997) channel shape prediction varies with channel width.

6.4.6 *Comparison of Regime Theory methods*

During the 7 months following the initiation of the MR, the channel within Breach 1 was eroded, increasing its cross-sectional area by some 15 times. Figure 6.15 shows a cross-section through the breach, with the channel just after its formation and 7 months later. On the basis of frequent site visits, the majority of the change occurred during the first few months following the breaching of the seawall. The initial high spring tides caused the most dramatic erosion of the channel; since then, change has not been as obvious. It may be assumed that the eventual channel equilibrium will be similar to the cross-sectional profile, as measured some 7 months following the breaching. However, it is not known what the eventual equilibrium channel size will be, and how the long the process will take.

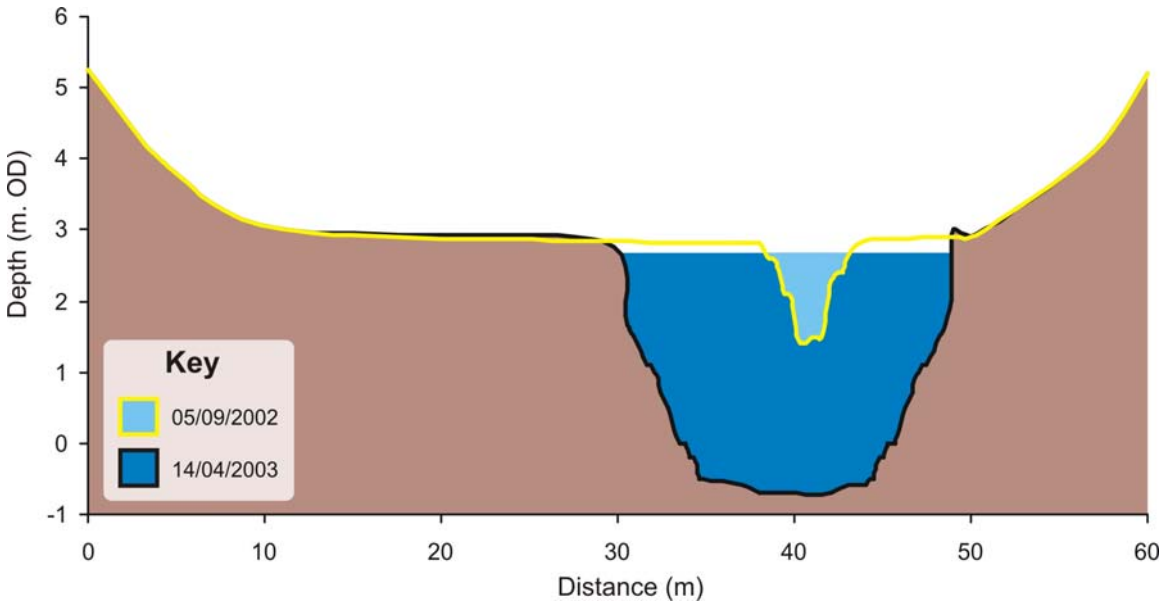

Figure 6.15: Cross-section of the channel within Breach 1, measured shortly after breaching and 7 months later (Note: the edges of the embankment are shown on either side of the channel).

On the basis of experimental research, it has been found that $T_0 < \sim 0.01 T_R$ (Shimizu, 1991; cited in Yalin and Ferreira da Silva, 2001); where T_0 = adjustment period of the channel, and T_R = the time for channel equilibrium to be reached. Hence, if it is assumed that the adjustment period of the channel within Breach 1 was reached after the first set of high spring tides, which lasted 7 days, this relationship would indicate that it takes at least 700 days for channel equilibrium to be reached. However, these 700 days would need to coincide with spring tides, of sufficient height to flood the channel in the breach. About 40 % of all the tides occurring at Freiston Shore are of sufficient height (Fig. 6.16). Hence, the method predicts that it will take at least 1750 days, i.e. nearly 5 years, for channel equilibrium to be established.

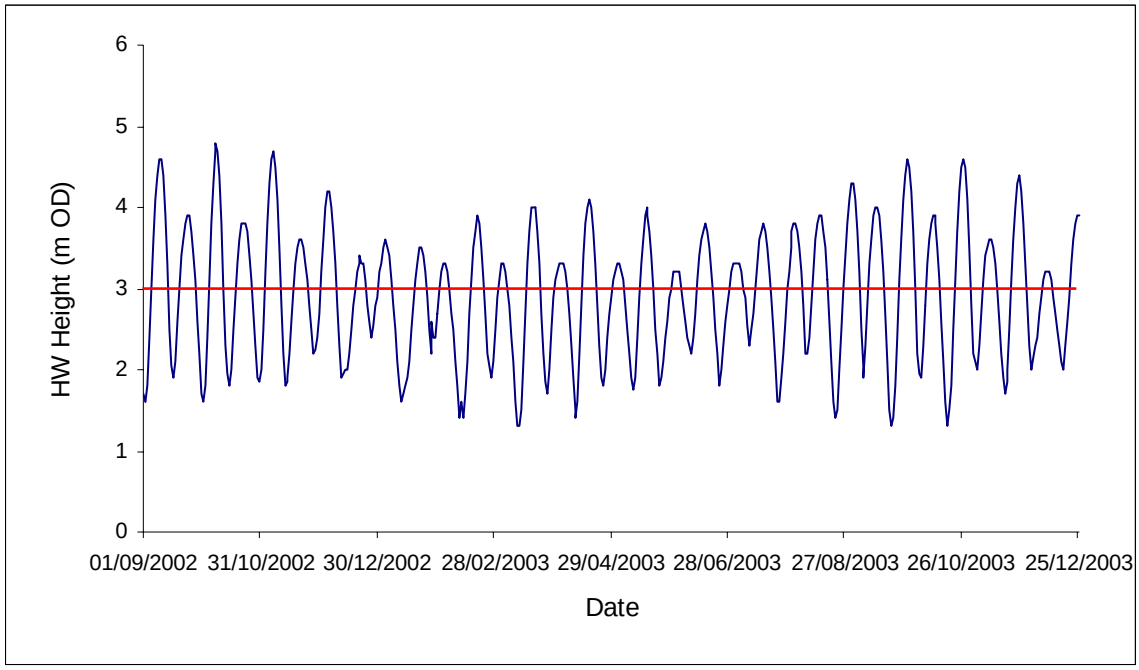

Figure 6.16: The tidal height at HW, over a 15 month period, abstracted from the Boston (Dock Sill) Tide Tables (Note: the red line represents the height necessary for flow into the MR site).

The predicted dimensions of the equilibrium channel were calculated, using both regime methods (Fig. 6.17) with the measured data (initial cross-section; current speed; and grain size); these have been plotted against the cross-section measured on 14/04/2003, which has been used to provide an approximate guideline for the equilibrium channel. The Yalin method predicted a wide, deep channel, with a cross-sectional area of 233 m^2 over 3 times the size of the measured channel (60.3 m^2). In contrast, the Inglis method predicted a much narrower and shallower channel; this was wider than the measured channel, but shallower, with a cross-sectional area of 60.2 m^2. The channel predicted through applying the Yalin method was much larger than the measured actual channel size; this can be explained on the basis of the grain size used in the calculation; as stated previously, this method does not provide accurate predictions for grain sizes of less than 0.15 mm. Further, the channel dimensions were predicted again using the Yalin method, with a grain size of 0.15 mm (Fig. 6.18). This latter approach predicted a comparable channel cross-sectional area of 63.6 m^2 to that derived using the Inglis method and to the measured channel.

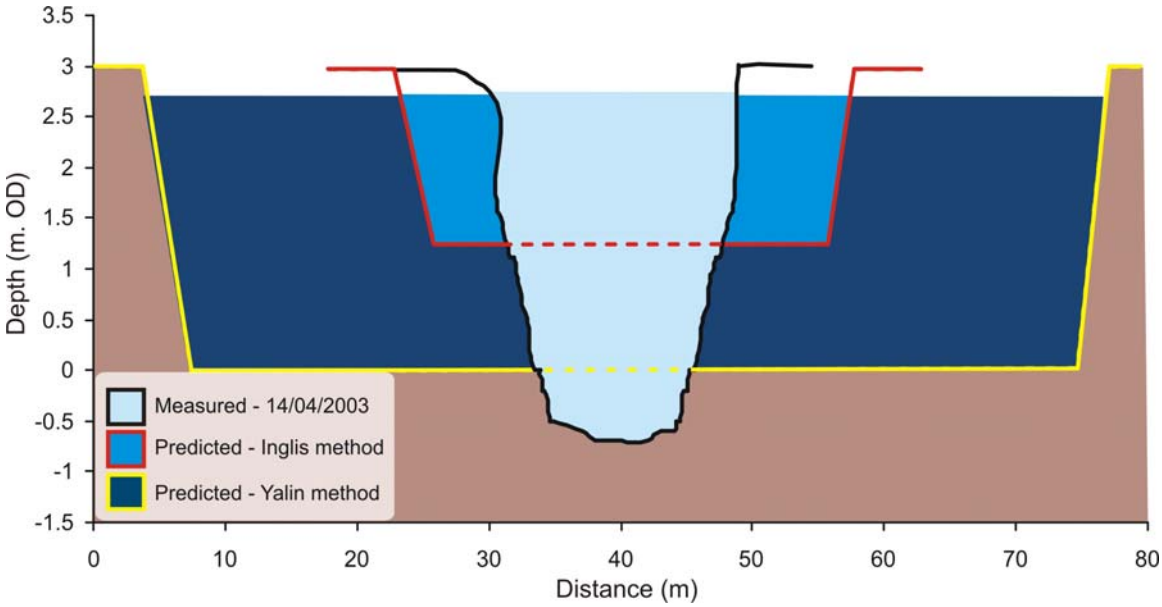

Figure 6.17: The predicted and measured cross-section of the channel within Breach 1 (using the measured cross-section and currents), using both methods for calculating the equilibrium channel (adopting a mean grain size of 0.06 mm).

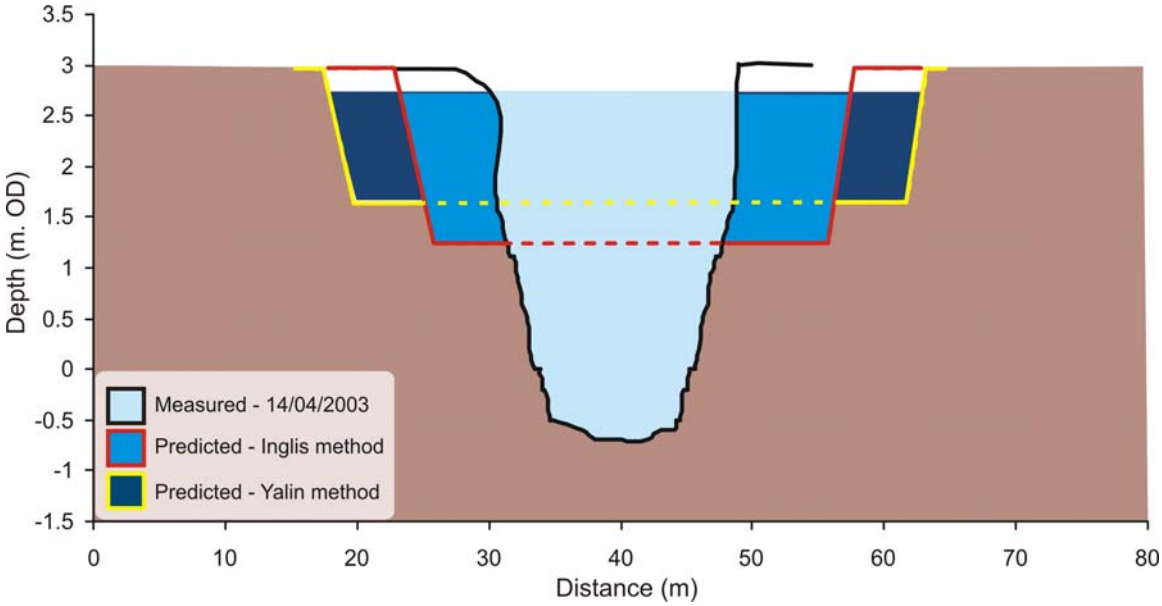

Figure 6.18: The predicted and measured cross-section of the channel within Breach 1 (using the measured cross-section and currents), with the Inglis method assuming a grain size of 0.06 mm and the Yalin method assuming 0.15 mm.

The grain size used in the calculation of channel size was varied, to observe if the channel shape could be simulated, without altering the method of calculation (Fig. 6.19). The Yalin method was incapable of reproducing the measured channel shape, as it could not predict a deep, narrow channel. The most appropriate channel shape was achieved using a mean grain size of 0.25 mm; this was twice the width of the actual measured channel, with a cross-sectional area of 83.6 m^2. The Inglis method was capable of predicting similar channel

dimensions to those measured, using a grain size of 0.01 mm; this was equivalent to the D_{10} (at which 10 % of the sediment was finer) value.

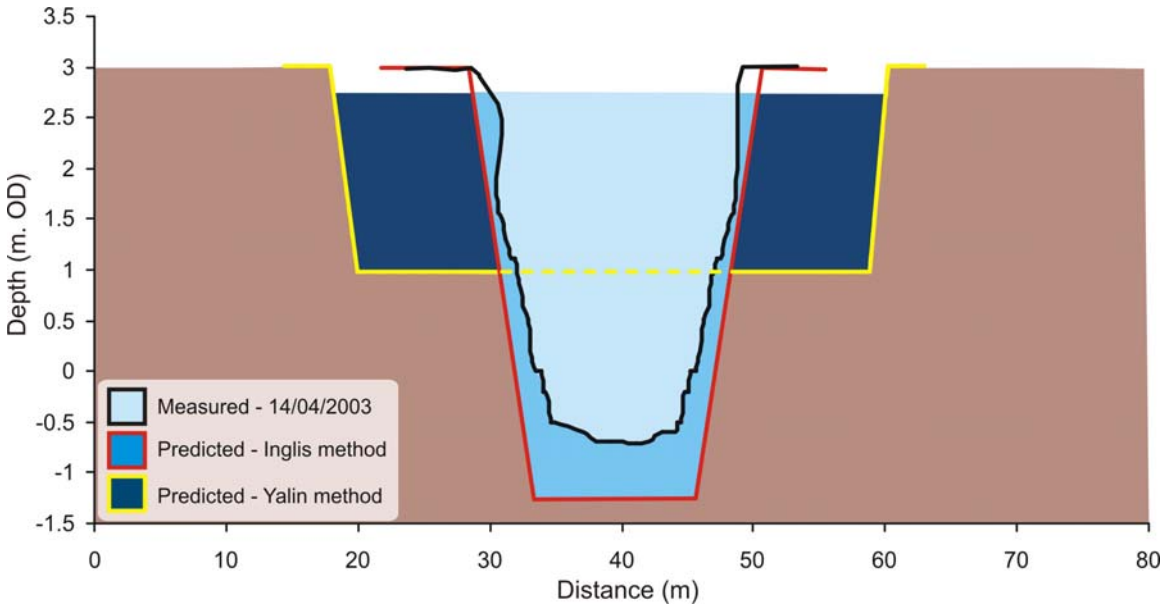

Figure 6.19: A cross-section of both the predicted and measured equilibrium channels within Breach 1, with the mean grain size being varied to provide the closest possible correlation with the actual measured channel (Inglis method, D_{50} = 0.01 mm; Yalin method, D_{50} = 0.25 mm).

6.4.7 *Changes in the Plan Form of the Channels*

Another method used to study the evolution of the channels within the breaches, was to examine their change in terms of their plan view area. These data were derived on the basis of geo-referenced vertical aerial photography, combined with RTK-GPS measurements. The change in the plan view area of the channels, within the breaches, provides a further indication of the rate of change of the channel dimensions. Thus, an indication is provided as to whether the channels are reaching equilibrium, or still undergoing change.

The (3) channels within the breaches underwent a rapid phase of erosion, during the first 1 – 2 months following the initiation of the MR scheme (Fig. 6.20). Subsequently, the channels continued to erode at a relatively linear rate, for ~10 months. The channels within Breaches 1 and 3 have since remained relatively stable, with only a small increase in the plan view area of the channel within Breach 3, from the most recent measurements. In contrast, the channel within Breach 2 (the middle channel) continued to erode, at a slightly reduced rate to that of the initial rapid erosion. This rate of change has fluctuated, but has remained relatively high, throughout the 27 months of measurements. In addition to this continuing rate of erosion within Breach 2, the natural creek to which it is connected has undergone erosion; it has increased in width, from ~ 5 m to ~ 25 m (Fig. 6.21). This pattern of change has meant that the potential discharge entering and leaving the channel has increased. The channel is still

being subjected to rapid erosion; thus, it does not appear to be reaching, at the present time, dynamic equilibrium. The natural creeks connected to the channels, within Breaches 1 and 3, have experienced erosion, but to a lesser extent. These natural creeks have not been eroded as dramatically as the natural creek connected to Breach 2; they widened and deepened to double their size, from a width of 3 to 6 m and a depth of 2 to 4 m (Plate 6.4).

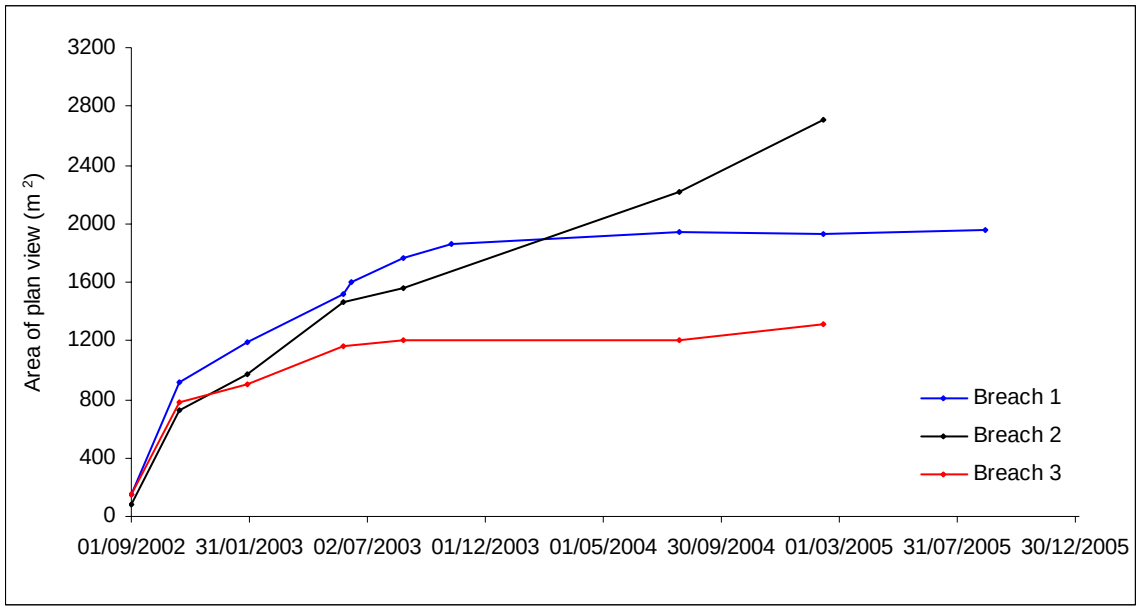

Figure 6.20: The plan view area of the channels within the 3 breaches, over time (Figure 6.21 shows how plan view area increases while channel width remains similar).

In addition to calculating the plan view area of the channels, through the RTK-GPS and aerial photography, the widest point of the channel was also recorded for the 3 channels within the breaches (Fig. 6.22). Interestingly, all the (3) channels have increased in their width at relatively constant rates, following the initial rapid erosion. The channels within Breaches 1 and 3 have both increased in their width, at similar rates. The channel within Breach 2 has increased in its width at a more rapid, but less constant rate.

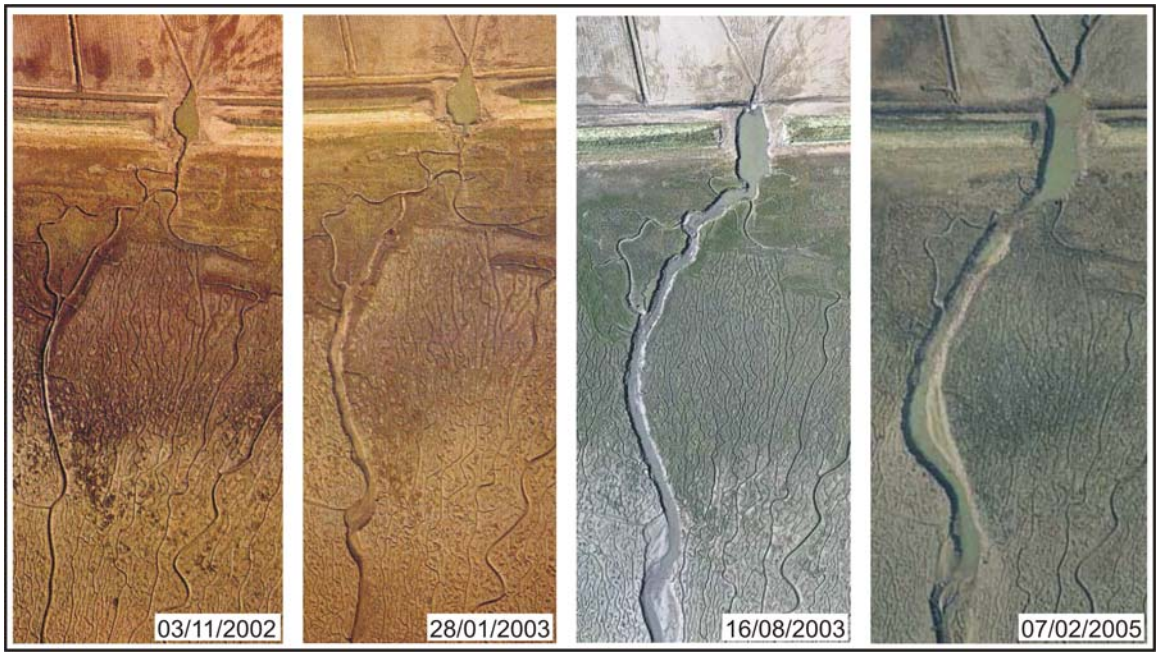

Figure 6.21: The plan view of the channel within Breach 2 and the natural creek it is connected to, based upon systematic aerial photography, over a 2 year period following the initiation of the MR. Note: for scale the embankment was 20 m wide.

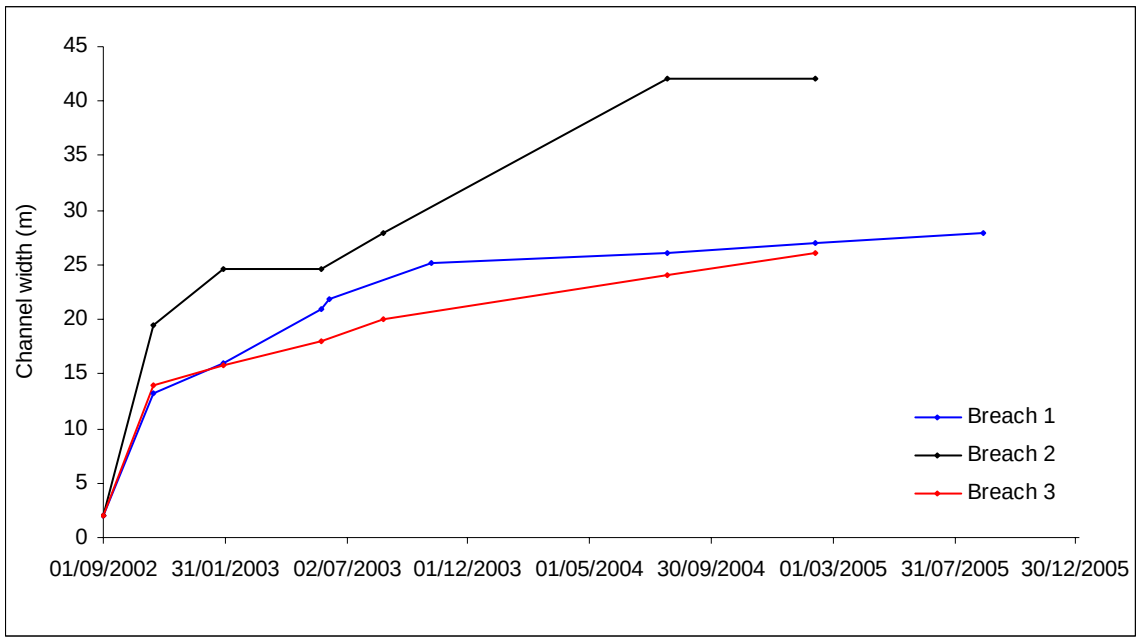

Figure 6.22: Change in the peak width of the channels within the breaches, over the area affected by erosion, over time; this has been extrapolated from aerial photography, together with RTK-GPS data.

6.5 DISCUSSION

The main period of erosion in the channels within the breaches occurred during the first few months, following the breaching of the embankment; during this time, they eroded to some 10 – 15 times their original sizes. Since this period of rapid erosion, the rate of change diminished; this is consistent with the findings of a laboratory experiment undertaken by

Shimizu (1991; cited in Yalin and Ferreira da Silva, 2001), where it was stated that a channel will undergo a period of rapid erosion, followed by a much longer period of smaller changes. Using the relationship derived from this study, it was predicted that it would take 5 years for the channels to reach dynamic equilibrium. This expression has not been used in any other field-based studies, so no comparisons can be made. However, a natural retreat at Motney Hill, in the Medway Estuary, Essex, UK, was subject to high levels of erosion inside the breached site, which was found to be still eroding some 70 years following the breaching (French, 1999). The breached site had been reclaimed several centuries earlier, and was lower than the marshes of the estuary, owing to compaction and dewatering. This, combined with the tight confines of the original breach, created strong currents on the flood (as seen at Freiston Shore) and ebb, and led to a rapid initial rate of erosion inside the breached site. Despite the similarities between Motney Hill and Freiston Shore, the changes associated with the natural and managed realignments were different, i.e. the erosion at Motney Hill was focused inside the breached site, while at Freiston Shore it was predominantly around the breaches and over the intertidal flats. Owing to the differences between the sites, it is proposed that the site at Freiston Shore may reach a dynamic equilibrium much more rapidly than was achieved at Motney Hill, with the prediction of 5 years remaining realistic.

On the basis of the analyses in this chapter, it has been demonstrated that deriving an equilibrium channel, through the regime theory, is somewhat difficult. Such predictions are highly sensitive to the variables used in their calculation; as such, it is important to utilise highly accurate data in the calculations. The Inglis and Allen (1957) method for calculating the width and hydraulic depth of the equilibrium channel, combined with the Cao and Knight (1997) method for predicting the channel shape, gave the most realistic predictions to what the eventual channel equilibrium is thought to be. For the Inglis and Allen (1957) method to provide meaningful results, accurate measurements of the mean grain size and water discharge need to be obtained. These combined methods have provided realistic results for this particular study, but require validation for other sites. The results obtained for the regime channel, for the present investigation, are based upon the assumption that the channels equilibrium will be similar to that of their present form; and they are not to undergo any other dramatic change.

There are other methods to calculate the regime channel equilibrium that have not been used in this study; however, they have been highlighted as possible methods for predicting breach dimensions at future MR sites (Townend, in press-a). These methods use the hypsometry of the site to calculate the profile of the MR site (Townend, in press-b). The most reliable of these methods for predicting the breach width was applied at Freiston Shore; however, it was

unable to predict as deep a channel as measured (Townend, pers. comm., 2006). There are two possible reasons for the channels within the breaches being much deeper than expected:
(i) the profile of the intertidal flat was in regime with the natural conditions (prior to the MR), and the increased water flow over the intertidal flats, from the drainage of the MR, caused the natural creeks to be scoured out, which, in turn, caused the bed of the channels within the breaches to be eroded. This created a much lower intertidal flat profile within the creeks and the channels within the breaches, allowing the intertidal flats to drain more rapidly; and
(ii) the sediment under the embankment was very stable and well compacted, with concrete reinforcements present, which would hinder the lateral erosion of the channels within the breaches, forcing vertical erosion.

The best method for predicting the size and shape of breaches in embankments, as part of the MR scheme at Freiston Shore, was through using the Inglis and Allen (1957) method to predict the channel width and hydraulic depth and the Cao and Knight (1997) method to calculate the channel shape. To use the Inglis and Allen (1957) method, a rate of flow into the MR site is necessary; this can be calculated through constructing a probable hypsometry using the total plan area and volume (Townend, in press-b). The tidal prism method (Equation 6.2) used in the design of the MR at Freiston Shore, predicted a necessary breach width of 152 m; this would have been a sufficient width for the breaches, if the MR site had not been lower than the saltmarsh (Section 5.2). Despite this method predicting a realistic breach size at Freiston Shore, this type of approach does not incorporate sufficient information about the site conditions (sediment type and site hypsometry), and so for predicting the necessary size of future breaches in embankments this type of approach has limited applicability.

The erosion of the channels within Breaches 1 and 3 has, at the present time, reduced; in comparison, the channel within Breach 2 maintains a relatively constant rate of erosion. Breach 2 appears to have become the dominant drainage route, and, as such, it is where the majority of flow is focused during the draining of the MR site. This pattern could be owing to: (a) the topography of the site, focusing the flow into this particular breach; or (b) the channel being connected with the most efficient natural drainage creek, allowing more discharge to leave the MR than Breaches 1 and 3. In addition to the continued erosion of the channel within Breach 2, the natural creek to which it is connected has also experienced erosion; this, in turn, is considered to be primarily a result of the MR site drainage scouring the creek. Some erosion has been experienced in the natural creeks connected to the other breach sites, but it has not been as extensive. Such dominance of one of the breaches would

be difficult to predict, making the regime theory for sites with multiple breaches an even more complex problem.

During the development of the channels, some difficulties were encountered in measuring accurately the changes occurring to the channels; in particular, the cross-sectional profile and the hydrodynamics within the channels. Such a limitation has restricted the analysis of changes in the channels, for the validation of the regime models. A particular omission was the lack of knowledge of the flow discharge during a range of spring tides, as the ABR was scoured out of the channel bed. The main control on the development of channels within the breaches appears to be the tidal height, controlling the flow entering the channels, together with its duration. Predictions for the equilibrium channel width and shape were obtained. However, as the channels have yet to reach an equilibrium, it is unknown if these predictions are realistic. Continued monitoring of the channels within the breaches is necessary, as well as the validation of this particular method at other MR sites.

6.6 CONCLUDING REMARKS

The channels within the breaches in an embankment, eroded following the initiation of a MR scheme. The erosion was rapid in the initial few months following the breaching, after this, a more constant rate of erosion was experienced, with the most recent measurements showing channels up to 20 times wider than they were originally. It has been predicted that it will take 5 years for the channels to reach a dynamic equilibrium.

Deriving the dimensions of an equilibrium channel, through the Regime Theory, can provide both realistic and unrealistic predictions. The method is sensitive to the input values, so care must be taken in using accurate measurements. To predict the necessary width and hydraulic depth for future MR breaches it is advised that the Inglis and Allen (1957) method is used, with the Cao and Knight (1997) method then being applied to calculate the channel shape. However, care must be taken as these methods have not been tested extensively and may not be applicable at all sites.

In cases where multiple breaches are made in an embankment, it must be remembered that the breaches may develop at different rates. At Freiston Shore all 3 breaches developed differently, with the central breach eroding to become nearly twice as wide as the others. Even if an accurate prediction for breach width is achieved for the site, some breaches may silt up while some may erode, owing to variations in the local topography and drainage patterns.

The main controls on the size of the breaches necessary for a MR site are the site hypsometry, the tidal range and the sediment type. However, many potential MR sites are in areas of alluvium, and the cohesive nature of these sediments remains poorly understood and highly variable. The sediment making up embankments may or may not be of a local source and could also be at varying levels of compaction and drainage. Thus more detailed research is required into the properties of sediments at potential MR sites.

6.7 PLATES

Plate 6.1: A seaward view of the channel within Breach 1, shortly after it was created (22/08/2002). Note: the width of the channel at the bed was 2 m.

Plate 6.2: A seaward view of the channel within Breach 1, some 2 months after the initiation of the MR scheme (October 2002). Note: the width of the channel was 20 m.

Plate 6.3: A seaward view of the channel within Breach 1, from the most recent site visit (05/09/2005). Note: the widest point of the channel was 28 m.

Plate 6.4: The point in the natural creek connected to the artificial channel within Breach 1, where the channel has been eroded (25/11/2003). The photograph is looking landward, the flow in the creek is from the drainage of the MR site. Note: the creek to the right is approximately 3 m in width, whilst the eroded area varies, in width, from 6 to 10 m.

CHAPTER 7: THE ENHANCED DEVELOPMENT OF A CREEK SYSTEM OVER AN INTERTIDAL ZONE, IN RESPONSE TO MANAGED REALIGNMENT

7.1 INTRODUCTION

Research into intertidal creek formation has been focused mainly in estuarine environments, which experience limited creek development on mudflats and sandflats. However, insufficient research has been undertaken over wider intertidal zones, with extensive sandflats and mudflats; here, different processes and formations occur compared to the estuarine environments. From the previous work it was found that a number of variables are important in the development of creek networks: position relative to the tidal frame; slope of the intertidal zone; type of sediment; and the water and sediment yield. If these variables, or any factors controlling these variables, undergo a sudden change, then creeks over the intertidal zone may experience change. The breaching of a coastal embankment has caused a change in these variables, leading to an unbalance in the system. In turn, this should result in a change in the system, and an eventual new dynamic equilibrium being reached.

A unique data set is available for this study, allowing an investigation into the development of an intertidal creek system under natural conditions, over a 10 year period; likewise, over a 3 year period following anthropogenic modification to the system (in the form of a managed realignment). The 2 periods of creek development will be compared, to see if the anthropogenic changes to the system have impacted the creek system over the intertidal zone.

7.2 BACKGROUND

Following the MR, high flood current speeds (2.5 m s^{-1}) were experienced in the channels within the breaches, during the initial high spring tides (Chapter 6). Following HW during the spring tides soon after the breaching of the embankment, the MR site acted as a "reservoir", gradually releasing water through the channels in the breaches during the falling stage of the tide through to the following HW (Section 5.2). This "unnatural" discharge enhanced sediment dynamic processes over the adjacent intertidal zone (Symonds and Collins, 2005). The natural creeks, which were connected to the artificial channels in the breaches, were full throughout much of the LW period. This pattern led to excess water escaping from the creeks, by overbank flow (Plate 7.1); this, in turn, caused overland sheetflow to occur on the exposed intertidal zone (Plate 7.2). Such flows become concentrated into natural gullies and existing creeks, over the lower intertidal zone, causing an enhancement in the natural creek development (Plate 7.3).

7.3 METHODS

Combinations of past (prior to the MR) and recent (since the MR) data were used in the present investigation. The past data were obtained from aerial photography (1:5000 scale), collected every 6 months on behalf of the EA, since 1991; these provide a generalised summary of the creek development before the MR. In addition to the use of photography, an innovative measurement technique was used to record changes in the evolution and development of the tidal creeks. An RTK-GPS was used, with backpack positioning and logging devices, to collect high-resolution positional data, to complement and validate the aerial photography. From these data, the headward extension rates of the creeks were calculated, using the first survey as a baseline. Following each survey, the total landward extension was established for each creek, relative to the initial survey; this provided the total headward extension rate, over that period. These values were used also to predict the annual headward extension rate. A transect was measured, to establish the cross-sectional area of the creeks, which were then compared over time.

7.4 RESULTS

7.4.1 *Aerial Photography*

On the basis of the aerial photography, the development of the creek system before and after the MR were examined and compared. Three sets of aerial photographs were used to establish creek evolution on the intertidal zone, since the initiation of the MR; only the results from the major creeks are shown, to simplify the diagram. The first aerial photograph was obtained 1 month before the MR, the second 2 months after and the third 5 months after. The main areas of change were the small creek systems in Zone B and their associated larger drainage channels (Fig. 7.1). The other areas of change were the channels in the breaches in the embankment (Chapter 6), as highlighted by the erosional Zones A.

The main reason for the enhanced development of the creek system over the intertidal zone was a difference in levels between the MR site and the adjacent saltmarsh (Section 5.2). This caused ‘unnatural’ flows to occur in the natural creeks connected to the artificial channels in the breaches, which led to overbank flow occurring at points along the creeks; the most notable of these was on the creek connected to the Breach 1. Water flowed over the bank on a tight meander bend, and then, by overland flow, it travelled over the intertidal zone (the ‘inferred flow’ over the intertidal flats, on Fig. 7.1). It was this flow which appears to have caused the enhanced creek development and has only existed since the MR was initiated.

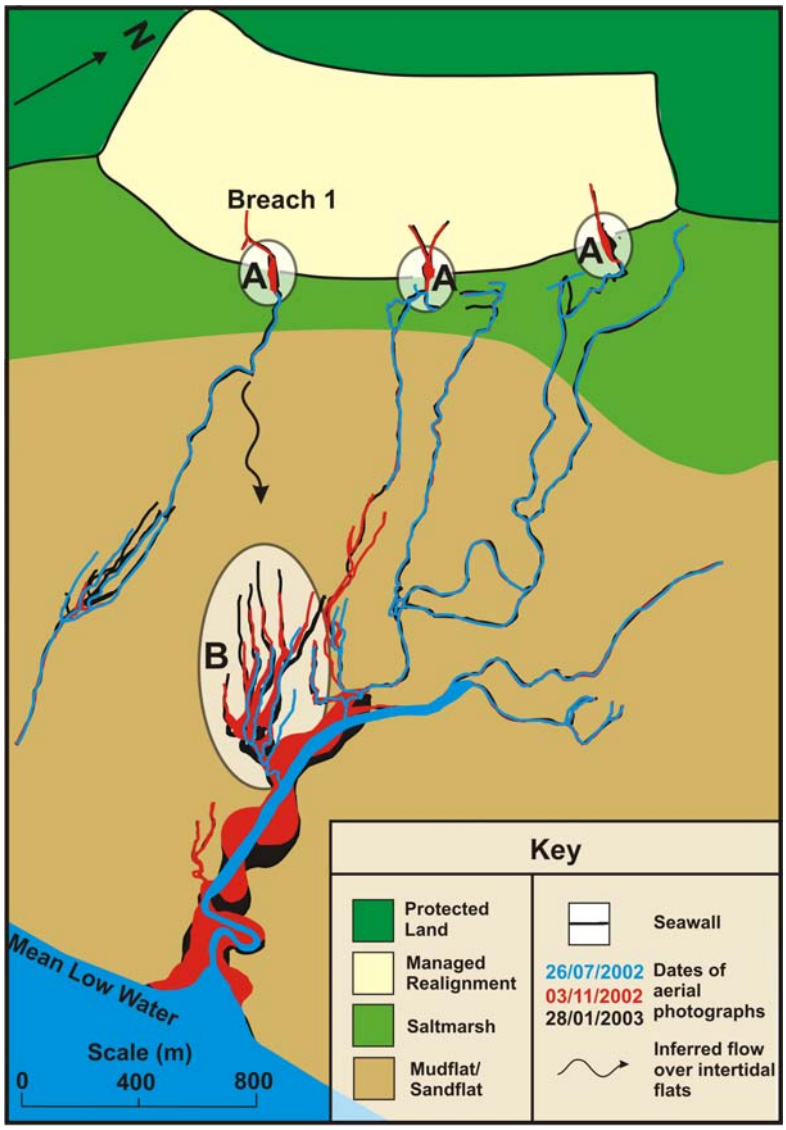

Figure 7.1: The development of the creeks over the intertidal zone, based on sequential aerial photography. Note: Zones of different erosional processes are highlighted by A and B (see text).

Due to the nature of change experienced in Zone B, this area has been examined in more detail using aerial photography, both before and after the MR. The creek patterns on Figure 7.2, row A, show the creek system before the MR was initiated, whilst row B shows it after the MR was completed. The lines represent the main axis of the creek; for simplicity of representation, there is no relationship between the line width and the width of the creek. Over the 10 years before the MR, the creek system in the south corner of the diagrams (Fig. 7.2) extended some 160 m; most of this occurred between 1992 and 1998. Between 1998 and 2002, the creek system became more complex through the addition of tributaries. Since the MR, the rate of headward extension and the drainage density have increased dramatically, with some 380 m of headward extension between 26/07/2002 and 31/05/2003. In addition, the creek system which originates in the centre of the diagrams and extends to the northwest, was relatively stable prior to the MR, and had by 28/01/2003 extended to the seawall.

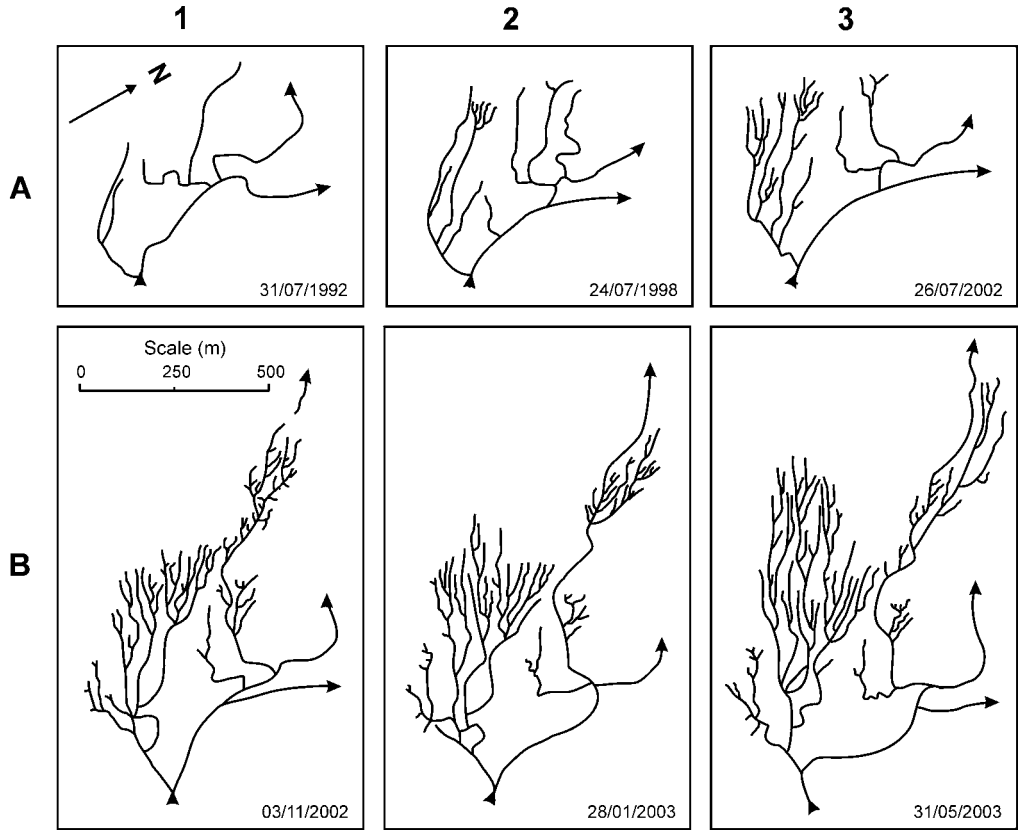

Figure 7.2: The development of a creek system, extrapolated from sequential aerial photography, within the lower intertidal zone at Freiston Shore: with the creeks in (A) and (B) being before and after the MR, respectively. The arrows represent flood flow through the creeks.

7.4.2 *RTK-GPS*

The overall headward extension of the creeks within Zone B over an 18-month period, are shown in Figure 7.3. The distances are expressed in terms of being relative to the distance the creek has extended since the baseline survey, some 3 months after the breaching; at this time, some extension is likely to have already taken place. From the data presented, two different processes appear to be occurring within the creeks. The headward extension rates in Creeks 2 and 3 have increased logarithmically. However, the extension in Creeks 1 and 4 has decreased exponentially, i.e. the most recent measurements appear to indicate a cessation in headward extension. It is also worth noting that the overall distances of extension vary between the two sets of creek; with Creeks 2 and 3 having extended around 600 m each, and Creek 1 having extended only 200 m, and Creek 4 only 60 m.

The annual headward extension rates appear to indicate that Creeks 1 and 2 were initially dominant. Following the first survey, a change was experienced and Creek 3 became dominant (Fig. 7.4). Over the summer of 2003 (June to October), the rates of extension reduced dramatically in all the creeks, e.g. in Creek 3 it dropped from 490 m yr^{-1}, to 120 m yr^{-1}. Over the following 6 months, the rates in Creeks 2 and 3 increased to 350 m yr^{-1}; in comparison, the other creeks had negligible rates of headward extension (< 50 m yr^{-1}). The

latest measurements, from September 2005, showed that the creeks were no longer extending in a headward direction, without any "nick points" to identify their most headward location. Instead, they joined with small drainage runnels over the upper intertidal zone (Plates 7.4 & 7.5). In the absence of a "nick point", the creek lengths could not be established. As such, measurements of the cross-sectional area and the profile of the thalweg are discussed below, to represent the creek development.

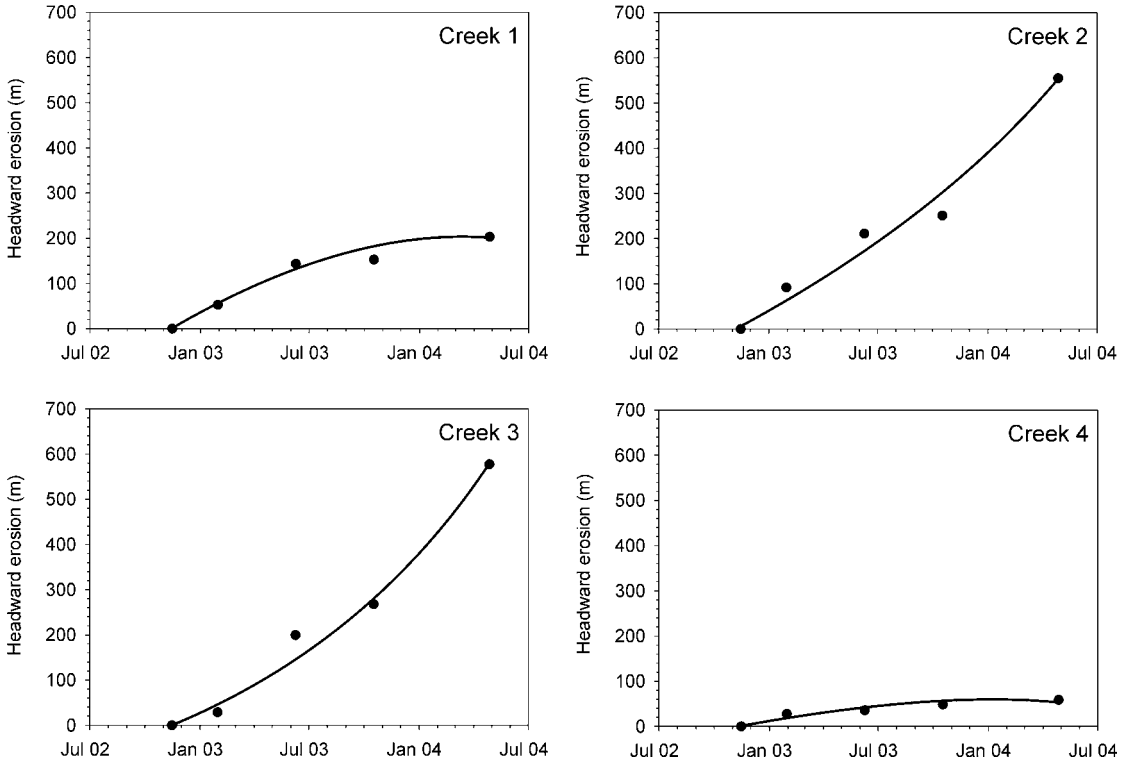

Figure 7.3: Total headward extension of the 4 creeks in erosional Zone B (see Fig. 4.1 for creek labelling), since the first measurements (15/11/2002).

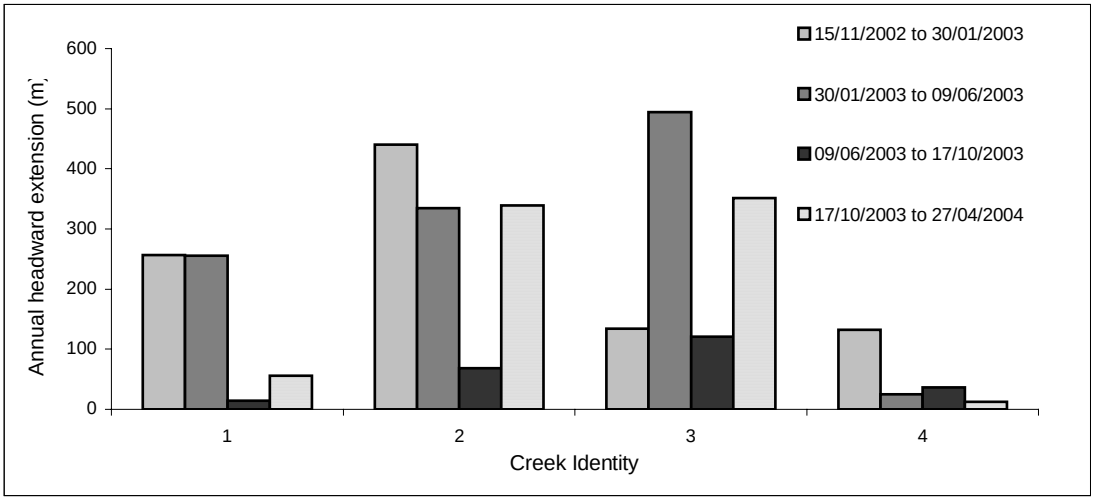

Figure 7.4: Calculated annual headward extension rates for the surveyed creeks, over an 18-month period.

The surveys show that the cross-sectional areas of Creeks 1 and 4 have exhibited similar patterns of change (Fig. 7.5). Following a period of rapid erosion, between September and November 2002[1], the cross-sectional areas of these creeks have gradually reduced. Creek 4 showed an initial period of erosion, from November 2002 to the end of January 2003; following this, it has been silting up. In contrast, the cross-sectional area of Creeks 2 and 3 continued to erode rapidly, from November 2002 until October 2003 (Creek 2) and April 2004 (Creek 3). Between then and the measurements undertaken in September 2005, the creeks have been silting up rapidly. The cross-sectional areas of Creeks 2 and 3 have fluctuated by 9 and 13 m^2, respectively, over the 3 years. The final cross-sectional area of Creek 3 is very similar to its original size. Overall rates of change were not as great at Creeks 1 and 4, where the cross-sectional area varied by 6 and 3 m^2, respectively. The shape of the Creeks 2 and 3 changed with the cross-sectional area; steep sided, deep creeks (1.5 m) were present during the highest rates of change in area (June to October 2003); these changed to being much shallower (0.75 m), with gently sloping banks, following the period of extensive siltation (Fig. 7.6).

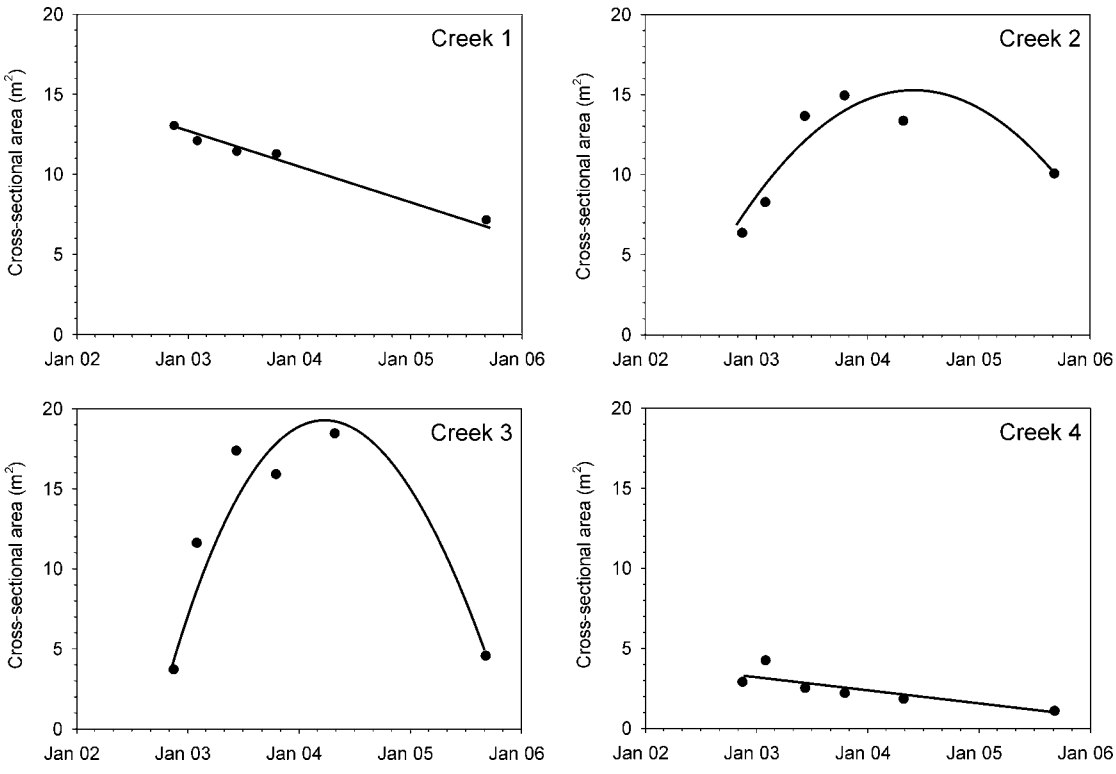

Figure 7.5: The cross-sectional area of the creeks in Zone B, across a transect (Fig. 7.6), over a 3 year period. Note: due to an equipment problem, no measurement was undertaken at Creek 1 in April 2004.

[1] It was not possible to measure this change, as it occurred unexpectedly and very rapidly. Over a 5 day period the creek system changed, from being small drainage runnels to relatively substantial creeks (Plates 7.2 & 7.6).

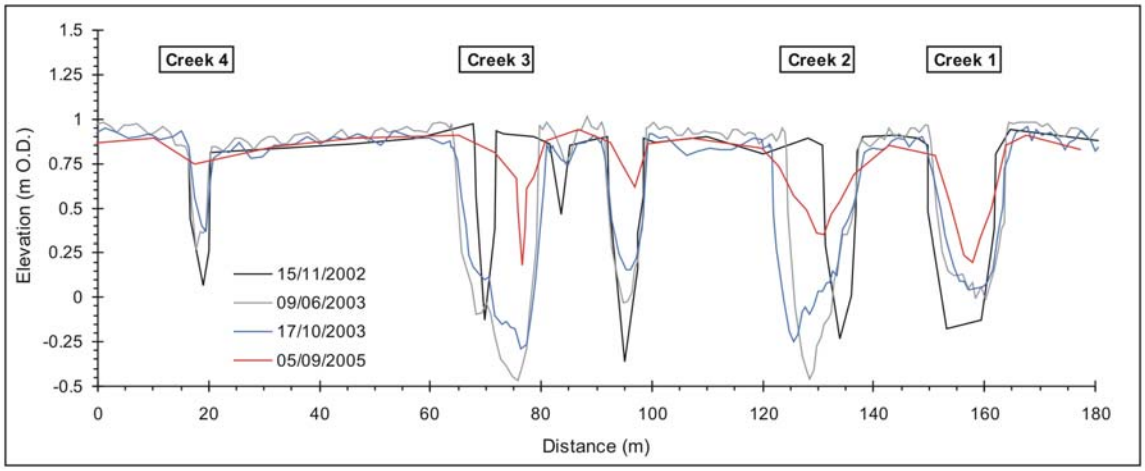

Figure 7.6: Transects across the creek system on the lower intertidal zone, with 4 measurements over a 3 year period.

The rate of the headward extension and the change in bed level of the creeks is shown in the profile of the thalweg (Fig. 7.7). This data set emphasizes the quantity of sediment eroded, during the headward extension of the creeks; likewise, that deposited when the creek system silted up. Once again, Creeks 2 and 3 are shown to be the dominant creeks, eroding and accreting more rapidly than Creeks 1 and 4. Within Creeks 2 and 3, some 0.5 – 1 m of sediment was deposited on the bed, over a 500 m length, between October 2003 and September 2005; in comparison, Creeks 1 and 4 had a maximum of 0.25 m of sediment deposited, over the same period. Sediment deposited in Creek 2 can be seen by comparison of photographs taken during *Deployment 3* (24/11/2003) and during the most recent RTK-GPS measurements (05/09/2005). Interestingly, a scaffold pole deployed originally in Creek 2 (in 2003) was only just visible in 2005; this shows that at least 0.5 m thickness of sediment has been deposited (Plates 7.7 & 7.8).

On the basis of the assumption that the erosion/accretion rates, calculated from the creek cross-sections, are uniform along the length of the creeks, the volumes of sediment change were estimated. Over the 3 year period, 2,060 m^3 of sediment accreted in Creek 1. Some 3,650 m^3 of sediment was eroded between November 2002 and October 2003, whilst 2,500 m^3 of sediment was deposited between October 2003 and September 2005. Creek 3 had 7,370 m^3 of sediment eroded between November 2002 and April 2004, whilst 5,200 m^3 of sediment was deposited from April 2004 to September 2005. Between November 2002 and January 2003, 270 m^3 of sediment was eroded from Creek 4, whilst 1,280 m^3 of sediment was deposited from January 2003 to September 2005. Overall, 11,300 m^3 of sediment was eroded from the creek systems during the erosional phase; in comparison 11,050 m^3 of sediment was deposited when the creeks silted up.

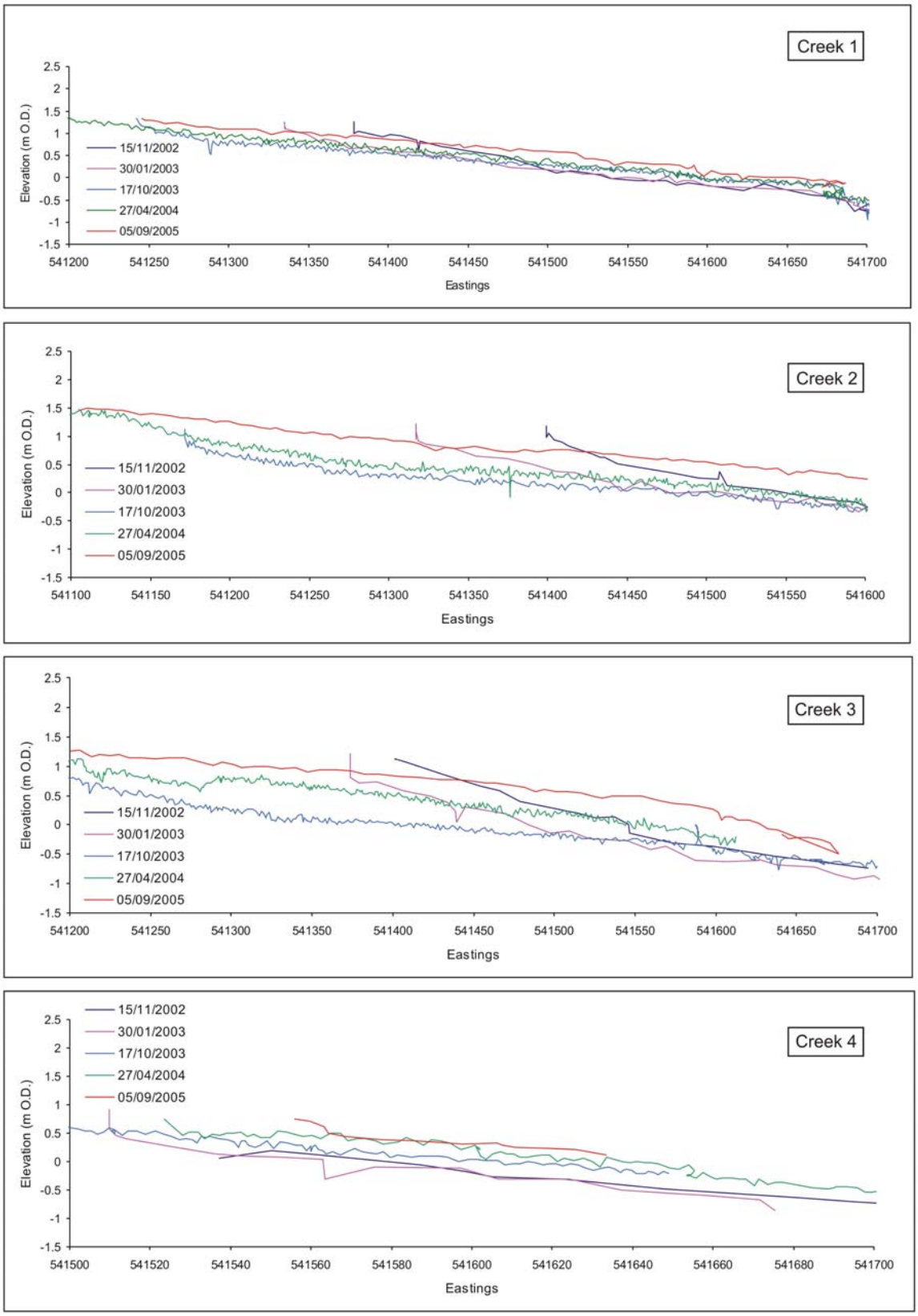

Figure 7.7: Profile of the thalweg along the creeks, with 5 of the RTK-GPS measurements shown, over a 3 year period.

7.4.3 *Offshore Bathymetry*

Bathymetric surveys of the Lower Road Channel (Fig 3.1), undertaken between June 2000 and June 2005 (by the Port of Boston Authority) reveal periods of erosion and accretion (Table 7.1). The calculations were undertaken based upon the volume difference for areas where data were available between consecutive surveys, above a -8 m ACD level; such an example is shown in Figure 7.8. The initial survey from June 2000 was used as a baseline, i.e. no change could be derived. The surveys undertaken in June 2000 and May 2002 did not extend over as large an area as the later surveys (1.3 km^2, compared to 5.1 km^2). As such, the rates of change established from June 2000 to April 2003 relate to a smaller area of the channel.

On the basis of the (2) surveys undertaken prior to the MR, the Channel can be seen to have been accreting, at a rate of around 70,000 m^3 km^{-2}; however, it is not known if this was part of a longer-term trend. When the greater part of the 11,300 m^3 of sediment was eroded from the creek system on the intertidal flats (August 2002 – early 2003 (see above)), the Lower Road Channel was eroding rapidly, at a rate some 4 times higher than the accretion rate had been, over the previous 2 years. Between April 2003 and May 2004, the Channel accreted at a rate much lower than that of the previous erosion; at the same time, the creek system over the intertidal flats was also predominantly accreting. From May 2004 to June 2005, when all of the creeks over the intertidal zone were silting up, some 650,000 m^3 of sediment was eroded from the Lower Road Channel. Overall, since the MR, 840,000 m^3 of sediment has been removed from the Lower Road Channel; in the previous 2 years, some 175,000 m^3 of sediment was deposited within the Channel.

Table 7.1: Change in volume of the Lower Road Channel area, between June 2000 and 2005.

Survey Date	**Annual rate of Change, m^3 km^{-2}**	**Cumulative Change, m^3**
June 2000	0	0
May 2002	70813.4	176443.5
April 2003	-273239.3	-149166.7
September 2003	21113.2	-95328.0
May 2004	24397.3	-12377.3
June 2005	-127292.6	-661569.4

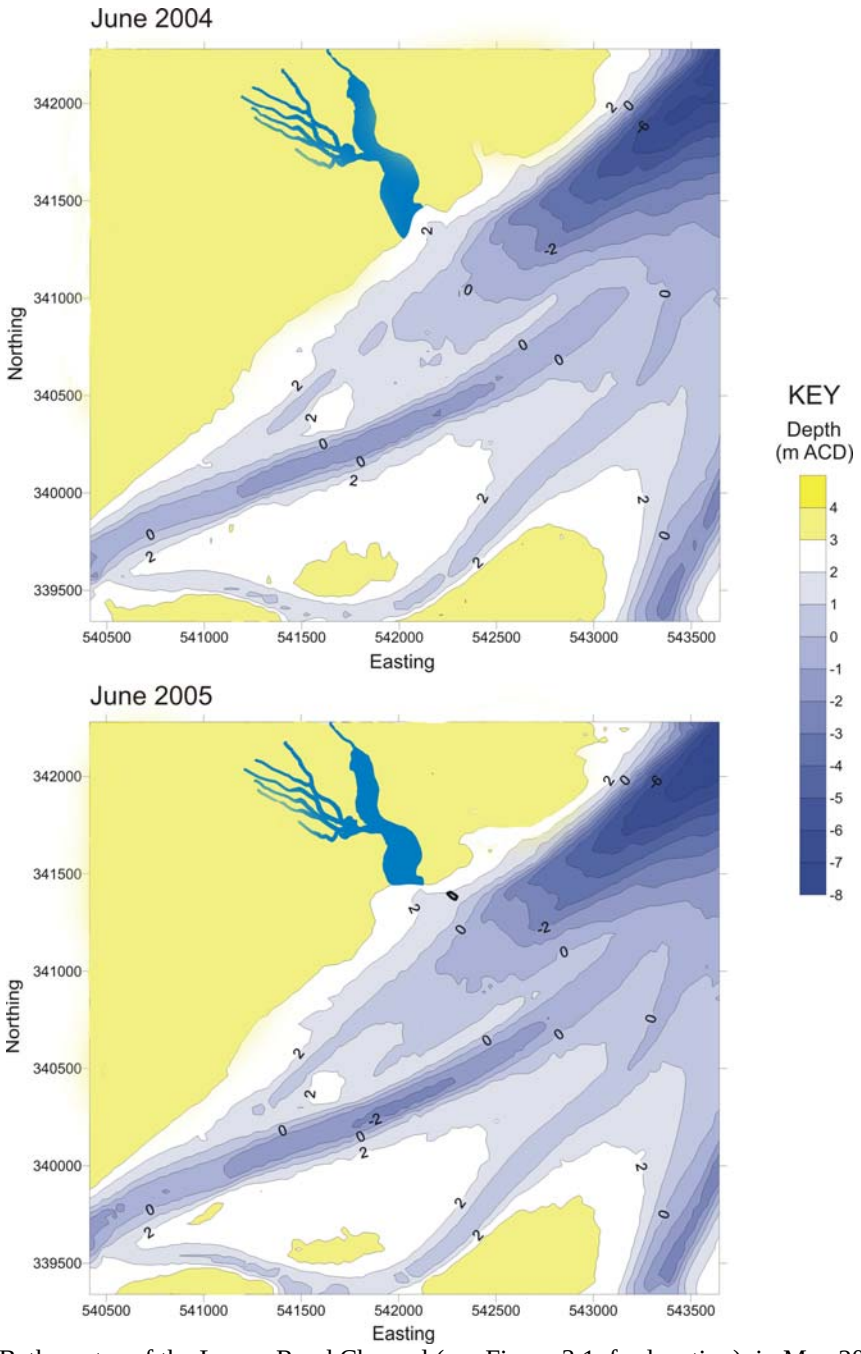

Figure 7.8: Bathymetry of the Lower Road Channel (see Figure 3.1, for location), in May 2004 and June 2005, with the creek system superimposed on the adjacent intertidal zone. Note: the areas shown in yellow/green are intertidal flats, where no data were collected; as such, the contours should be ignored.

7.5 DISCUSSION

The creation of a MR at Freiston Shore was directly related to the enhanced development of a creek system over the mid-intertidal zone for 2 years following the MR. Throughout low tide, during spring tides, the MR gradually released the water which had flooded the site during the preceding high water. This draining of the MR led to overbank flow occurring in the creeks connected to the artificial channels in the breaches, causing unnaturally high overland flow across the intertidal flats, which became focused in natural depressions and existing small

creeks. Natural sheetflow from rainfall was identified by Mwamba and Torres (2002) as intermittently controlling the headward erosion of low-order intertidal creeks. In the present study the sheetflow can be regarded as the primary control on the rates of headward extension, as the flow occurred regularly. From various empirical relationships established for fluviatile systems, it has been demonstrated that channel dimensions are controlled mainly by water discharge (Schumm, 1985). As such, the natural conditions, which initiate and support the development of a creek system over the intertidal zone, were enhanced by water draining from the MR site. Instead of the natural sheetflow associated with the last phase of the ebb tide, which naturally lasts for up to 30 minutes, the sheetflow caused by the MR continued until the subsequent tide reflooded the area (up to 6 hours). This enhancement in the sheetflow caused the creek system to develop into a larger network than it would have done with just the natural flow. Hence, when the sheetflow ceased, the creek system rapidly silted up and returned to the natural equilibrium, prior to the MR.

Aerial photographs of the creeks revealed changes in the pattern of the drainage network and the rates of headward extension, before and after the implementation of the MR. Natural creek development was associated with a rate of headward extension of around 16 m yr^{-1}; since the MR, this increased to a peak of around 400 m yr^{-1}. These rates are considerably higher than most rates from previous studies, with headward extension rates of up to a few metres annually recorded in marshes in North Norfolk, UK (Steers, 1977) and in the Bahia Blanca Estuary, Argentina (Perillo and Iribarne, 2003). However, natural rates of 500 m yr^{-1} were recorded over the coastal plains of the Mary River, northern Australia (Knighton *et al.*, 1992). These high rates were attributed to a large tidal range (6 m in the nearby macro tidal gulf), relatively flat plains and the availability of pre-existing channel lines (in the form of palaeochannels). This shows that although the anthropogenically enhanced headward extension of the creeks at Freiston Shore were high, similar natural rates have been recorded.

Low annual headward extension rates were experienced during the summer in 2003 (between June and October); this was in spite of high spring tides experienced during this period. This pattern indicates that the rates were not related directly to the tidal heights and their frequency, but could be due also to seasonal effects. Further, waves may influence creek development, by weakening the sediment surface or eroding parts of the banks; however, more research is needed into this particular effect. Only a single set of summer data was available, so it is not known whether this was an abnormal result, or if headward extension rates are reduced during the summer months.

The rapid development of a creek system over the intertidal flats at Freiston Shore was recorded over a 2-year period, in the following year the creek system silted up and reverted back to its original state. On the basis of the measurements collected, it has been possible to study the overall evolution of the creek system. As such, creek development can be divided into a number of stages:

(i) initial and rapid extension of all of the creeks, in response to overland flow;

(ii) tributaries added, whilst rapid extension of the original creeks was still occurring;

(iii) concentration of flow into the main creeks, where rapid extension was still taking place, and siltation in the other creeks; and

(iv) cessation of overland flow, causing rapid siltation within all of the creeks, reverting back towards their initial form.

Stage (iv) appears to have occurred because the overland flow, which caused the original enhanced development of the creek system, had reduced dramatically. The creek development was related directly to the efficiency of the channels in the breaches in draining the MR site, i.e. the length of time of the discharge and the quantity of water flowing over the intertidal zone. Following the MR, the channel within Breach 1 increased in width and depth, to accommodate the discharge, causing the MR site to drain much more rapidly than predicted. Finally, the natural creeks (connected to the channels in the breaches) have eroded, to contain the enhanced discharges associated with drainage of the MR site. Overbank flow was prevented in these creeks, limiting sheetflow over the intertidal zone. Hence, rapid development of the creek system ceased when the natural creeks, connected to the breaches, became sufficient in size to accommodate all of the discharge resulting from drainage of the MR site. Development of the creek system until Stage (iv) (see above), follows closely two fluvial models, described in detail by Schumm *et al*. (1987); (a) expansion by headward growth; and (b) the extension of rapidly growing, long channels, with tributaries added to fill the drainage networks as suggested by Glock (1931). This pattern of creek development can be thought of as representative of intertidal flats similar to those at Freiston Shore. However, the rate of the development in the present study is not representative of natural conditions.

Creek development over the mid-lower intertidal flats, together with erosion around the breaches, has released sediment from the intertidal zone. The associated predicted quantity was found to be approximately equal to that deposited during their infilling. Sediment eroded from channels within the breaches is thought to have been deposited inside the MR site; here, rates of accretion of 4 to 5 cm yr^{-1} were recorded, adjacent to the breaches.

The anthropogenic impacts, which have been recognised as effecting the development of creeks, are either; by impairing their evolution and development through the construction of

embankments, or by directly affecting the creeks through dredging (Allen, 2000). The present investigation has shown how the creation of a managed realignment at Freiston Shore can also effect the development of creeks. This was in the form of an enhanced development for 2 years after the initiation of the MR, followed by the rapid siltation of the creek system over 1 year, returning it to its original state.

During the initial development of the creek system, sediment was eroded from the intertidal flats and the adjacent subtidal channel. As the creek development over the intertidal flats ceased, sediment deposition took place in the adjacent channel. During siltation of the creek system, the adjacent channel was extensively eroded; sediment eroded from the channel, over this period, was some 50 times greater than that deposited in the adjacent creek system. Excess sediment may have been deposited within the large channel on the intertidal flats, into which the creek system drains; this eroded extensively, following the MR (Fig. 7.1). However, because of the size and stability of the channel, ground surveying could not be undertaken; as such, its cross-sectional area and thalweg profile are not known. Sediment eroded (650,000 m^3) from the subtidal channel, adjacent to the intertidal flats, must have been transported to other areas of The Wash.

7.6 CONCLUDING REMARKS

Since the initiation of a MR, enhanced erosion has been experienced on a creek system over the intertidal flats. Such erosion can be attributed to the MR, due to a difference in level between the MR and the adjacent saltmarsh. The MR site acted as a reservoir following high water spring tides, gradually releasing water during the subsequent low water; this caused higher rates of erosion than expected in the channels within the breaches. There was a continual dynamic adjustment to the MR, which resulted in an unpredicted enhancement in the creek development over the mid-intertidal zone. The natural creeks over the intertidal zone experienced a higher water discharge, which is the primary control on channel size, causing a change in the character of the creek system. The MR caused similar sheetflow to that during the natural draining of the last phase of the ebb tide, which originally formed the creek system; the difference between the natural ebb sheetflow and the sheetflow related to drainage of the MR, was that the latter lasted much longer and was associated with a higher velocity, which caused an enhancement to the natural creek development.

The enhanced creek development (> 20 times the natural headward extension) continued for 2 years following the MR; over the next 12 months the creek system silted up and returned to its original (natural) equilibrium. The drainage of the MR, through the channels within the breaches in the embankment and the natural creeks they connect to, controlled the

development of the creeks over the intertidal zone; their size dictates the drainage of the MR site and whether sheetflow occurs over the intertidal zone. When these channels and creeks reached a size capable of containing the high flows associated with the drainage of the MR site, the sheetflow ceased over the adjacent intertidal flats; hence, the erosive development of the creek system also ceased. The absence of sheetflow over the intertidal flats 'starved' the creek system of the flow necessary for its development, causing the system to silt up rapidly; subsequently the creeks reverted back to their original (natural) form.

The impact of the MR enabled a detailed investigation into the natural and anthropogenically enhanced development of a creek system over an intertidal mudflat and sandflat. The available data have shown that a combination of two fluvial models, fit with the development observed. These were the models summarised by Schumm et al. (1987); (a) expansion by headward growth; and (b) the extension of rapidly growing, long channels, with tributaries added to fill the drainage networks as suggested by Glock (1931). The initial formation of the tidal creeks, at Freiston Shore, is considered to be due to subtle variations in the surface topography, focusing any sheetflow. In these areas of concentrated flow, "nick points" are created and initiate the head of a tidal creek. Subsequently, headward erosion becomes the dominant process, determining the creek length.

Sediment was eroded from the intertidal flats and the adjacent subtidal channel, immediately following the MR; however, this is considered to have been transported to another area of The Wash. As flow over the intertidal flats decreased, the subtidal channel started to accrete. When the overland flow stopped and the creek system silted up, the sediment is considered to have been transported from the subtidal channel and redeposited over the intertidal flats.

7.7 PLATES

Plate 7.1: The creek connected to the channel in Breach 1, during low water. The creek is 'unnaturally' full of water during this phase of the tide, when water is escaping over the banks and flowing over the intertidal flats, as sheetflow (05/09/2002).

Plate 7.2: The ABR deployed on the lower intertidal site at the start of *Deployment 1* (05/09/2002). Note: the whole of the surrounding intertidal flats are flooded, with overland sheetflow.

Plate 7.3: Sheetflow over the lower intertidal zone, flowing into the “nick point” of a creek; this is causing rapid headward extension of the creek (05/09/2002).

Plate 7.4: A “nick point” at the landward extent of a creek, in the developing creek system (15/01/2003).

Plate 7.5: No evidence of “nick points”, with the creek system continuing into small drainage runnels, over the upper intertidal flats (05/09/2005). Note: compare with Plates 7.3 and 7.4 (see text).

Plate 7.6: The ABR deployed on the lower intertidal site at the end of *Deployment 1* (10/09/2002). There is an absence of any overland flow over this area of the intertidal flats, in response to the rapid development of the creek system (visible behind the ABR, in the Plate). Note: compare with Plate 7.2 (see text).

Plate 7.7: A view of Creek 2, looking landward, during *Deployment 3* (24/11/2003).

Plate 7.8: A similar view of Creek 2 (05/09/2005), to that shown in Plate 7.7, looking landward. The scaffold pole deployed in the centre of the creek, used in *Deployment 3*, is only just visible; this indicates that, since then, > 0.5 m thickness of sediment has been deposited.

CHAPTER 8: CREEK AND INTERTIDAL ZONE INTERACTION, IN TERMS OF SEDIMENT AND WATER MOVEMENT

8.1 INTRODUCTION

The majority of previous studies undertaken into the interaction of creeks with intertidal zones have been based upon creek systems located within saltmarsh environments (Bayliss-Smith et al., 1979; Healey et al., 1981; French and Stoddart, 1992; and Pringle, 1995). In such environments, overmarsh (occurring on spring tides) and undermarsh tides (occurring on tides other than springs) are experienced. The creek system at Freiston Shore was located on the mid- to lower intertidal zone and, as such, overbank tides were experienced during every tidal inundation irrespective of the stage within the spring/neap cycle. The creek system, which consisted of a dense linear-dendritic network with blind-ended channels (Fig. 8.1), has been subjected to an enhanced development, following the initiation of the MR scheme (Chapter 7). The longest of these creeks extended to near the seaward edge of the saltmarsh; thus, the creek network was located over the lower to upper intertidal zone where the surficial sediment is predominantly made up of fine-grained sediment (< 63 μm). The system consisted of 4 main creeks, which flow into a single creek; this, in turn, flowed into a larger channel that was connected (to landward) to Breaches 2 and 3 and (to seaward) flowed into The Wash.

The aim of this part of the study is to investigate the interaction between a developing creek system and the intertidal flats, to assess the role of tidal creeks and intertidal flats in the transport of sediment. Most past investigations of sediment transport at Freiston Shore have used the bedform morphology and the direction orientation of surface ripples and internally-preserved structures, to indicate bedload transport (Amos and Collins, 1978; and Collins et al., 1981), i.e. direct measurements of bedload transport have not been collected. The present investigation has incorporated bedload transport measurements; these should enhance the bedload transport measurements collected by Amos (1974), over the intertidal zone at Freiston Shore. A number of bedload transport formulae have been derived on the basis of laboratory experiments (Carling, 1996); against this background, the present study has used various equations, to predict the transport rates. The outputs of these predictions have been compared to the measured rates, to identify the most accurate method for the prediction of bedload transport in such an environment.

8.2 METHODS

8.2.1 *Data Collection*

This part of the study utilises data from 3 ABRs and 8 bedload samplers, collected over the lower intertidal zone during *Deployment 3* (Fig. 4.1(b)). Creek 2 was studied (Fig. 4.1(a)); ABRs were deployed in the deepest part of the creek and on each bank (Fig. 8.1). Four bedload samplers were set up on each bank, with the samplers facing at 90° to each other. In this way, measurements of (net) bedload transport were obtained in the longshore and cross-shore directions.

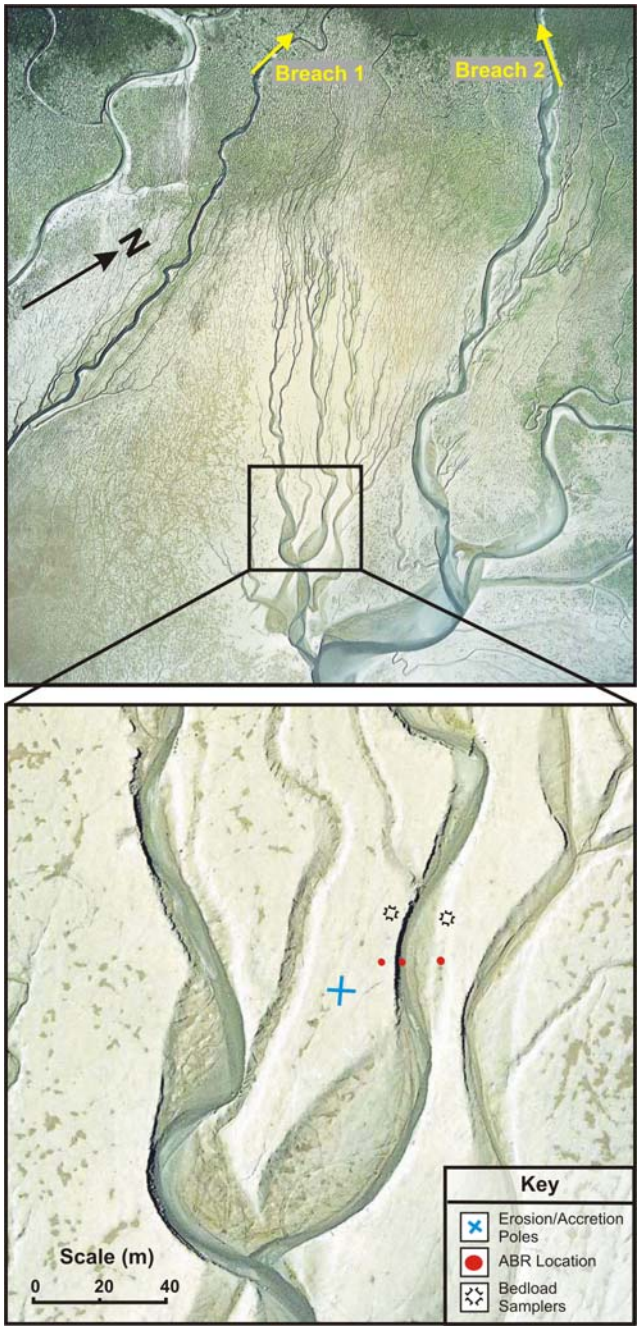

Figure 8.1: Aerial photographs of the creek system surrounding the instruments deployed as part of *Deployment 3*.

8.2.2 *Bedload transport predictions*

A number of possible formulae were considered, for the calculation of bedload transport. Elsewhere, it has been established that different theories may result in very different predictions of sediment transport rates (in particular) and directions (Heathershaw, 1981). Laboratory-derived formulae, based on the Bijker approach to the combination of wave and current shear stresses, such as that by Ackers and White (1973), have been shown not to represent the field data accurately (Soulsby, 1997). Further, a formula presented by Ribberink (1998), was considered as not being suitable for sediment finer than 0.2 mm, or under waves of a short period (< 3 s). Both of these characteristics occur over the intertidal zone at Freiston Shore; as such, this particular method was not considered to be capable of accurate predictions of bedload transport. Finally, the method described below, derived from Soulsby (1997), was used in the calculation of the bedload transport rates, under waves and tidal currents; it was considered to be appropriate to calculate the bedload transport, under conditions prevailing at Freiston Shore.

The sequential steps of the Soulsby (1997) method of bedload transport prediction are listed below.

The radian frequency of the waves is calculated using:

$$\omega = 2\pi / T_p \tag{8.1}$$

The bed level, relative to an arbitrary datum is calculated through:

$$\xi = \omega^2 h / g \tag{8.2}$$

$$\eta = \xi^{1/2}(1 + 0.2\xi) \qquad for \xi \le 1$$

$$\eta = \xi[1 + 0.2\exp(2 - 2\xi)] \qquad for \xi > 1$$

$$k = \eta / h \tag{8.3}$$

The amplitude U_w of the wave orbital velocity, just above the bed and due to a monochromatic (single frequency) wave, is:

$$U_w = \frac{\pi H_s}{T_p \sinh(kh)} \qquad \text{[Note: sinh (z) = ½(e}^{z}\text{-e}^{-z}\text{)]} \tag{8.4}$$

where,

T_p = peak wave period (s)

h = depth (m)

g = acceleration due to gravity (9.81 m s^{-1})

H_s = significant wave height (m)

The orbital amplitude of wave motion at the bed is calculated using:

$$A_w = \frac{U_w T_p}{2\pi} \tag{8.5}$$

In order to calculate the bed roughness, for D_{50} = 100 μm:

$$z_0 = (100 \times 10^{-6} / 12) = 1.0 \times 10^{-5} \tag{8.6}$$

Thus, the rough-bed wave friction factor is calculated through:

$$f_{wr} = 1.39\left(\frac{A_w}{z_0}\right)^{-0.52} \tag{8.7}$$

where υ = kinematic viscosity, $\upsilon = 1.36 \times 10^{-6}$ m^2 s^{-1}

The wave Reynolds number is used to find the type of flow:

$$R_w = \frac{U_w A_w}{\upsilon} \tag{8.8}$$

If $R_w \le 5 \times 10^5$, laminar flow occurred and so the dimensionless coefficients become B=2 and N=0.5,

When $R_w > 5 \times 10^5$, smooth turbulent flow was present, so B=0.0521 and N=0.187

The smooth-bed wave friction factor is shown by:

$$f_{ws} = BR_w^{-N} \tag{8.9}$$

Thus, $f_w = \max(f_{wr}, f_{ws})$ (8.10)

The amplitude of oscillatory bed shear-stress, due to waves, becomes:

$$\tau_w = \frac{1}{2}\rho f_w U_w^2 \tag{8.11}$$

Which is converted to the skin-friction Shields parameter, due to waves:

$$\theta_w = \frac{\tau_w}{g(\rho_s - \rho)d} \tag{8.12}$$

The drag coefficient C_D of the steady current, in the absence of waves, is found by interpolation of Table 8.1 where:

$$z_0 / h = 0.00001 / 2 = 2 \times 10^{-5}$$

Table 8.1: Values of C_D using the DATA 13 method (from Soulsby (1997)).

z_0/h	10^{-2}	10^{-3}	10^{-4}	10^{-5}
Value for C_D	0.01231	0.00458	0.00237	0.00145

From Table 8.1, C_D =0.00145

Using the specific values from Table 8.2, the coefficients *b*, *p* and *q* are calculated, using equation 8.13 and substituting *p* and *q* for *b*, and taking *J* = 8.8 in accordance with the DATA13 method shown in Soulsby (1997).

$$b = (b_1 + b_2 \left|\cos\phi\right|^J) + (b_3 + b_4 \left|\cos\phi\right|^J) \times \log_{10}(f_w / C_D) \qquad (8.13)$$

Table 8.2: Fitting coefficients for the current boundary layer, using the DATA 13 model (from Soulsby (1997)).

	1	**2**	**3**	**4**
b	0.47	0.69	-0.09	-0.08
p	-0.53	0.47	0.07	-0.02
q	2.34	-2.41	0.45	-0.61

In order to calculate the current-only bed shear-stress

$$\tau_c = \rho C_D \overline{U}^2 \qquad (8.14)$$

The relative current strength, in relation to the combined waves and tidal currents, can be found through:

$$X = \tau_c / (\tau_c + \tau_w) \qquad (8.15)$$

Hence, the dimensional mean shear-stress becomes:

$$Y = X\left[1 + bX^p (1 - X)^q\right] \qquad (8.16)$$

The mean bed shear-stress during a wave cycle, under combined waves and currents, can then be calculated:

$$\tau_m = Y(\tau_c + \tau_w) \qquad (8.17)$$

The mean Shield's parameter, over the wave cycle, is given by:

$$\theta_m = \frac{\tau_m}{g(\rho_s - \rho)d} \tag{8.18}$$

The dimensionless grain size then has to be calculated, for the threshold Shield's parameter to be known:

$$D_* = \left[\frac{g(s-1)}{\upsilon^2}\right]^{1/3} d \tag{8.19}$$

$$s = \rho_s / \rho \tag{8.20}$$

The threshold Shield's parameter is:

$$\theta_{cr} = \frac{0.30}{1+1.2D_*} + 0.055\left[1 - \exp\left(-0.020D_*\right)\right] \tag{8.21}$$

The dimensionless bedload transport rates, in the direction of the tidal current (x) and perpendicular to it (y), are calculated then using

$$\Phi_{x1} = 12\theta_m^{1/2}(\theta_m - \theta_{cr}) \tag{8.22}$$

$$\Phi_{x2} = 12(0.95 + 0.19\cos 2\phi)\theta_w^{1/2}\theta_m \tag{8.23}$$

$$\Phi_x = \max\left(\Phi_{x1}, \Phi_{x2}\right) \tag{8.24}$$

$$\Phi_y = \frac{12(0.19\theta_m\theta_w^2 \sin 2\phi)}{\theta_w^{3/2} + 1.5\theta_m^{3/2}} \tag{8.25}$$

To obtain the volumetric bedload transport rates,

the values of Φ_x and Φ_y are multiplied by $\left[g\left(s-1\right)d^3\right]^{1/2}$ (8.26)

This approach provides output values for:

q_{bx} = component of q_b, travelling in the direction of the current;

q_{by} = component of q_b, travelling at right angles to the current; and

ϕ = angle between current direction and direction of wave travel

8.3 RESULTS

8.3.1 *Within the Creek*

The flow in the creek was rectilinear, flowing at 260° (to landward, on the flood) and 90° (to seaward, on the ebb) (Fig. 8.2). The initial flood flow and final ebb flow within the creek were not parallel to the banks, but at an angle of 30° relative to the bank; this was caused by the localised topography of the creek, as the flow followed the thalweg. The meanders in the creek caused the flow to shift from one side of the creek, to the other.

Overall, the duration of the ebb flow was 50% longer than the flood, i.e. 4.5 compared to 3 hours. However, the flood tide was associated with higher current speeds, with the flood tidal current peak being 0.54 m s^{-1} (over 6 tidal cycles), whilst the ebb peak was 0.39 m s^{-1} (Fig. 8.3). The peaks in suspended sediment concentration (SSC) coincided with the peaks in the tidal current speed, occurring during the first phase of the flood and the last phase of the ebb (Fig. 8.4). The quantity of suspended sediment present in the creek was higher than predicted, with the OBS sensor becoming 'saturated' during most of the peaks, when the SSC was higher than 140 mg l^{-1}. Allowing for the absence in the peaks of the SSC, a negative flux was calculated, i.e. with more sediment being transported seaward, than to landward. However, as the measurements for tidal current speed and SSC were only recorded at 0.25 and 0.5 m above the creek bed, respectively, and there have been no detailed studies on the tidal current speed and SSC distributions through tidal creek cross-sections, the actual total net flux cannot be determined.

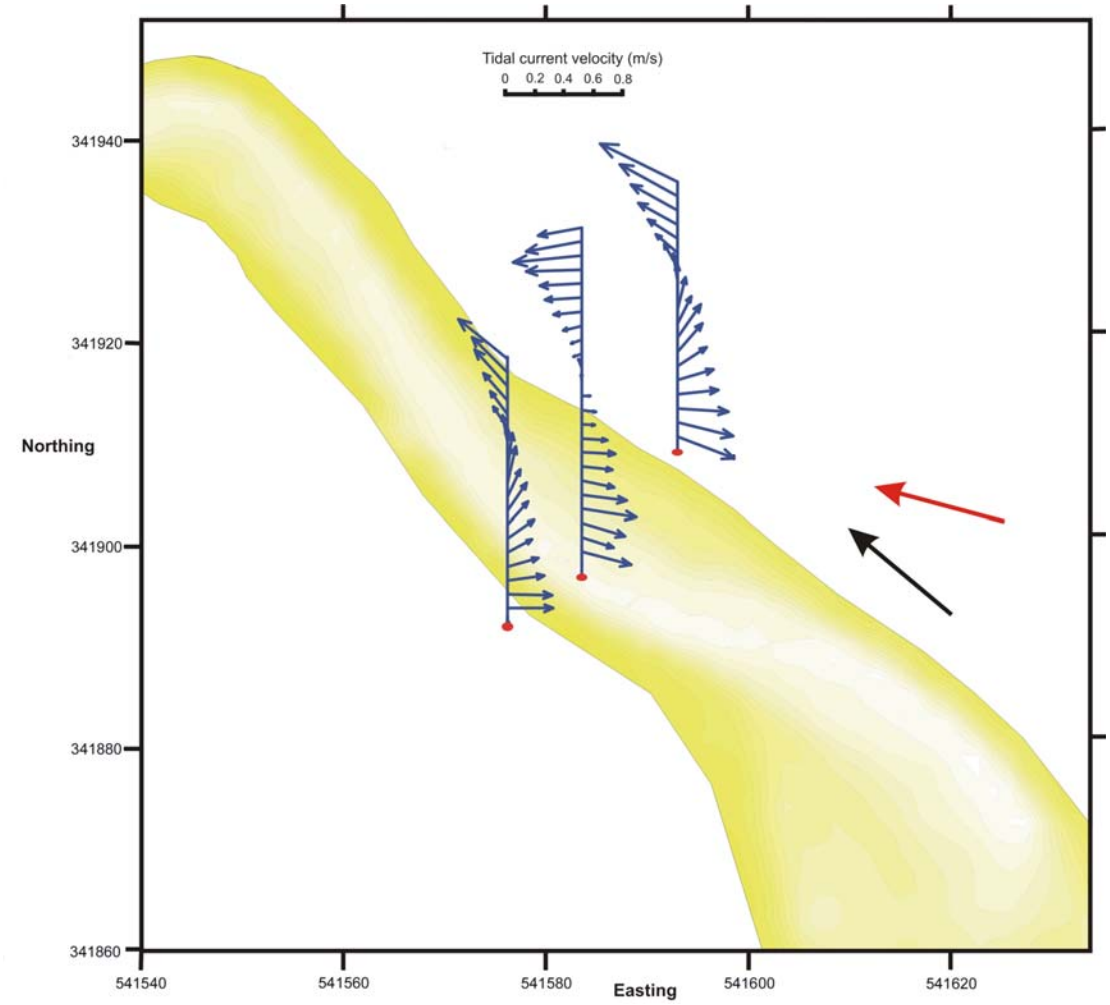

Figure 8.2: The measured tidal current velocities shown as a vector diagram, with each series of vectors being obtained from the ABR, located in that position, throughout a tidal cycle. The vectors at the top of each series represent the first phase of the flood tide, with subsequent measurements (below) every 15 minutes, until the final measurement at the bottom of the series is the last phase of the ebb tide. The separate arrows represent the prevailing wave directions.

Wave activity recorded inside the creek was lower than on the adjacent intertidal zone (Fig. 8.5). Only approximately 17% of the wave energy, during the period of the highest wave energy over the intertidal flats (26/11/2003 am) was experienced within the creek (Fig. 8.6). In contrast, during an earlier period of wave activity (25/11/2003 am), with lower wave heights, the wave energy inside the creek was 66% that of the energy on the adjacent intertidal flats. The average wave direction, between the 2 tides with the highest wave energies, showed some variation (Table 8.3). The two arrows shown on the intertidal flat on Figure 8.2 represent wave directions; 25/11/2003 (am), the black arrow is running near parallel with the banks, of this section of the creek; 26/11/2003 (am), the red arrow is at an angle to the banks of the creek. The 25 to 40° difference in wave direction appears to have caused the reduction in wave energy inside the creek, on 26/11/2003 (am). The reduction in wave energy experienced within the creek is considered to have been the result of a sudden

increase in water depth, between the intertidal flats and the creek bed, reducing the wave height; this, combined with the creek bed being 1 m deeper than the intertidal flats, results in lower wave energies being recorded within the creek. However, the reason for the variability in wave energy reduction, between the intertidal flats and the creek, is unknown.

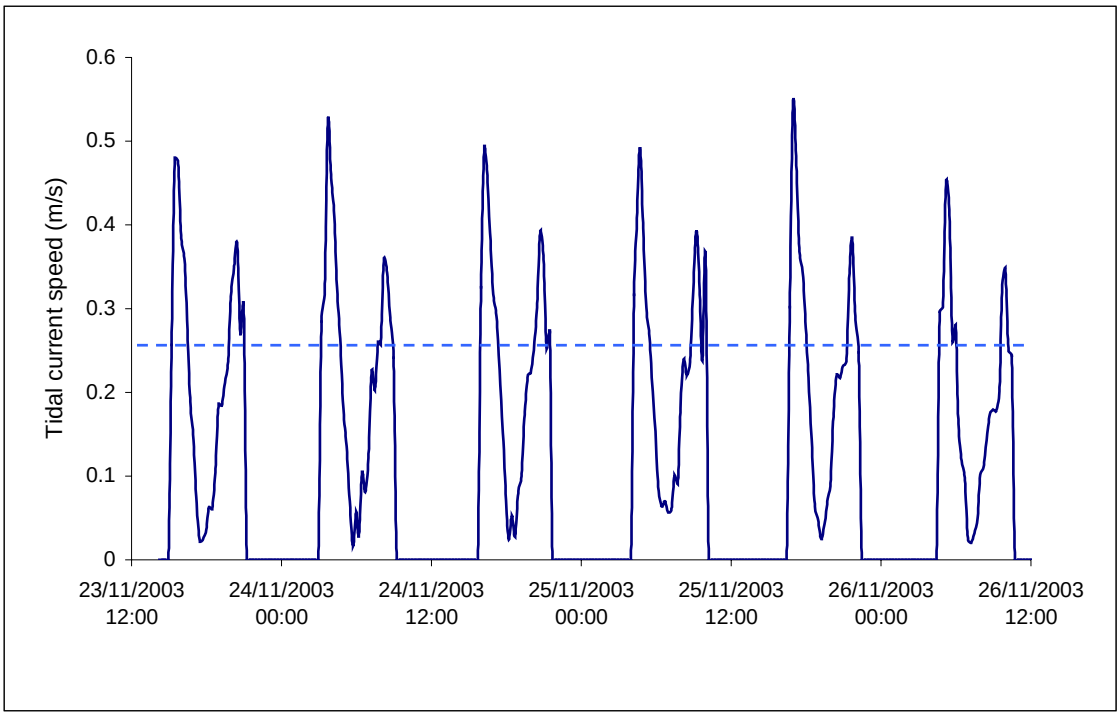

Figure 8.3: Tidal current speed throughout *Deployment 3,* within the creek. The critical threshold for transport of fine grained sediment (70 μm) is shown by the blue dashed line, calculated using the equations from Soulsby (1997).

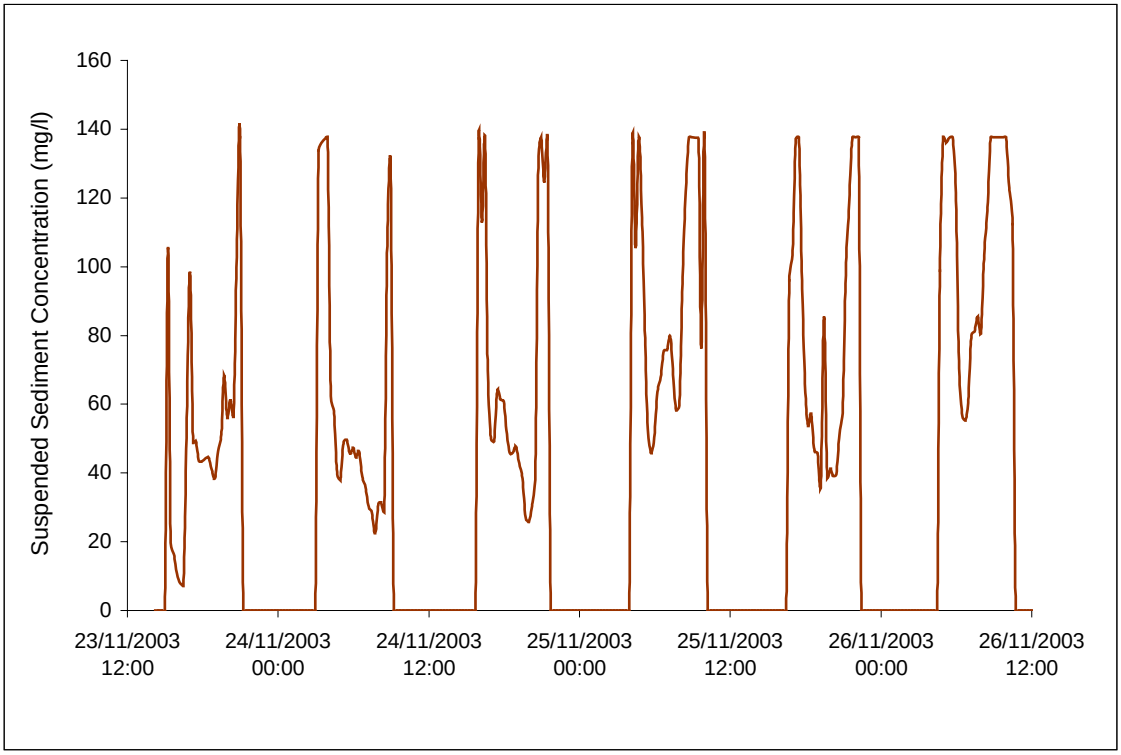

Figure 8.4: Suspended Sediment Concentration (SSC) throughout *Deployment 3*, within the creek.

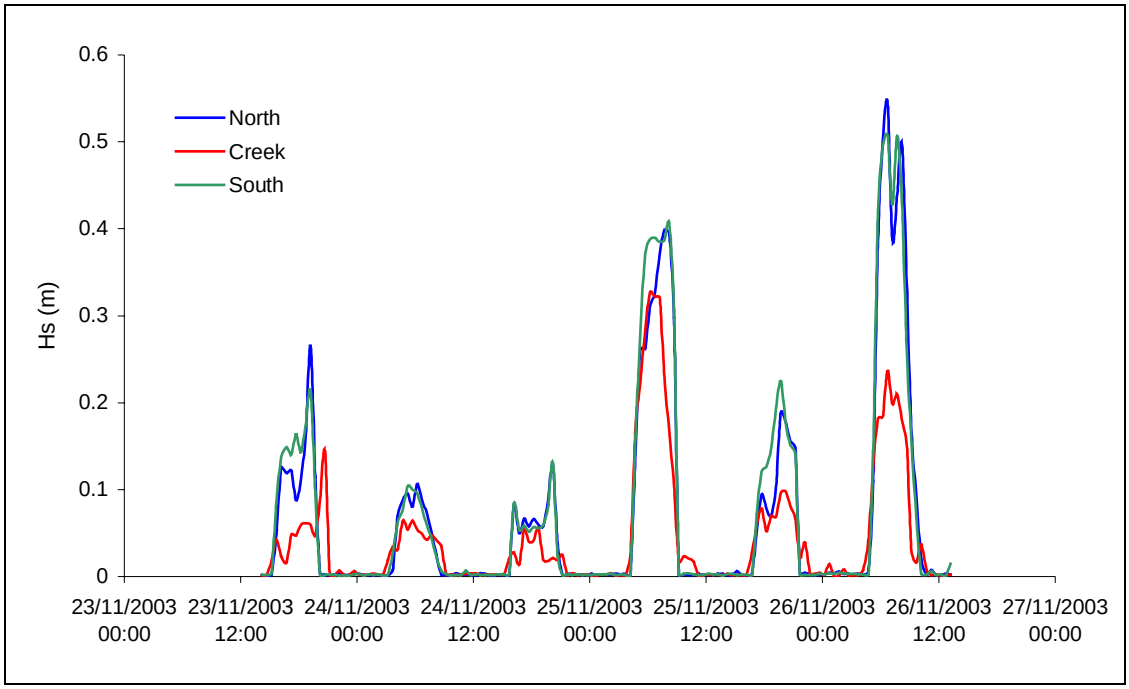

Figure 8.5: Significant wave height measured at the 3 locations (see Figure 4.1(b)), over *Deployment 3*.

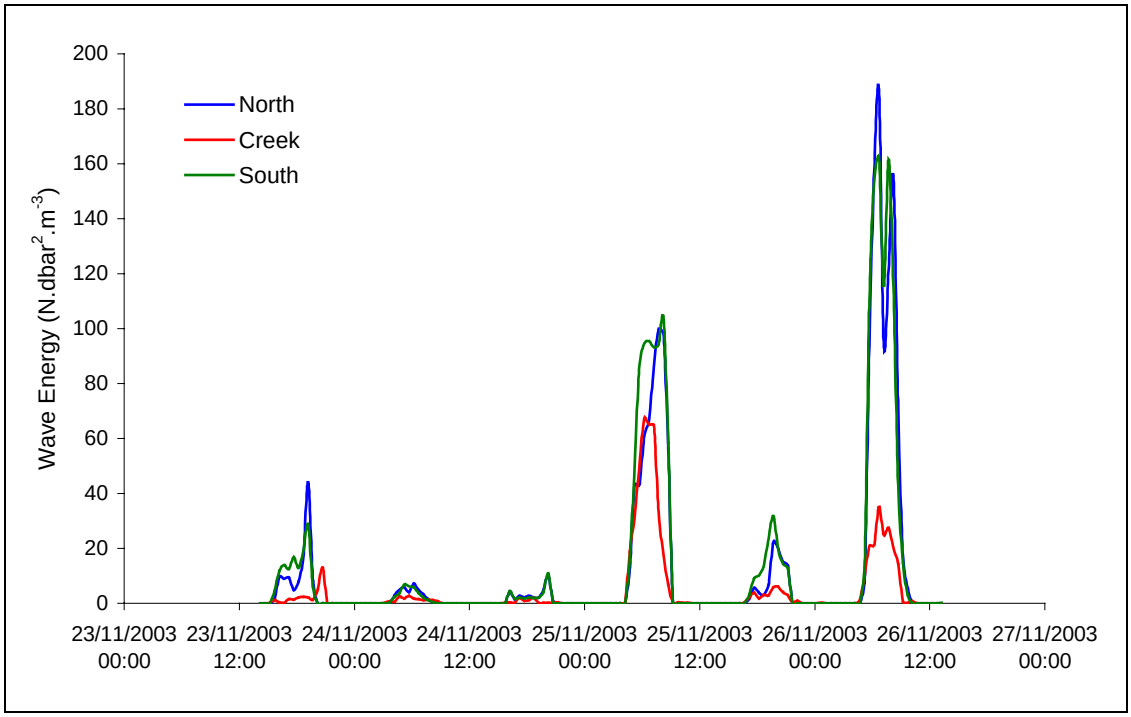

Figure 8.6: Wave energy at the 3 locations (see Figure 4.1(b)), over *Deployment 3*.

Table 8.3. The dominant wave direction over the (two) tides with the highest recorded wave activity (see Figure 8.6).

Location	Time	Wave Direction (from)
North of Creek	25/11/2003 (am)	146°
	26/11/2003 (am)	106°
Within Creek	25/11/2003 (am)	116°
	26/11/2003 (am)	110°
South of Creek	25/11/2003 (am)	140°
	26/11/2003 (am)	117°

As bankfull stage was reached within the creek, there was an increase in the current speed, with the peak flow occurring immediately afterwards (Fig. 8.7). Throughout the deployment, it took between 30 and 45 minutes for the water in the creek to rise the 0.5 m, from the height of the instrument above the bed (0.5 m) and the height of the banks above the bed (1 m), to reach bankfull stage. The highest frequency sampling period of the ABRs was every 15 minutes; as such, at most 2 measurements were obtained leading up to the bankfull stage. Similarly, as the water level fell below the banks, during the ebb tide. Peaks in SSC occurred before the flood bankfull stage was reached, while similar peaks were also observed shortly after bankfull stage was reached, these correlated with peaks in the tidal current speed (Fig. 8.8).

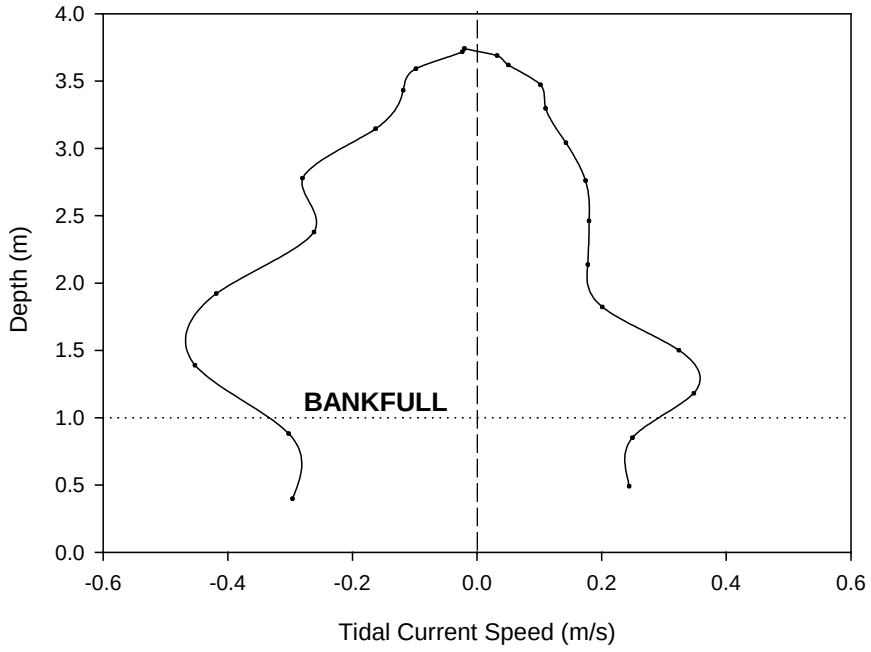

Figure 8.7: Tidal current speed against water depth within the creek, over a tidal cycle (26/11/2003 am). (Note: The negative tidal current speeds are during the flood stage of the tide and the positive are during the ebb stage)

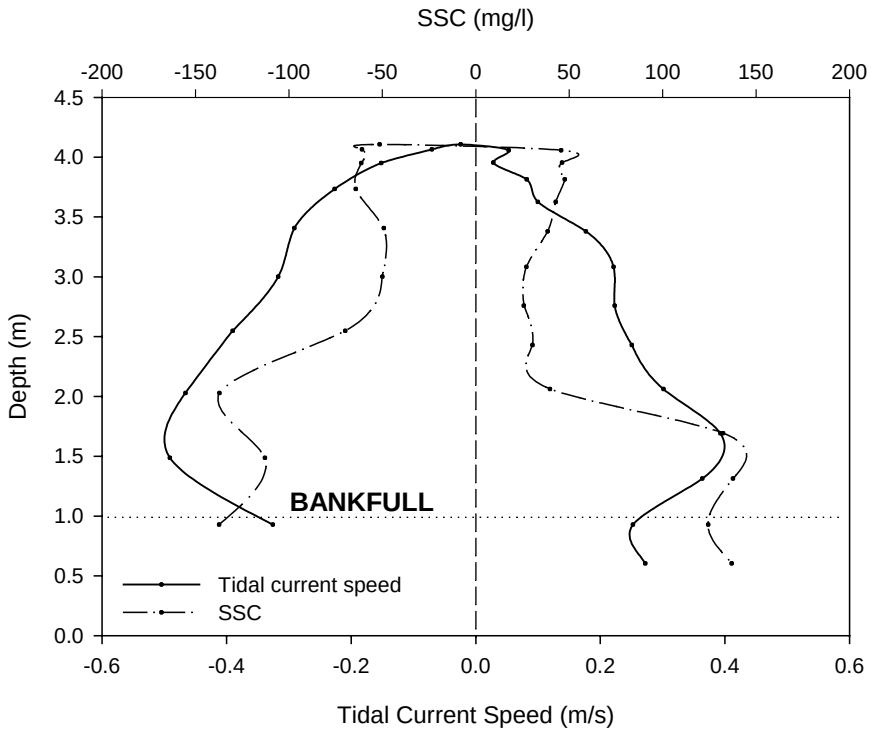

Figure 8.8: Tidal current speed and SSC, plotted against the water depth within the creek over a tidal cycle (24/11/2003 pm).

8.3.2 *Intertidal flats (i.e. the northern and southern banks of the creek)*

Flow within the creek lasted for 30 minutes longer, at the beginning and end of the tidal inundation, compared with the adjacent intertidal flats; during this time the creek drained any water and suspended sediment left on the adjacent intertidal flats. The north bank of the creek experienced higher peaks in flood and ebb tidal current speeds, by some 0.1 m s^{-1} (Fig. 8.9): in contrast, the SSC was either lower, or similar to that on the south bank (Fig. 8.10). The SSC peaked during the first phase of the flood and last phase of the ebb, coinciding with the peak tidal current speeds. The highest SSCs were during the flood stage of the tide, with peaks roughly 25 mg l^{-1} higher than those during the ebb. When the significant wave height exceeded 0.25 m (25/11/2003 am and 26/11/2003 am), the SSC peak switched, from flood-dominant to ebb-dominant; this was more emphasised on the north bank of the creek. Under these higher wave conditions, the SSC on the north and south banks of the creek were approximately equal.

The direction of the tidal flow was similar on the north and south bank of the creek. The initial flood flow was in a landward direction, followed by a clockwise rotation throughout the tide, until seaward flow during the last phase of the ebb (Fig. 8.2). The general

hydrodynamics and sediment dynamics of the intertidal flats will be exmained in more detail in Chapter 9.

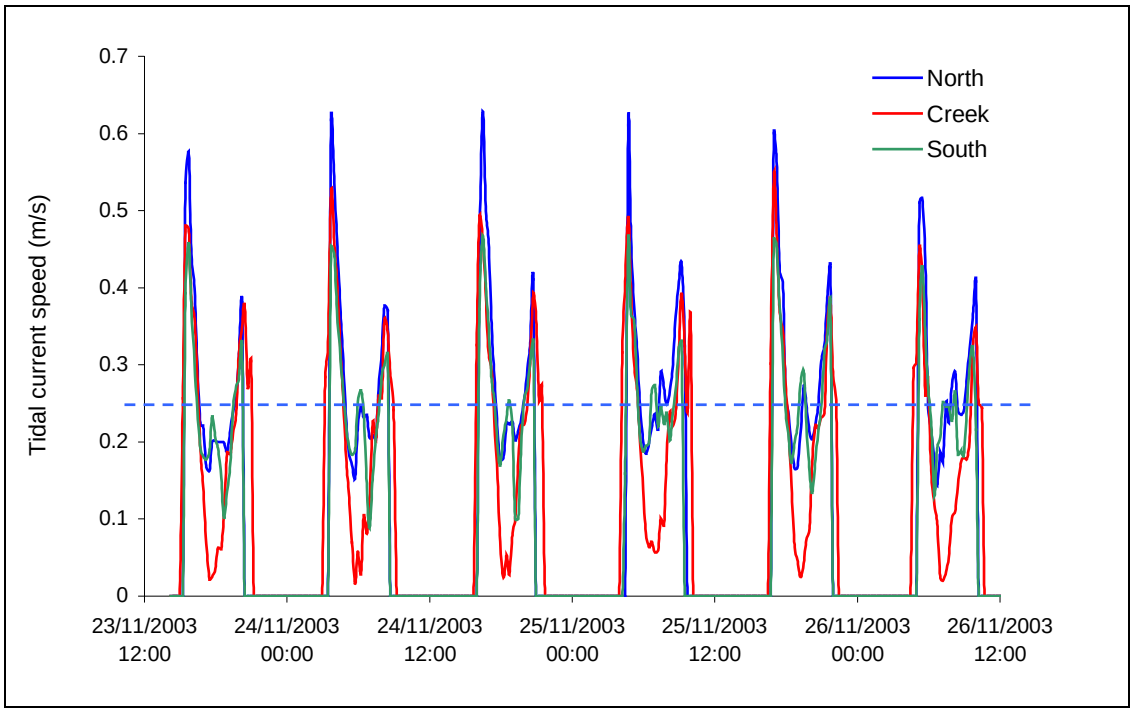

Figure 8.9: The tidal current speed measured at all 3 sites, over *Deployment 3*. The critical threshold for transport of fine grained sediment (70 μm) is shown by the blue dashed line, calculated using the equations from Soulsby (1997).

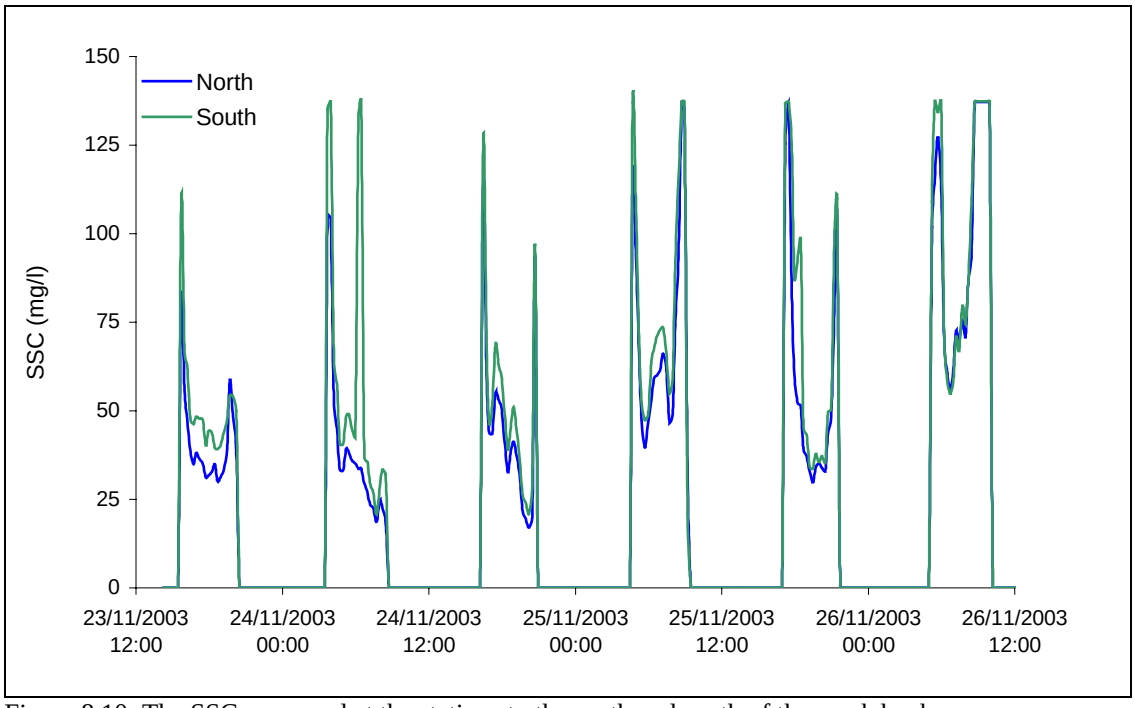

Figure 8.10: The SSC measured at the stations to the north and south of the creek banks, over *Deployment 3*.

8.3.3 *Bedload Transport*

Bedload transport was recorded during the final tidal inundations, with each inundation consisting of 2 consecutive tides as the bedload samplers could only be recovered once a day. From the data available on significant wave height (*Hs*) (Fig. 8.5), two tides were identified with greater wave activity; these coincided with the periods of bedload transport (Figure 8.11). This relationship indicates, importantly, that prevailing wave conditions are a major factor in the transport of material, as bedload. The peak *Hs* values associated with times where no bedload transport was recorded were below 0.25 m; it was > 0.4 m, during periods of measured bedload transport. However, a previous study has shown this design of bedload trap to be inefficient with efficiency rates of 1 – 10 % (Amos, 1974). The periods when no bedload transport was recorded, were not necessarily periods when no bedload transport occurred, rather the efficiency of the traps meant that no bedload was measured. If the sediment surface is assumed to be composed of sediment of 70 μm, then the critical current speed to initiate bedload transport is 0.25 m s^{-1}, on the basis of the equations from Soulsby (1997). Bedload transport was recorded during events when wave activity enhanced the bedload transport (Fig. 8.11). Owing to the low efficiency of the bedload traps, highlighted by the absence of bedload caused by tidal currents despite the current velocity exceeding the critical threshold for the transport of fine sand, the rates of bedload transport are not reliable. The rates of bedload transport described are relative and will be used for comparison between tides and to examine the composition of sediment transported.

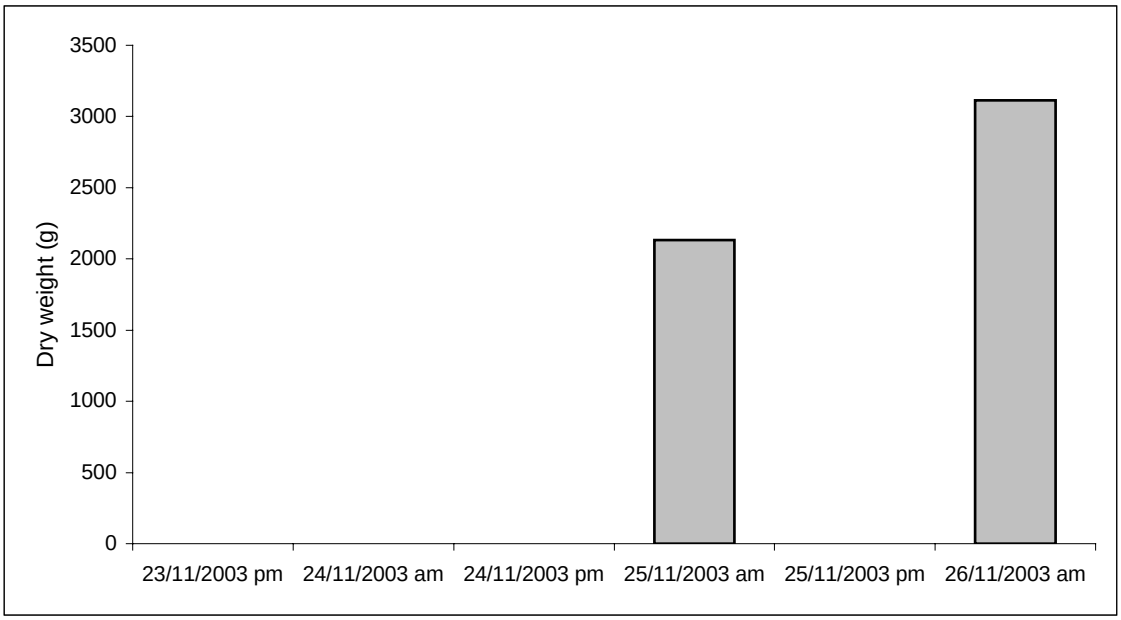

Figure 8.11: The tides when bedload transport occurred, together with the total dry weight of bedload collected during each of the tides.

On the north bank of the creek, the quantity of fine-grained (< 63 μm) and sand-sized (> 63 μm) sediment, transported as bedload, was greatest during the higher significant wave heights

(26/11/2003 am) (Fig. 8.12), as opposed to the period of bedload transport with lower waves (25/11/2003 am) (Fig. 8.13), i.e. the mean *Hs*, between the tides, changed from 0.3 to 0.35 m, whilst the peak changed from 0.4 to 0.5 m (Fig. 9.5). Over the two periods of bedload transport, the quantity of sand-sized sediment increased by more than double that of the fine-grained sediment (Fig. 8.14). The total amount of sediment transported, as bedload, increased by between 55 and 130 g (i.e. a 25 to 50 % increase).

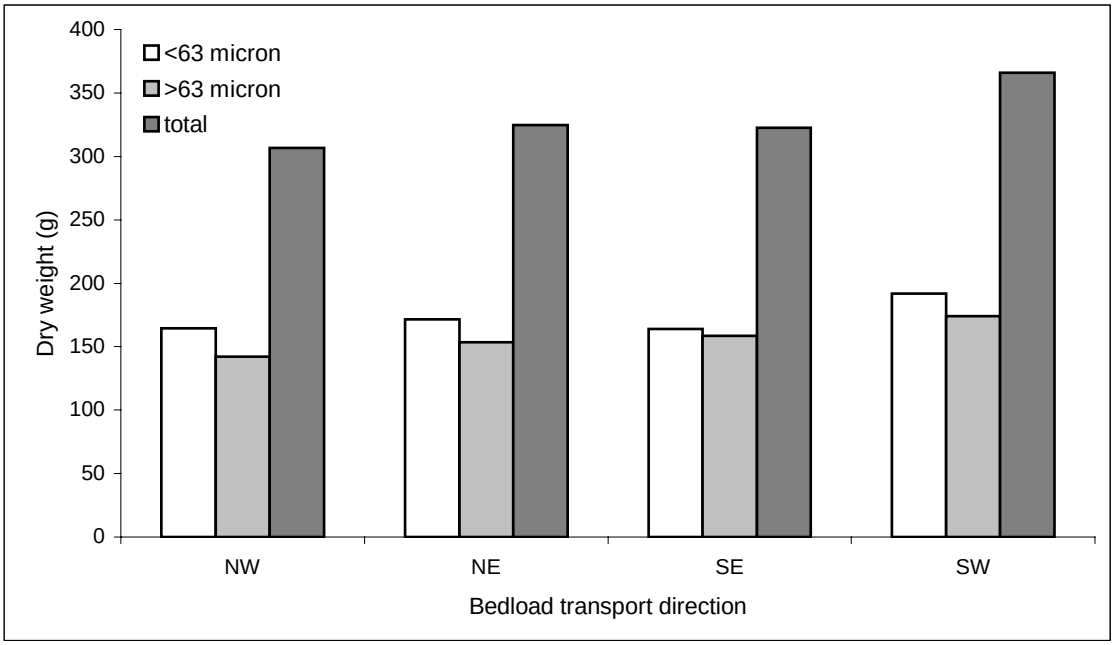

Figure 8.12: The direction and quantity of sediment transported, as bedload, on the north bank of the creek, during the period of highest wave activity (26/11/2003 am).

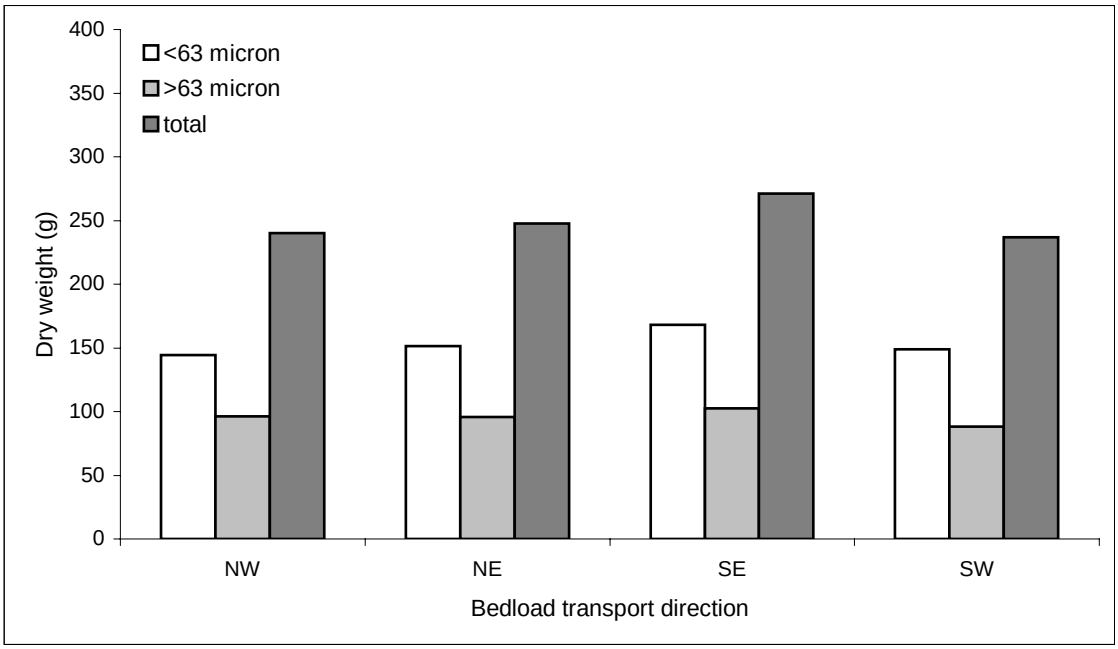

Figure 8.13: The direction and quantity of sediment transported, as bedload, on the north bank of the creek, during the period of bedload transport with smaller waves (25/11/2003 am).

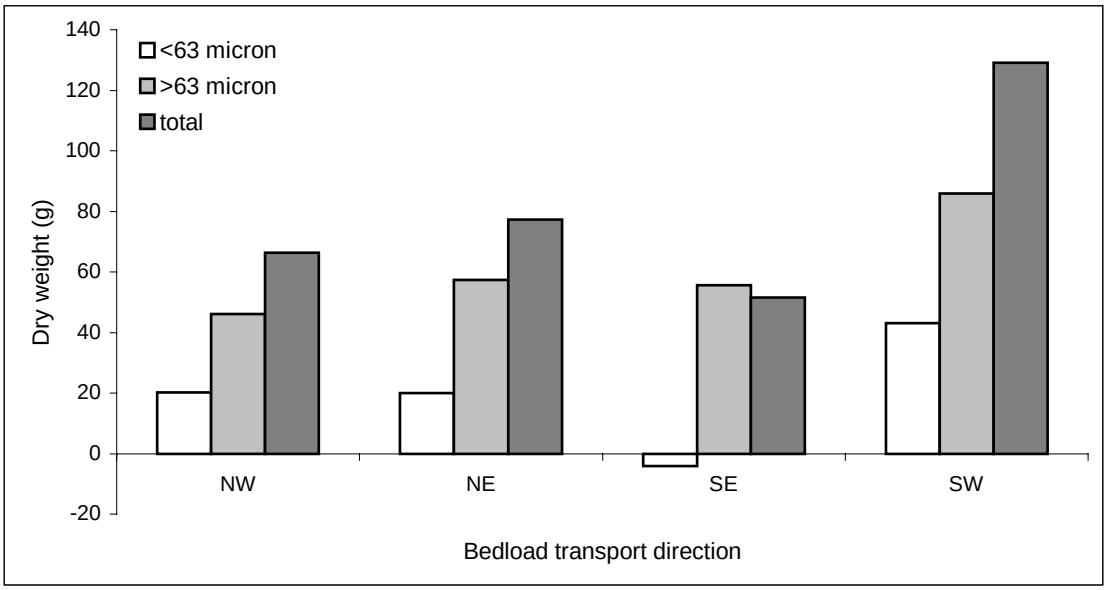

Figure 8.14: The difference between quantities of bedload transported during the period of higher wave conditions and the period of lower wave conditions, in each direction on the north bank of the creek.

The south bank of the creek experienced similar increases in bedload transport to the north bank, between 25/11/2003 am (Fig. 8.15) and 26/11/2003 am (Fig. 8.16), as the wave height increased. The percentage of fine-grained to sand-sized sediment was, on average, 10 % higher following the first period of wave activity, compared to the second, when the concentration of sand-sized sediment increased. The greatest increase in directional bedload transport, between the 2 inundations, was towards the SW (away from the creek) and the SE (Fig. 8.17). The quantity of sand-sized sediment transported as bedload towards the SW increased by 160 g; this was more than double that transported during the initial period of bedload transport. In comparison, the bedload transported towards the SE contained an increase in fine-grained sediment of 70 g; this was 50 % more than during the first period of bedload transport measurements. The smallest increase in bedload transport was towards the NW; this increase consisted mainly of sand-sized grains. Overall, the increase in sand-sized sediment in transport was double that of fine-grained sediment, between the two periods of bedload transport. The composition of sediment, transported as bedload, varied with wave height; as the wave height increased, the percentage of sand-sized sediment transported increased.

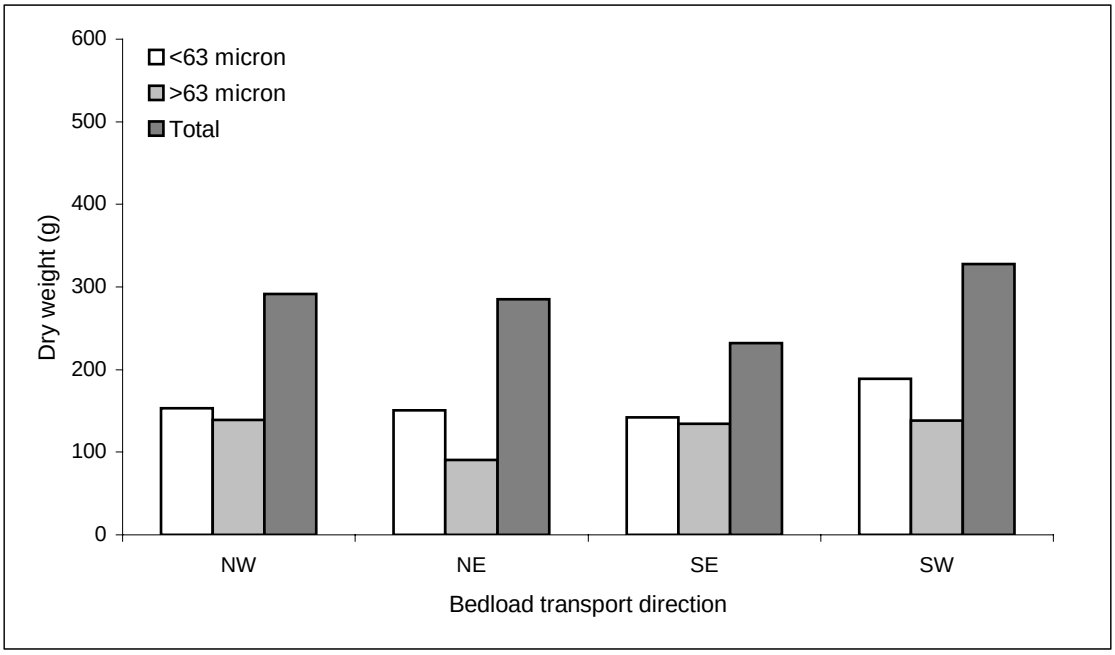

Figure 8.15: The direction and quantity of sediment transported as bedload, to the south of the creek, during the period of bedload transport with smaller waves (25/11/2003 am).

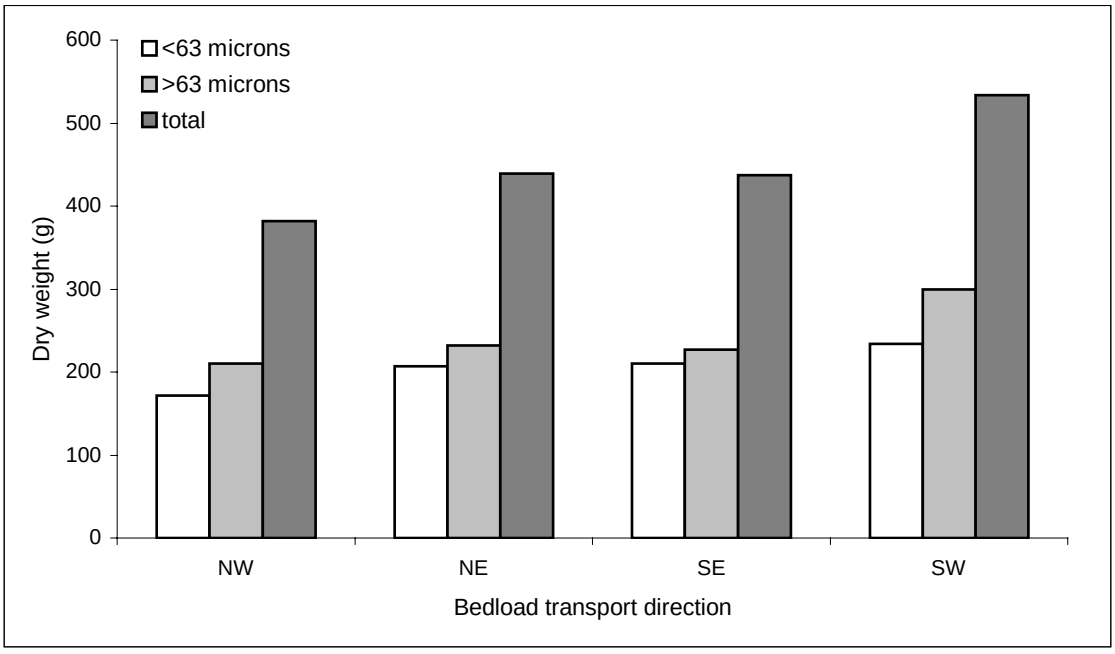

Figure 8.16: The direction and quantity of sediment transported as bedload, to the south of the creek, during the period of highest wave activity (26/11/2003 am).

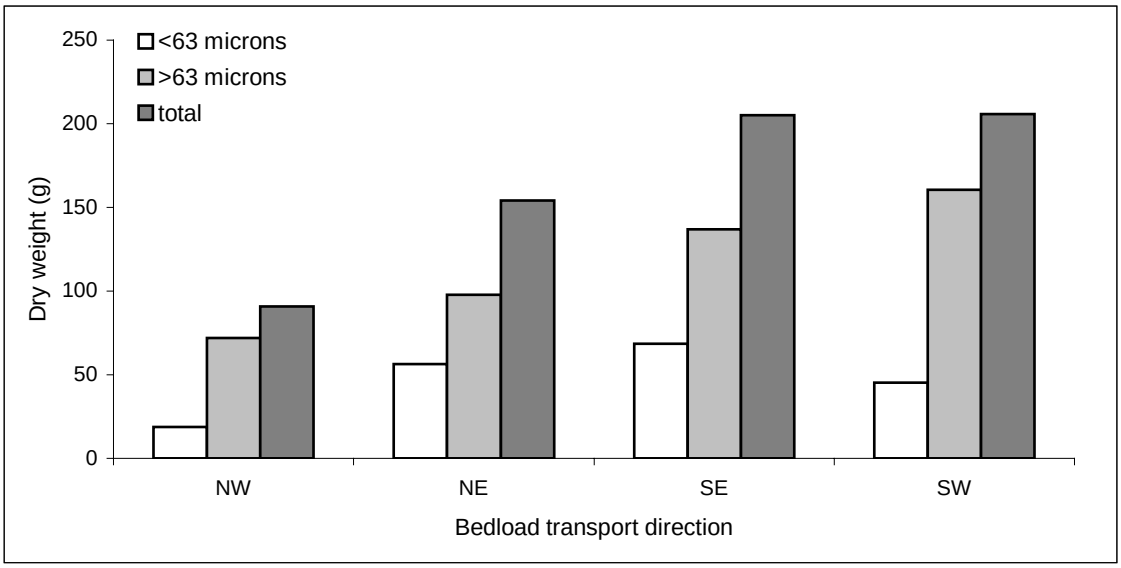

Figure 8.17: The difference between quantities of bedload transported during the period of higher wave conditions and the period of lower wave conditions, in each direction on the south bank of the creek.

The total bedload transported over the intertidal flats, on the north and south banks of the creek, provides an indication of the total bedload transport over the intertidal flats adjacent to the creek system. During the first period, the rates were similar in all directions; nonetheless, the bedload transport towards the SW was highest, whilst transport towards the SE was lowest (Fig. 8.18). During the second period, transport to the SW was again highest, i.e. 20 % more than towards the SE and NE, and 30% more than towards the NW (Fig. 8.19). The percentage of fine-grained sediment (by dry weight) in the bedload changed from 59 % within the first period, to 49 % in the second. An increase in significant wave height of 0.1 m, between the first and second period of transport, caused a 45 % increase in the bedload transport. The overall quantity of sediment transported, as bedload, was higher on the south bank of the creek.

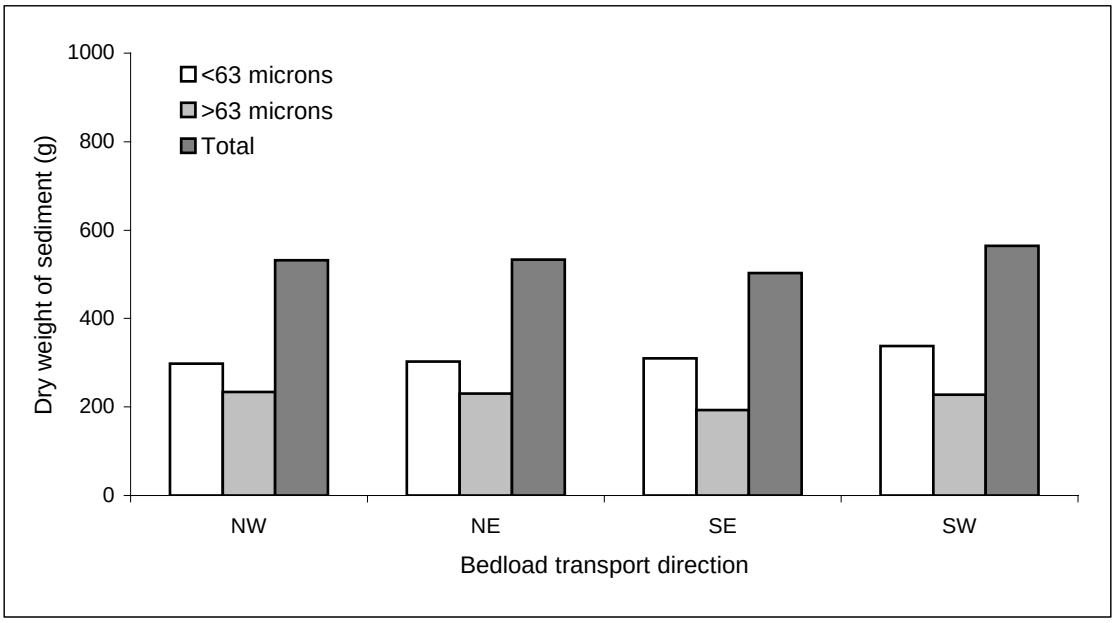

Figure 8.18: Total sediment transported by bedload, on the north and south banks (25/11/03 am).

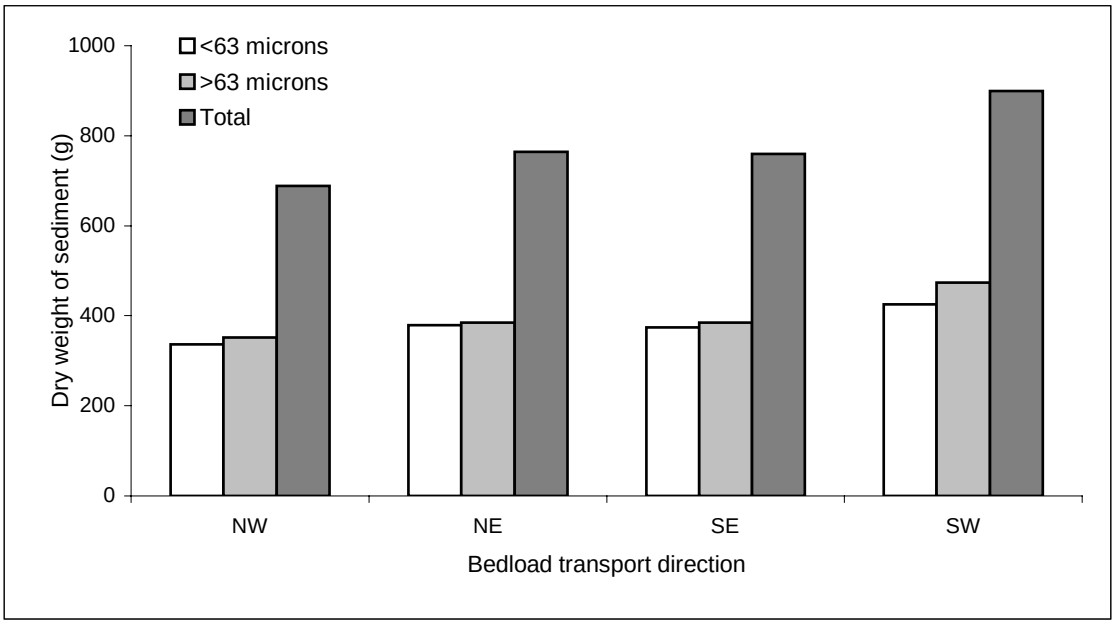

Figure 8.19: Total sediment transported by bedload, on the north and south banks (26/11/03 am).

The longshore movement of bedload over the intertidal flats was greater than the cross-shore movement (Figs. 8.20 & 8.21). On the north bank this was only noticeable during the period of greatest wave height; on the south bank, it was evident throughout both periods of bedload transport. More sediment was transported on the south than the north bank, with a maximum difference of 200 g, over 25 % more through a tidal cycle. During each period of bedload transport, the relative quantities of fine-grained and sand-sized sediment transported in longshore and cross-shore directions were similar.

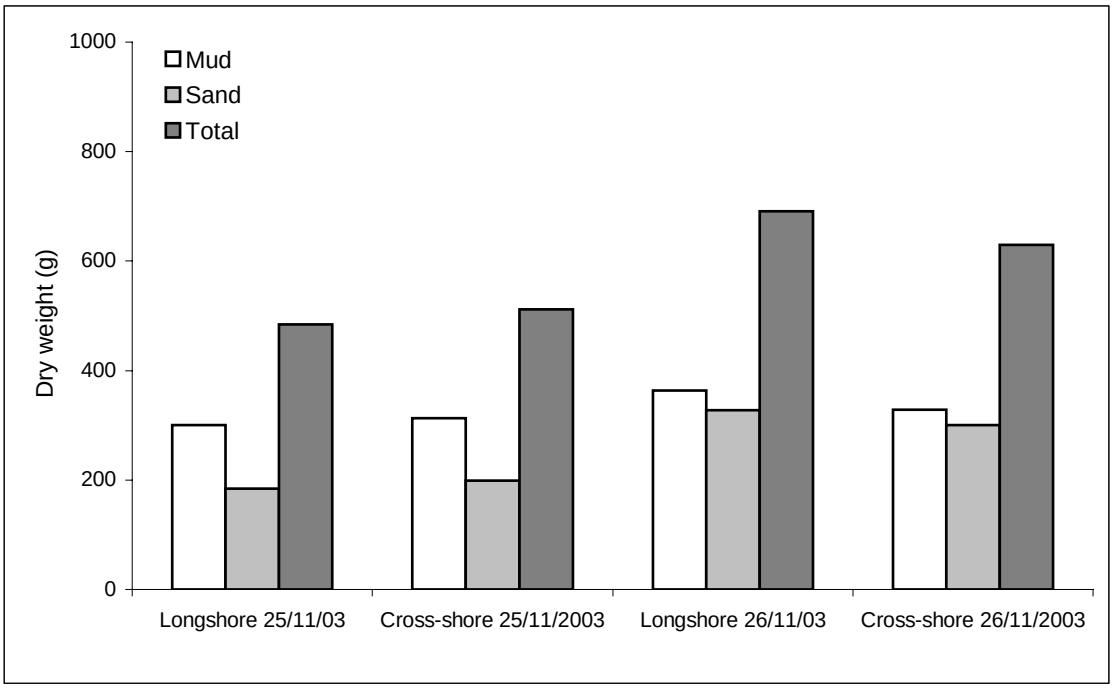

Figure 8.20: Longshore and cross-shore bedload transport, over the 2 inundations, on the north bank.

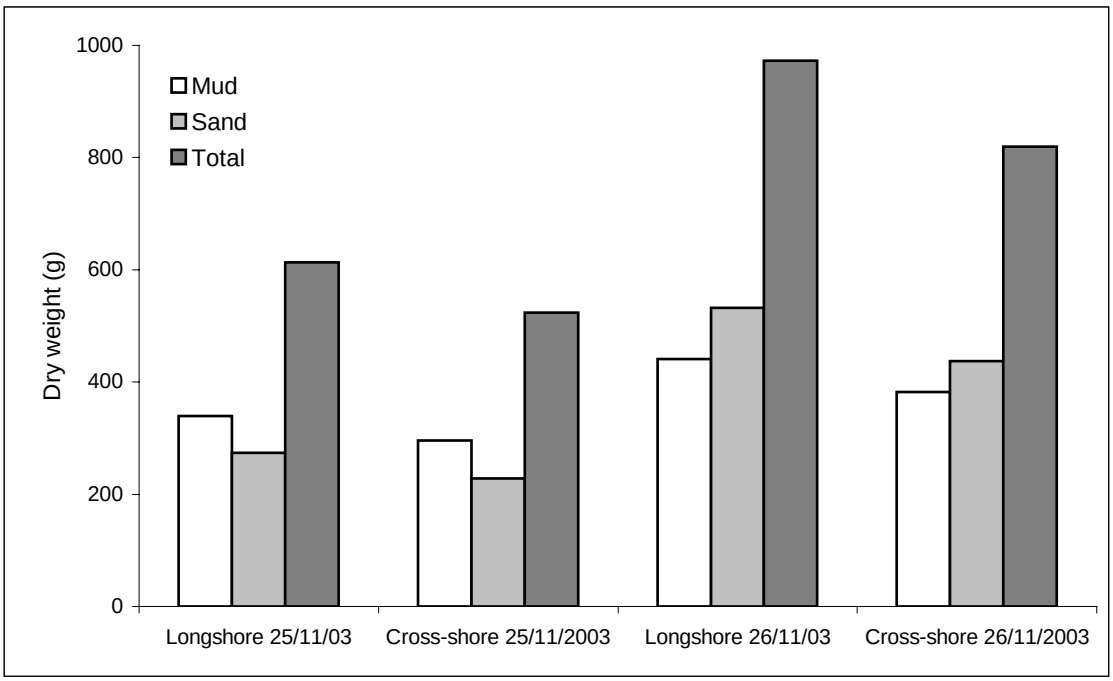

Figure 8.21: Longshore and cross-shore bedload transport, over the 2 inundations, on the south bank.

The sediment transported as bedload on the south (Fig. 8.22) and north (Fig. 8.23) banks, was of similar composition during both of the periods of bedload transport measurements. The sediment shows a bi-modal distribution in grain size, with peaks in the grain size distribution in fine silt (10 μm) and very fine sand (100 μm); 40 % of the sediment transported as bedload was very fine sand, between 63 and 125 μm. The sediment was poorly sorted, skewed towards sand-sized sediment, strongly bi-modal and the primary mode displayed a sharp peak (Buller and McManus, 1979). The variation between the composition of the sediment transported as bedload on the north and south banks, during both periods of bedload transport, showed that more fine-grained sediment was transported on the north bank and more sand-sized sediment was transported on the south bank (Fig. 8.24). The fine-grained (< 63 μm) sediment collected as bedload are considered to have settling velocities that are too low (W_s < 0.2 cm s^{-1}), for the individual grains to be transported as bedload rather than suspended load. The fine-grained sediment, sampled as bedload, may have been eroded from the bed and transported as larger floccules held together by cohesive bonds, or they may have been part of an appreciable concentration of suspended silt transported close to the bed (McCave, 1979).

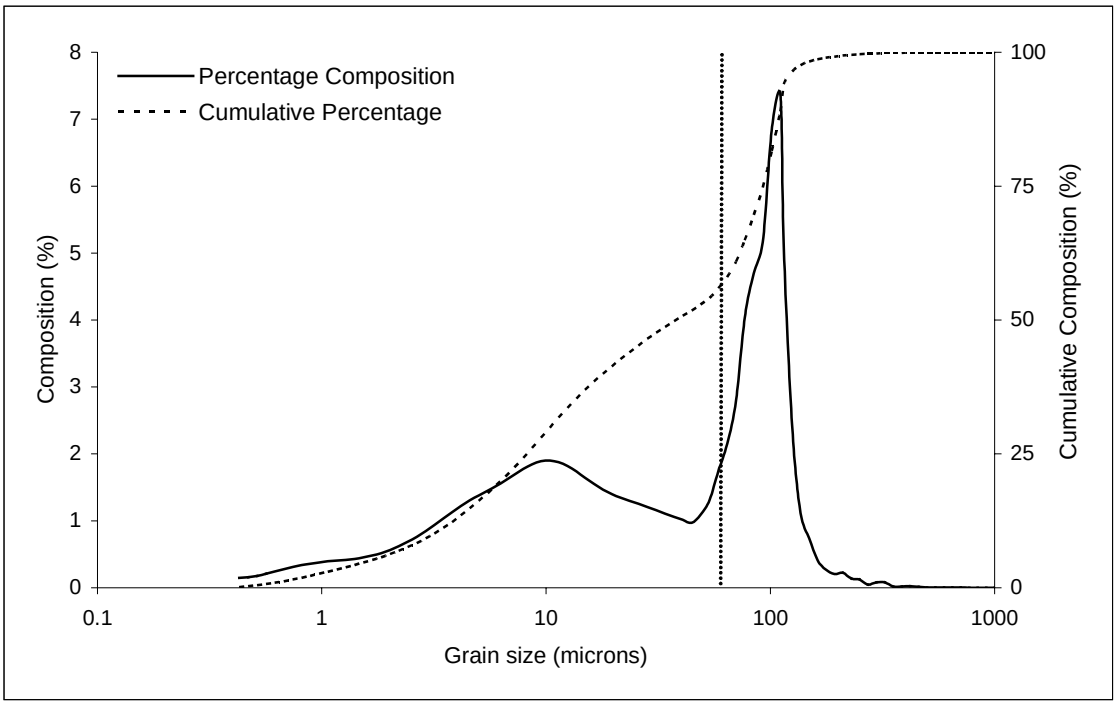

Figure 8.22: Averaged grain size of sediment transported as bedload, to the south of the creek, on 25/11/2003 am. The dotted line represents the 63 μm boundary.

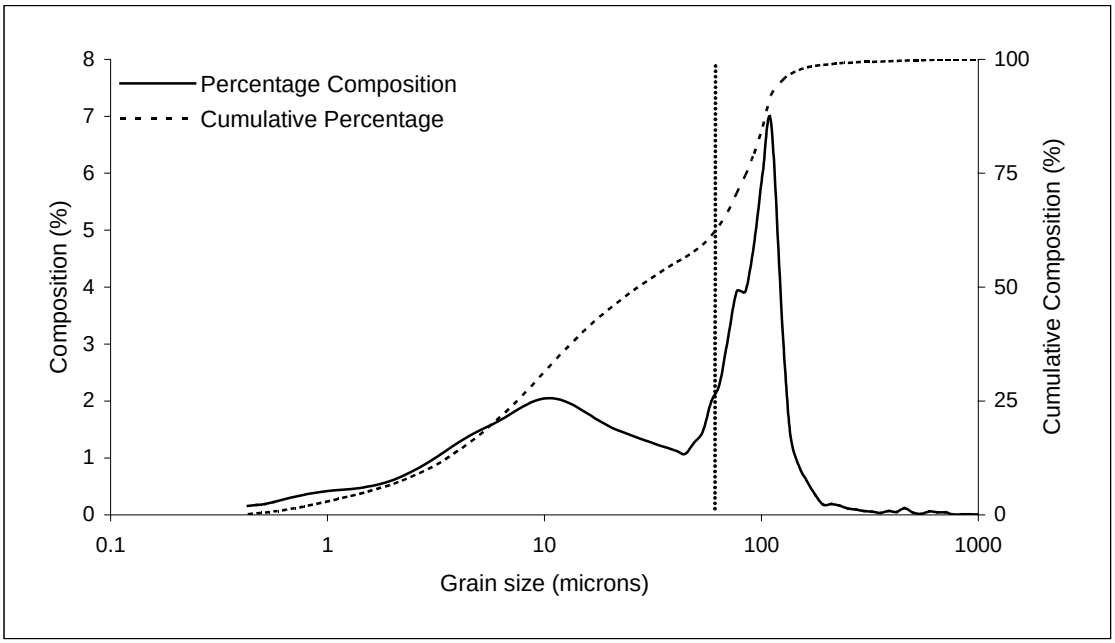

Figure 8.23: Averaged grain size of sediment transported as bedload, to the north of the creek, on 25/11/2003 am. The dotted line represents the 63 μm boundary.

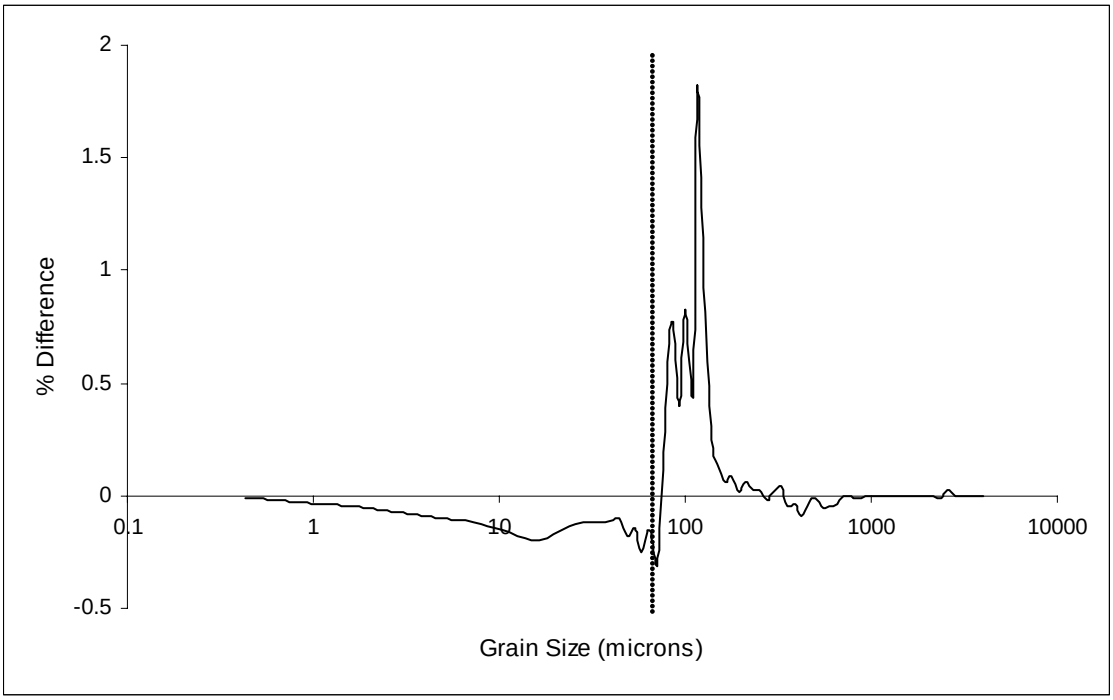

Figure 8.24: Averaged grain size of the sediment transported as bedload on the south bank minus that on the north bank, from 25/11/03 am. The dotted line represents the 63 μm boundary.

The sediment transported as bedload in different directions was compared for grain size composition, on the north and the south banks of the creek. The grain size distributions were all of a similar bi-modal distribution to the average distributions shown in Figures 8.22 and 8.23. No patterns were present in the sediment transported in different directions or in longshore and cross-shore directions, indicating that the samples deposited in each direction

were transported simultaneously, but in different directions owing to wave induced current oscillations and tidal current rotation.

8.3.4 *Bedload Transport Predictions*

Bedload transport rates were derived using all measurements collected throughout the deployment, allowing predictions of the bedload transport under all the wave and tidal conditions measured. These derived rates, based upon the Soulsby (1997) method for combined waves and currents, reveal that the rates for q_{bx} represent, predominantly, the predicted bedload in response to tidal currents; in comparison, q_{by} values represent bedload transport in response to wave activity. The predicted q_{bx} rates reveal 2 peaks within a tidal cycle (Fig. 8.25); these correlate with peaks in the tidal current speed and the period of shallowest water, i.e. during the first phase flood and last phase ebb. Minimal or no bedload transport, in response to the tidal current, was predicted during slack water (Fig. 8.26). During 2 of the last 3 tidal cycles of the deployment the predicted bedload transport in response to the tidal current increased, this coincided with an increase in the *Hs*. The value of q_{by} is unaffected by tidal current velocities; however, it shows strong peaks, dependent upon the prevailing wave conditions (Fig. 8.27).

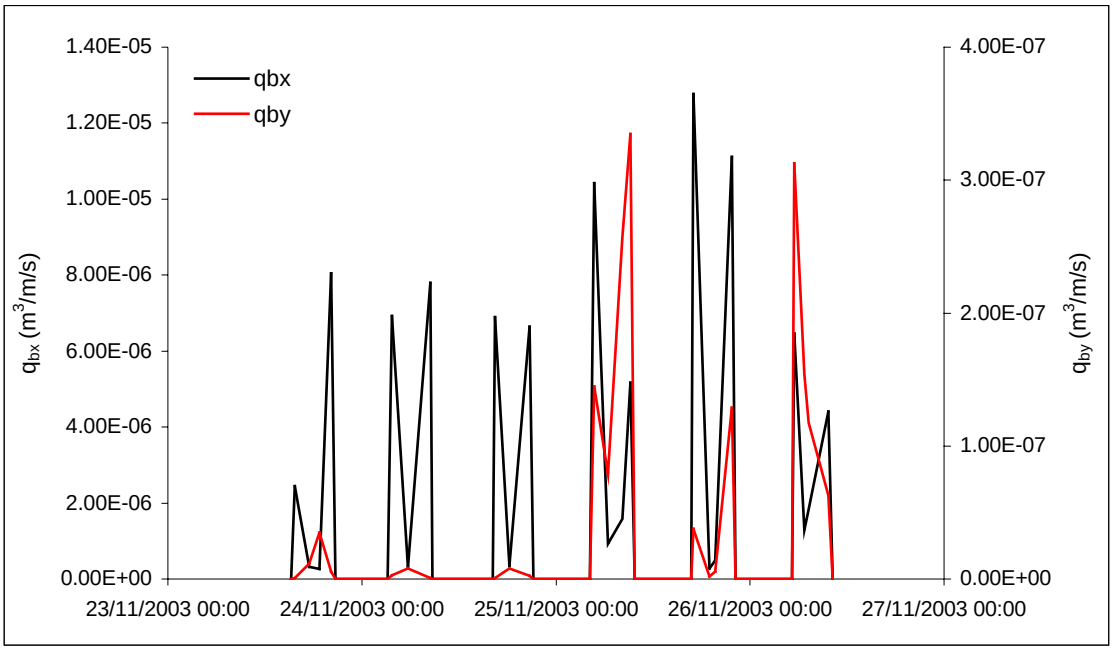

Figure 8.25: Predicted values of q_{bx} and q_{by}, without any modification incorporated for the presence of cohesive sediment, based upon flow measurements from the south bank.

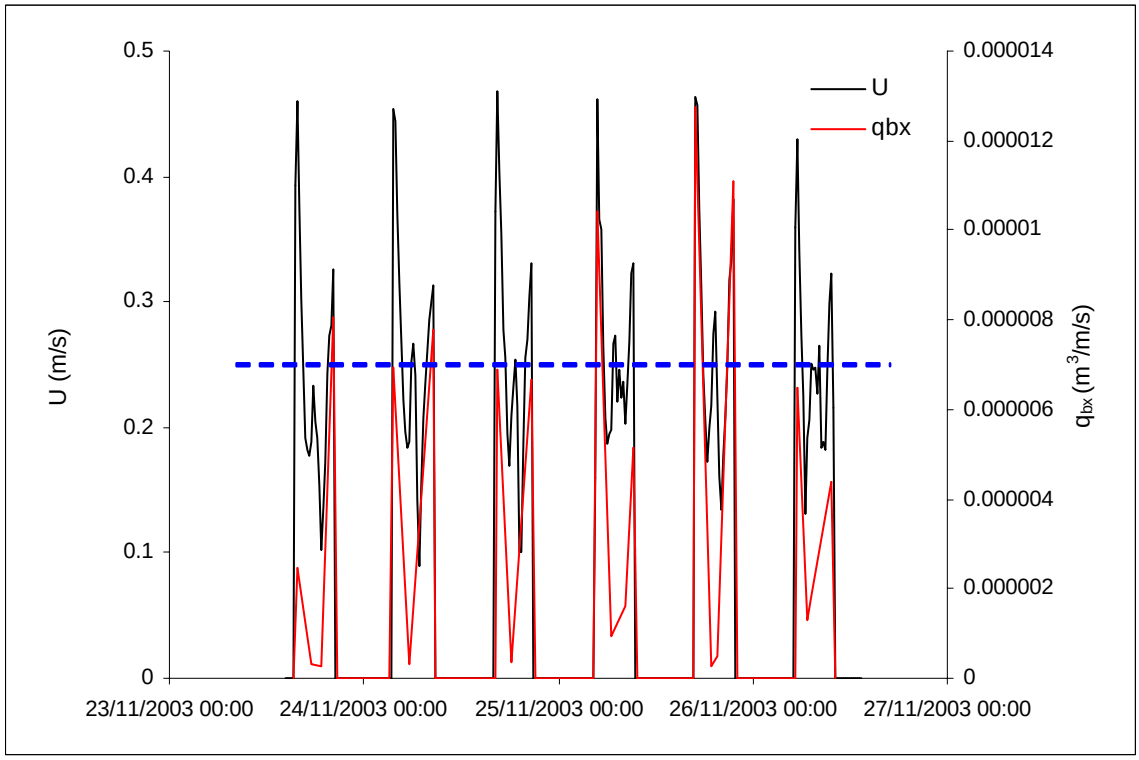

Figure 8.26: The relationship between the tidal current speed recorded at 0.25 m above the bed and the predicted q_{bx}, from measurements obtained on the south bank, with the critical threshold for transport of fine grained sediment (70 μm) shown by the blue dashed line, calculated using the equations from Soulsby (1997).

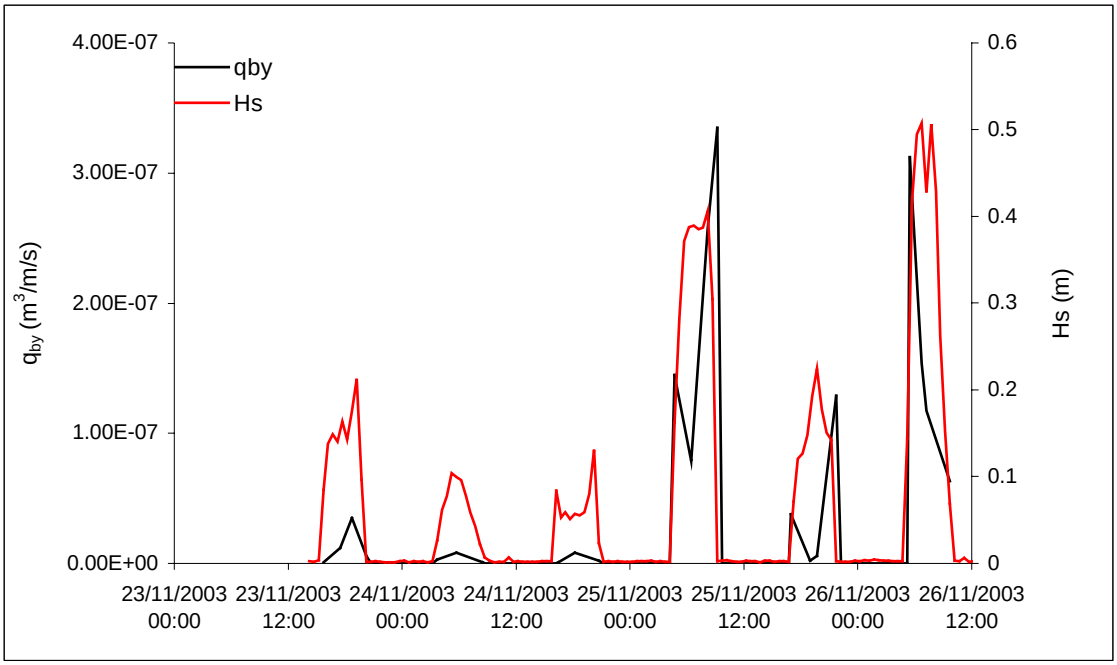

Figure 8.27: The relationship between *Hs* and q_{by}, derived on the basis of measurements obtained from the south bank.

A further correction was made to the bedload transport calculations, to take into consideration the composition of the bed, i.e. accommodating sediments with > 30% (dry weight) of clay-

sized particles. On the basis of a study undertaken by Panagiotopoulos et al. (1997), this percentage composition of sedimentary material was found to be sufficient to dominate the erosional characteristics of bed material. At such levels of clay content, sand-sized particles are no longer in material contact; as such, pivoting is not the primary mechanism for the initiation of grain motion; instead, it is controlled by the clay fraction. Owing to its cohesive nature, this fraction is able to withstand higher steady current flows, before erosion occurs. The critical unidirectional (current-induced) bed shear stresses, required to erode fine-grained sand, has been found to be increased by 90 %, in the presence of clay. The increase was higher, by 50 to 90 %, for clay quantities in excess of 11 to 14% (Panagiotopoulos et al., 1997). Under oscillatory flow conditions, the critical wave-induced orbital velocity was found to increase linearly, with mud content, when the clay fraction was in excess of 11 %. This approach reduced the q_{bx} values by an order of magnitude, with high bedload transport rates predicted in the direction of the current (Figs. 8.28 & 8.29). The predicted rates, with τ_c increased by 50 %, show the bedload transport in the same direction as the tidal current, peaks during the first phase of the flood, while the transport perpendicular to the tidal current, peaks during the last phase of the ebb. The predicted rates, with τ_c increased by 90 %, show the same pattern for the transport perpendicular to the tidal current, while the bedload transport in the same direction as the current peaks during both the first phase of the flood and the last phase of the ebb.

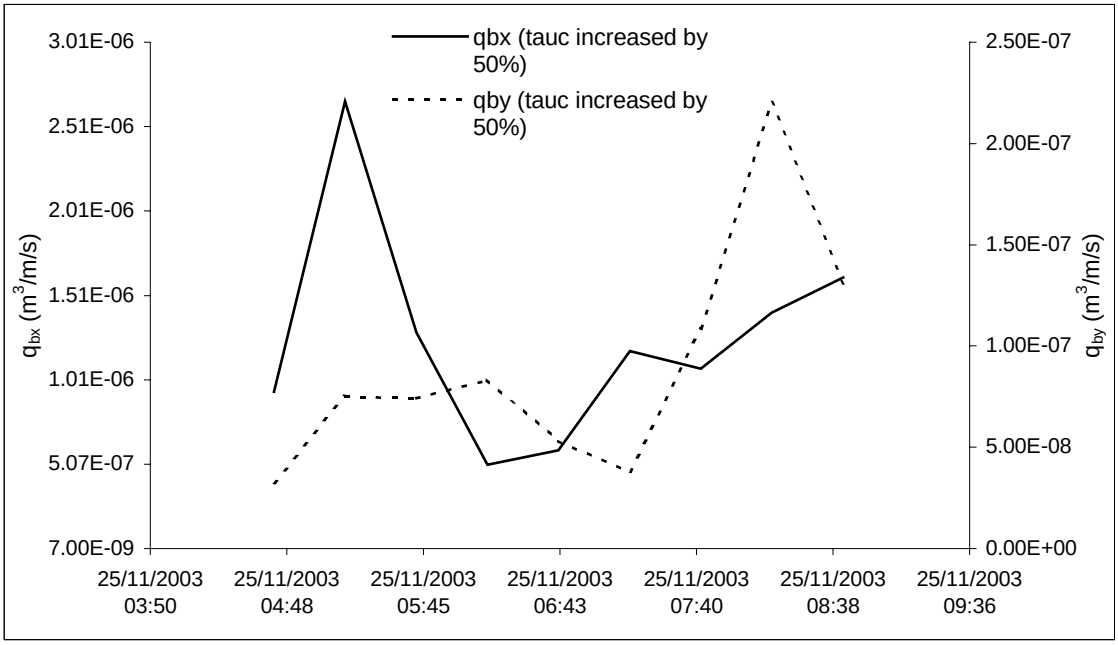

Figure 8.28: Predicted values of q_{bx} and q_{by}, with a 50% increase in τ_c, on the south bank, over the initial tide when bedload transport was recorded.

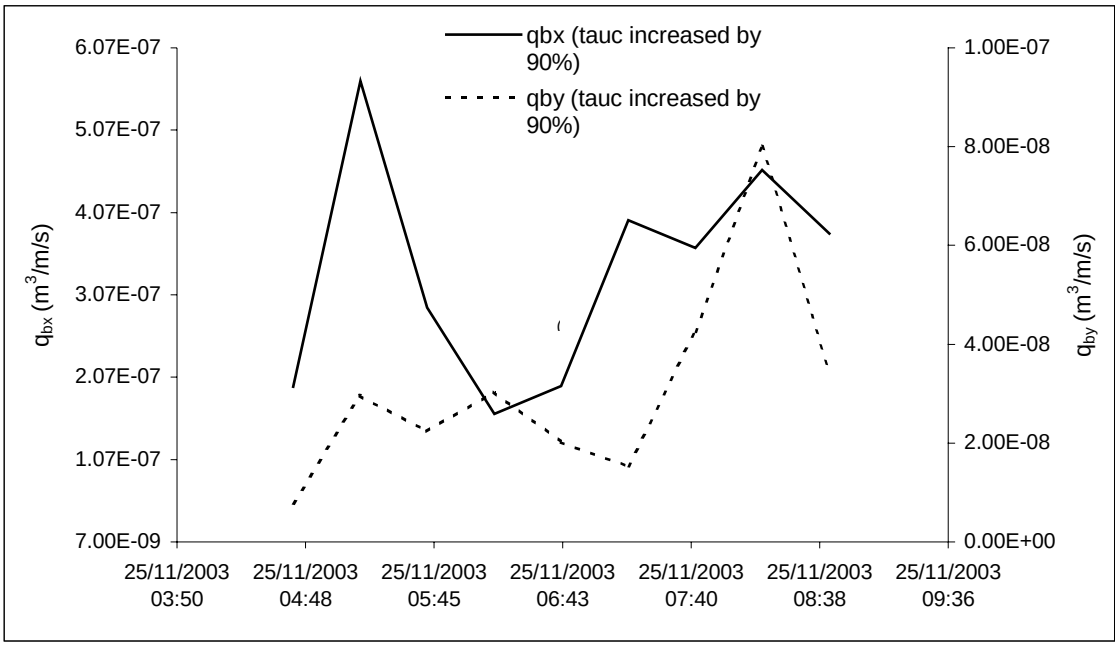

Figure 8.29: Predicted values of q_{bx} and q_{by}, with a 90% increase in τ_c, on the south bank over the first tide when bedload transport was recorded.

From hydrodynamic measurements, q_{bx} and q_{by} rates were predicted for the north and south banks of the creek; these reveal that higher bedload transport rates should have occurred on the north bank, whereas more sediment was transported as bedload on the south bank (Fig. 8.30). However, predicted bedload transport rates perpendicular to the tidal current are higher to the south. This highlights the difficulty in predicting accurate rates of bedload transport, as even when an area is subject to greater wave heights and tidal currents than another area, it may not have higher rates of bedload transport, as factors such as the localised topography may influence the rates. Overall, q_{bx} rates dominate the predicted bedload transport; their peaks are some 2 orders of magnitude greater than the peak q_{by} rates.

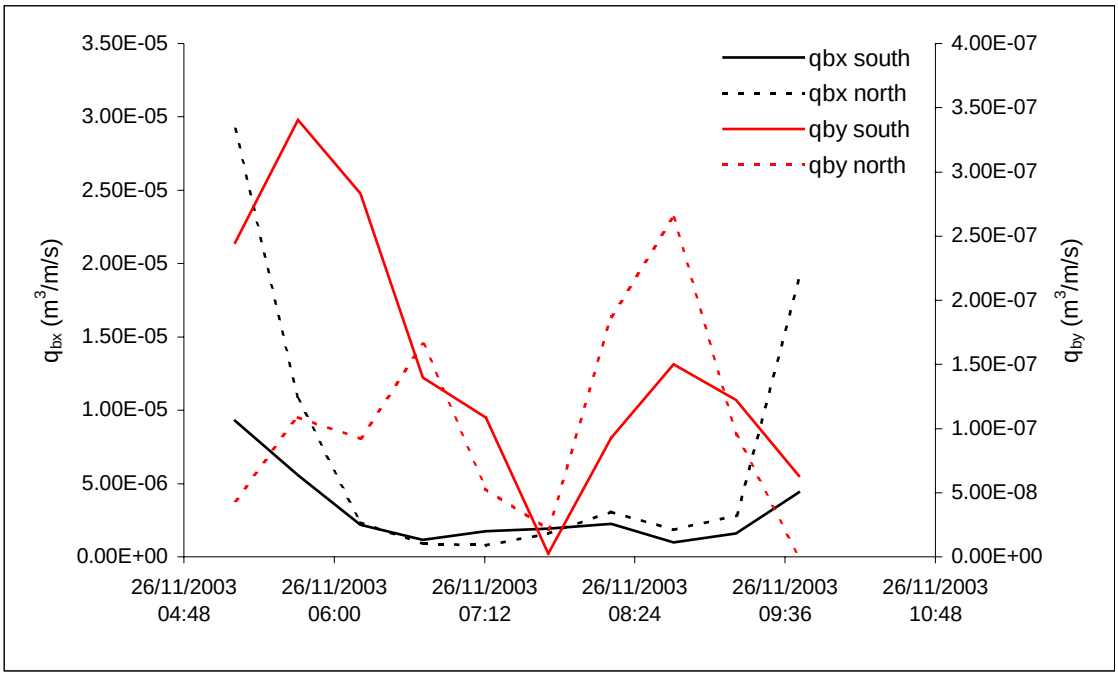

Figure 8.30: Comparison of the predicted q_{bx} and q_{by} rates, to the north and south of the creek, over the period with the highest wave activity.

On the basis of a more detailed investigation over a tidal cycle, the variation in the peak q_{bx} can be seen to vary very rapidly, depending upon the hydrodynamic conditions measured during the first phase of the flood (Fig. 8.31). For example, if the 'first phase flood' was recorded following a water depth of 0.5 m, high bedload transport rates would be predicted. However, if this stage was not recorded and the initial measurement was obtained in a water depth approaching 1 m, the predicted transport rates could be up to an order of magnitude lower. In addition, high-resolution instrumentation at varying heights above the intertidal flats are required during the first phase flood and last phase ebb in order to accurately predict the rates of bedload transport and to be able to calculate the net transport throughout a tidal cycle.

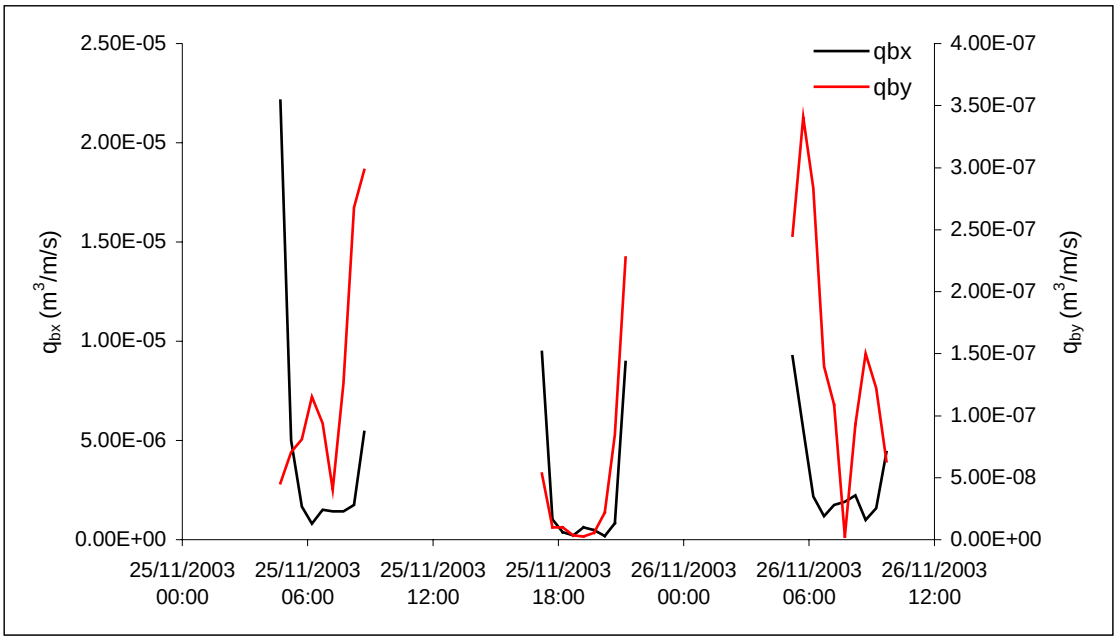

Figure 8.31: Predicted values of q_{bx} and q_{by} over the deployment period (Note: predicted values were calculated every 30 minutes, from the measurements obtained on the north bank).

8.4 DISCUSSION

The tidal currents in the creek were flood dominant, although the ebb phase of the tide had a longer duration. Unfortunately, associated peaks in SSC were not recorded (as the OBS became saturated (Section 9.3.1)); the width of the peaks infer that higher and longer duration peaks were experienced during the ebb tide; this would indicate that the creek was acting as an exporter of sediment. Flow within the creek lasted for 30 to 45 minutes longer than on the adjacent intertidal flat, at the beginning and end of the tidal cycle; during these periods, large quantities of sediment were transported within the creek. Intertidal creeks acting as exporters of sediment have been identified elsewhere; for example, tidal creeks within the saltmarsh of the Westerschelde estuary, south-west Netherlands (Hemminga et al., 1996). The peak tidal current speeds within the creek, at Freiston Shore, occurred following bankfull stage, during both the flood and ebb stages of the tidal cycle. Previous investigations have found that within creeks on the upper area of the saltmarsh, the peak flood current speed occurs after bankfull stage, while the peak ebb tidal current speed occurs when the water is only present within the creeks (Dyer, 1986). The peak ebb tidal current occurs following bankfull in saltmarsh creeks as the creeks have developed to drain the saltmarsh, and so the majority of the shallow water over the saltmarsh will flow into the creeks, creating higher tidal current speeds within the creeks when the saltmarsh has drained, i.e. after bankfull. In contrast, the creek system on the mudflat examined in the present study, was enhanced in order to drain overland flow from the drainage of the MR; however, much of the overland flow had, by the

time of this study, ceased (see Chapter 6), resulting in the creek system only draining a small area of the intertidal flats, causing lower tidal current speeds.

In order to establish, fully, the effects of bankfull stage, on the flow conditions inside the creek, higher-resolution sampling would be required. The sampling frequency adopted (the most frequent sampling possible with the ABRs) obtained only a maximum of 2 measurement bursts (including a 60 s tidal burst and a 512 s wave burst) before the bankfull stage was reached; more are necessary nearer to the creek bed to obtain detailed information on the hydrodynamic interaction between the creek and the adjacent intertidal flats. Nonetheless, the peak flow in the creek was observed to occur just after bankfull stage; peaks in the SSC occurred before and after these peak flows.

The initial peak in the SSC was in response to the initial flow of water inside the creek, causing resuspension of loosely-deposited material. The second peak, following bankfull stage, correlated with the peak observed on the adjacent intertidal flats; this was in response, in turn, to the initial flow over the flats, resuspending the loosely-consolidated surficial sediments (Ke and Collins, 2000). The peak in the SSC experienced in the creek, at the same time as the ebb peak over the intertidal flats, was related to suspended material flowing into the creek. The second SSC peak within the creek occurred after the water level dropped back below bankfull; this resulted from the final drainage of surface waters from the intertidal flat, becoming focused into the creek, transporting sediment already in suspension, whilst, at the same time, resuspending sediments within the creek.

The flow out of the MR site, which led initially to the enhanced development of the creek system (Chapter 7), did not affect the creek throughout *Deployment 3*. The main creek connected to the channel within Breach 1 had, by this time, been eroded to such an extent that it was capable of containing the water draining from the MR, following HW on spring tides, without any overbank flow occurring.

The intertidal zone, on the basis of the measurements obtained, appeared to act as a net importer of sediment. Peak tidal current speeds occurred during the first phase of the flood, generally coinciding with the peak in SSC. This peak in tidal current speed differed between the banks of the creek, by 0.1 to 0.15 m s^{-1}, with the highest being on the north bank (where another creek was located just 10 m away, to the north, possibly causing the increase in current speed). The peak tidal current speeds observed within the creek were similar to those observed on the adjacent intertidal flats. However, the creek current speed dropped to nearly

zero at high water whereas, over the flats, a small increase in tidal current speed was recorded.

The small creek investigated here (within the lower intertidal zone) differed to most studied previously, which incorporated either mature saltmarsh creeks or much larger channels (Kestner, 1975; Ward, 1979 and 1981). Accordingly, the measurements obtained show very different conditions to those of the other creeks and channels. For example, most of the latter were associated with higher velocities, than the surrounding intertidal zone, e.g. the tidal channel in the Danish Wadden Sea had much higher velocities (1.2 m s^{-1}) than the adjacent intertidal flat (0.35 m s^{-1}) (Vinther et al., 2004).

When the significant wave height exceeded 0.25 m, the peak SSC on the intertidal flats switched from flood- to ebb-dominant. When the wave height was sufficient to entrain the surface sediment, the SSC switched to ebb-dominant, making both the intertidal flats and the creeks exporters of sediment. Hence, intertidal flats accrete during calm periods and erode during rough weather, when high wave activity is present; this agrees with the findings from the Dutch Wadden Sea, The Netherlands, by Janssen-Stelder (2000). Such a pattern has been noted in previous work by Gao and Collins (1997) and Vinther et al. (2004), when wave action caused a change from flood dominance to ebb dominance in the eastern Solent and the Danish Wadden Sea.

During periods of low wave energy no bedload transport was measured over the intertidal flats at Freiston Shore, owing to the low efficiency of the bedload samplers (Novak, 1959; Graf, 1971; Amos, 1974; and Carling, 1996), as the critical transport threshold for fine sand (70 μm) was 0.25 m s^{-1} and the maximum current speed was 0.6 m s^{-1}. Hence, the bedload transport rates recorded have been used to show the relative rates over the deployment and the type of sediment transported.

On the intertidal flats at Freiston Shore, the rates of bedload transport were similar in the 4 directions measured; however, the longshore transport away from the mouth of The Wash was the highest. The rates of bedload transport, in each direction sampled, varied spatially; the south transported more sediment than the north bank, owing to the topography surrounding the bedload samplers, for example, the presence of creeks interrupting the intertidal flat, reduces the area over which bedload transport can be initiated and thus reduces the potential quantity of sediment transported as bedload (Fig. 8.1). The sediment transported as bedload had a bi-modal distribution, with peaks in fine silt and very fine sand, with very fine sand being the most common grain size. The fine silt was sampled as bedload through two

possible forms of transport; as bedload with numerous grains held together in compacted floccules, which had been eroded from the bed by wave activity; and in suspension close to the bed. The composition of the sediment transported, as bedload, varied with wave height; the ratio of sand-sized to fine-grained sediment increased with wave height.

The total bedload transport rates, calculated using the method of Soulsby (1997) showed peaks in bedload transport coinciding with the peaks in the tidal currents, and an enhancement to the bedload transport when wave activity was superimposed.

A limitation in calculating bedload transport rates from field data is considered to have been related to the resolution of the measurements, i.e. whether the very first phase of the flood and the very last phase of the ebb were recorded. If such periods of high tidal currents and low water depths (just after the ABRs were inundated), together with moderate wave heights, were recorded, then the predicted bedload transport rates were much higher than if the first measurement was obtained at a water depth of 1 m.

8.5 CONCLUDING REMARKS

Within tidal creeks and over the adjacent intertidal flats, the peaks in suspended sediment transport occurred during the first phase of the flood and the last phase of the ebb. Exchanges of sediment between the creek and the intertidal flats were observed, with the most important being sediment from the intertidal zone being transported into the creek during the last phase of the ebb. During the last phase of the ebb tide, high SSC over the intertidal flats and within the creek resulted from high tidal current speeds; these transported sediment already in suspension and resuspended sediment, deposited during the preceding slack water. A second peak in SSC was experienced in the creek, as the water level fell below the bankfull depth; this was from the draining of the surface waters from the adjacent intertidal flats, carrying suspended sediment into the creek. The levels of suspended sediment were higher in the creek than over the adjacent intertidal flats and the creek remained flooded for 30% longer. These findings agree with the function of a tidal creek, as described by Allen (2000b); i.e. they distribute tidal waters and suspended sediment over the creek banks during the flood, returning the tidal prism and any undeposited silt to the sea, as the tide ebbs.

Wave activity over the intertidal zone enhanced, generally, the sediment transport: more bedload and suspended sediment transport took place when waves were superimposed, although various other parameters affected also the transport rates: the tidal currents; water depth; wave direction; sediment composition; and sediment stability. The prevailing wave height was found to affect the composition of the sediment transported as bedload; as the

wave height increased, the proportion of sand-sized sediment transported increased. The direction of net sediment transport varied depending on the prevailing wave conditions. During the spring tides recorded, net landward transport was experienced over the intertidal flats, under calm conditions; this changed to seaward transport during periods with significant wave heights greater than 0.25 m. Rates of bedload transport were generally similar in all directions; however, longshore transport just dominated over the cross-shore transport.

The Soulsby (1997) approach predicted that bedload transport would occur under strong tidal currents, with no wave activity. Nonetheless, for future studies, resolution of the tidal currents is important; for example, if the first measurement was obtained when the water was 1 m deep, a very different bedload transport rate will result than under the same conditions with an initial depth of 0.5 m. There are a number of limitations with the work undertaken here, with respect to the bedload transport recorded. A representative rate of sampling, both spatially and temporally, is difficult to achieve; for example, fluctuations in the rate of bedload transport at different states of the tide could not be established. The transport of sediment over the intertidal zone, together with that within the creeks, is a highly complex process; on the basis of the observations of this study, it is still not completely understood and is difficult to predict accurately. The efficiency of the bedload transport traps was low, resulting in no bedload transport being recorded during periods of low wave activity.

CHAPTER 9: SEDIMENT DYNAMICS OVER AN INTERTIDAL ZONE

9.1 INTRODUCTION

Researchers have studied Freiston Shore since the 1950s, with a variety of studies providing a background to the present investigation (Table 3.1). Data are available prior to the land reclamation of 1980, since the reclamation, and following MR (2002) of the original 1980 reclamation site. As such, an extensive data set is available to investigate the impact of anthropogenic changes, on the hydrodynamics and geomorphology of the intertidal zone. The aim of this Chapter is to describe the sediment dynamic and hydrodynamic conditions over the intertidal zone, and, wherever possible, to compare the present situation with those of the past to identify any changes that have occurred over the last 35 years. Understanding the natural processes, in particular the tidal currents, wave climate, sediment transport and sediment stability, over intertidal flats is necessary prior to the initiation of any coastal management (Gao and Collins, 1995). Once an understanding of the natural processes is established, any impacts from anthropogenic changes on the intertidal zone can be identified. These impacts need to be recognised to predict how different forms of coastal management will effect the surrounding natural environment, which is important for deciding on suitable forms of coastal management for the future. This Chapter utilises an increase in the accuracy of measurements, which newly available equipment has provided, to attempt to refine the past findings and thus improve the general understanding of the environment.

The wave conditions over the intertidal flats and inside the MR site were measured, to examine the effectiveness of the different sub-environments of the intertidal flats at dissipating wave energy. Factors affecting suspended sediment concentrations in the waters overlying the intertidal zone were investigated, as it was found previously that storm conditions in the North Sea could increase the level of suspended sediment ten-fold over the intertidal flats at Freiston Shore (Evans and Collins, 1975). However, previous studies have not identified the effect of locally varying tidal currents and wave conditions on the suspended sediment. At other intertidal flat locations, it has been shown that any simple empirical relationship between SSC and tidal height, related strongly to the tidal current, is generally obscured (French and Spencer, 1993). There are a number of possible reasons for this lack of correlation: the deposition and resuspension of sediment during the tidal cycle; sediment mobilisation by wind-waves; and any variations in the background concentration of sediment, from offshore areas (Evans and Collins, 1987; and Luternauer et al., 1995). Measurements of erosion/accretion have been used in the present investigation to identify seasonal changes in bed level and their spatial variability over the flats. The associated

compositions of the surficial sediments were analysed, then compared with the rates of erosion/accretion change, to identify any existing correlations. These data have been combined with those from an earlier study, where no definite trends in bed level change were identified (Amos, 1974), to establish any patterns in the combined data and to see if there has been any change over time.

9.2 METHODS

Data collected by the ABRs and the sediment samplers, during 4 deployments, have been utilised (Section 4.3). Supplementary hydrodynamic data have been used: (a) from the wave buoy at the mouth of The Wash; and (b) from 3 wave/tide recorders deployed across the intertidal zone, at Butterwick Low (Section 4.8.5). Erosion/accretion data were used, together with surficial sediment samples obtained from the monthly sampling programme, which extended over an 18-month period (Section 4.4). Supplementary erosion/accretion measurements were collected over the saltmarsh (Section 4.8.3).

The high-frequency data collected from the ABRs were processed using the WAVELOG TURBIDITY 1.02 software (made available by Valeport Ltd. 2002). The processing involved:

(i) the calculation of the mean level and tidal slope for each burst;
(ii) the de-trending of the bursts, to remove the low-frequency tidal components;
(iii) the application of a frequency-dependent correction to the pressure fluctuations, to correct attenuation at the high-frequency end of wave spectrum; and
(iv) the calculation of the summary wave parameters and the frequency spectrum, from the corrected water surface record.

Synoptic wave conditions at the different measured sites were then compared, to calculate the extent of wave dissipation over the intertidal zone, in accordance with the procedure of Moeller et al. (1996).

9.3 RESULTS

9.3.1 *Hydrodynamics*

The sampled tidal heights were compared to those which occurred from 2002 to 2004 to examine their representation of wider-ranging conditions (Fig. 9.1). This comparison showed the tides sampled during this study represent the upper part of the tidal ranges, i.e. approaching spring tides.

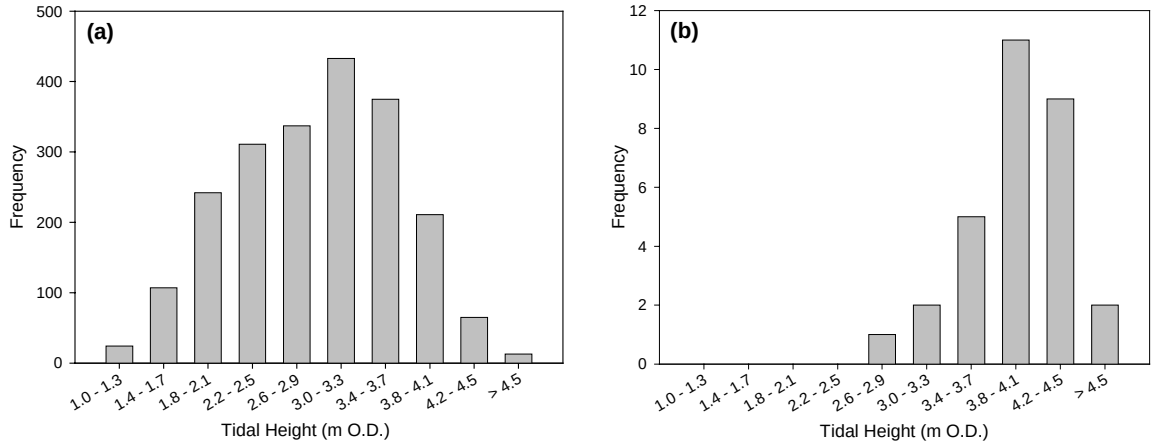

Figure 9.1: (a) Frequency of tidal (predicted) height, for all tides from 2002 to 2004; and (b) frequency of the tides measured during *Deployments 1 – 4* (for details, see text).

The hydrodynamic conditions measured over the upper and lower intertidal zones, throughout *Deployments 1* and *4* are shown in Figures 9.2 to 9.5. The peak tidal current speeds were generally associated with the first phase of the flood and the last phase of the ebb; this pattern was more emphasised over the lower intertidal zone. The current speed was higher over the lower (with peak values ranging from 0.3 to 0.5 m s^{-1}), compared to the upper intertidal zone (with peak values ranging from 0.2 to 0.3 m s^{-1}). The upper intertidal zone often experienced a third peak, of similar magnitude to the first phase and last phase peaks, just before HW; this peak occurred simultaneously with the peak flow entering the MR site through the channel within Breach 1 (Fig. 9.6). The peak water depth at the upper intertidal site did not coincide with that of the channel within Breach 1; water continued to flow into the MR site until the water level over the adjacent saltmarsh dropped to a certain elevation. This was owing to the fact that the channels within the breaches were not of a sufficient size to allow the quantity of water necessary to fill the MR site to the same water level as present over the adjacent saltmarsh (Chapter 6). This meant that water continued flowing into the MR site after HW was experienced on the saltmarsh, resulting in different tidal curves inside the MR site and over the saltmarsh (Chapter 5).

The tidal current speeds during *Deployment 1* increased as the tidal range increased, throughout the deployment. The first 3 tides, when the tidal height was increasing from neap to spring tides, had lower current speeds than those of the later tides during the peak spring tidal heights. However, tidal current speed was not related directly to the tidal height; this can be seen clearly over the lower intertidal zone during *Deployment 1* (Fig. 9.3), when the peak tidal current speeds were experienced during tides 0.5 m lower (on 07/09/2002 am & pm) than the peak tidal height (09/09/2002 am & 10/09/2002 am).

The SSC peaked during the first and last phases of the tidal cycle, with more defined and consistent peaks over the lower intertidal zone. However, throughout *Deployments 1 – 3*, the OBS became saturated during the peak values of some of the tides; as such, the peak concentrations were not recorded. The gain setting was altered for *Deployment 4*, when peak values were recorded. The SSC decreased in a shoreward direction; the lower intertidal zone (site 3) had peak concentrations of 154 to 294 mg l^{-1}, whilst the upper intertidal zone (site 1) had peaks of 108 to 255 mg l^{-1}. The percentage of the spring tides at which the OBS became saturated, over *Deployments 1 – 3*, decreased shorewards; the OBS became saturated during 45 % of the tides measured over the upper intertidal zone, and during 73 % of the tides measured over the lower intertidal zone.

Wave conditions influenced the SSC, at both of the sites. Overall, the SSC appeared to vary more as a result of the prevailing wave conditions, than in response to tidal currents. The wave conditions varied over the deployments, with the significant wave height (*Hs*) ranging from 0.05 to 0.5 m; in comparison, the peak wave period (*Tp*) varied from 1.5 to 9 s. *Hs* was greater over the lower intertidal zone than the upper location; this was in response to wave energy being dissipated over the intertidal flats (discussed in more detail in Section 9.3.2).

The ratio between the duration of the flood and ebb phases of the tide, over the upper intertidal zone, was 0.8 : 1. Over the lower intertidal zone, at lower tidal ranges, the ratio of flood to ebb was similar (Fig. 9.7); during spring tides, with larger tidal ranges, the ratio was 0.64 : 1 (Fig. 9.8). The asymmetry of the tide varied temporally over the lower whilst it remained relatively constant over the upper intertidal zone.

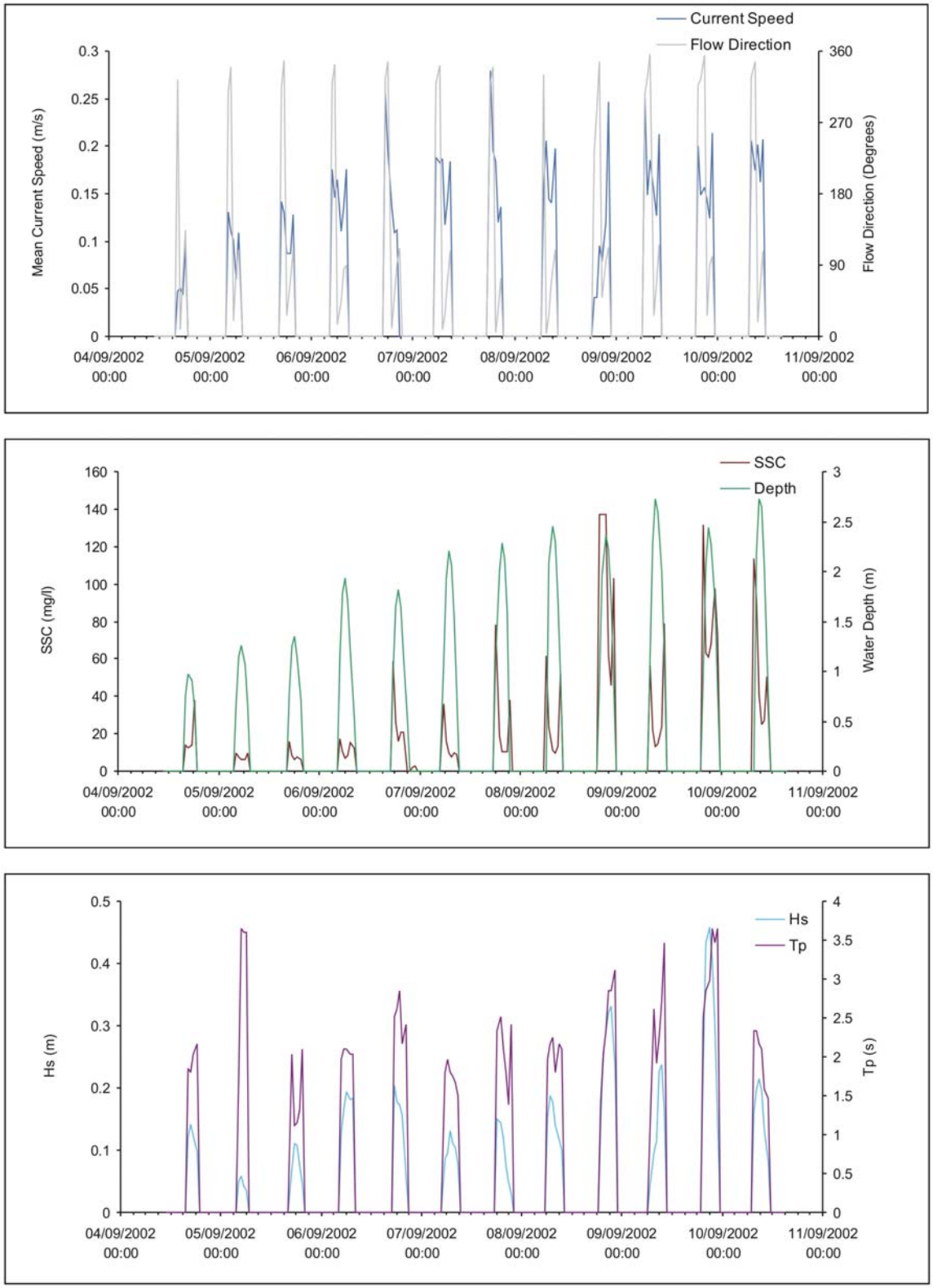

Figure 9.2: The hydrodynamic and sediment dynamic conditions during *Deployment 1*, over the upper intertidal zone (site 1).

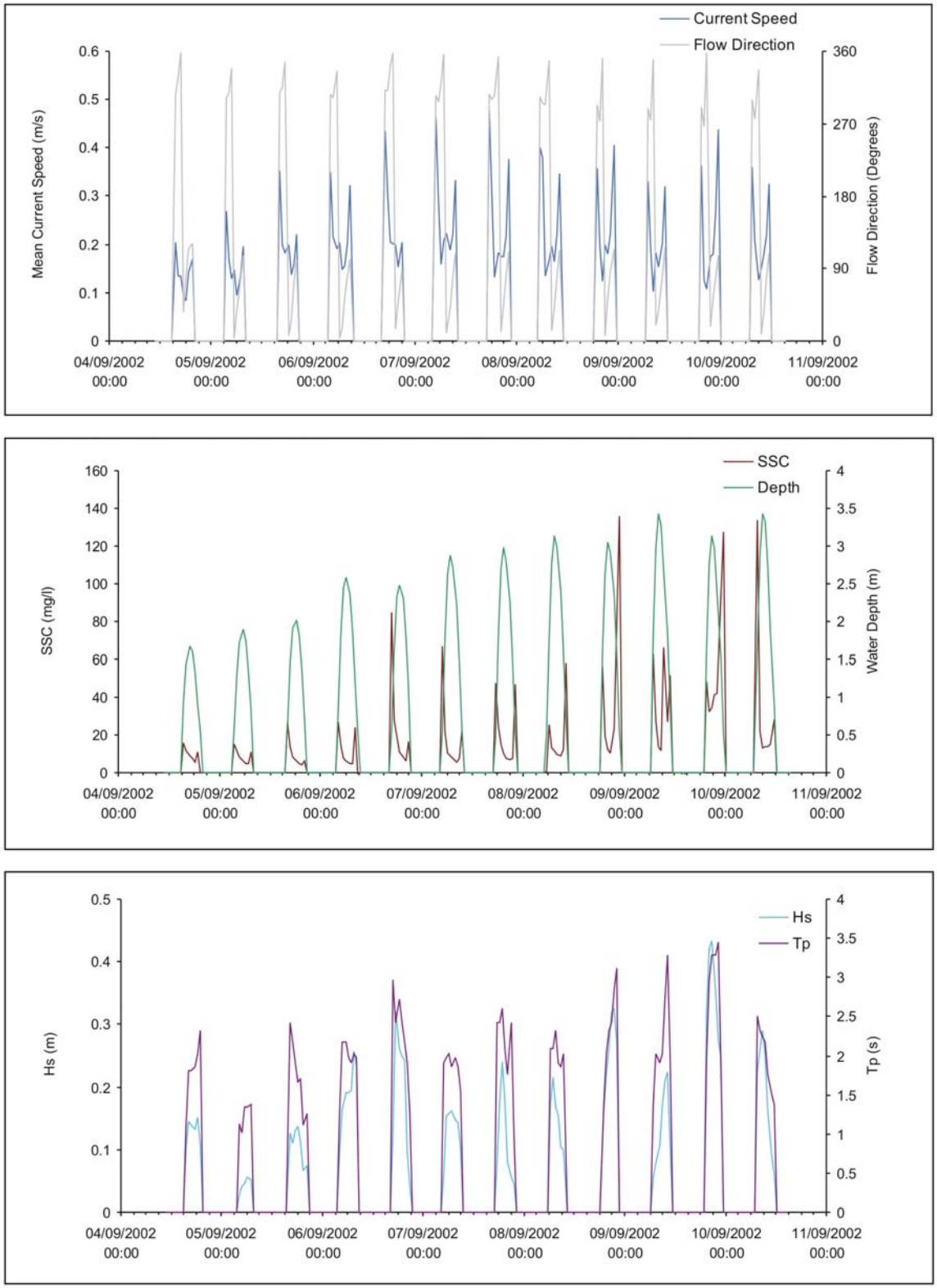

Figure 9.3: The hydrodynamic and sediment dynamic conditions during *Deployment 1*, over the lower intertidal zone (site 3).

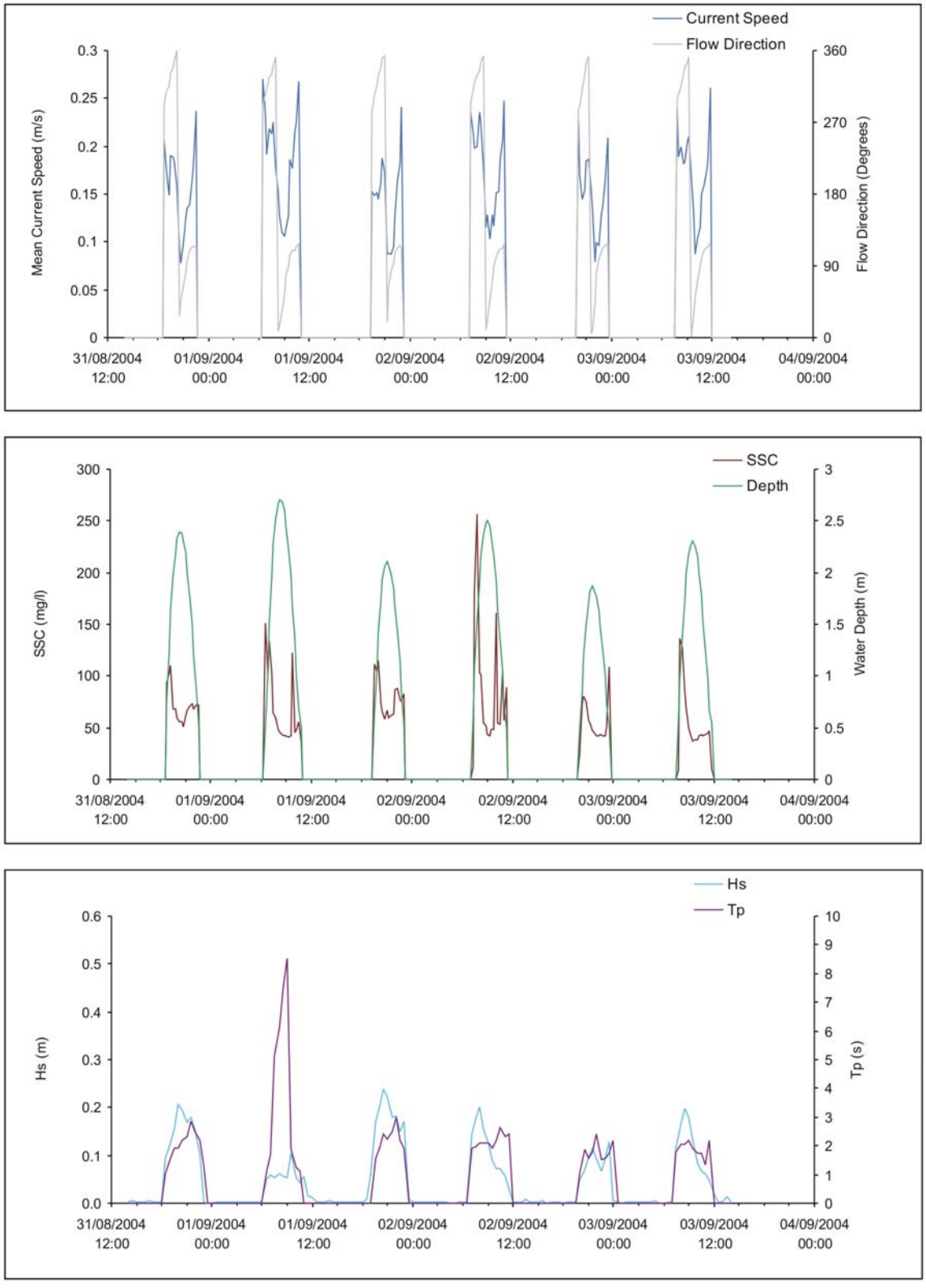

Figure 9.4: The hydrodynamic and sediment dynamic conditions during *Deployment 4*, over the upper intertidal zone (site 1).

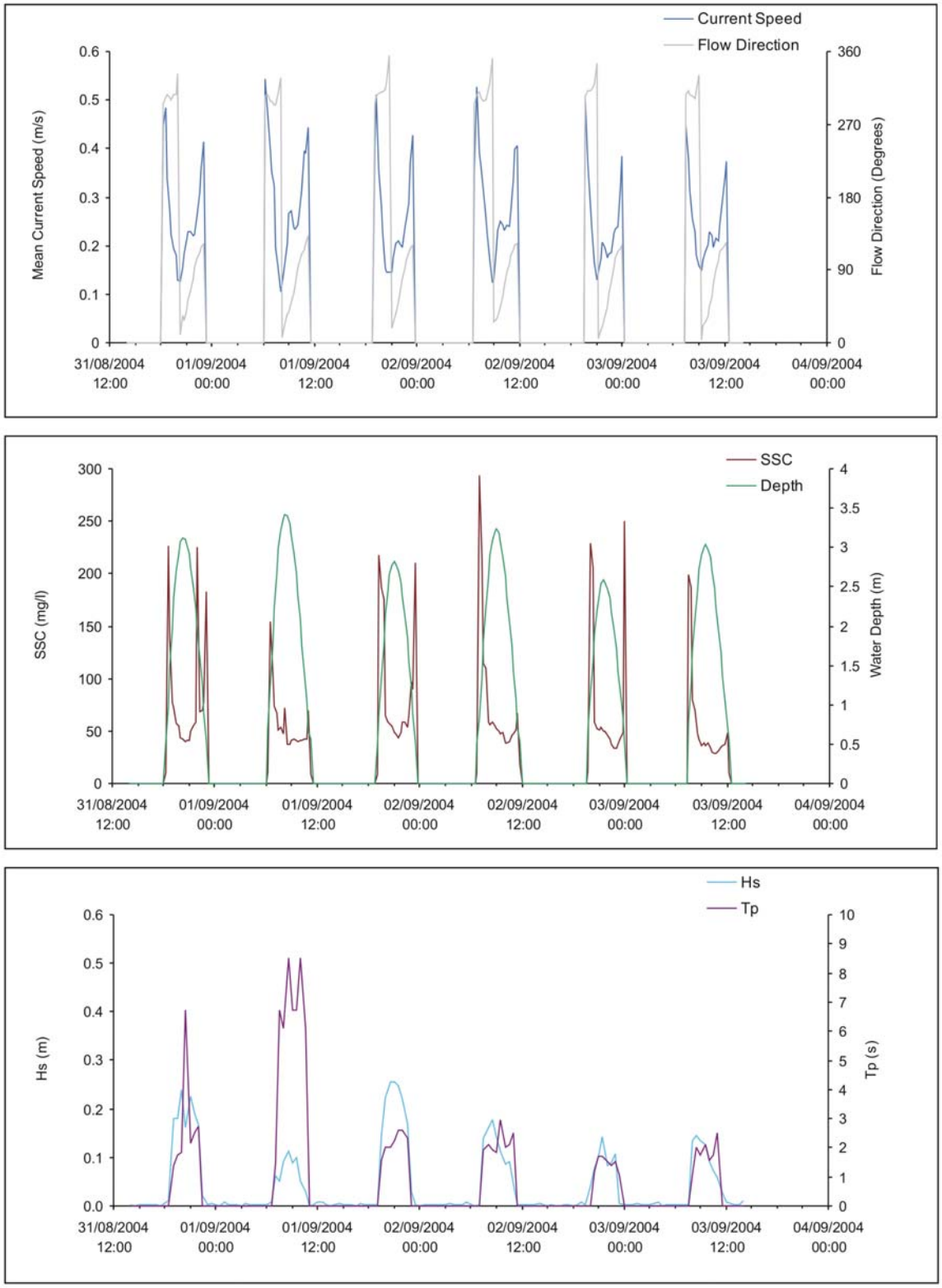

Figure 9.5: The hydrodynamic and sediment dynamic conditions during *Deployment 4*, over the lower intertidal zone (site 3).

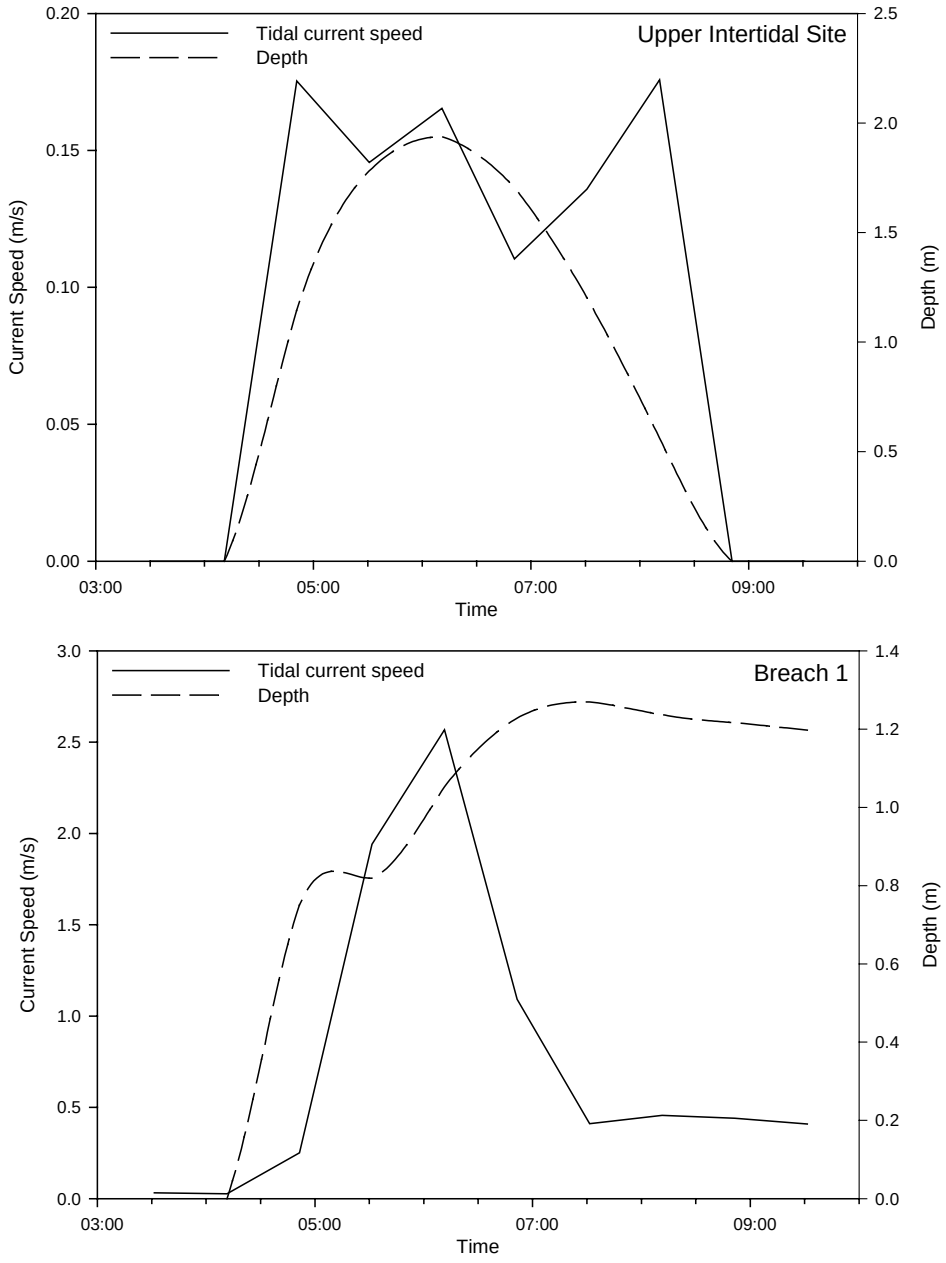

Figure 9.6: Tidal current speed and water depth over the upper intertidal zone (site 1), in the channel within Breach 1 (i.e. the only breach studied), on 06/09/2002.

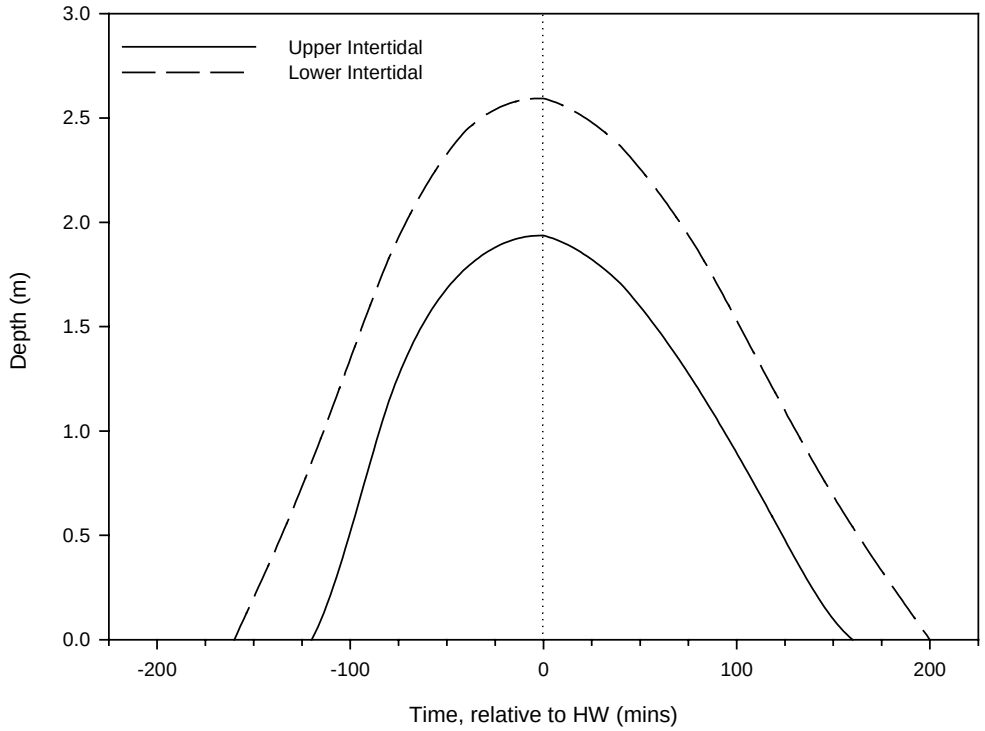

Figure 9.7: The tidal curve at the upper and lower intertidal zones, during a lower tidal range.

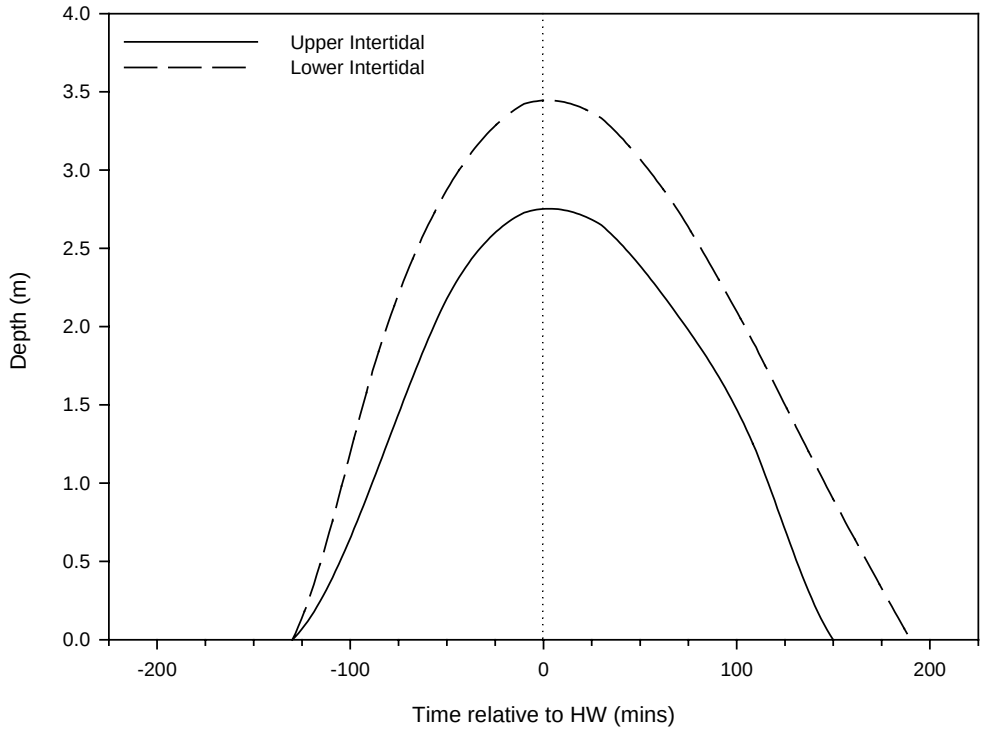

Figure 9.8: The tidal curve at the upper and lower intertidal zones, during a spring tide.

At the upper and lower intertidal zones, the tidal current rotated in a clockwise direction (Fig. 9.9). At the start of the flood, the tidal currents were directed towards the shore at ~ 300°;

they then rotated, such that at HW they were perpendicular to the shoreline. Finally, at the end of the ebb the currents were directed towards ~ 100°, in a direction away from the shoreline. The rotation of the currents, throughout the tidal cycle, was not as well defined over the upper as it was over the lower intertidal zone. The tidal current speed over the upper intertidal zone remained high throughout the flood phase of the tide; it peaked generally during the first part of the flood phase of the tide. Over the lower intertidal zone, there was a consistent peak during the first phase flood, with a gradual reduction in the tidal current speed throughout the ensuing part of the flood. This pattern was followed by an increase in the tidal current speed during the ebb phase of the tide, reaching a peak during the last part of the ebb.

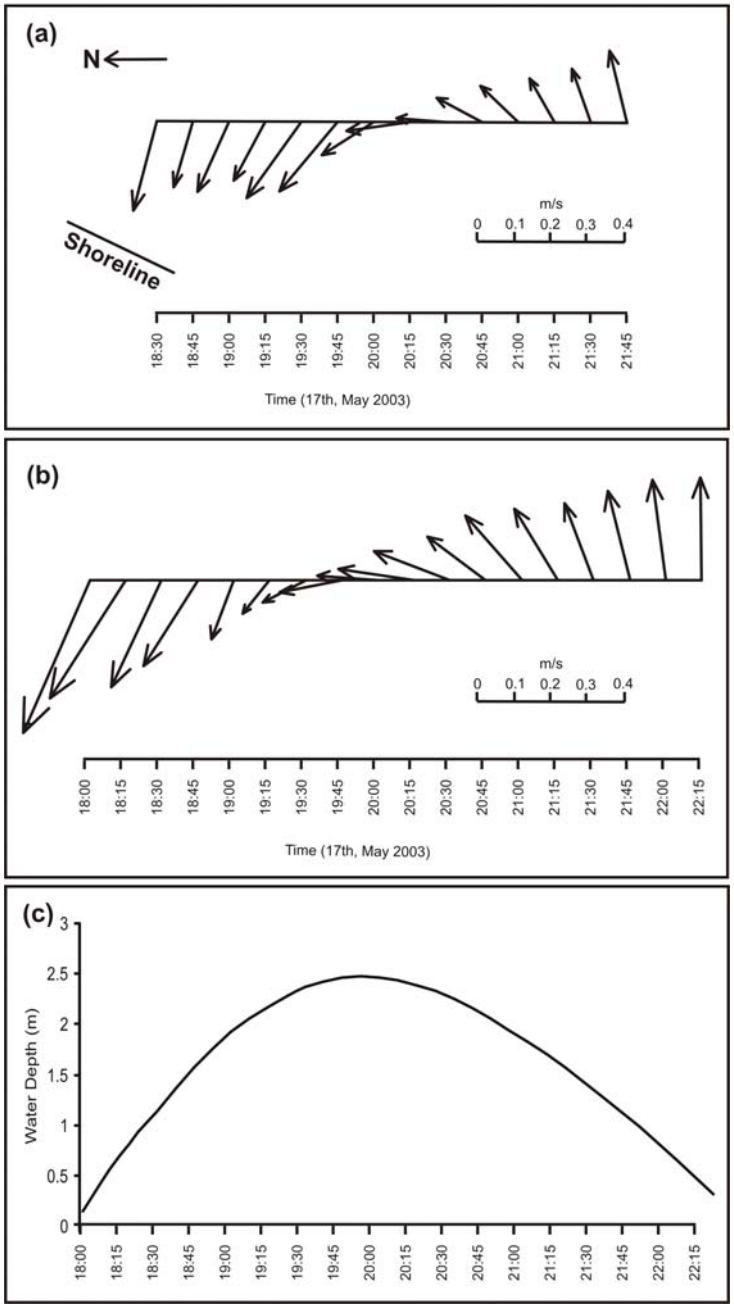

Figure 9.9: Tidal current velocity vectors and water depth, over a tidal cycle: (a) the upper intertidal zone; (b) the lower intertidal zone; and (c) the water depth (measured at the lower intertidal zone).

Comparison with Previous Studies

A number of similarities and differences can be identified, between recent (2002 to 2005) and past (1972, 1980/81, 1990s) measurements. The direction of the tidal currents has remained similar in spite of anthropogenic changes, with clockwise rotation of the tidal currents throughout the tidal cycle; this is noted in past measurements and within the recent data (Evans and Collins, 1975). During the present study, the tidal curve asymmetry varied across the intertidal zone; it was more asymmetrical with a longer ebb tide over the lower than the upper intertidal zone. Such a pattern was observed during earlier investigations (Evans and Collins, 1975; and Ke and Collins, 2000), although the opposite was also recorded (Collins et al., 1981). The tidal current speeds have shown some disparity between present and past measurements, over the upper and lower intertidal zones, and are discussed separately below. The differences discussed are greater than any variation in results, which may have been caused through the use of different instrumentation.

1) *Upper Intertidal zone*: In general, the tidal currents were similar to those observed in previous years, although there were a few anomalies. Tidal current speeds recorded in 1980 were ~ 0.2 m s^{-1} higher than those measured previously (Ke and Collins, 2000) and as part of the present investigation, during similar tidal heights (peaks ~ 0.25 m s^{-1}) (Fig. 9.10). Fluctuations have occurred in the peak tidal current speed through the measurements over the last 30 years, but no pattern could be established. The peak tidal current speed recorded at HW, shown in Figure 9.6, was recorded in previous studies (Collins et al., 1998), although it was not as well defined during those measurements (Fig. 9.10).
2) *Lower Intertidal zone*: The tidal current speeds have remained consistent throughout the period of measurements; only a few minor variations can be identified, between the past and present. For the lower tidal ranges, with maximum water depths of < 1.6 m, recent measurements showed higher tidal current speeds (Fig. 9.11). These were more pronounced first phase flood and last phase ebb peaks, than in previous measurements (Collins et al., 1998; and Ke and Collins, 2000). For the larger tidal ranges (peak water depths > 2.3 m), the tidal current speeds recorded in the present study were similar to those of previous measurements; however, the recent measurements were associated with higher tidal current speeds (~ 0.1 m s^{-1}), during the ebb phase of the tide (Fig. 9.12). It should be noted that a similar peak around HW, to that measured over the upper intertidal zone, was present also over the lower intertidal site during the present and past measurements (Ke and Collins, 2000); this indicates that this is a natural peak and is not related to the anthropogenic changes over the intertidal flats.

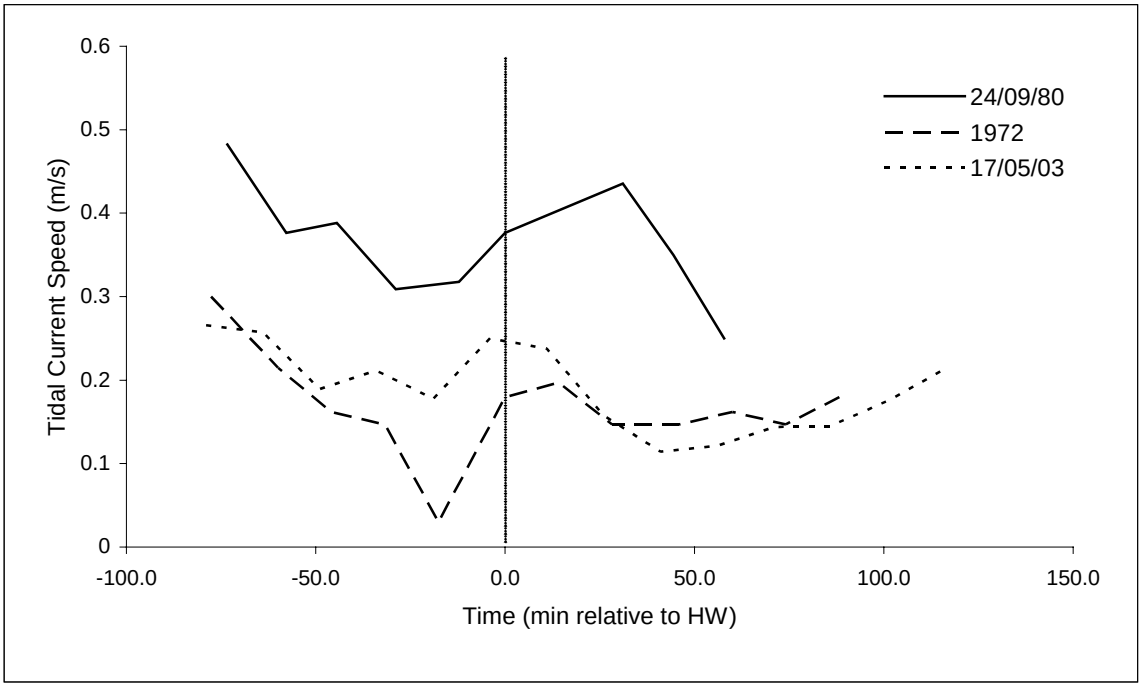

Figure 9.10: Comparative tidal current speeds over the upper intertidal flats, during tides of similar heights from 1972, 1980 and 2003 (Collins et al., 1981; and Collins et al., 1998).

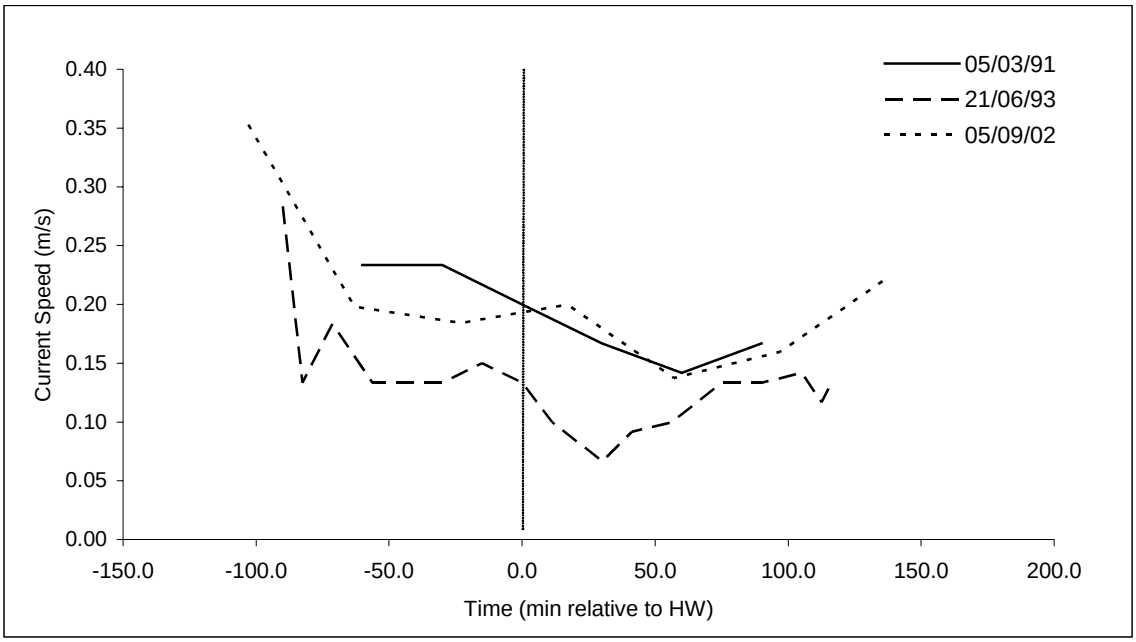

Figure 9.11: Tidal current speeds during tides with a peak water depth < 1.6 m, over the lower intertidal zone, between 1991 and 2002 (Collins et al., 1998; and Ke and Collins, 2000).

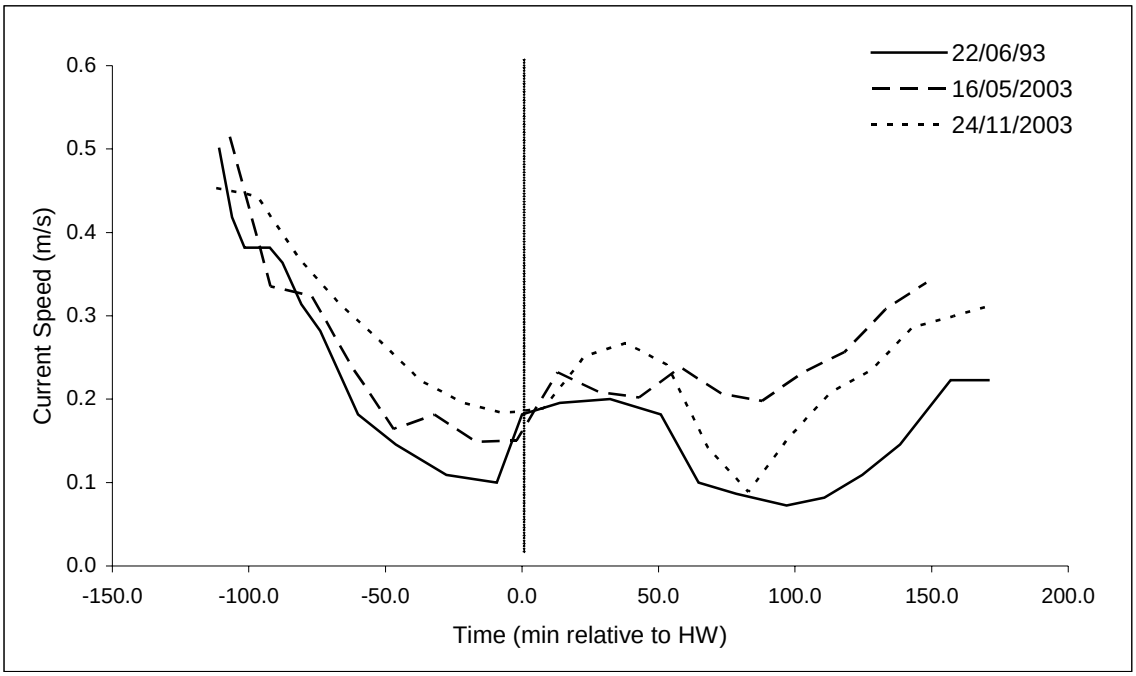

Figure 9.12: Tidal current speeds during tides with a peak water depth > 2.3 m, over the lower intertidal zone, between 1993 and 2003 (Ke and Collins, 2000).

9.3.2 *Wave conditions*

The direction of waves over the intertidal zone, ranged from 65 to 185°, throughout the 4 deployments (Fig. 9.13) (Note: the shoreline is orientated at 45° (Fig. 3.1)). The direction varied over consecutive tides, throughout the deployments. The dominant directions, 90 to 105° and 165 to 180°, are considered to represent waves generated by different mechanisms. The waves travelling from 60 to 105° had higher wave periods (3 to 4.2 s) than from the other directions (2 to 3 s) and their orientation show that they originated from the mouth of The Wash, i.e. they are swell waves from the North Sea. The waves travelling from 105 to 180° were originated from the direction of the south-eastern shoreline of The Wash, i.e. they were locally-generated wind waves formed within The Wash.

There is a seasonal cycle in the significant wave height, recorded at the mouth of The Wash, as can be identified in the data collected between June 1999 and May 2000 (Fig. 9.14). This shows an increase in wave height after September, with a peak in December. The wave height decreased then until February; it then remained relatively constant until May. This seasonal pattern in wave height is typical in this area (Addison, 2005). There was a difference of 0.2 m between the wave heights in June 1999 and May 2000; this is based upon the annual variation in the wave conditions.

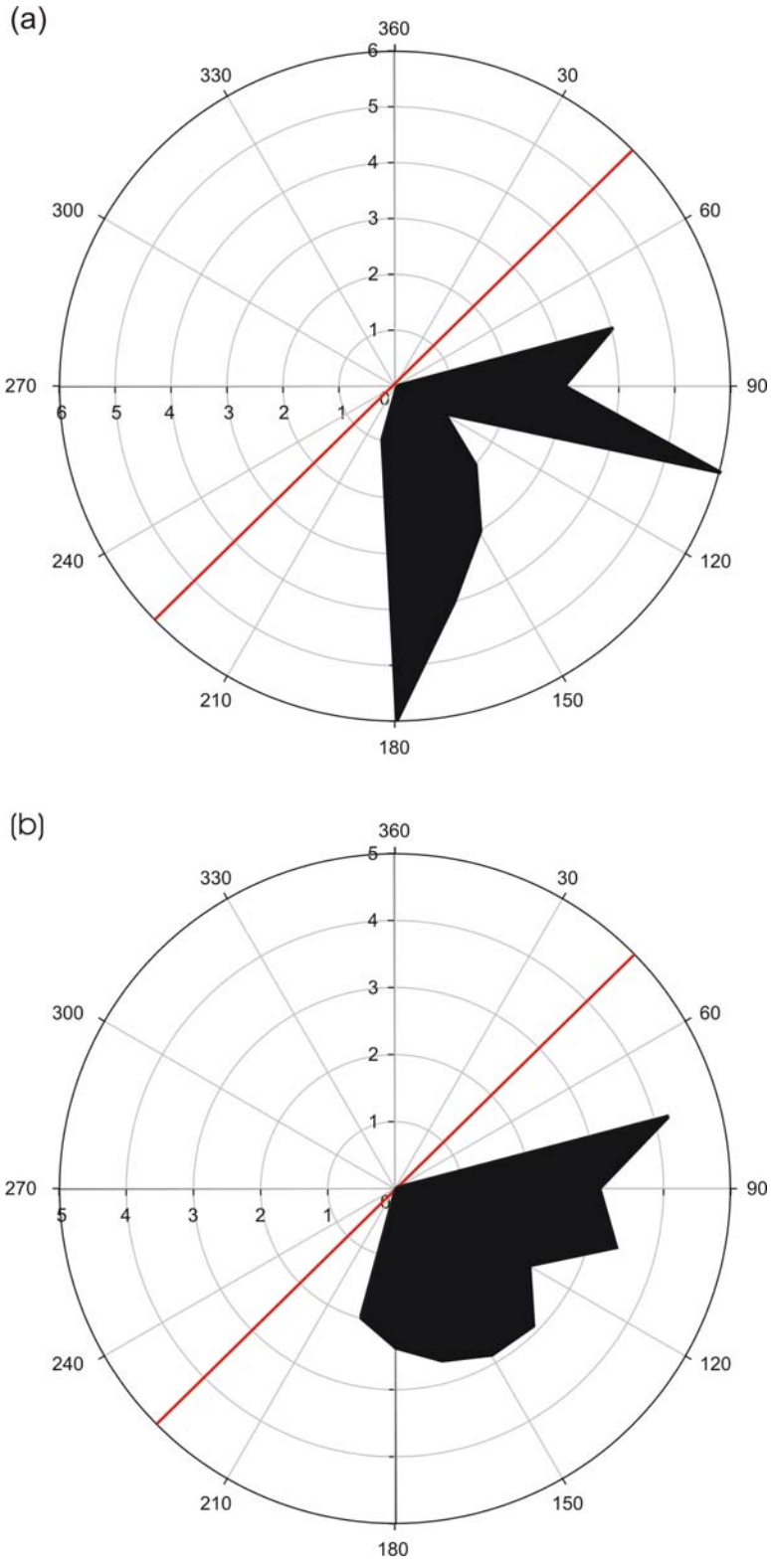

Figure 9.13: Rose diagrams of wave conditions, at HW for each tide measured in the 4 deployments, over the lower intertidal zone, showing; (a) the frequency of the wave direction, with the measurements averaged into groups of 15°; and (b) the corresponding peak wave period recorded at HW. Note: the bold line represents the orientation of the shoreline, at Freiston Shore.

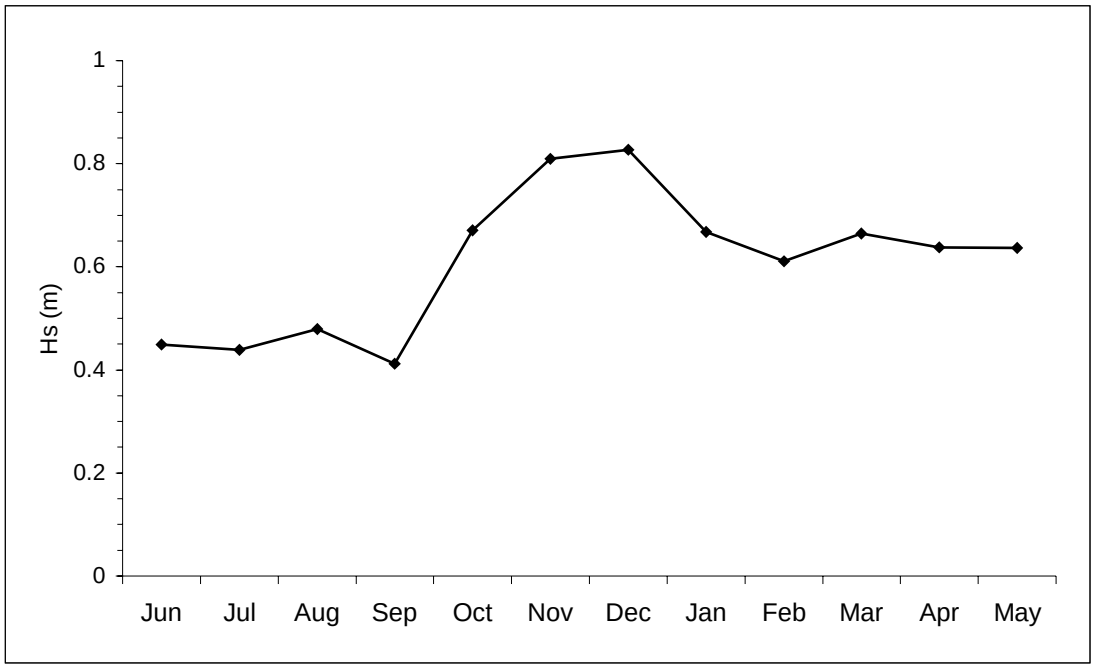

Figure 9.14: Significant wave heights between June 1999 and May 2000, obtained from the EA Wave-rider Buoy measurements, at the mouth of The Wash.

The significant wave height measured at three locations over the intertidal flats at Butterwick Low are shown in Figure 9.15. Site 1 at Butterwick Low (Site BL1) was saltmarsh on the upper intertidal zone; Site BL2 was located on the mid-intertidal zone, on mudflat; and Site BL3 was mudflat, located on the lower intertidal zone (Fig. 4.6). The *Hs* decreased across the intertidal zone, with the greatest wave heights being at Site BL3, with a peak mean monthly *Hs* value of 22.6 cm, during April 2000. In comparison, Site BL1 was associated with mean monthly *Hs* of less than 6 cm, throughout the measurements. Sites BL2 and BL3 reveal a similar pattern in *Hs*, with Site BL3 consistently experiencing wave heights some 5 cm greater than at Site BL2.

Surprisingly, the measured *Hs* over the saltmarsh was higher during the summer months; at this time, the saltmarsh vegetation was at its most dense (Jefferies et al., 1981), than during winter, when much of the vegetation was not present. Overall, the *Hs* over the intertidal flats were similar to those measured at the mouth of The Wash. Sites BL2 and BL3 both showed an increase in *Hs*, from June to a peak in December, as did those at the mouth of The Wash. In contrast, the *Hs* at Sites BL2 and BL3 were highest in April 2000; however, at the mouth of The Wash, the waves during this period were no higher than those of the surrounding months. Such variation might be related to wind waves, generated inside The Wash; the similarities described relate to waves entering The Wash from the North Sea.

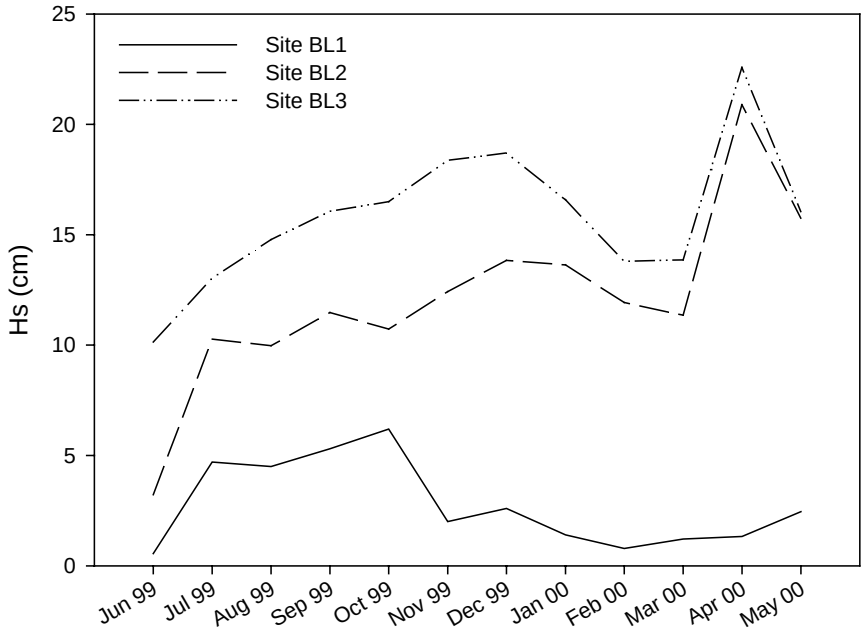

Figure 9.15: Significant wave height at 3 locations on the intertidal flats at Butterwick Low, from June 1999 to May 2000, obtained by the Environment Agency (Note: for station locations, see Figure 4.6).

Wave Attenuation

Summary statistics of 170 wave records collected through the 3 deployments with the ABRs situated at Freiston Shore on the upper (site 1) and lower (site 3) intertidal zones, between September 2002 and August 2004, are listed in Table 9.1. These data were collected throughout the tidal cycle, with water depths during the individual records varying over the lower from 0.5 to 3.5 m, from 0.5 to 2.5 m over the upper intertidal zone and from 0.5 to 1.6 m at the site inside the MR. The wind fluctuated in strength throughout the measurements, but was consistently in an onshore direction, from the south. The upper and lower intertidal zones remained unvegetated throughout the year, while during *Deployment 4* the MR site and saltmarsh were both densely vegetated.

Throughout *Deployments 1* and *2*, the maximum wave energy over the upper intertidal was 10 to 25 % higher than that over the lower, while the maximum *Hs* was also greater over the upper site by ~10 %. However, the mean *Hs* was higher at the lower intertidal site compared to the upper site, by ~5 % through *Deployments 1* and *2*. The mean, maximum and minimum *Hs* all decreased across the intertidal zone, from the lower intertidal site to the MR site, during *Deployment 4*. Between the lower and upper intertidal sites, the maximum and mean *Hs* reduced by 2 cm. In contrast, the wave energy increased between the lower and upper intertidal sites. During *Deployment 4*, the wave conditions inside the MR site were minimal, with maximum and minimum *Hs* values of 0.04 and 0.02 m respectively. These results

confirmed field observations that, as expected, the MR site only experienced wind waves formed inside the site, and owing to the limited fetch these were small. Throughout all the deployments there was minimal wave attenuation between the lower and upper intertidal sites.

Frequency histograms of significant wave height, over the 3 locations throughout *Deployment 4*, are shown in Figure 9.16. The upper experienced higher peak wave heights (> 0.24 m) than the lower intertidal zone, while the lower had a higher frequency of waves from 0.06 to 0.24 m than the upper intertidal zone.

The mean significant wave heights experienced at Freiston Shore over the enclosed MR site, the upper (Site FS1) and lower (Site FS3) intertidal sites, are plotted with the mean significant wave height of 208 sampled bursts over the saltmarsh (Site BL1), upper (Site BL2) and lower (Site BL3) intertidal sites at Butterwick Low (established by Cooper (2005)) (Fig. 9.17). The sites at Butterwick Low were located some 1 km to the north-east of the deployments at Freiston Shore and were considered to be comparable in terms of wave attenuation as the mean significant wave heights over the lower intertidal zones were similar. The profile represents the relative position of the measuring sites from both studies, i.e. their elevation and distance from the embankment is plotted on the same profile across the intertidal zone. The combined significant wave heights show a rapid decrease in wave height between the upper intertidal zone (Sites BL2 & FS1) and the saltmarsh (Site BL1). The saltmarsh appears to be highly effective in dissipating the waves, with very similar wave conditions prevailing over the saltmarsh and inside the MR site.

Table 9.1: Summary of wave characteristics, collected by ABRs measuring simultaneously high-frequency data at different locations over the intertidal zone (for deployment details, see Section 4.3).

Deployment 1 – September 2002

	Hs (m)		Change in *Hs* (%)
	Upper	Lower	Upper - Lower
Maximum	0.46	0.43	6.98
Minimum	0.06	0.06	0.00
Mean	0.16	0.17	-6.22
	E ($N.dBar^2.m^{-3}$)		Change in *E* (%)
	Upper	Lower	Upper - Lower
Maximum	132.4	118.1	12.11
Minimum	0.6	0.6	6.67
Mean	20.7	22.7	-8.58

Deployment 2 – May 2003

	Hs (m)		Change in *Hs* (%)
	Upper	Lower	Upper - Lower
Maximum	0.44	0.40	10.00
Minimum	0.26	0.29	-10.34
Mean	0.35	0.36	-3.58
	E ($N.dBar^2.m^{-3}$)		Change in *E* (%)
	Upper	Lower	Upper - Lower
Maximum	123.8	97.6	26.84
Minimum	43.7	51.8	-15.64
Mean	79.9	83.4	-4.20

Deployment 4 – September 2004

	Hs (m)			Change in *Hs* (%)		
	MR Site	Upper	Lower	MR - Upper	Upper - Lower	MR - Lower
Maximum	0.04	0.22	0.24	-81.82	-8.33	-83.33
Minimum	0.02	0.1	0.11	-80.00	-9.09	-81.82
Mean	0.03	0.16	0.18	-82.58	-12.92	-84.83
	E ($N.dBar^2.m^{-3}$)			Change in *E* (%)		
	MR Site	Upper	Lower	MR - Upper	Upper - Lower	MR - Lower
Maximum	0.8	41.4	36.1	-97.85	14.68	-97.53
Minimum	0.1	8.0	7	-97.76	14.86	-97.43
Mean	0.5	21.9	21.7	-97.58	0.92	-97.56

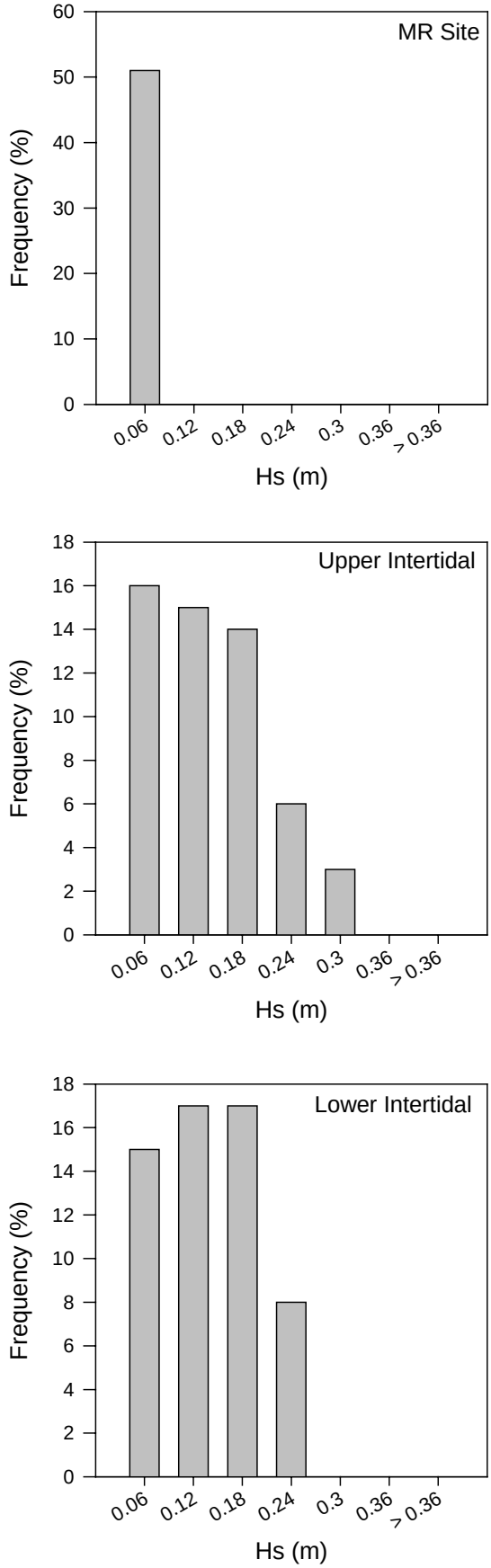

Figure 9.16: The frequency distribution of *Hs* classes (with only the upper limits shown), during *Deployment 4* at the 3 locations (for details, see Section 4.3.4).

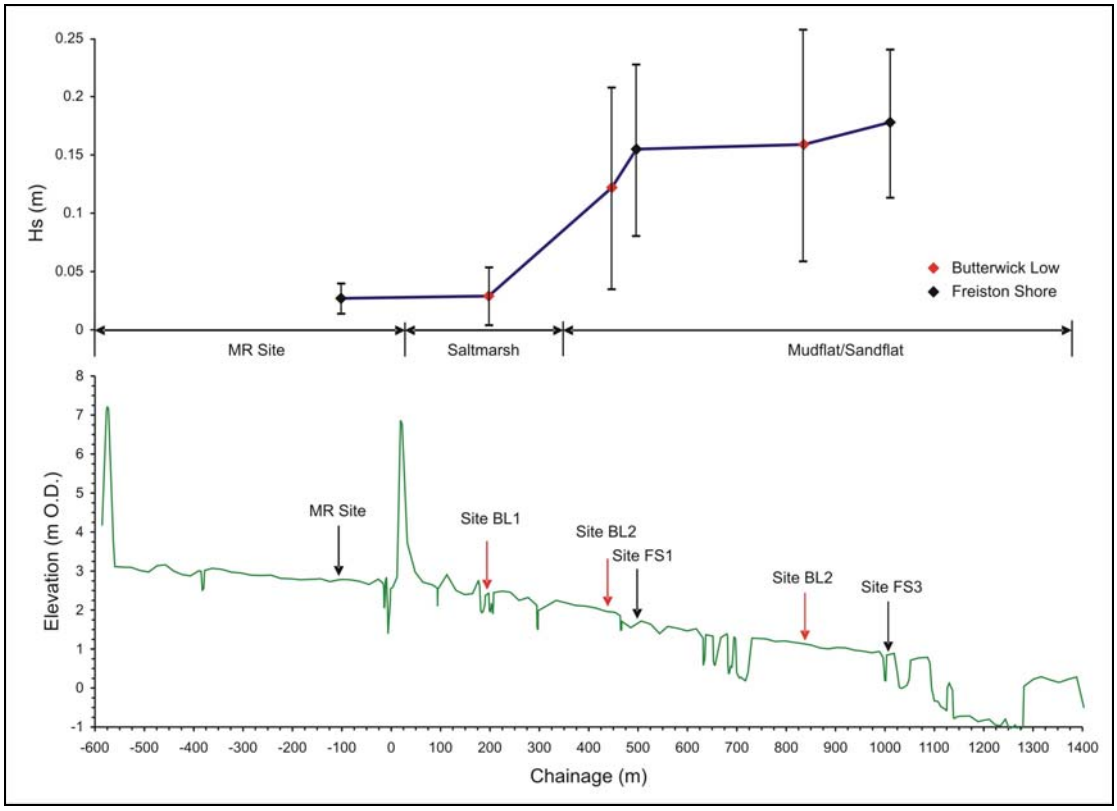

Figure 9.17: Profile across the intertidal zone at Freiston Shore, showing the location of the sites used in *Deployment 4* at Freiston Shore, shown with black arrows, together with the study undertaken by Cooper (2005) at Butterwick Low in 2000, shown with red arrows. The corresponding average significant wave heights over the deployments and standard deviations are shown.

Changes in wave spectra

The variation in wave height and energy, over the intertidal zone, provides a general indication of the levels of wave attenuation over the sandflat, mudflat and saltmarsh. A more detailed representation of the wave transformation occurring can be examined by reference to the wave spectra, at the various locations. Two examples are shown, from *Deployment 1*, in Figures 9.18 & 9.19; these were obtained from consecutive tides; the first representing 'average' wave energy conditions, whilst the second is associated with 'high' wave energy conditions. The measurements were taken during HW, to maximise the water depth and minimise any possible influence of the tidal currents, as advised by Moeller and Spencer (2003). The summary wave conditions has shown that during both tides, the upper intertidal zone experienced greater significant wave heights than the lower intertidal zone (Figs. 9.2 & 9.3): 0.23 m compared to 0.22 m (09/09/2002 am); and 0.46 m compared to 0.43 m (09/09/2002 pm). Similar *Tz* values were recorded, of 2.3 s (09/09/2002 am) and 2.7 s (09/09/2002 pm), respectively. In the 'average' energy case, the low frequency (high period) waves were preferentially attenuated between the lower and upper intertidal zones, while the higher frequency (low period) waves increased their spectral energy, i.e. there was a

redistribution of the energy to the higher frequencies (Fig. 9.18). During the 'high' wave energy case, the peak was at a high frequency; this was attenuated between the upper and lower intertidal zones (Fig. 9.19). Despite the reduction in the peak in the wave spectra, there was an increase in the high-frequency wave energy present at the upper, compared to the lower intertidal zone. High-frequency waves appear to have increased preferentially over the mudflat, whilst the low frequency waves were attenuated.

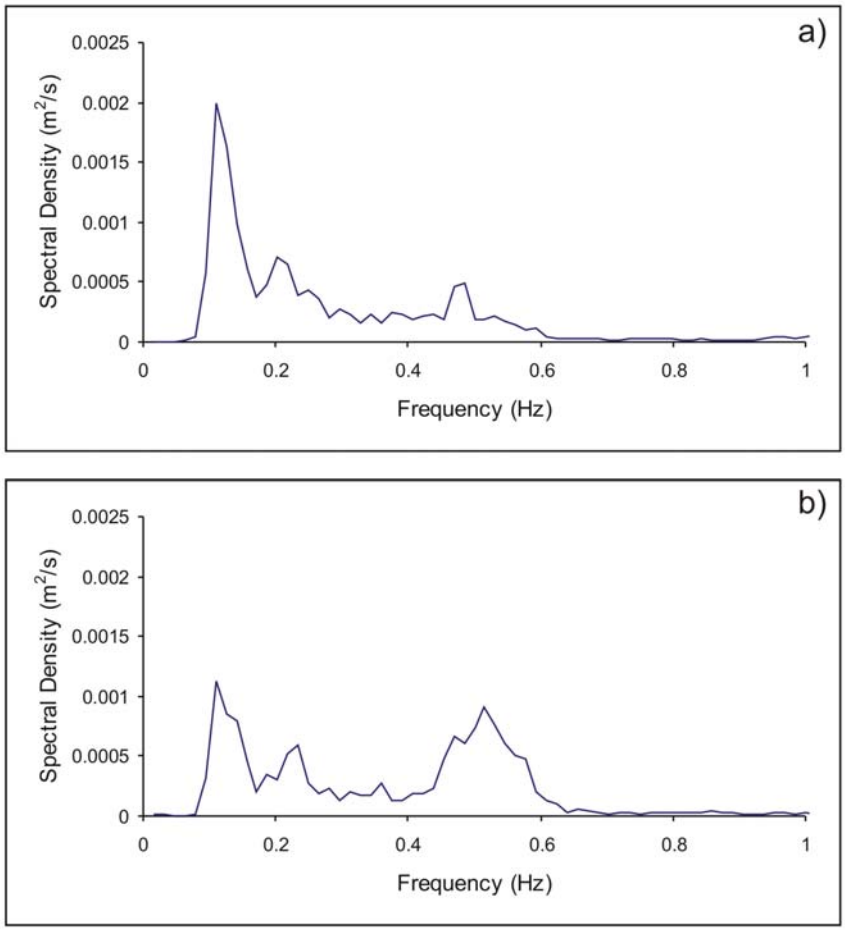

Figure 9.18: Comparison of the spectral densities, during HW on the morning of 09/09/2002, over: (a) the lower intertidal zone (site 3); and (b) the upper intertidal zone (site 1).

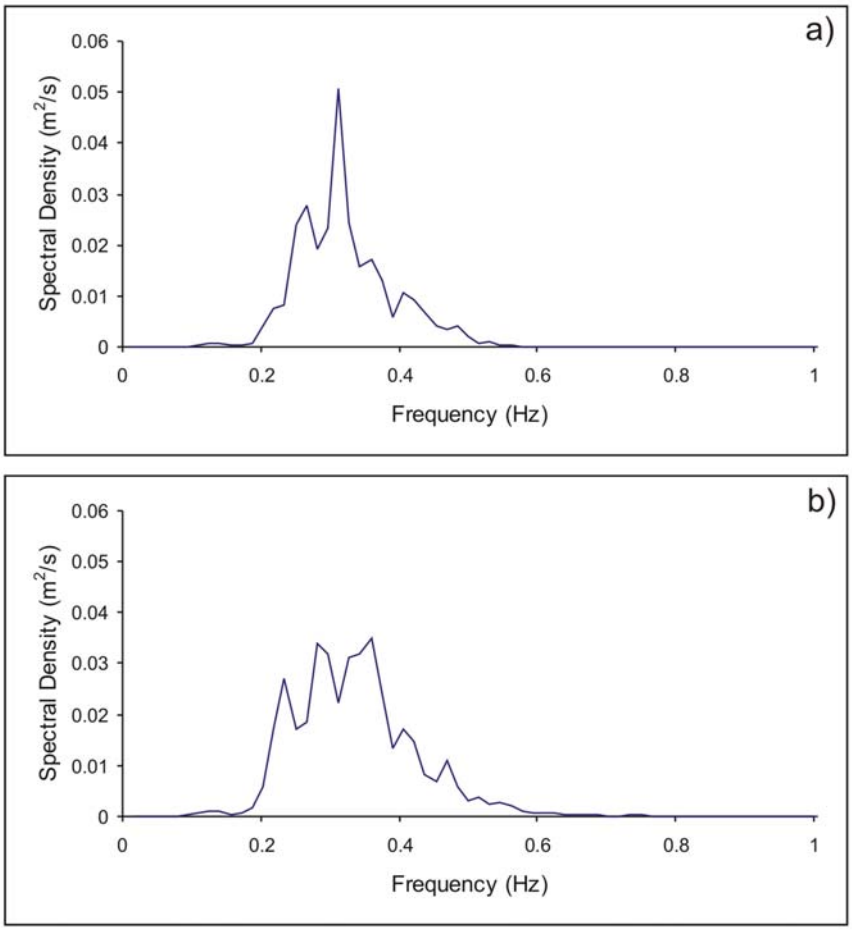

Figure 9.19: Comparison of the spectral densities, during HW on the afternoon of 09/09/2002, over: (a) the lower intertidal zone (site 3); and (b) the upper intertidal zone (site 1).

Influence of waves on SSC

In order to quantify the influence of varying wave conditions on the SSC over the intertidal zone, it is necessary to examine initially the relationship between tidal current speed and SSC. Periods of minimal wave activity were used (*Hs* < 0.2 m), in an attempt to ensure that any locally-generated suspended sediment was mobilised solely by the tidal currents. Over the 4 deployments, 6 tides suitable for analysis were identified for the lower and 4 for the upper intertidal zone. These tides were preceded by calm weather conditions, preventing the SSC over the intertidal flats from being enhanced by wave action in the North Sea, as recorded by Evans and Collins (1975).

The peak values of SSC and tidal current speed, obtained from the flood and the ebb phases of the tidal cycle, show an exponential[1] growth relationship between tidal current speed and SSC (Fig. 9.20), with a significance of 99 % at both locations (upper intertidal zone ($F_{1,6}$ = 98.9, P < 0.01); lower intertidal zone ($F_{1,10}$ = 48.04, P < 0.01)). On the basis of this relationship, the

[1] Note: from the different relationships tried, this gave the best correlation.

measured SSC was plotted against the predicted SSC, derived on the basis of tidal current speed (Fig. 9.21).

During the first 7 tides of *Deployment 1*, the predicted SSC was similar to those measured; this indicates that, during this period, the wave activity was not affecting suspended sediment levels over the intertidal zone. However, during the later tides of the deployment (from 8th to 11th September), the measured SSC was much higher than predicted by the curvilinear relationship. It may be assumed that this difference was related primarily to wave activity over the intertidal zone, causing resuspension of sediment. Consequently, the peak *Hs* was plotted against the difference between the measured and predicted (on the basis of the tidal currents alone) SSCs (Fig. 9.22). Both locations showed a positive linear correlation at a 99 % significance level (upper intertidal site ($F_{1,10} = 12.9$, $P < 0.01$); lower intertidal site ($F_{1,10} = 11.8$, $P < 0.01$)).

Owing to a problem with the gain setting on the OBS, it was not possible to investigate increases in SSC associated with periods of high tidal current activity (on high spring tides), combined with high wave heights (*Hs* > 0.6 m). Under such conditions, the OBS became saturated. The gain setting for the OBS was corrected for *Deployment 4*. Unfortunately, throughout this deployment, minimal wave activity was experienced. As such, no further measurements were obtained of the interaction between the wave activity and SSC.

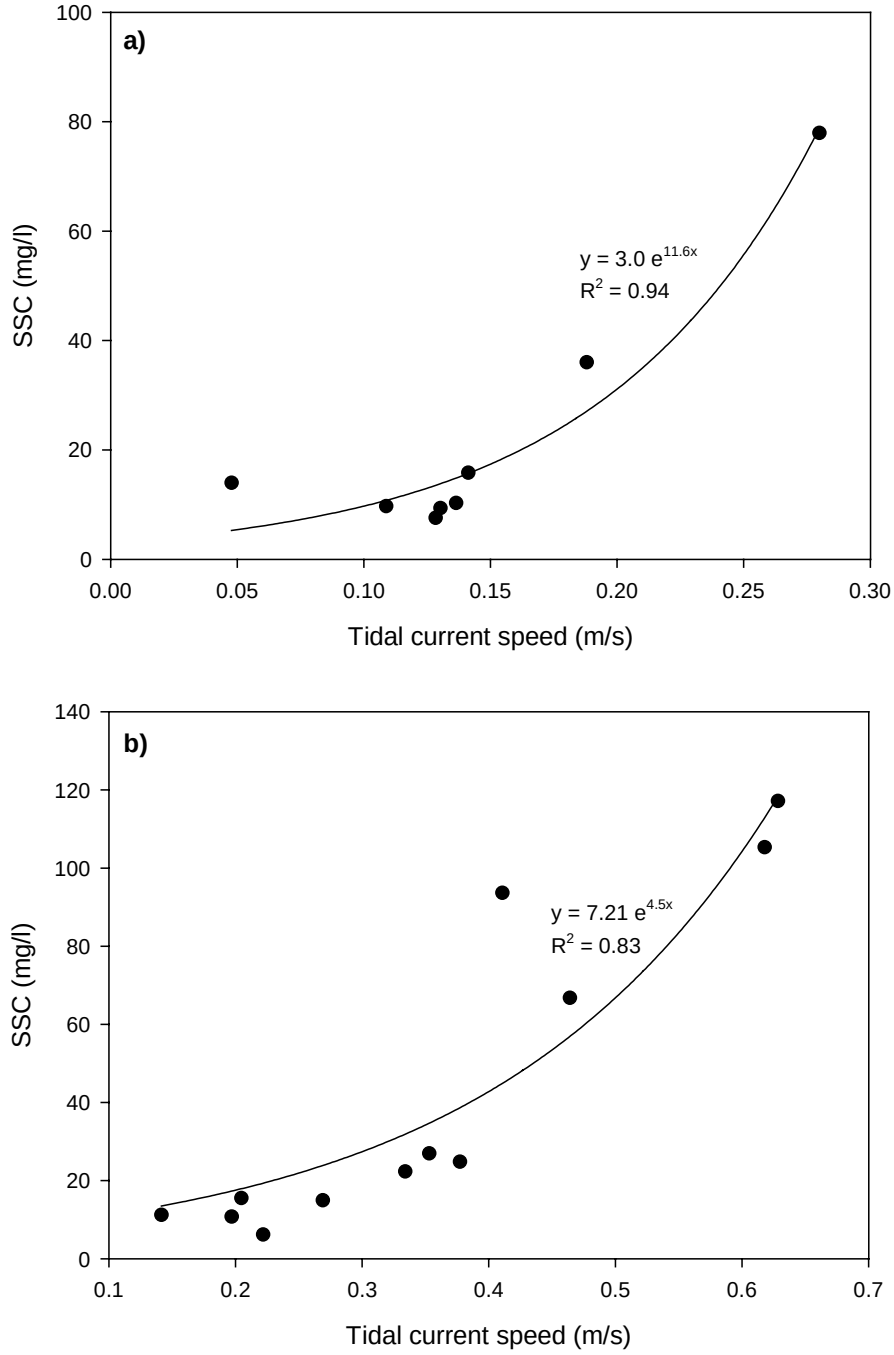

Figure 9.20: The correlation between peak SSC and peak tidal current speed, during periods of minimal wave activity, from Sept 2002 and Nov 2003: (a) upper intertidal zone; and (b) lower intertidal zone.

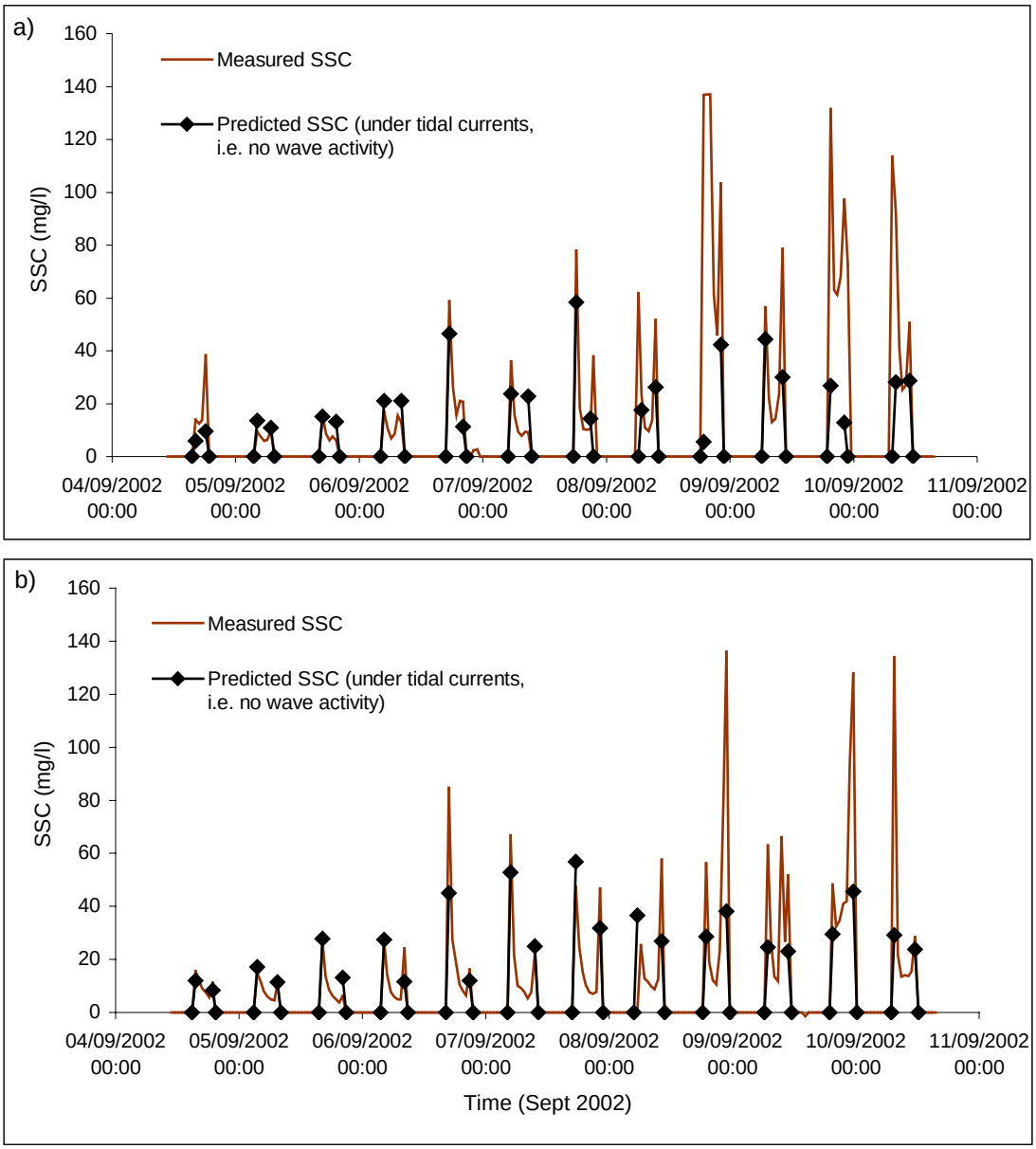

Figure 9.21: The predicted tidally induced SSC, plotted against the measured SSC: (a) the upper intertidal zone; and (b) the lower intertidal zone.

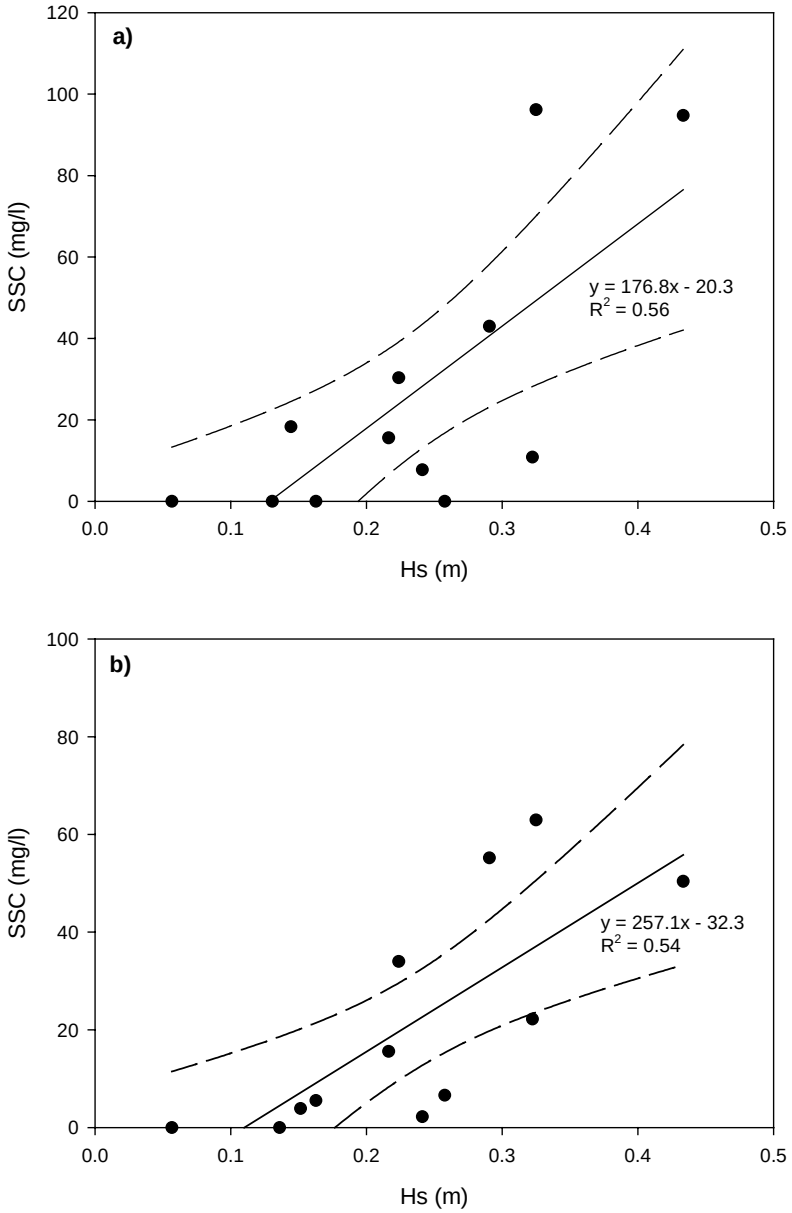

Figure 9.22: The peak Hs against the predicted tidally averaged wave induced SSC; (a) upper intertidal zone; and (b) lower intertidal zone. Note: the dashed line represents the 95 % confidence intervals.

9.3.3 *Sediment Transport*

Suspended Sediment

The quantity and the composition of sediment transported in suspension varied with water depth, time and location over the intertidal flats (Figs. 9.23 & 9.24). The suspended sediment samplers collected sediment in suspension, at set heights above the bed over the upper and lower intertidal zones during *Deployment 4*. Pairs of tides were sampled, owing to the timing of LW (Section 4.3.4). Over both of the sites, the level of suspended sediment collected was highest during the first pair of tides sampled.

On the lower intertidal zone, the quantities of fine-grained (< 63 μm) sediment collected, at 0.25 m and 0.5 m above the bed, were similar. The quantity of fine-grained sediment decreased gradually, as the depth decreased. However, the amount of sand-sized (> 63 μm) sediment collected varied. The first set of tides was associated with a large amount of sand-sized sediment (a dry weight of 2 g) present at 0.25 m and none at 0.5 m. During the other tides there was only slightly more sediment at 0.25 m, than at 0.5 m. The distribution of suspended sediments within the water column above the upper was more uniform than above the lower intertidal zone. There was a peak in both fine-grained and sand-sized sediment at 0.25 m above the bed, together with a general reduction in the quantity of sediment as depth decreased. The suspended sediment transported over the upper intertidal zone was predominantly fine-grained, while over the lower intertidal zone it was made up of approximately equal amounts of fine-grained and sand-sized sediment (Fig. 9.25). The amount of sediment in suspension was much higher over the lower than the upper intertidal zone, especially at heights of 0.5 and 0.75 m. At both locations, throughout the spring tides monitored, the total amount of sediment transported decreased with height above the bed; this pattern was found previously during neap and spring tides by Evans and Collins (1975). On the upper intertidal zone, such a decrease was abrupt, with the amount in suspension at 0.5 and 0.75 m being less than a third of that in suspension at 0.25 m (Fig. 9.26). On the lower intertidal zone, there was a more gradual reduction, as the height above the bed increased.

The SSC measured by the ABRs at 0.5 m above the bed during *Deployment 4*, on the upper and lower intertidal zones, do not show the same temporal pattern as the suspended sediment collected by the samplers (Figs. 9.4 & 9.5). The ABR measurements showed the peak SSC was during the tide on 02/09/2004 am; however, the measurements from the suspended sediment samplers during this tide were smaller than those from the first set of tides. The wave conditions, measured by the ABRs, showed minimal wave activity throughout the entire deployment, with a peak wave height of 0.25 m (over the lower intertidal zone) occurring on 01/09/2004 pm, which was in the second set of suspended sediment samples (labelled 02/09/2004). The reason for the discrepancy between the ABRs and the suspended sediment samplers is related to the different methods of measurement, with the ABRs recording more accurate measurements of SSC.

The suspended sediment samplers provide representative values of the quantities of suspended sediment, at set depths above the bed. However, these values cannot be converted into a measure of SSC, as the volume of water from which the sediment was collected is not known. Instead, the measurements have been utilised to show the relative distribution of suspended sediment throughout the water column; thus, to provide an indication of what the

ABRs have measured. The ABRs measured at 0.5 m above the bed; however, the suspended sediment samplers indicate that this level represents high, but not peak, values of suspended sediment within the water column.

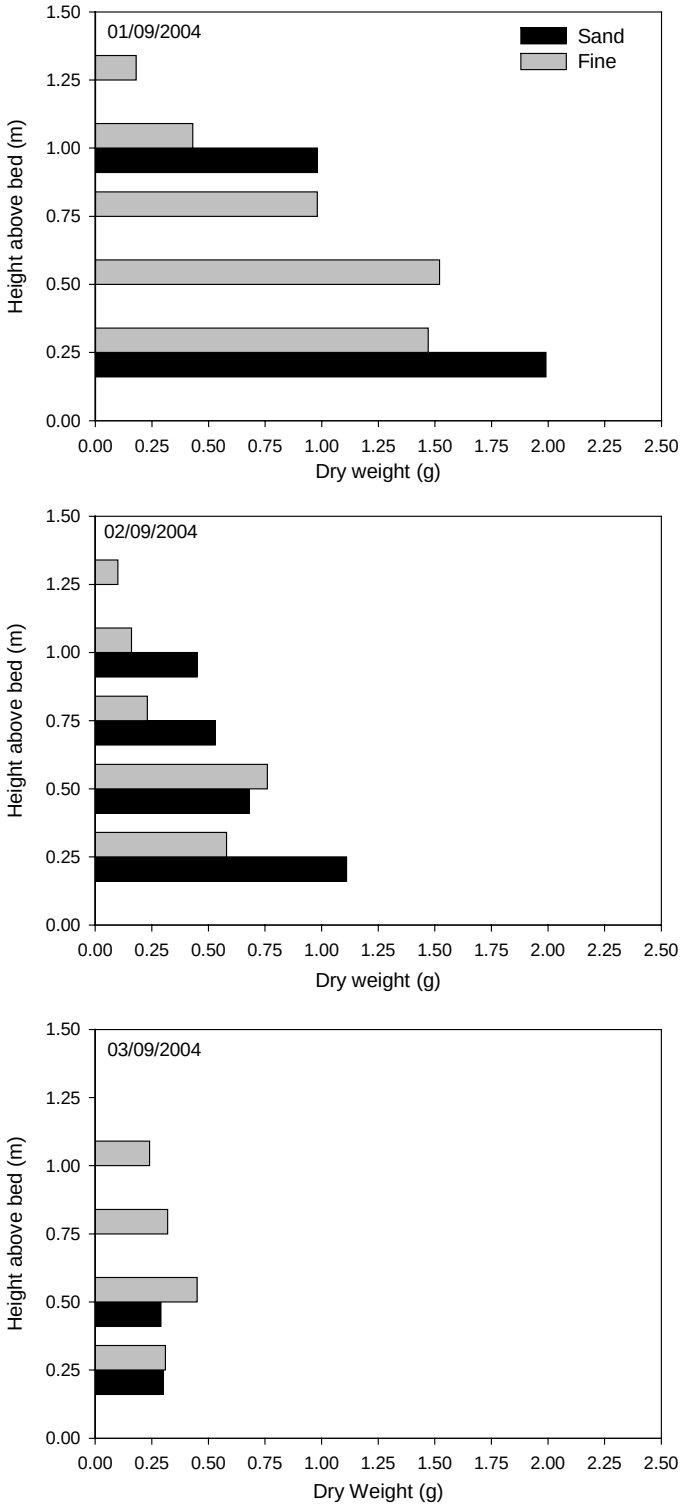

Figure 9.23: The dry weight of sand-sized (> 63 μm) and fine-grained (< 63 μm) sediment collected by the suspended sediment samplers, over the lower intertidal zone (site 3) throughout *Deployment 4*.

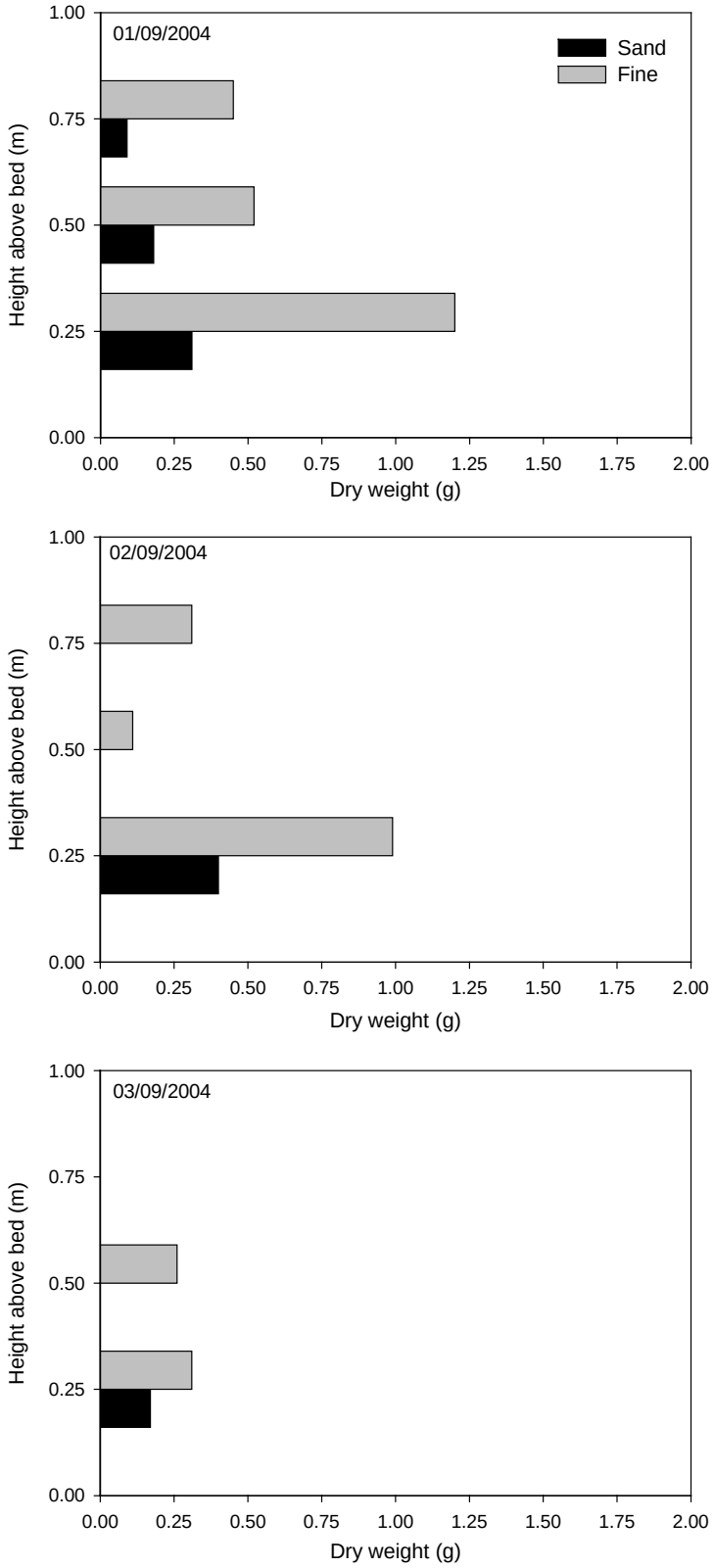

Figure 9.24: The dry weight of sand-sized (> 63 μm) and fine-grained (< 63 μm) sediment collected by the suspended sediment samplers, on the upper intertidal zone (site 1) throughout *Deployment 4*.

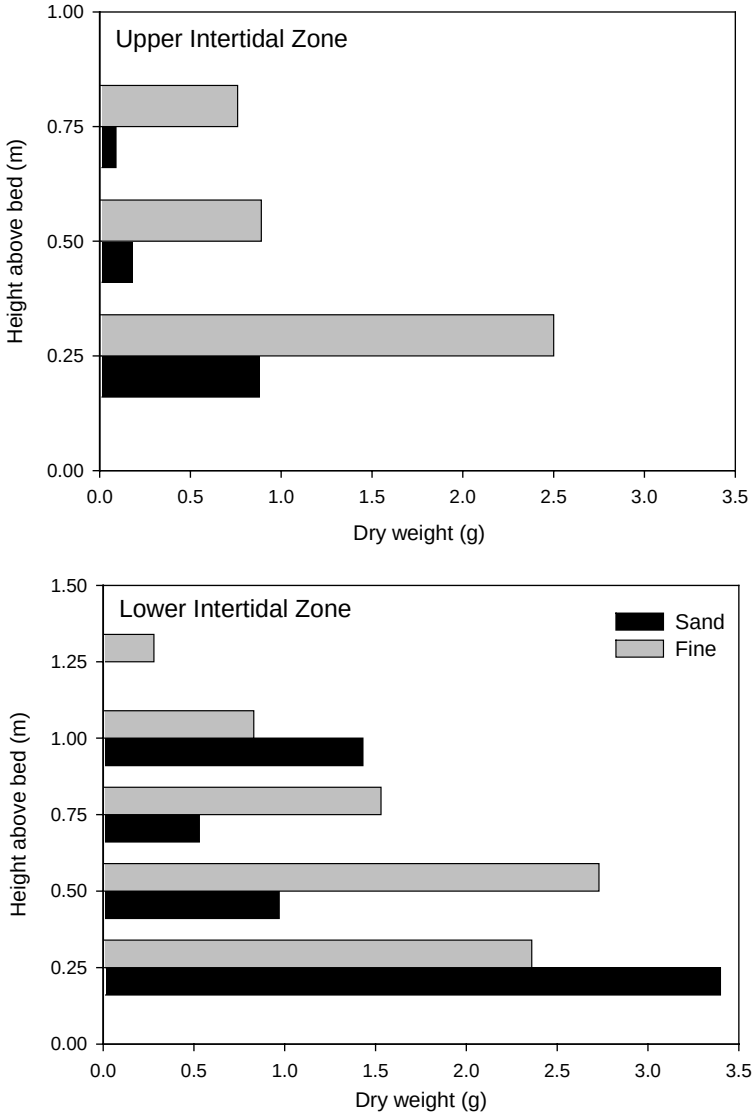

Figure 9.25: The total dry weight of sand-sized and fine-grained suspended sediment, collected at each depth over *Deployment 4*, on the upper and lower intertidal zones.

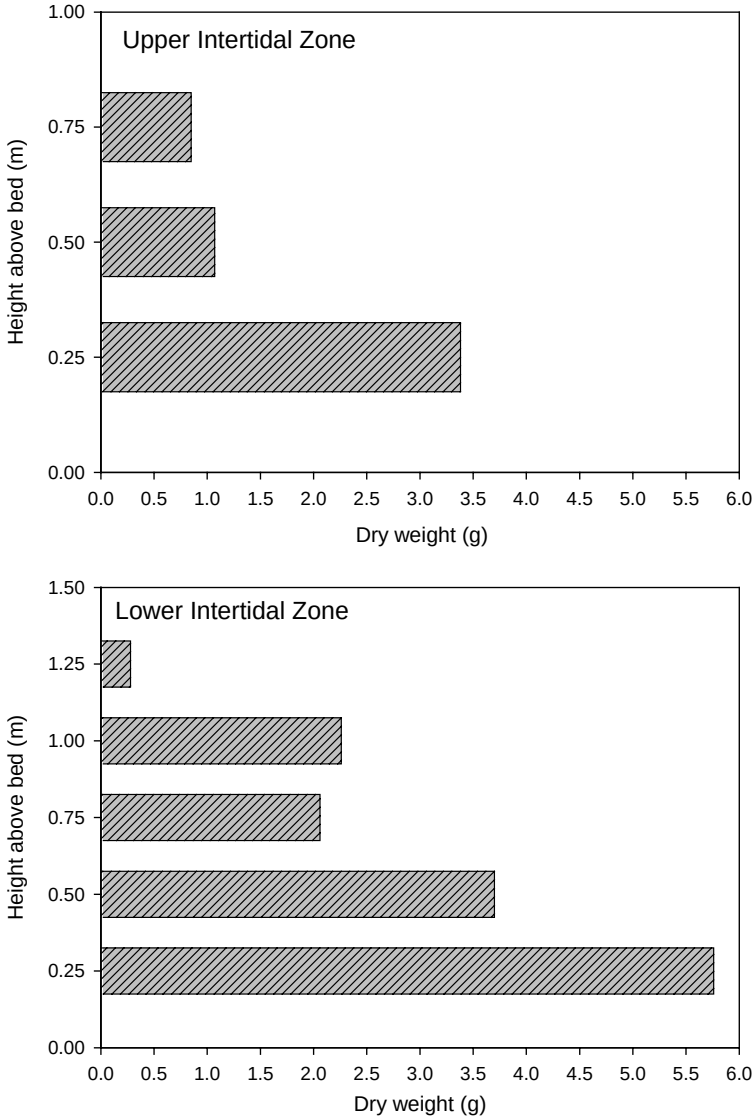

Figure 9.26: The total dry weight of all the suspended sediment collected, at each depth over *Deployment 4*, on the upper and lower intertidal zones.

Bedload Transport

During the deployments of the bedload samplers (*Deployments 3* & *4*, with a total of 12 tidal cycles measured) only 2 periods of transport, in this mode, were identified. Bedload transport was recorded over the lower intertidal[2] zone only when the peak *Hs* over the tidal cycle exceeded 0.4 m; however, the bedload samplers were found to have very low efficiency resulting in no bedload transport being measured during periods of low activity (Section 8.3.3).

[2] Note: The 2 periods of bedload transport were during *Deployment 3*, when no bedload samplers were deployed at the upper intertidal zone. Consequently, it is unknown if any bedload transport occurred there.

9.3.4 *Erosion/Accretion*

Bed level changes in the longshore (parallel with the shoreline) and cross-shore (perpendicular to the shoreline) directions showed either erosion or accretion; at all 3 sites, the change was greater in a cross-shore direction (Fig. 9.27). Unfortunately, between August and December 2003 no measurements could be obtained at the lower intertidal zone (site 3), as cockle dredging was taking place (Section 4.4). Nonetheless, from the measurements available, the lower intertidal zone experienced accretion from December 2003 to June 2004, with the rate peaking at 12.3 cm yr^{-1}, during April (Fig. 9.28). A period of erosion followed, from July to October 2004, when the peak erosion rate was 15.7 cm yr^{-1}. Site 2 was predominantly erosional throughout the 18 months, with occasional isolated periods of accretion. The highest rates of erosion were in December 2003 and March 2004, with rates of 19.4 cm yr^{-1} and 14.5 cm yr^{-1}, respectively. The rates of bed level change on the upper intertidal zone (site 1) were much lower, switching frequently between erosional and accretional. The peak accretion rate occurred during May 2003, at 8.6 cm yr^{-1}, and the peak erosion rate was during July 2004, at 11.4 cm yr^{-1}.

The cumulative change in bed level over the 18-month period is shown for each location over the intertidal flats in Figure 9.29. The upper intertidal zone was accretional until June 2004, then erosion ensued; this led to the bed level having been eroded by 1.5 cm, over 18 months. The mid-intertidal zone was subjected to persistent erosion throughout the 18 months, with the bed having been eroded by 7.6 cm. The lower intertidal zone experienced accretion from January to June 2004, before a period of erosion from July to October 2004; this meant that the bed accreted 0.3 cm, over these 10 months. The switch from accreting to eroding on the upper and lower intertidal zones may be related to the creek development over this area, described in Chapter 7. The creek system was eroding until it started accreting sometime between April 2004 and September 2005. The sediment that was deposited over these areas may have been supplied from erosion of the creeks, while the change to erosion over the intertidal flats could have been due to the creek system switching to accreting.

From measurements collected by Sue Brown from CEH and supplied by the EA, the saltmarsh adjacent to the MR site was found to have been already accreting before the MR site was initiated; since then, it has continued to do so at a similar rate (Fig. 9.30). The rate of accretion was lowest over the landward part of the saltmarsh. The peak rates of ~ 1.5 cm yr^{-1} varied: from the middle of the saltmarsh, during the winter months; to near the seaward edge of the saltmarsh, during the summer months. The intertidal zone adjacent to the saltmarsh suffered erosion throughout the summer; during the winter it accreted, whilst the most seaward part of the saltmarsh eroded. The saltmarsh has maintained a stable accretional rate

following the MR, with the peak rate remaining much higher than the predicted regional rise in sea level (~ 1 mm yr^{-1}) (Andersen et al., 2000).

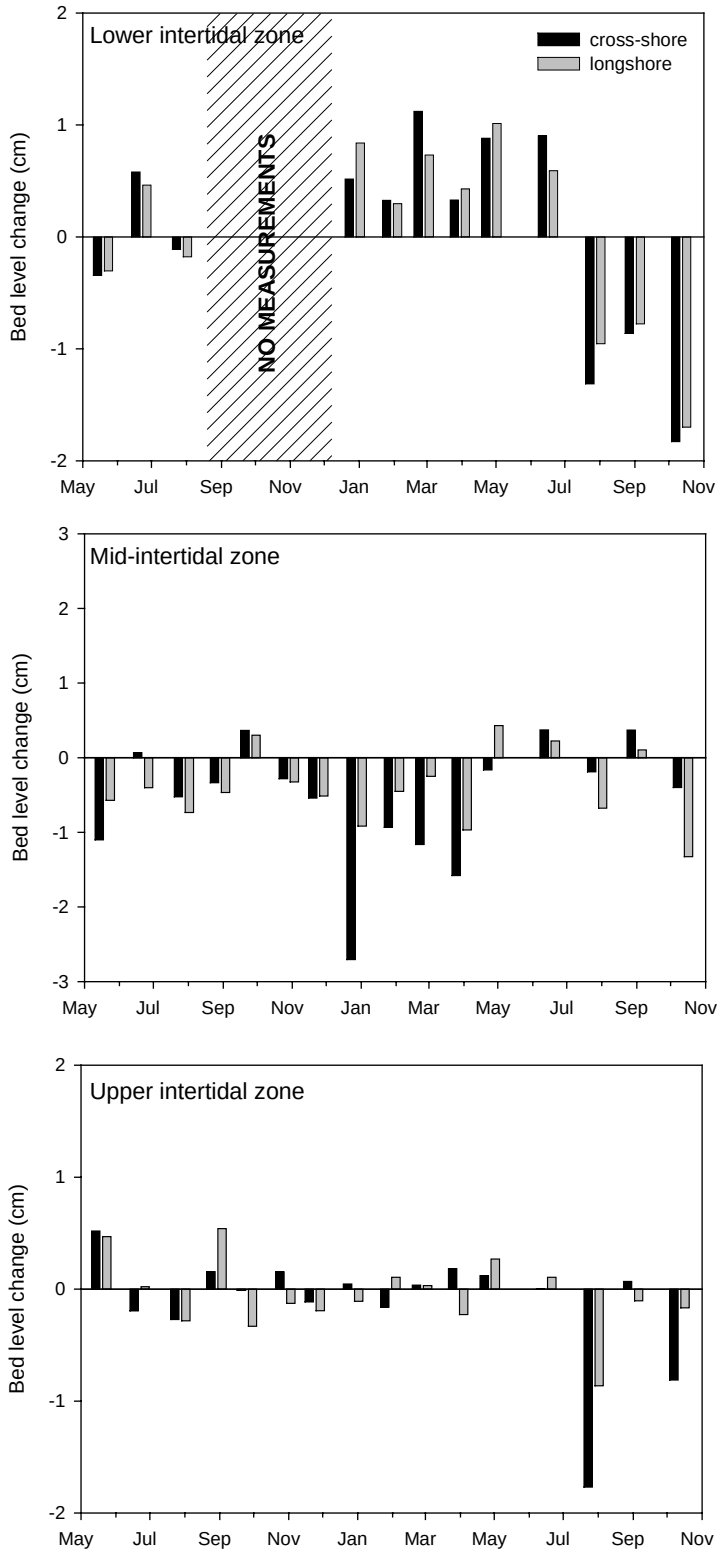

Figure 9.27: The monthly average bed level change, in longshore and cross-shore directions, at the 3 sites over the intertidal zone, from April 2003 to October 2004 (Note: erosion = negative; accretion = positive).

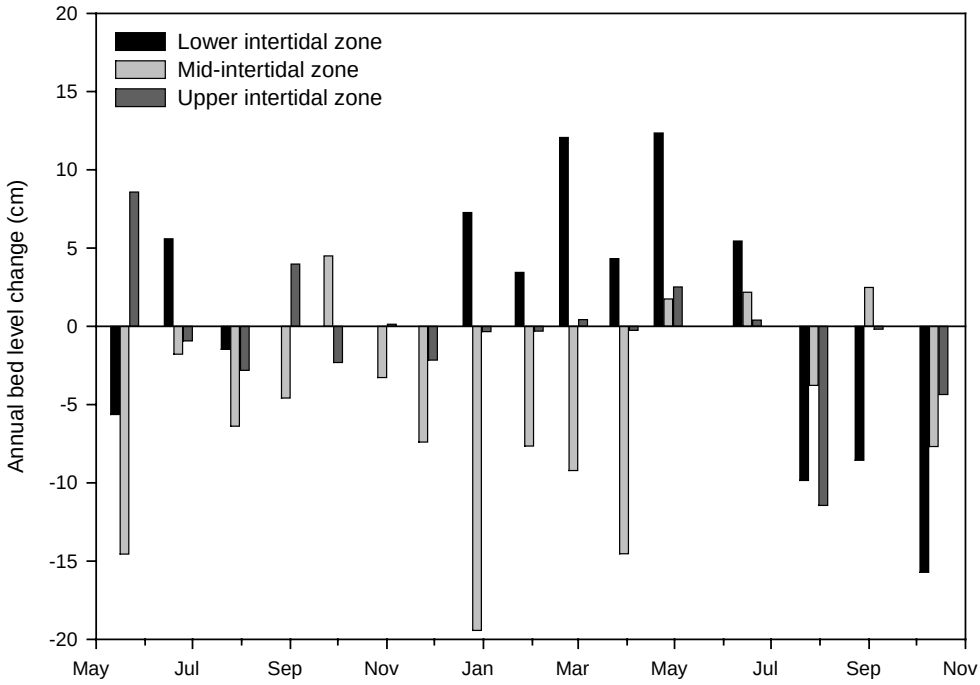

Figure 9.28: The average annual rate of bed level change at the 3 sites over the intertidal zone, from April 2003 to October 2004 (Note: erosion = negative; accretion = positive).

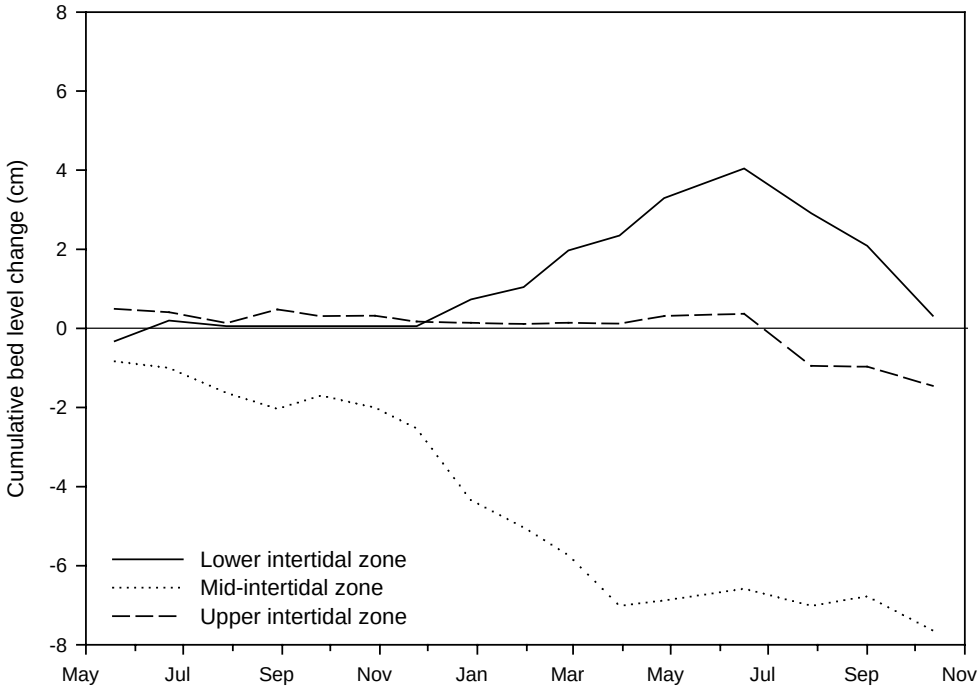

Figure 9.29: The cumulative change in bed level at the 3 sites over the intertidal zone, from April 2003 to October 2004 (Note: erosion = negative; accretion = positive).

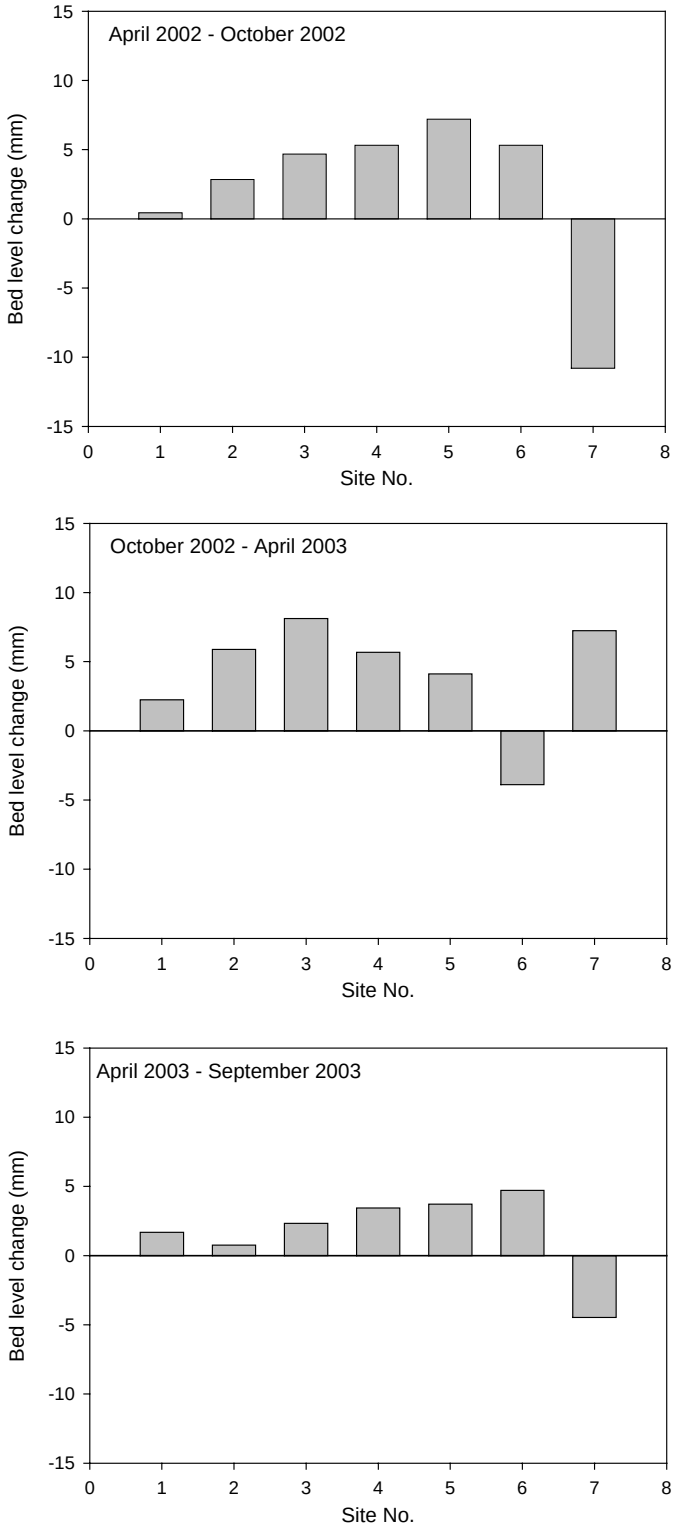

Figure 9.30: The average change in bed level, over the saltmarsh adjacent to Breach 1, from April 2002 to September 2003. Site number 1 was adjacent to the embankment, with the following sites located farther to seaward across the 200 m wide saltmarsh until site 7, which was located on the mudflat (for locations, see Fig. 4.5). Data collected by Sue Brown of CEH and supplied for the present investigation by EA.

Comparison with Previous Studies

The rates of bed level change measured by Amos (1974), between October 1972 and November 1973, showed that the intertidal flats at Freiston Shore were predominantly accretional (Fig. 9.31). However, the lower intertidal zone and an isolated area on the mid-intertidal zone were erosional. The erosion/accretion stations located over the intertidal zone at sites 1 to 3 from the present study, were located along the profile line CA/1 used by Amos (1974); the site on the upper intertidal zone was in the same location as the 4th station along from the embankment (CA 1/3), the site on the mid-intertidal zone was located landward of the 5th station (CA 1/4) and the site on the lower intertidal zone was located seaward of this, near the 6th station (CA 1/5). Over the same seasonal period as the measurements of Amos (1974) (December to November), the recent data show: annual accretion of 0.3 cm at the lower intertidal zone; erosion of 5.1 cm at the mid-intertidal zone; and erosion of 1.6 cm at the upper intertidal zone. From 1972 to 73, the upper intertidal zone accreted by 3.5 cm, the mid-intertidal zone eroded by 1 cm and the lower intertidal zone accreted by over 10 cm (Fig. 9.32). The rates of accretion measured during 1973 were much higher than those of 2004, although the relative magnitude of the changes at the sites was similar. The lower intertidal zone accreted at the highest rate, whilst the mid-intertidal zone eroded the most; and the least change was experienced at the upper intertidal zone. The only seasonal pattern that can be identified from the two data sets is, during both studies, the upper and lower intertidal zones accreted between January and June. However, during the recent study they then started to erode; in the past study, they continued accreting.

Between October 1971 and September 1981, the whole of the area seaward of the upper intertidal zone was recorded as having eroded by 20 to 25 cm (Van Smirren and Collins, 1982). The change from a location predominantly accreting during 1972 to 73, to being eroded 20 cm by 1981, was considered to be due either: (a) to hydraulic adjustment, in response to the land reclamation of 1980; or (b) to the development of a localised area of erosion, within an overall pattern of accretion within The Wash embayment.

For regional comparison, a sediment core collected on the Wrangle saltmarsh, 7 km to the north-east of Freiston Shore, has shown that the sedimentation rates of the saltmarsh were variable. The saltmarsh at Wrangle is in front of an old seawall, constructed between 1800 and 1900; hence this is an area where there has been no anthropogenic interference for a long time. Using ^{137}Cs as an indication of dating, it was found that following an erosional event in 1978, the saltmarsh accreted at 1.37 gr cm^{-2} yr^{-1} but after 1986 this rate dropped to 0.72 gr cm^{-2} yr^{-1} which it remained at until the present (Tsompanoglou, 2003).

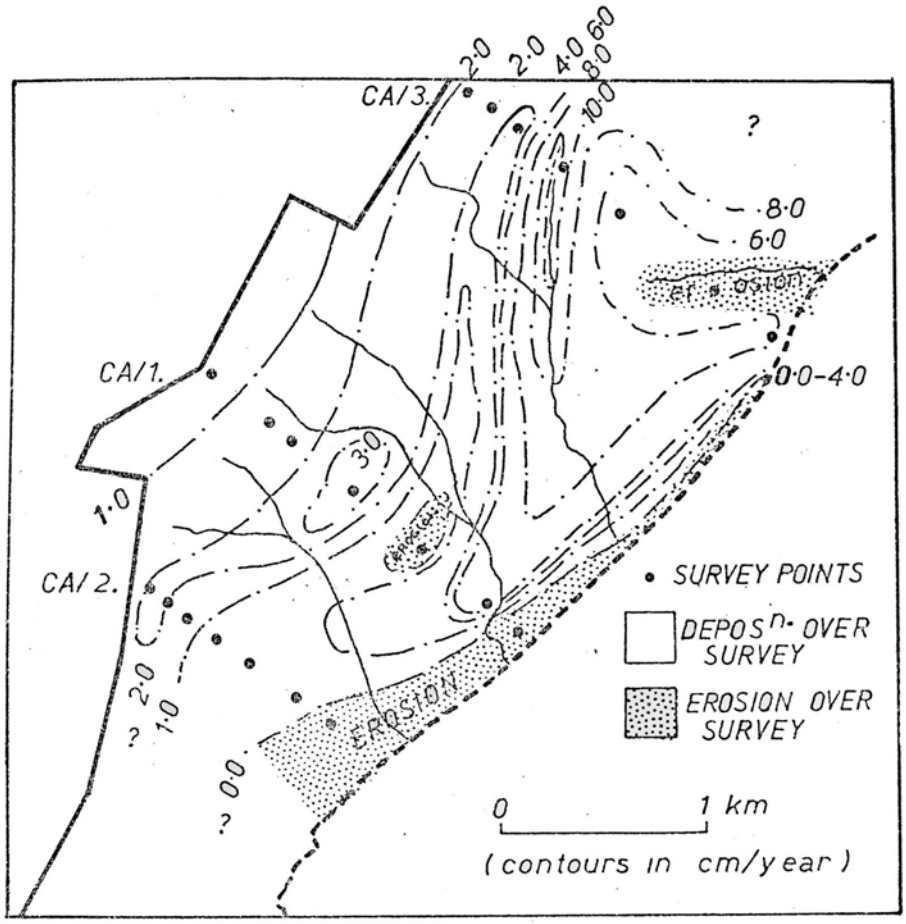

Figure 9.31: A contour plot of the rates of bed level change measured at Freiston Shore, between October 1972 and November 1973 (from Amos, 1974).

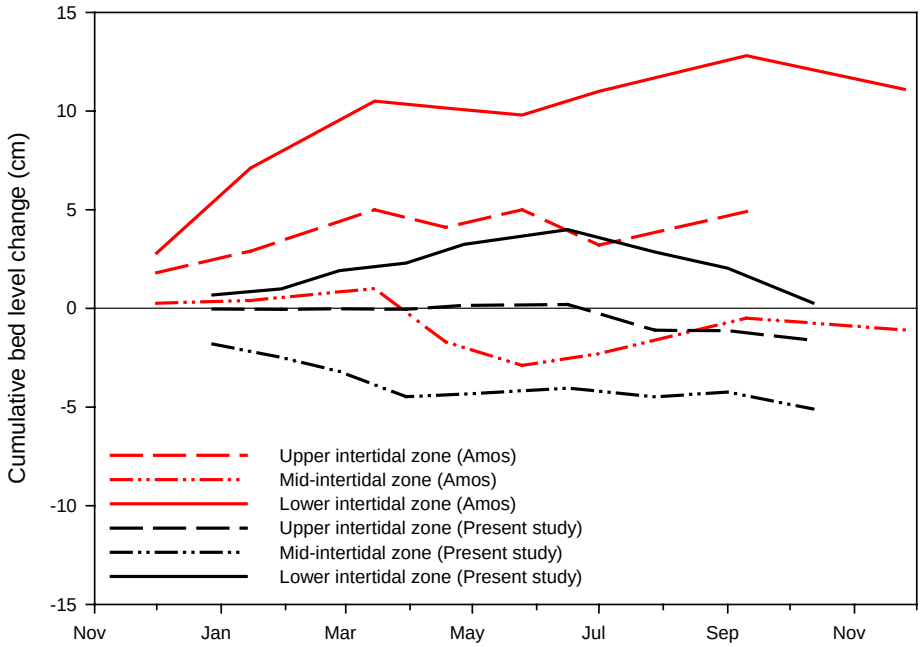

Figure 9.32: Cumulative erosion/accretion rates derived from the present study and from the study by Amos (1974). The data from the present study are represented by black lines, which vary in style to show the location of the measurements.

9.3.5 *Sediment Samples*

Surficial sediment samples were collected at the 3 erosion/accretion measurement sites (Fig. 4.1(a)) over 12 months, from November 2003 to October 2004. The variability in the grain size will be considered, in terms of mean grain size and proportion of fine- to coarse-grained material. The mean grain size of the surface sediment varied temporally and spatially (Fig. 9.33). The grain size at the upper and mid-intertidal zones followed very similar trends throughout the year, in terms of peaks and troughs in the mean grain size; while, the lower intertidal zone showed slightly more variation. At the lower intertidal zone, from November to December 2003, the mean grain size remained relatively stable at ~70 μm; from January to March, it decreased gradually to a minimum of 45 μm. A slight increase was experienced in April; this was followed again by a gradual decrease until mid-June, when the grain size was 49 μm. The grain size then increased until the final surficial sediment sample, collected in mid-October 2004, when the grain size was 99 μm. The mean grain size at the upper intertidal zone remained at ~70 μm from November 2003 to April 2004; it then peaked at 80 μm in May and decreased to a minimum grain size of 56 μm in June 2004. It then increased to maximum mean grain size of 94 μm in October 2004. The mean grain size at the mid-intertidal zone followed this same pattern, with slightly higher peaks and lower troughs than was experienced over the upper intertidal zone.

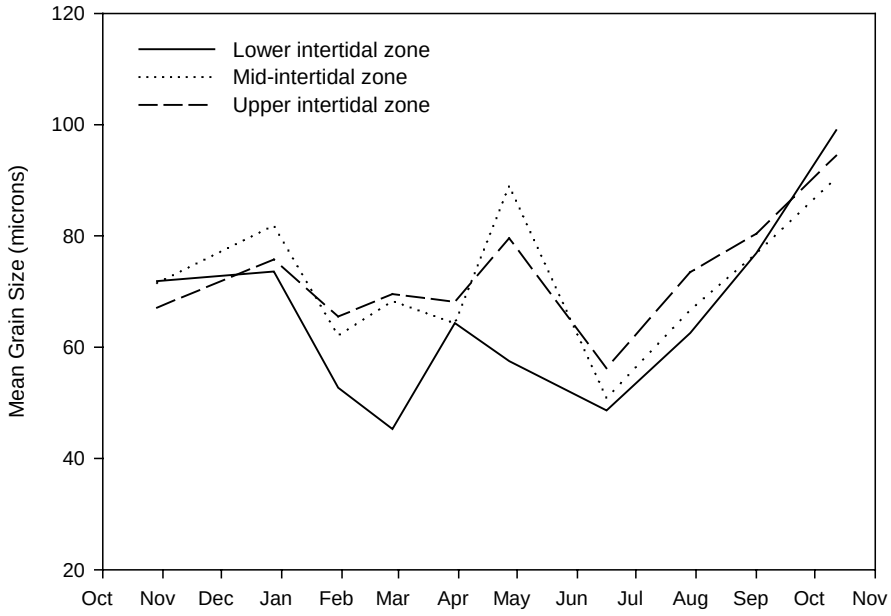

Figure 9.33: The mean grain size at the 3 sites, over the 12-month sampling period (October 2003 – 2004).

Overall, a high proportion of sand-sized sediment (> 63 μm), in comparison to fine-grained sediment (< 63 μm), was present within the surficial sediments of the 3 locations over the intertidal zone, during October 2003; this decreased gradually until February 2004 (Fig. 9.34). The proportion of sand-sized, in relation to fine-grained sediment, fluctuated at varying rates at all 3 sampling sites during the spring months. However, from July 2004 the proportion of sand-sized sediment increased until the final measurements were obtained in October 2004. As with the mean grain size, the proportion of sand-sized to fine-grained sediment at the upper and lower intertidal zones showed similar patterns, while the mid-intertidal zone had a contrasting pattern. There were low proportions of sand-sized sediment during May at the upper and lower intertidal zone (31 % and 50 %, respectively), whilst the mid-intertidal zone was associated with a high proportion (78 %) of sand-sized sediment in May.

The lower intertidal zone showed the greatest variation in the proportion of fine- to coarse-grained sediment, with a variation of 51 %, while at the upper and mid-intertidal zones the proportion only varied by 33 % and 35 % respectively (Fig. 9.34). The highest proportion of sand-sized sediment, to fine-grained sediment, was at the lower intertidal zone with a peak of 85 % during October 2004. The mean proportion of sand-sized sediment, over the 12 months was: 57 % at the lower; 61 % at the mid-; and 40 % at the upper intertidal zone. The mid- and lower intertidal zones were dominated by sand-sized sediment, whilst the upper intertidal zone was dominated by fine-grained sediment. Overall, there was a decrease in the proportion of sand-sized sediment to fine-grained sediment over the intertidal flat, in a landward direction. This pattern relates to a decrease in wave and tidal energy across the intertidal flats as noted by Evans and Collins (1987). Wave and tidal current activity increase the resuspension and transport of sediment. Hence, areas of the intertidal zone exposed to strong wave energy and tidal currents will be associated with the resuspension of finer-grained sediments; this creates a lag deposit of coarse sand surficial sediments. This characteristic was found also in 1981, when the intertidal zone was eroded. At this time, the surficial sediment was composed of coarser-grained sediment, than in 1973, when the area had been accreting (Van Smirren and Collins, 1982).

The dominant process occurring over the intertidal flats, i.e. erosion or accretion, affected the grain size of the surficial sediment (Fig. 9.35). From July 2004, all sampling locations on the intertidal flats experienced erosion; at the same time, the proportion of sand-sized sediment in the surficial sediment increased. The relationship between the rate of bed level change and the surficial sediment composition was more defined at the lower than at the upper or mid-intertidal zones. From February to June 2004, two periods of accretion at the lower intertidal zone were accompanied by an increase in the proportion of fine-grained sediment; a period of

erosion was associated with a corresponding increase in the proportion of sand-sized sediment. The lower intertidal zone was the only location to have a statistically significant correlation (to 95 %) between the percentage of sand-sized sediment and the corresponding rates of erosion/accretion (Fig. 9.36): upper intertidal zone ($F_{1,8} = 2.09$, $P > 0.05$); mid-intertidal zone ($F_{1,8} = 0.08$, $P > 0.05$); and lower intertidal zone ($F_{1,7} = 9.2$, $P < 0.05$). Erosion led to an increase in the proportion of sand-sized sediment; accretion caused an increase in the proportion of fine-grained sediment.

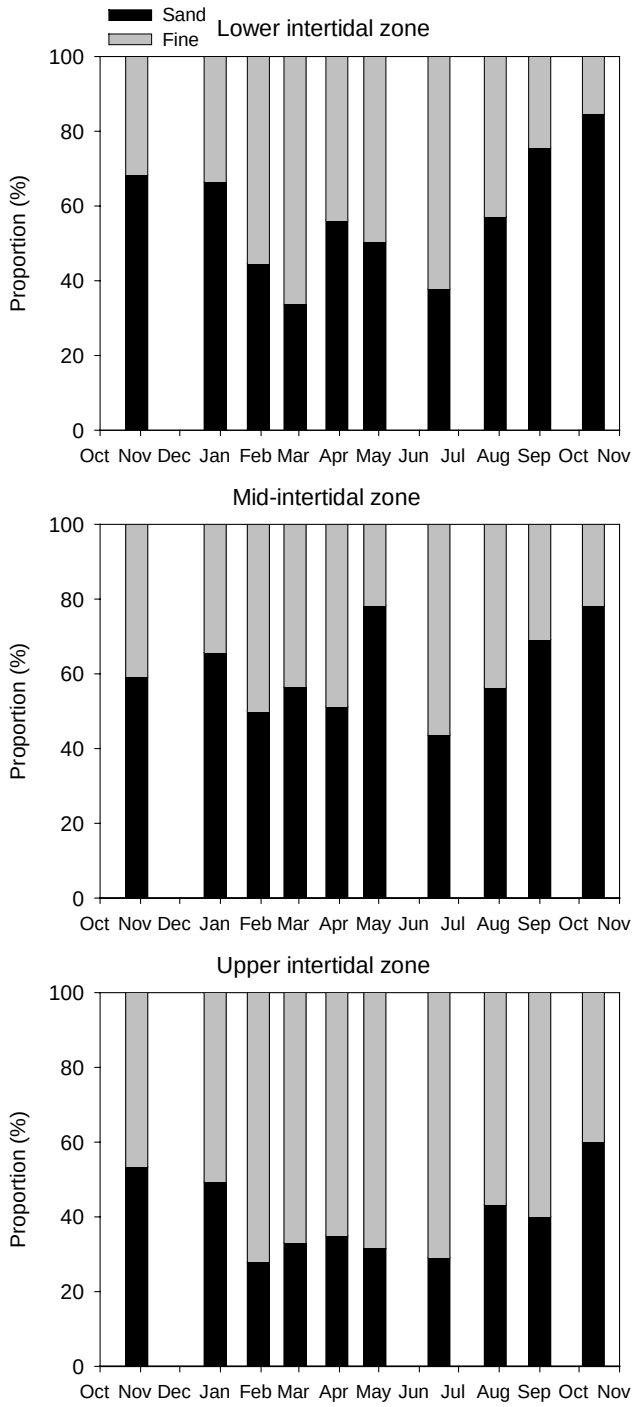

Figure 9.34: The proportion of sand-sized particles (> 63 μm), to fine-grained particles (< 63 μm), over the 12 month sampling period (October 2003 – 2004) at the 3 sites on the intertidal zone.

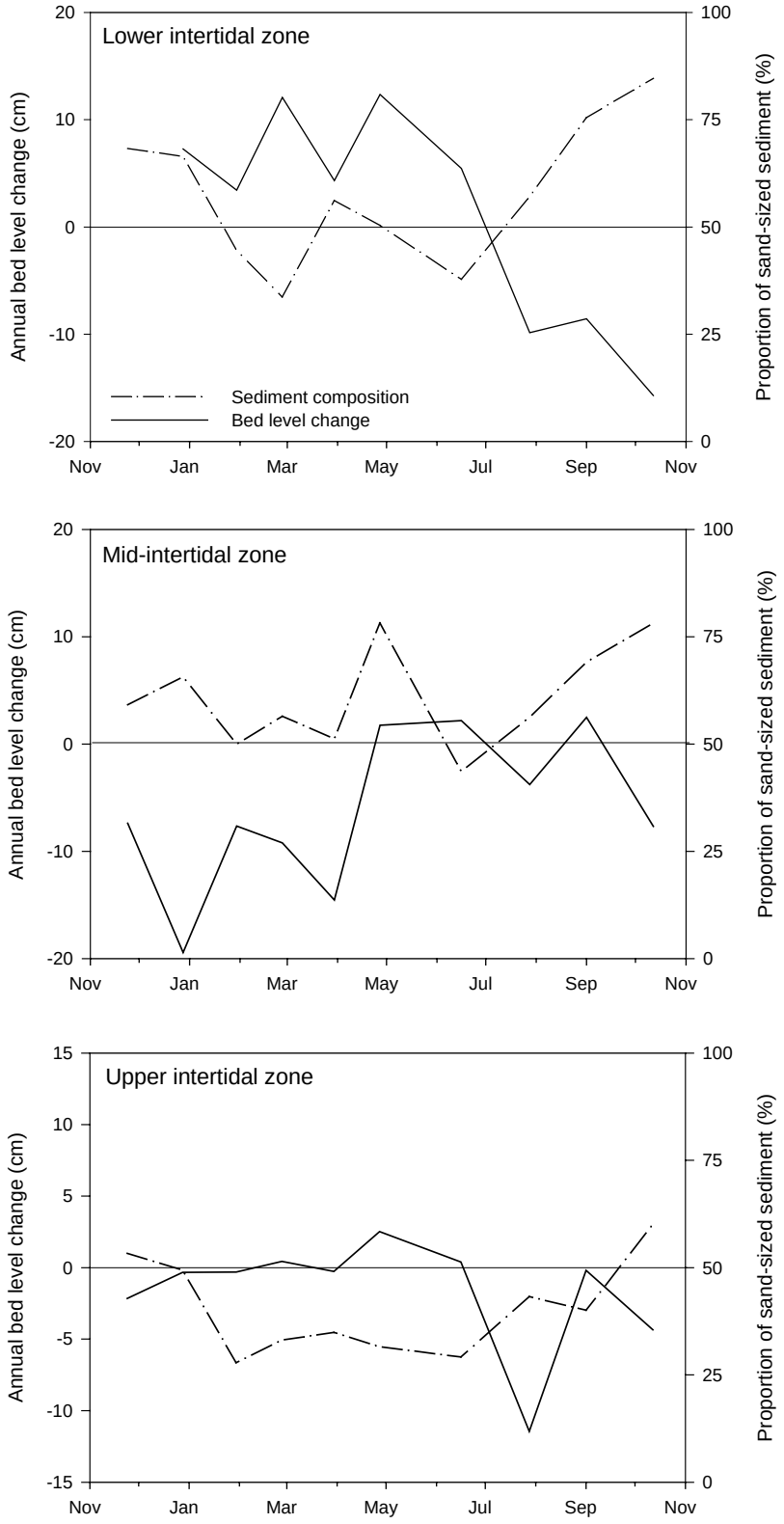

Figure 9.35: Comparison of the annual rates of bed level change and the sediment composition at the 3 sites, from December 2003 to October 2004 (Note: erosion = negative; accretion = positive).

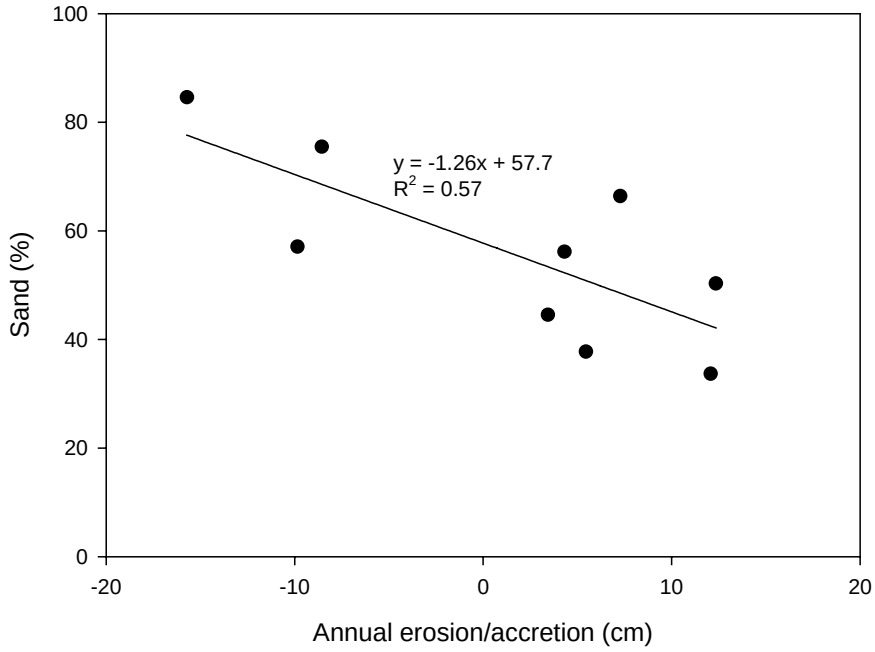

Figure 9.36: Correlation between the composition of the surficial sediment and the corresponding rates of erosion/accretion, at the lower intertidal zone.

9.4 DISCUSSION

The hydrodynamic conditions over the intertidal flats during spring tides appear to have remained relatively consistent over time. The general characteristics are similar, nowadays, to those identified in the various previous studies (Amos, 1974; Evans and Collins, 1975; Collins, Amos and Evans, 1981; Evans and Collins, 1987; Ke, Collins and Poulos, 1994; Ke, Evans and Collins, 1996; and Ke and Collins, 2000). The tidal current speed peaks during the first phase of the flood and the last phase of the ebb tide, with the flood peak generally being the higher (Ke and Collins, 2000). The tidal curve is asymmetrical, with longer ebb than flood period, to accommodate the higher flood current speeds; this is more emphasised over the lower intertidal zone, where the asymmetry varies with tidal range. The tidal curve over the lower intertidal zone became more asymmetrical as the tidal range increased towards spring tides; over the upper intertidal zone, it was not noticeably affected. This variation in the observed asymmetry in the tidal current speed and tidal curve are consistent with the interpretation proposed by Ke and Collins (2000), i.e. that the asymmetry of the tide is related strongly to the stage of the spring/neap cycle. The asymmetry in the tidal current speed, together with the duration of the flood and ebb stages of the tide, can be used to determine if an intertidal flat is eroding or accreting (Van Straaten and Keunen, 1958; Postma, 1967; and Elliott, 1986). Based upon the findings of other studies, where similar asymmetries in the tidal curve and tidal currents were experienced (Anderson, 1973; Bayliss-Smith et al., 1979; Carling, 1982; French and Clifford, 1992; Zhang, 1992; Amos, 1995; and Leonard et al.,

1995), the prevailing conditions in The Wash indicate that sediment should accumulate over the intertidal zone during spring tides. A similar, weaker, process should occur during neap tides (Ke et al., 1996).

Clockwise rotation of the tidal currents, from the first phase flood to the last phase ebb, was present; this was more pronounced on the lower intertidal zone than at the upper, as the rotation at the upper intertidal site started shortly before HW. At both locations, the observed tidal current direction at the start of the flood was around 300º; it was around 100º at the end of the ebb. These observations are in agreement with the earlier findings of Evans and Collins (1975). The present study identified a peak in the tidal current speed occurred over the upper and lower intertidal zones, at the point in the tidal cycle as when flow began into the MR site. Such a peak had been recorded previously (Ke and Collins, 2000), but had not been as well defined over the upper intertidal zone as it was during the present investigation. The slight enhancement noted in the measurements of this study, may be related locally to the water flowing into the MR site, causing acceleration in the tidal current speed over the upper intertidal zone. The proposed enhancement in peak tidal current speed around HW over the upper intertidal zone has not impacted the area. Owing to the presence of a small peak prior to the creation of the MR, combined with a similar peak being present over the lower intertidal zone before the MR, it is likely that the peak over the upper intertidal zone is natural and not related to the MR.

The erosional phase over the intertidal zone, associated with an increase in tidal current speeds in 1980 (Van Smirren and Collins, 1982), is considered to have taken place over a limited period of time. Such high current speeds, as were observed at that time, have not been recorded during the present investigation. Conditions appear to have reverted to those observed previously, i.e. as in 1972. The studies undertaken by Collins et al. (1998) and Ke and Collins (2000), represent similar tidal current speeds, in 1981 and 1991-3, to those that occur today over the upper intertidal zone. The increase in tidal current speed, it was suggested, could have been attributed to a hydraulic readjustment to land reclamation (Van Smirren and Collins, 1982). Thus, the erosion associated with the high current speeds, measured by Van Smirren and Collins (1982), can only have lasted for 1 to 2 years if it was associated with the embankment built as part of the land reclamation; the reclamation was undertaken in 1979-1980 and the measurements from 1981 show that the high current speeds had ceased. This period of erosion was either: a short-term rapid phase of erosion caused by a land reclamation (i.e. the creation of an embankment over the saltmarsh), similar to the short-term erosional response of the intertidal creek system following the initiation of the MR (Chapter 7); or, a natural change associated with high current speeds and erosion between

1972 and 1980. The embankment associated with the reclamation would have reduced the local tidal prism; this, in turn, would have affected the "regime" of the intertidal zone, causing a brief period of instability over the intertidal zone (Inglis and Kestner, 1958). The creation of an embankment is generally thought to lead to a reduction in the tidal current velocities; this leads to the seaward displacement of the location where hydrodynamic conditions are sufficiently slowed to cause deposition (Evans and Collins, 1987). However, in the case of Freiston Shore the embankment was constructed too far to seaward and, as such, did not leave sufficient width for the intertidal flats to accrete and develop. As the intertidal flats had been narrowed, the flats did not dissipate the tidal currents; this caused higher tidal currents over the flats, resulting in erosion of the mudflats.

During the period of the measurements a clear seasonal trend was observed in the wave climate at the mouth of The Wash. Peak wave heights occurred during the winter months (December to February); mixed wave conditions were present in autumn (September to November) and spring (March to May); whilst the lowest wave heights were over the summer (June to August) (Addison, 2005). Wave heights measured over the adjacent intertidal flats, such as Freiston Shore, showed a similar seasonal trend. The intertidal flat observations of the present study showed that minimal wave dissipation occurred over the mudflats and sandflats. Although they were effective in reducing the energy of the higher period waves, which resulted in the redistribution of the energy to the lower period waves. The preferential reduction of the low frequency waves was also found at the Tillingham marshes in Essex, east coast of the UK (Möller and Spencer, 2003), which have similar characteristics to the intertidal flats at Freiston Shore; the saltmarshes form a narrow belt (< 700 m wide) between the seawall protected agricultural land and the intertidal mudflats, which extend up to 4 km. Möller and Spencer (2003) concluded that the site characteristics, such as substrate type, micro-topography and marsh surface vegetation as opposed to the meteorological conditions, were crucial in explaining and therefore predicting wave spectra transformations. This would explain why similar wave spectra transformations were witnessed at Tillingham and Freiston Shore.

The saltmarsh was the most effective zone of the intertidal flats in dissipating wave energy; this is in agreement with the findings from other intertidal flat environments (Möller and Spencer, 2003), where the saltmarsh vegetation has been found to be the main cause of wave dissipation (Neumeier and Ciavola, 2004). The wave conditions experienced inside the MR site at Freiston Shore were similar to those over the saltmarsh; this indicates that vegetation inside the MR acts in the same way as over a natural saltmarsh, i.e. preventing the wave height from increasing above a certain height.

The waves experienced over the intertidal flats have been classified, in previous and the present investigations, into two types: (a) wind waves travelling from the south, which are generated locally within The Wash; and (b) swell waves travelling from the east, which originate in the North Sea and travel through the mouth of The Wash (Amos and Collins, 1978). The peak wave periods observed during the present study varied with wave direction. The average *Tp* for the swell waves ranged from 3 to 4.5 s; for the locally-generated wind waves the *Tp* ranged from 2 to 3 s. Both wave types had a similar frequency of occurrence. In a previous study, the swell waves were observed to have a period of 2 s, with the locally-generated waves having a period of 1 s; while the locally-generated waves occurred more frequently than the swell waves (Amos and Collins, 1978). The recent measurements show that swell waves were dissipated more over the mudflats and sandflats, whilst the locally-generated waves often gained more energy over this part of the intertidal zone. Dyer (1998) considered that on mudflats the short period, locally-generated wind waves can be erosive, whilst longer period swell waves have less of an impact. This pattern indicates that the predominant locally-generated waves, observed by Amos and Collins (1978), over the intertidal zone are more likely to cause erosion, than accretion.

The measured SSC in the waters overlying the intertidal flat at Freiston Shore correlated strongly with the tidal current speeds, with peaks in both occurring simultaneously. This pattern has been seen on other intertidal flats, such as in Namyang Bay, the Yellow Sea, South Korea (Adams Jr. et al., 1990). At Freiston Shore, the peak SSCs during the first phase flood and last phase ebb varied with tidal current speed; this, in turn, was dependent upon the tidal range. As predicted, highest tidal current speeds were associated with spring tides; these coincided generally with the highest SSCs. Overall, the measured levels of SSC decreased from LW towards HW, over the intertidal flats, with the higher concentrations occurring towards the base of the water column. These patterns are in agreement with the results of previous work undertaken at Freiston Shore (Evans and Collins, 1975; and Collins et al., 1981). The observed SSC was found to increase exponentially with an increase in tidal current speed. Similarly, increased wave activity caused a linear increase in SSC. A significant wave height greater than 0.15 m was found to be sufficient to resuspend sediment over the intertidal flats. A linear relationship between wave height and SSC was observed in a previous investigation, where small amplitude waves (less than 5 cm) were found to be capable of suspending fine-grained sediment in shallow water (Anderson, 1972). Owing to the pressure sensor on the ABRs being 0.5 m above the bed, the impact of waves on the SSC in shallow water could not be observed during the present investigation.

The SSC was found here to increase exponentially with an increase in tidal current speeds, and linearly with an increase in wave height. In general, waves are important in the resuspension of intertidal flat sediments (Amos, 1995). The rapidly oscillating flows, under wind-induced waves, result in much higher shear stresses than those caused by tidal currents alone (Postma, 1988; and Pethick, 1996). For example, at Portishead on the Severn Estuary, the mean measured sediment concentrations were increased three-fold, in response to wave action (Whitehouse and Mitchener, 1998). The oscillatory motion weakens the sediment water interface, causing resuspension of the otherwise consolidated sediments. The bed shear stress under waves is related inversely to water depth; hence, erosion will occur predominantly during the first phase and last phase of the tidal inundation (Madsen and Grant, 1976; and Amos and Collins, 1978). An ambient level of suspended sediment is often present in the overlying waters; this may be related to 'external' events, such as storms in adjacent water bodies. Collins et al. (1981) observed that storm conditions outside of The Wash embayment could increase the SSC by an order of magnitude over the intertidal flats. The maximum suspended sediment content carried over the intertidal flats was found to be normally of the order of 200 mg l^{-1}; under storm conditions in the adjacent North Sea, it had previously been recorded to be as high as 2,000 mg l^{-1} (Evans and Collins, 1975). It appears that material suspended in the North Sea can, eventually, be transported to, and deposited on, the intertidal flat system of The Wash. On the basis of data collected, a schematic representation of the relative effects of tidal currents, waves and external sources, on the SSC over intertidal flats, was established (Fig. 9.37). The diagram shows a simplistic representation of the factors controlling the SSC based on actual data. However, data still need to be collected under higher wave conditions and during storms in the North Sea, to validate the diagram.

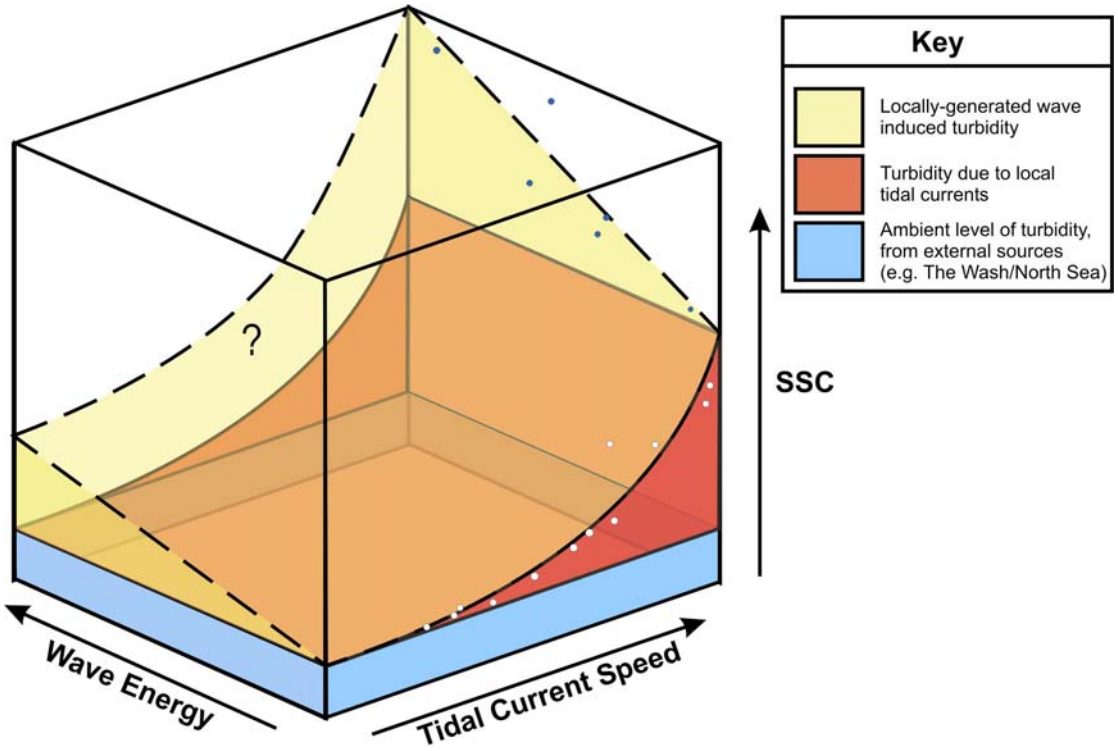

Figure 9.37: A schematic representation of the controls on suspended sediment concentration over an intertidal zone. Relative data points obtained from the intertidal zone at Freiston Shore, as part of the present study have been added.

The pattern of erosion and accretion, which occurred at all of the monitoring sites on the intertidal flats during this study, agrees with the previous findings of Amos (1974) and Van Smirren & Collins (1982). The measured rates of erosion and accretion varied temporally, with the peak levels of erosion being higher than those of accretion. Fluctuations in erosion and accretion on the upper intertidal zone were found here not to be as high as those on the mid- and lower zones. However, it must be considered that the upper zone was located at a higher elevation on the flat; as such, it would not remain inundated for as long as the other sites, and would be exposed to weaker tidal currents. The erosion and accretion rates over the intertidal flats were more pronounced in a cross-shore, rather than longshore, direction. Such an outcome may have been in response to dominant wave and tidal propagation in a cross-shore direction, i.e. perpendicular to the shoreline. In the present study, there was a progressive increase in the magnitude of the fluctuations between erosion and accretion in a seaward direction, as also noted by Amos (1974).

An erosional phase at the mid-intertidal zone occurred concurrently with an accretional phase at the lower intertidal zone. Increased erosion on the mid-intertidal zone may have supplied the material in suspension that was deposited subsequently over the lower intertidal zone; this suggests that sediment may be reworked and redeposited over the intertidal flats. Few apparent seasonal trends were found in the present data set, except that erosion tended to

occur in the summer and autumn. This was not the expected result, as the summer months are considered generally to show an increase in accretion; these would allow finer-grained sediment to settle out, in response to a reduction in the frequency and intensity of waves (Amos and Mosher, 1985; Kirby et al., 1993; Boorman et al., 1998; and O'Brien et al., 2000). In addition, over the summer months, there is an increase in bio-stabalisation of the surficial sediments by algal mats (Paterson et al., 2000), as observed over the upper intertidal zone at Freiston Shore (Plate 9.1). Although Amos (1974) concluded Freiston Shore to be an accretional environment, the present investigation has shown that erosional phases still occur. The present study has demonstrated that Freiston Shore has been undergoing a prolonged period of erosion since the summer of 2002, with estimated erosion of 4,000 m^3 yr^{-1} of sediment across a 100 m wide stretch of the intertidal zone; this phase may be part of a natural cycle similar to those described by French (2001) and thus may not be cause for concern. However, it is possible that this has been caused by the breaching of the seawall at the MR and has only been occurring since August 2002. The MR may have caused an increase in the rates of erosion since the measurements by Amos (1974) through the water draining from the MR following HW during spring tides. The sheetflow resulting from the drainage of the MR caused the enhancement of a creek system over the intertidal flats and had the potential to erode the surface sediment of the intertidal flats.

The composition of the surficial sediment over the intertidal flats was found to be associated with the rates of erosion and accretion. As under accretional conditions, there was an increase in the proportion of fine-grained sediment; under erosion, the proportion of sand-sized sediment increased. Such modification was in response to the reworking of the surficial sediments by wave and tidal action.

9.5 CONCLUDING REMARKS

The anthropogenic changes at Freiston Shore over the last 30 years are considered to have resulted in a number of changes over the intertidal zone. For example, the high tidal currents and high rates of erosion, recorded by Van Smirren and Collins (1982) in 1980, are considered to have resulted from the construction of an embankment in 1979-80. The MR has not significantly affected the tidal currents and sediment transported across the intertidal flats; however, the sheetflow which occurred as a result of the MR, may have resulted in more erosion over the intertidal flats than experienced under natural conditions, causing the difference between the rates recorded following the MR and those prior to it (in 1973-74). Other affects have been identified, as described in Chapters 5 & 6: erosion of the channels within the breaches in the embankment; and the enhanced development of a creek system over the intertidal flats.

The wave conditions in The Wash have been found to be associated with a seasonal trend. Peak wave conditions were shown to occur in the winter months, with isolated periods of high wave activity during the autumn and spring. The lowest wave conditions occur during the summer months. Surprisingly, the rates of erosion and accretion over the intertidal flats did not follow the same seasonal trend over the period of measurement, with erosion taking place during the summer months. Therefore, other factors, such as the tidal and biological activity, must have been important in influencing the rate of bed level change. During the period of measurement the intertidal flats were predominantly erosional, whilst the saltmarsh was accretional.

Suspended sediment was transported during all of the tides measured, with the presence of waves increasing the SSC. The first phase flood and last phase ebb were identified as being important phases in the transport of suspended sediment. In the absence of wave activity, tidal currents resuspended sediment as the water initially flooded the intertidal flats (Plate 9.2). With waves present, it is shown that the quantity of sediment resuspended increases dramatically. Hence, even minimal wave activity in very shallow waters and at the edge of the tidal incursion, will suspend sediment (Dyer, 1998). The initial influx of suspended sediment, caused by the first phase of the flood, was not recorded by the ABRs; these instruments could only commence recording in water depths greater than 0.5 m. In future studies, the tidal currents and SSC during these periods should be measured; this should provide a more accurate indication of the flux of sediment. To be able to describe and predict changes in the sediment movement caused by varying conditions over intertidal flats is "essential for maintaining or creating a successful coastal defence" (Dyer, 1986).

The intertidal zone at Freiston Shore was shown to be effective in dissipating wave energy. Also, the wave energy dissipation rates over the saltmarsh were much higher, than over the mudflats, stressing its importance for coastal protection. As such, forms of coastal protection that aim to create saltmarsh should be encouraged, in suitable areas, as they use the natural environment to improve the coastal defence.

9.6 PLATES

Plate 9.1: An algal (*Enteramorpha* sp.) mat present over the upper intertidal zone at Freiston Shore (29/08/2003).

Plate 9.2: Suspended sediment within the surface waters, during the first phase flood of the tide, over a creek within the lower intertidal zone (05/09/2005).

CHAPTER 10: DISCUSSION AND CONCLUSIONS

10.1 DISCUSSION

10.1.1 *Sediment Dynamics*

In relation to the aims of the managed realignment; i.e. firstly to create a sustainable flood defence scheme, through the establishment of saltmarsh and, secondly, to avoid adverse impacts on existing habitat and the adjacent saltmarsh and intertidal flats, the scheme at Freiston Shore has fulfilled the former but not the latter. The MR site has provided a sustainable flood defence; it should continue to do so, for the foreseeable future. The majority of the MR site was colonised by halophytic vegetation after 12 months, whilst its elevation has been increasing, at up to 5 cm yr^{-1}. The wave activity experienced inside the MR site is similar to that over the adjacent saltmarsh; this indicates that the site should provide adequate protection from wave activity, when the breached embankment is eventually eroded away (however, over a 3 year period, it has suffered only minimal erosion). On the other hand, the creation of the MR site has produced adverse effects on the existing adjacent saltmarsh and intertidal flats. High levels of erosion have occurred in the channels within the breaches in the embankment, which also eroded areas of saltmarsh. Likewise, rapid expansion of an original creek system has resulted in erosion of the mudflats and sandflats.

Anthropogenic changes have been found to affect the hydrodynamics of the water column over the intertidal flats. The construction of an embankment in 1980, for land reclamation purposes, produced a short-term increase in the tidal current speeds and a subsequent period of erosion. The creation of the MR did not cause any change in the magnitude of the tidal currents, but may have caused an increase in the general erosion rates over the intertidal flats and a definite increase in the erosion rates of a creek system over the mid-intertidal zone and of the channels within the breaches.

The main impacts of the MR, on the surrounding intertidal zone, lasted for 2 years after the embankments were breached. In this time, the channels within the breaches and the natural creeks to which they are connected, eroded sufficiently to allow the MR to drain at the same rate (in terms of tidal curve) as the surrounding intertidal flats. As the creeks eroded sufficiently to contain all the drainage water from the MR, the development of the creek system over the mid- to lower intertidal zone ceased and it silted up. Overland flow from the draining of the MR caused enhanced creek development and, possibly, erosion of the intertidal flats. Some 3 years after the initiation of the MR, the channels within the breaches and the natural creeks to which they are connected were still eroding; however, they appear to

be near a dynamic equilibrium, with conditions following the MR. The negative impacts[1] of the MR at Freiston Shore, which had ceased mainly 2 years after the MR site was created, are considered to be negligible, in relation to the saltmarsh created and improvement in long-term coastal protection.

Erosion of the channels within the breaches, together with the rapid expansion of a creek system, were caused by a difference in elevation between the MR site and the adjacent saltmarsh, to seaward; the saltmarsh was 0.5 to 1 m higher, than the area of the MR site by the breached embankment. This difference in level caused water to enter the MR site at high current speeds during high water spring tides; this, in turn, resulted in rapid erosion of the channels within the breaches, as they enlarged in order to adapt to the flow entering the site. During the ensuing low water period, the MR site acted as a 'reservoir', holding back the waters and draining only gradually through the channels within the breaches. During the initial spring tides which flooded the MR site, such drainage continued, until the subsequent HW re-flooded the site. However, as the water flowing into the site eroded the channels within the breaches, drainage of the site became more rapid. Approximately 18 months after the breaching of the embankment, the tidal curve inside the MR site was nearly synchronous with that over the adjacent saltmarsh. The water draining from the MR site flowed into natural creeks, which had been connected artificially to channels within the breaches. These systems were small creeks, which responded naturally to the flooding and draining of the saltmarsh; however, they were not sufficiently large to contain all of the water flowing out of the MR site. As the breaches in the embankments were eroded, the MR site drained more rapidly; hence, the natural creeks to which they were connected were enlarged, to accommodate the volume of water draining from the MR. Two years after the MR was initiated, the natural creeks were observed to accommodate all of the water draining from it. However, up to this point, the natural creeks could not contain all of the water flowing out of the MR site; as such, much of this escaped from the creeks, as overbank flow. Such flow proceeded then over the intertidal flats, as sheetflow, which became ultimately channelled into small drainage rills; these connected to an existing creek system, over the intertidal flats. The enhancement to the natural flow, as experienced in this creek system, eroded rapidly large quantities of sediment from the intertidal mudflats and sandflats. The enhanced development lasted for 2 years, and in the following 12 months the creek system silted up until it had nearly reverted back to its original state prior to the MR. Over these 3 years, the complete development of this creek system, caused by an anthropogenic change modifying the intertidal system, was observed. Such a rapid change in a creek system, resulting from

[1] Note: these were; the rapid erosion of the channels within the breaches; the enhanced development of a creek system over the intertidal flats; and the possible erosion of the intertidal flat surface.

anthropogenic change, has not been documented previously; neither has such rapid siltation in creeks, as occurred when the anthropogenic change ceased affecting the intertidal flats. Such patterns emphasise the theory of a dynamic equilibrium existing for intertidal zones, as proposed by Brookes (1996) and Bassoullet et al. (2000). When an anthropogenic change upset the equilibrium of an intertidal flat, rapid erosion of a creek system ensued. Likewise, when the effect of the anthropogenic change ceased, the creek system infilled rapidly, returning to a state similar to that which existed before the anthropogenically induced change, i.e. to a dynamic equilibrium. The intertidal flats were "geomorphologically responsive" to anthropogenic changes, in the form of the creation of a MR site: however, when the surrounding area was stabilised, the intertidal zone returned to its original form, in agreement with the theory by Werritty (1997).

The majority of the erosion experienced in the channels, within the breaches in the embankment, occurred within the first few months following the MR. The area of the channels increased by 5 times, over the first 2 months following their creation. After this initial period of rapid erosion, the rate reduced (although the most recent measurements obtained, some 3 years later, showed that the channels were still eroding, but not at such a rapid rate, as previously). The Regime Theory was used to calculate the eventual shape and size of the channels within the breaches of the embankment. The calculations require: (a) either measurements, or predictions, of the discharge of the channels; (b) the quantity of sediment transported; (c) the mean grain size of the sediment transported; and (d) the settling velocity of the grains. Through the use of the Regime Theory method (Inglis and Allen, 1957), together with the Cao and Knight (1997) method for calculating channel shape, a realistic prediction of the final dimensions and shape of the channels was calculated. On this basis, it was predicted that it would take 5 years for the channels, within the breaches, to reach a dynamic equilibrium (Shimizu, 1991; as cited in Yalin and Ferreira da Silva, 2001).

The dominant hydrodynamic regime over the intertidal flats did not appear to represent the long-term changes in bed level. The hydrodynamic conditions indicate that the intertidal zone should be an accretional environment, according to the findings of Wang and Eisma (1988); however, the intertidal flats were predominantly eroding. The saltmarsh and lower intertidal zone at Freiston Shore were found to be accretional, whilst the upper and mid-intertidal zones were erosional. However, the erosion/accretion measurements obtained during the present study were collected just after the initiation of the MR scheme. The measurement period coincided with a phase of high headward extension of the creek system, over the intertidal flats, i.e. over the same area as the erosion/accretion measurements. Therefore, the erosion measured over the mid- and upper intertidal zones may be related to the MR scheme, owing

to the increased sheetflow produced by the MR; this caused, possibly, instability in the surficial sediments, leading to erosion. However, it is possible that the erosion was caused or enhanced by the presence of the creek system. Drainage of the intertidal zone directs water into the creeks; as such, any sediment would be transported into the creeks, then be transported towards the subtidal channel. There was spatial variability in the response of the intertidal flats, as part of the lower intertidal flats experienced accretion over an 18 month period; in contrast, an area located 300 m to landward was associated with high rates of erosion. Previous measurements undertaken by Amos (1974) showed similar spatial variability in erosion/accretion rates, with the mid-intertidal zone eroding and the lower intertidal zone accreting. The main difference between the findings of the present study and that of Amos (1974), is that the previous measurements showed that the intertidal flats were predominantly accreting at high rates (up to 12 cm yr^{-1}), the only area of erosion, the mid-intertidal zone, had low rates (1 cm yr^{-1}). However, recent measurements show that only the lower intertidal zone was accreting, at a peak rate of 0.36 cm yr^{-1}; the remainder of the intertidal flats was eroding, at rates of up to 5.1 cm yr^{-1}. The two sets of data show similar patterns at each site, but with much lower accretion rates and higher erosion rates associated with the recent measurements; this suggests that, either the intertidal flats are now subjected to more erosion as part of a natural cycle, or that the MR has caused an increase in the levels of erosion and a decrease in the levels of accretion.

In addition to monitoring the impacts of the MR on the intertidal zone, hydrodynamic and sediment dynamic measurements were undertaken to help in the understanding of wide intertidal flats and to be able to predict or model how various conditions may affect them. The addition to the already existing knowledge of these environments, provided by the present investigation, will be of particular use for predicting the impacts of MRs at different sites or to ascertain what form of coastal management, if any, would be the most suitable.

The frequency of the hydrodynamic measurements used to predict the bedload transport were important, as the main periods of bedload transport over the intertidal flats at Freiston Shore were during the first and last phases of the tidal cycle. The low water depth maximises the effect of the wave-induced shear stresses on the intertidal sediment surface, increasing the chance of mobilising sediments.

The levels of suspended sediment were enhanced by the presence of wave activity, with a significant wave height > 0.15 m being necessary to enhance the SSC over the intertidal flats. The SSC was found to increase at a linear rate with increasing significant wave heights; however, insufficient periods of high (Hs > 0.2 m) wave activity were recorded, for a

complete analysis. When a large number of measurements were available during periods of low wave activity, it permitted an investigation to be undertaken into the effect of varying tidal current speeds, on the SSC. The SSC was found to increase exponentially, with an increase in tidal current speed.

The wave conditions in The Wash show a seasonal trend. Peak wave heights occur during the winter, isolated periods of high wave activity during autumn and spring, and low wave activity during summer. The rates of erosion/accretion over the intertidal flats do not appear to follow the same seasonal trend as the wave conditions. As such, wave conditions alone do not control the levels of erosion/accretion over the intertidal flats; other factors are important, such as the prevailing tidal conditions, which affects the stability of the sediment surface.

With only minimal wave attenuation over the mudflats and sandflats, the majority of the attenuation of wave activity occurred over the saltmarsh. The saltmarsh vegetation attenuates the wave energy, whilst the presence of only small waves and low velocity tidal currents cause the saltmarsh to accrete. The ability of saltmarsh vegetation to attenuate wave activity, to such an extent, emphasises that the process of managed realignment is a realistic form of sustainable coastal management. The landward realignment of a seawall creates a new intertidal area, and, when this is vegetated, it enhances coastal protection by dissipating wave energy. Similarly, such a development encourages deposition, whilst permitting the landward retreat of the intertidal flats, in response to a rising sea-level.

Creeks within a developing system over an intertidal zone were found to behave in a similar way to saltmarsh creeks (Ward, 1981; French and Clifford, 1992; and Allen, 2000b); they supply water and sediment to the adjacent intertidal zone during the flood, removing it during the ebb tide. The differences between these creeks and those within saltmarshes, are that they flood their banks during every tidal cycle, acting as net exporters of sediment. The reason for this pattern may be associated with the fact that there is overbank flooding during every tide, which creates large amounts of turbulence; in comparison, underbank tides create little disturbance (Bayliss-Smith et al., 1979; and Healey et al., 1981). The low levels of disturbance caused by underbank tides allows sediment to be deposited on the banks and the bed of the creeks; on overbank tides, erosion and transport of bed material occurs, as the emptying of the intertidal zone causes higher velocities in shallow water depths (Allen, 2000b). Erosion caused by the draining of the intertidal zone will be greater over the intertidal flats compared to the saltmarsh, as there is no halophytic vegetation to provide stabilisation of the bed.

10.1.2 *Instrumentation*

The use of RTK-GPS was very effective in tracking the development of both creek systems and the channel lying within the breach in the embankment. This method provided a relatively cheap and effective way of surveying large areas of intertidal flat, rapidly and accurately. The method is diverse, in that it can be utilised to measure a wide range and scale of formations, at varying resolutions. For the purpose of the present study, the RTK-GPS was used to: (a) track the development of a creek system; (b) monitor the change in elevation of the thalwegs, together with the measurement of a transect across the creeks; and (c) to study the cross-sectional changes. Each set of these measurements was undertaken within approximately 2 to 3 hours, as the area surveyed (near low water mark) was exposed only for a short period of time, during each tide. In addition, the backpack position and logging device, which collected the data, was not cumbersome; this permitted measurements over the intertidal flats to be obtained relatively easily. Finally, the base station could be set up rapidly and, following set up, was left to communicate the positional corrections to the backpack position devices; the devices were able to communicate up to a distance of ~ 5 km apart; this was adequate for surveys of wide intertidal flats, such as those at Freiston Shore.

10.2 CONCLUSIONS

The main conclusions resulting from this study are summarised below; they have been separated into two sections, relating to the nature of the findings. Firstly, conclusions relating to the MR will be outlined. Secondly, the findings associated with the understanding of sediment dynamic conditions over the intertidal flats of The Wash are described.

10.2.1 *Managed Realignment*

1) In terms of coastal protection, the MR scheme at Freiston Shore has been successful. The site was colonised by halophytic vegetation, increased its elevation by the accretion of sediment and now experiences low wave activity. It has provided a sustainable form of coastal protection, mimicking the natural response to sea-level rise and, thus, reducing "coastal squeeze".
2) High rates of erosion were experienced as a result of the MR: in the channels within the breaches in the embankment; and with a creek system over the intertidal zone expanding rapidly.
3) Erosion occurred because the area of the MR site adjacent to the breached embankment was 0.5 to 1 m lower than the saltmarsh, on the seaward side of the embankment.
4) The most rapid period of erosion of the channels, within the breaches, was during the initial few months following the breaching of the embankment. After this period, the

channels continued to erode; this is predicted to continue for around 5 years after the breaching.

5) Some 2 years following the breaching of the embankment, the 3 channels in the breaches and the natural creeks (to which they were connected), had grown to the extent that the MR site was drained at the same time as the saltmarsh; as such, the natural creeks could contain all the water flowing out of the MR site.
6) Application of the Regime Theory has allowed predictions to be made of the eventual channel width and hydraulic depth. This method is useful for the prediction of the width necessary, tending towards stability, for future breaches in embankments.
7) The rate of headward extension of the creeks, over the intertidal flats, was 20 times higher following the establishment of the MR, than it had been under previous 'natural' conditions.
8) The enhanced development of the creek system over the intertidal flats was related directly to drainage of the MR site. Water draining the MR site overflowed the natural creeks; as such, it flowed over the intertidal flats as sheetflow, causing the enhanced development of the creek system.
9) The enhanced development of a creek system, over intertidal mudflats and sandflats, occurs through headward extension of creeks and the elaboration of the creek system, through the addition of tributaries.
10) When sheetflow over the intertidal flats ceased, owing to the enlargement of the natural creeks to a size capable of containing all the flow from the drainage of the MR site, some 2 years after its creation, the creek system rapidly silted up.
11) The quantity of sediment removed initially during the rapid development of the creeks was, in terms of volume, approximately equal to that which was ultimately deposited in the creeks.
12) The intertidal flats are in a dynamic equilibrium, changing when there is a modification to the controlling system; then reverting back, when the system changes to its original form.
13) Creeks over the intertidal flats act in a similar way to saltmarsh creeks, supplying and removing water and sediment to the adjacent intertidal zone. The main difference identified was that the creeks over the intertidal flats acted as exporters of sediment, whereas the saltmarsh creeks act as importers.
14) Note: The RTK-GPS was a very successful method to study a rapidly developing creek system, over a wide intertidal zone; as such, it should be considered in any similar future studies.

10.2.2 *Intertidal Flats*

1) There have been no significant changes in the hydrodynamic conditions over the intertidal flats, since the previous studies, which commenced in 1973.
2) Despite the prevailing hydrodynamic conditions indicating an accretional environment, the intertidal flats have been predominantly eroding, with only the lower intertidal flats and the saltmarsh experiencing net accretion. The reason for this erosion is unknown, but it may be associated with a natural cycle of erosion/accretion; or, it is related most probably to the MR site and the development of the creek system, changing the dynamic equilibrium of the intertidal flats.
3) The creation of an embankment as part of a land reclamation scheme, caused originally an increase in the tidal current speeds, this, in turn, led to enhanced erosion over the intertidal flats. However, breaching of the embankment, as part of the MR scheme, did not affect the tidal current speeds over the adjacent intertidal flats; however, it may have increased the rates of erosion over the intertidal flats.
4) SSC increased exponentially, with an increase in tidal current speed. This pattern was more marked over the lower, rather than the upper, intertidal zone.
5) As the significant wave height increased, the SSC increased with a roughly linear correlation. A significant wave height of 0.15 m was found to be necessary to enhance the SSC.
6) Bedload transport was greater in the longshore than the cross-shore direction, with transport to the SW dominating, i.e. landward into The Wash embayment.
7) Bedload transport predictions were sensitive to the water depth of the measurements: much higher bedload transport rates were predicted in shallow water (0.5 m) than deeper water (1 m).
8) The majority of the sediment transport (bedload and suspended load), occurred in periods of shallow water, i.e. during the first phase flood and last phase ebb of the tide.
9) The wave climate in The Wash is seasonal, with the peak in wave activity during the winter, the lowest wave activity in the summer and variable wave conditions during spring and autumn.
10) Wave conditions do not control the rates of bed level change over the intertidal flats, but factors such as the tidal conditions and biological processes are important.
11) The majority of the wave energy is attenuated over the saltmarsh, with the mudflats and sandflats not dissipating the wave conditions significantly.

10.3 RECOMMENDATIONS

10.3.1 *Future Research*

Monitoring should continue at Freiston Shore as, 3 years after the breaching of the embankment, some changes related to the MR site are still occurring. The channels within the breaches are still eroding; as such, it will be useful to measure the total extent of their change and to see how long it takes for a dynamic equilibrium to be reached, e.g. if the prediction of 5 years was accurate. The creek system over the mid- to lower intertidal zone is silting up rapidly; it would be interesting to see how it continues to develop.

More MR sites require detailed monitoring, both prior to and following the initiation of a MR; any impacts can be identified and the reasons for them recognised. This is essential if MR is to be used as a common form of sustainable coastal management, in the future. Important impacts have been found to be a result of MRs, but if this method is to be used regularly, all of the possible impacts need to be recognised. This approach will help in deciding on suitable MR sites, making scheme designers aware of any potential problems.

The prediction of the width and shape of channels, within breaches, for MRs is important; if the channel is too small then rapid erosion may be experienced. Unnecessary expense will be incurred, if the channel is too large. The Inglis and Allen (1957) method, investigated here, should be used at other sites, to see if the method is capable of predicting the channel width accurately. The Cao and Knight (1997) method should be used to predict the channel shape.

To fully understand the interaction between the creeks and the intertidal flats, the very first phase of the flood and last phase of the ebb need to be recorded, as the instruments used in the present study could only sample in a water depth greater than 0.4 m. It is important to measure more periods of high wave activity over the intertidal flats at Freiston Shore, to establish the influence of waves on the suspended sediment and bedload transport.

10.3.2 *Future Managed Realignments*

When considering applicable sites for future MRs, the most important consideration, based on the findings of this study, is that the proposed MR site acts a continuation of the slope of the intertidal zone (or is, at least, at the same elevation as the saltmarsh). This should prevent the erosion that was experienced over the intertidal zone at Freiston Shore, in the form of creek development. In addition, if the channels within the breaches are constructed to a sufficient size (according to the Inglis and Allen (1957) and Cao and Knight (1997) methods), erosion rates in these channels should be maintained as low.

In most cases, if the proposed MR site was reclaimed more than a few years previously, the site will have been drained and the sediment consolidated (in response to material settling, dewatering and agricultural practices); hence, the site will be at a lower elevation, than the adjacent saltmarsh. If this is the case and it is still considered that a MR would be a suitable form of coastal management, then two options area available to attempt to reduce impacts to an area.

(i) Ensure the channels within the breaches are of sufficient size to accommodate the volumes of water flowing into and out of the MR site. Similarly, be aware that erosion is likely to ensue in the natural creeks connected to these channels and over the intertidal flats.

(ii) Create breaches within the embankment, but not excavate any associated artificial channels; this allows the site to flood, but minimises the drainage of the MR site over the intertidal flats. This approach should ensure that the site gradually accumulates sediment, but will act as a lagoon until it has accreted to a sufficient elevation. This method should prevent dramatic erosion in any natural creeks and over the adjacent intertidal flats, although it may take a long time for the site to become a stable saltmarsh.

REFERENCES

ABP Research & Consultancy Ltd. 1998. Review of coastal habitat creation, restoration and recharge schemes. R.909, Southampton. 190 pp.

Ackers, P. and White, W.R. 1973. Sediment transport: a new approach and analysis. *Proc. ASCE*, 99: 2041-60.

Adams Jr., C.E., Wells, J.T. and Park, Y.-A. 1990. Internal hydraulics of a sediment-stratified channel flow. *Marine Geology*, 95: 131-145.

Addison, J. 2005. Temporal variations in the mechanisms controlling the sediment supplied to the intertidal flats of The Wash. *3rd Year Dissertation*, University of Southampton, 59 pp.

Allen, J.R.L. 1977. Changeable rivers: Some aspects of their mechanics and sedimentation. In: *River Channel Changes* (Ed K.J. Gregory), John Wiley & Sons, Chichester. pp. 15-45.

Allen, J.R.L. 1990. Salt marsh growth and stratification: a numerical model with special reference to the Severn Estuary, southwest Britain. *Marine Geology*, 95: 77-96.

Allen, J.R.L. 1991. Salt marsh accretion and sea-level movement in the inner Severn Estuary: the archaeological and historical contribution. *Journal of the Geological Society*, 148: 485-494.

Allen, J.R.L. 1992. Tidally influenced marshes in the Severn Estuary, southwest Britain. In: *Saltmarshes: Morphodynamics, Conservation and Engineering Significance* (Eds J.R.L. Allen and K. Pye), Cambridge University Press, Cambridge. pp. 123-147.

Allen, J.R.L. 1997. Simulation models of salt marsh morphodynamics: some implications for high-intertidal sediment couplets related to sea-level change. *Sedimentary Geology*, 113: 211-223.

Allen, J.R.L. 2000a. Historical set-back on saltmarshes in the Severn Estuary, SW Britain. In: *British Saltmarshes* (Eds B.R. Sherwood, B.G. Gardiner and T. Harris), Forrest Text, Ceredigion. pp. 397-417.

Allen, J.R.L. 2000b. Morphodynamics of Holocene salt marshes: a review sketch from the Atlantic and Southern North Sea coasts of Europe. *Quaternary Science Reviews*, 19: 1155-1231.

Allen, J.R.L. and Pye, K. 1992. Coastal saltmarshes: their nature and importance. In: *Saltmarshes: Morphodynamics, Conservation and Engineering Significance* (Eds J.R.L. Allen and K. Pye), Cambridge University Press, Cambridge. pp. 1-18.

Alsop, W., Swash, A., Richardson, D. and Collins, T. 2004. Case Studies: soft engineering techniques for high and low energy coasts. 6 pp.

Amos, C.L. 1974. Inter-tidal flat sedimentation of the Wash, E. England. *PhD Thesis*, Imperial College of Science and Technology, London. 441 pp.

Amos, C.L. 1995. Siliclastic tidal flats. In: *Geomorphology and Sedimentology of Estuaries. Developments in Sedimentology, 53* (Ed G.M.E. Perillo), Elsevier Science, Amsterdam. pp. 273-306.

Amos, C.L. and Collins, M.B. 1978. The combined effects of wave motion and tidal currents on the morphology of intertidal ripple marks: The Wash. U.K. *Journal of Sedimentary Petrology*, 48: 849-856.

Amos, C.L. and Mosher, D.C. 1985. Erosion and deposition of fine-grained sediments from the Bay of Fundy. *Sedimentology*, 32: 815-832.

Amos, C.L., Van Wagoner, N.A. and Daborn, G.R. 1988. The influence of subaerial exposure on the bulk properties of fine-grained intertidal sediment from Monas Basin, Bay of Fundy. *Estuarine, Coastal and Shelf Science*, 27: 1-13.

Anderson, F.E. 1972. Resuspension of estuarine sediments by small amplitude waves. *Journal of Sedimentary Petrology*, 42: 602-607.

Anderson, F.E. 1973. Observations of some sedimentary processes acting on a tidal flat. *Marine Geology*, 14: 101-116.

Andersen, T.J., Mikkelsen, O.A., Moller, A.L. and Pejrup, M. 2000. Deposition and mixing depths on some European intertidal mudflats based on ^{210}Pb and ^{137}Cs activities. *Continental Shelf Research*, 20: 1569-1591.

Ayles, C.P. and Lapointe, M.F. 1996. Downvalley gradients in flow patterns, sediment transport and channel morphology in a small macrotidal estuary: Dipper Harbour Creek, New Brunswick, Canada. *Earth Surface Processes and Landforms*, 21: 829-842.

Bassoullet, P., Le Hir, P., Gouleau, D. and Robert, S. 2000. Sediment transport over an intertidal mudflat: field investigations and estimation of fluxes within the "Baie de Marennes-Oleron" (France). *Continental Shelf Research*, 20: 1635-1653.

Bayliss-Smith, T.P., Healey, R., Lailey, R., Spencer, T. and Stoddart, D.R. 1979. Tidal flows in salt marsh creeks. *Estuarine and Coastal Marine Science*, 9: 235-255.

Blackwell, M.S.A., Hogan, D.V. and Maltby, E. 2004. The short-term impact of managed realignment on soil environmental variables and hydrology. *Estuarine, Coastal and Shelf Science*, 59: 687-701.

Blanchard, G.F., Paterson, D.M., Stal, L.J., Richard, P., Galois, R., Huet, V., Kelly, J., Honeywill, C., de Brouwer, J., Dyer, K., Christie, M. and Seguignes, M. 2000. The effect of geomorphological structures on potential biostabilisation by microphytobenthos on intertidal mudflats. *Continental Shelf Research*, 20: 1243-1256.

Boon, J.D. 1975. Tidal discharge asymmetry in a salt marsh drainage system. *Limnology and Oceanography*, 20: 71-80.

Boorman, L.A., Garbutt, A. and Barratt, D. 1998. The role of vegetation in determining patterns of the accretion of salt marsh sediment. In: *Sedimentary Processes in the Intertidal Zone* (Eds K.S. Black, D.M. Paterson and A. Cramp), Geological Society Special Publication 139, London. pp. 389-399.

Brampton, A.H. 1992. Engineering significance of British saltmarshes. In: *Saltmarshes: Morphodynamics, Conservation and Engineering significance* (Eds J.R.L. Allen and K. Pye), Cambridge University Press, Cambridge. pp. 115-122.

Brew, D.S. and Williams, A. 2002. Shoreline movement and shoreline management in The Wash, eastern England. *Littoral*, 2002: 313-320.

Brookes, A. 1996. River channel change. In: *River Channel Restoration: Guiding Principles for Sustainable Projects* (Eds A. Brookes and F.D. Shields), John Wiley & Sons, Chichester. pp. 221-242.

Brown, S.L. 1998. Sedimentation on a Humber saltmarsh. In: *Sedimentary Processes in the Intertidal Zone* (Eds K.S. Black, D.M. Paterson and A. Cramp), Geological Society Special Publication 139, London. pp. 69-83.

Buller, A.T. and McManus, J. 1979. Sediment sampling and analysis. In: *Estuarine hydrography and sedimentation* (Ed K.R. Dyer), Cambridge University Press, Cambridge. pp. 87-130.

Burd, F., Clifton, J. and Murphy, B. 1994. Sites of historical sea defence failure: phase II study, Institute of Estuarine and Coastal Studies, University of Hull, Hull, Report No. ZO38-94-F, 100 pp.

Cahoon, D.R., French, J.R., Spencer, T., Reed, D.J. and Moller, I. 2000. Vertical accretion versus elevational adjustment in UK saltmarshes: and evaluation of alternative methodologies. In: *Coastal and Estuarine Environments: sedimentology, geomorphology and geoarchaeology* (Eds K. Pye and J.R.L. Allen), Geological Society Special Publication 175, London. pp. 223-238.

Cao, S. and Knight, D.W. 1997. Entropy-based design approach of threshold alluvial channels. *Journal of Hydraulic Research, IAHR*, 35: 505-524.

Carling, P.A. 1978. The influence of creek systems on intertidal flat sedimentation. *PhD Thesis*, University College of Swansea, Swansea, 288 pp.

Carling, P.A. 1982. Temporal and spatial variation in intertidal sedimenation rates. *Sedimentology*, 29: 17-23.

Carling, P.A. 1996. In-stream hydraulics and sediment transport. In: *River flows and channel forms* (Eds G.E. Petts and P. Calow), Blackwell Science, Oxford. pp. 160-184.

Chang, H.H. 1985. River morphology and thresholds. *Journal of Hydraulic Engineering, Proceedings of the American Society of Civil Engineers*, 111: 503-519.

Chang, S.-C. and Evans, G. 1992. Source of sediment and sediment transport on the east coast of England: significant or coincidental phenomena? *Marine Geology*, 107: 283-288.

Chang, Y.-H., Scrimshaw, M.D., MacLeod, C.L. and Lester, J.N. 2001. Flood defence in the Blackwater Estuary, Essex, UK: the impact of sedimentological and geochemical changes on salt marsh development in the Tollesbury managed realignment site. *Marine Pollution Bulletin*, 42: 469-480.

Cheng, Y.-F. 2004. Examination of potential sites for a managed realignment scheme in the Western Solent. *MSc Thesis*, Southampton University, Southampton, 82 pp.

Christiansen, T., Wiberg, P.L. and Milligan, T.G. 2000. Flow and sediment transport on a tidal salt marsh surface. *Estuarine, Coastal and Shelf Science*, 50: 315-331.

Christie, M.C. and Dyer, K.R. 1998. Measurements of the turbid tidal edge over the Skeffling mudflats. In: *Sedimentary Processes in the Intertidal Zone* (Eds K.S. Black, D.M. Paterson and A. Cramp), Geological Society Special Publication 139, London. pp. 45-55.

Christie, M.C., Dyer, K.R., Blanchard, G., Cramp, A., Mitchener, H.J. and Paterson, D.M. 2000. Temporal and spatial distributions of moisture and organic contents across a macro-tidal mudflat. *Continental Shelf Research*, 20: 1219-1241.

Collins, M.B. 1976. Suspended sediment sampling towers as used on the intertidal flats of The Wash, eastern England. *Estuarine and Coastal Marine Science*, 4: 46-57.

Collins, M.B. and Amos, C.L. 1975. Written contribution to: The transportation and deposition of suspended sediment over the intertidal flats of the Wash. In: *Nearshore Sediment Dynamics and Sedimentation* (Ed J. Hails and A. Carr), John Wiley & Sons, London. pp. 304-306.

Collins, M.B., Amos, C.L. and Evans, G. 1981. Observations of some sediment-transport processes over intertidal flats, The Wash, UK. *Special Publication International Association Sedimentologists*, 5: 81-98.

Collins, M.B., Ke, X. and Gao, S. 1998. Tidally-induced flow structure over intertidal flats. *Estuarine, Coastal and Shelf Science*, 46: 233-250.

Cooper, N.J. 2005. Wave dissipation across intertidal surfaces in the Wash tidal inlet, Eastern England. *Journal of Coastal Research*, 21: 28-40.

Crooks, S. and Pye, K. 2000. Sedimentological controls on the erosion and morphology of saltmarshes: implications for flood defence and habitat recreation. In: *Coastal and Estuarine Environments; sedimentology, geomorphology and geoarchaeology* (Eds K. Pye and J.R.L. Allen), Geological Society Special Publication 175, London. pp. 207-222.

Cundy, A.B., Long, A.J., Hill, C.T., Spencer, C. and Croudace, I.W. 2002. Sedimentary response of Pagham Harbour, southern England to barrier breaching in AD 1910. *Geomorphology*, 46: 163-176.

Dail, H.J., Merrifield, M.A. and Bevis, M. 2000. Steep beach morphology changes due to energetic wave forcing. *Marine Geology*, 162: 443-458.

Darby, H.C. 1940. The drainage of the Fens. Cambridge University Press, London, 312 pp.

Davey, J.T. and Partridge, V.A. 1998. The macrofaunal communities of the Skeffling muds (Humber Estuary), with special reference to bioturbation. In: *Sedimentary processes in the intertidal zone* (Eds K.S. Black, D.M. Paterson and A. Cramp), Geological Society Special Publication 139, London. pp. 115-124.

Davy, A.J., Costa, C.S.B., Yallop, A.R., Proudfoot, A.M. and Mohamed, M.F. 2000. Biotic interactions in plant communities of saltmarshes. In: *British Saltmarshes* (Eds B.R. Sherwood, B.G. Gardiner and T. Harris), Forrest Text, Ceredigion. pp. 109-127.

Davidson-Arnott, R.G.D., van Proosdij, D., Ollerhead, J. and Schostak, L. 2002. Hydrodynamics and sedimentation in salt marshes: examples from a macrotidal marsh, Bay of Fundy. *Geomorphology*, 48: 209-231.

de Brouwer, J.F.C., Bjelic, S., de Deckere, E.M.G.T. and Stal, L.J. 2000. Interplay between biology and sedimentology in a mudflat (Biezelingse Ham, Westerschelde, The Netherlands). *Continental Shelf Research*, 20: 1159-1177.

Dearnaley, M.P., Waller, M.N.H., Spearman, J.R. and Dennis, J.M. 1994. Estuary regime, HR Wallingford, Wallingford. 32 pp.

Decho, A.W. 2000. Microbial biofilms in intertidal systems: an overview. *Continental Shelf Research*, 20: 1257-1273.

Dijkema, K.S. 1987. Geography of salt marshes in Europe. *Zeitschrift fur Geomorphologie*, 31: 489-499.

Doody, J.P. 1992. The conservation of British saltmarshes. In: *Saltmarshes: Morphodynamics, Conservation and Engineering Significance* (Eds J.R.L. Allen and K. Pye), Cambridge University Press, Cambridge. pp. 80-114.

Doody, P. and Barnett, B. 1987. The Wash and its environment. In: *The Wash and its environment*, 7, Nature Conservancy Council, Horncastle, Lincolnshire. 32. pp.

Duckworth, H. 2005. Erosion/accretion rates over and intertidal zone: The Wash, U.K. *3rd Year Dissertation*, University of Southampton. 59 pp.

Dugdale, R., Plater, A. and Albanakis, K. 1987. The fluvial and marine contribution to the sediment budget of The Wash. In: *The Wash and its environments* (Eds P. Doody and B. Barnett), Nature Conservancy Council, Peterborough. pp. 37-47.

Dyer, K. 1986. Coastal and estuarine sediment dynamics. John Wiley & Sons, Chichester, 342 pp.

Dyer, K.R. 1998. The typology of intertidal mudflats. In: *Sedimentary Processes in the Intertidal Zone* (Eds K.S. Black, D.M. Paterson and A. Cramp), Geological Society Special Publication 139, London. pp. 11-24.

Dyer, K.R., Christie, M.C. and Wright, E.W. 2000. The classification of intertidal mudflats. *Continental Shelf Research*, 20: 1039-1060.

Eisma, D. 1981. Supply and deposition of suspended matter in the North Sea. *Special Publication International Association of Sedimentologists*, 5: 415-428.

Eisma, D., de Boer, P.L., Cadee, G.C., Dijkema, K., Ridderinkhof, H. and Philippart, C. 1998. Intertidal deposits: river mouths, tidal flats, and coastal lagoons. CRC Press LLC, Florida. 524 pp.

Elliott, T. 1986. Siliclastic shorelines. In: *Sedimentary Environments and Facies* (Ed H.G. Reading), Blackwell Scientific Publications, Oxford. pp. 155-188.

Environment Agency. 2000. Anglian region: Shoreline monitoring data catalogue, Environment Agency, Peterborough. 13 pp.

Evans, G. 1959. The development of the coastline of the Wash, England. *Proceedings of the 2nd Coastal Geography Conference*, Coastal Studies Institute, Louisiana State University, Baton Rouge, 265-283.

Evans, G. 1965. Intertidal flat sediments and their environments of deposition in The Wash. *Quarterly Journal of the Geological Society of London*, 121: 209-245.

Evans, G. 1975. Intertidal flat deposits of The Wash, western margin of the North Sea. In: *Tidal Deposits* (Ed R.N. Ginsburg), Springer-Verlag, New York. pp. 13-20.

Evans, G. and Collins, M.B. 1975. The transportation and deposition of suspended sediment over the intertidal flats of The Wash. In: *Nearshore Sediment Dynamics and Sedimentation* (Eds J. Hails and A. Carr), John Wiley & Sons, Chichester. pp. 273-304.

Evans, G. and Collins, M.B. 1987. Sediment supply and deposition in The Wash. In: *The Wash and its environment* (Eds P. Doody and B. Barnett), 7, Nature Conservancy Council, Peterborough. pp. 48-63.

Folk, R.L. 1974. *Petrology of sedimentary rocks*. Hemphill Publishing Co., Austin, 182 pp.

Fonseca, M.S. 1996. The role of seagrass in nearshore sedimentary processes: a review. In: *Estuarine Shores: Evolution, Environments and Human Alterations* (Eds K.F. Nordstrom and C.T. Roman), John Wiley & Sons, Chichester. pp. 261-286.

French, C.E., French, J.R., Clifford, N.J. and Watson, C.J. 2000. Sedimentation-erosion dynamics of abandoned reclamations: the role of waves and tides. *Continental Shelf Research*, 20: 1711-1733.

French, J.R. 1993. Numerical simulation of vertical marsh growth and adjustment to accelerated sea-level rise, North Norfolk, UK. *Earth Surface Processes and Landforms*, 18: 63-81.

French, J.R. and Clifford, N.J. 1992. Characteristics and "event-structure" of near-bed turbulence in a macrotidal saltmarsh channel. *Estuarine, Coastal and Shelf Science*, 34: 49-69.

French, J.R. and Stoddart, D.R. 1992. Hydrodynamics of salt marsh creek systems: implications for marsh morphodynamic development and matter exchange. *Earth Surface Processes and Landforms*, 17: 235-252.

French, J.R. and Spencer, T. 1993. Dynamics of sedimentation in a tide-dominated backbarrier salt marsh, Norfolk, UK. *Marine Geology*, 110: 315-331.

French, J.R., Spencer, T., Murray, A.L. and Arnold, N.S. 1995. Geostatistical analysis of sediment deposition in 2 small tidal wetlands, Norfolk, UK. *Journal of Coastal Research*, 11: 308-321.

French, P.W. 1999. Managed retreat: a natural analogue from the Medway estuary, UK. *Ocean and Coastal Management*, 42: 49-62.

French, P.W. 2001. Coastal defences: processes, problems and solutions. Routledge, London, 366 pp.

Friend, P.L., Collins, M.B. and Holligan, P.M. 2003. Day-night variation of intertidal flat sediment properties in relation to sediment stability. *Estuarine, Coastal and Shelf Science*, 58: 663-675.

Friend, P.L., Lucas, C.H. and Rossington, S.K. 2005. Day-night variation of cohesive sediment stability. *Estuarine, Coastal and Shelf Science*, 64: 407-418.

Galehouse, J.S. 1971. Sedimentation analysis. In: *Procedures in sedimentary petrology* (Ed R.E. Carver), Wiley - Interscience, New York. pp. 69-92.

Gao, S. and Collins, M.B. 1994. Tidal inlet equilibrium, in relation to cross-sectional area and sediment transport patterns. *Estuarine, Coastal and Shelf Science*, 38: 157-172.

Gao, S. and Collins, M.B. 1995. On the physical aspects of the 'design with nature' principle in coastal management. *Ocean and Coastal Management*, 26 (2): 163-175.

Gao, S. and Collins, M.B. 1997. Changes in sediment transport directions in response to wave action and tidal flood tide asymmetry in an estuary. *Journal of Coastal Research*, 13: 198-201.

Gardline Surveys. 2003. Washbanks wave and tide data: interim report (6), operations and data review, September 6th 2002 to March 10th 2003, tide and wave measurements. 16 pp.

Glock, W.S. 1931. The development of drainage systems: a synoptic view. *Geographical Review*, 21: 475-482.

Gordon, D.C., Cranford, P.J. and Desplanque, C. 1985. Observations on the ecological importance of salt marshes in the Cumberland Basin, a macrotidal estuary in the Bay of Fundy. *Estuarine, Coastal and Shelf Science*, 20: 205-227.

Graf, W.H. 1971. Hydraulics of sediment transport. McGraw - Hill Series in water resources and environmental engineering, USA, 513 pp.

Halcrow U.K. 1999. Wash banks: Hobhole to Butterwick Low; hydrodynamic, geomorphic and environmental assessment, Halcrow Group Ltd, Lincoln. 27 pp.

Halcrow U.K. 2001. Wash banks flood defence scheme; monitoring report, Halcrow Group Ltd, Peterborough. 41 pp.

Harris, T. 2000. The habitat preferences of *Scrobicularia plana* (da Costa), (Lamellibranchia: Tellinacea), within the saltmarsh of the River Otter estuary at Budleigh Salterton, Devon, UK. In: *British Saltmarshes* (Eds B.R. Sherwood, B.G. Gardiner and T. Harris), Forrest Text, Ceredigion. pp. 155-164.

Harvey, A.M. 1977. Event frequency in sediment production and channel change. In: *River Channel Change* (Ed K.J. Gregory), John Wiley & Sons, Chichester. pp. 301-315.

Haxel, J.H. and Holman, R.A. 2004. The sediment response of a dissipative beach to variations in wave climate. *Marine Geology*, 206: 73-99.

Hazelden, J. and Boorman, L.A. 1999. The role of soil and vegetation processes in the control of organic and mineral fluxes in some western European salt marshes. *Journal of Coastal Research*, 15: 15-31.

Healey, R.G., Pye, K., Stoddart, D.R. and Bayliss-Smith, T.P. 1981. Velocity variations in salt marsh creeks, Norfolk, England. *Estuarine, Coastal and Shelf Science*, 13: 535-545.

Heathershaw, A.D. 1981. Comparisons of measured and predicted sediment transport rates in tidal currents. *Marine Geology*, 42: 75-104.

Hemminga, M.A., Cattrijsse, A. and Wielemaker, A. 1996. Bedload and nearbed detritus transport in a tidal saltmarsh creek. *Estuarine, Coastal and Shelf Science*, 42: 55-62.

Hooke, J.M. 1977. The distribution and nature of changes in river channel patterns: the example of Devon. In: *River Channel Changes* (Ed K.J. Gregory), John Wiley & Sons, Chichester. pp. 265-280.

Hooke, J.M. 1997. Styles of channel change. In: *Applied Fluvial Geomorphology for River Engineering and Management* (Eds C.R. Thorne, R.D. Hey and M.D. Newson), John Wiley & Sons, Chichester. pp. 237-268.

Horton, R.E. 1945. Erosional development of streams and their drainage basins: hydrophysical approach to quantitative morphology. *Bulletin of the Geological Society of America*, 56: 275-370.

Hoekstra, P., Bell, P., van Santen, P., Roode, N., Levoy, F. and Whitehouse, R. 2004. Bedform migration and bedload transport on an intertidal shoal. *Continental Shelf Research*, 24: 1249-1269.

HR Wallingford, CEFAS/UEA, Posford Haskoning and D'Olier, B. 2002. Southern North Sea sediment transport study, phase 2. EX 4526, HR Wallingford, Oxford. 146 pp.

HR Wallingford, ABPmer and Pethick, J. in press. Review and formalisation of geomorphological concepts and approaches for estuaries. FD2116/TR2, Lincoln. pp. 89-141

Hydraulics Research Station. 1972. The Wash water storage scheme field studies, part one: data collected in 1971. Ex601.

Hydraulics Research Station. 1974a. The Wash water storage scheme field studies: part three: data collected in 1972. DE15.

Hydraulics Research Station. 1974b. The Wash water storage scheme: numerical model studies of The Wash. DE17.

Hydraulics Research Station. 1975. The Wash water storage scheme: the distribution of surface sediments in the South East Wash and the influence of waves. DE24.

Inglis, C.C. and Kestner, F.J.T. 1958. The long-term effects of training walls, reclamation and dredging on estuaries. *Proceedings of the institute of Civil Engineers*, 9: 193-215.

Inglis, C.C. and Allen, F.H. 1957. The regimen of the Thames Estuary as affected by currents, salinities and river flow. *Proceedings of Civil Engineering Division Meeting*, 7: 827.

Jacobson, H.A. 1988. Historical development of the salt marsh at Wells, Maine. *Earth Surface Processes and Landforms*, 13: 475-486.

Janssen-Stelder, B. 2000. The effect of different hydrodynamic conditions on the morphodynamics of a tidal mudflat in the Dutch Wadden Sea. *Continental Shelf Research*, 20: 1461-1478.

Jefferies, R.L., Davy, A.J. and Rudmik, T. 1981. Population biology of the salt marsh annual *Salicornia europaea* agg. *Journal of Ecology*, 69: 17-31.

Ke, X. 1995. Sediment dynamics of saltmarshes and intertidal flats, southern and eastern England. *PhD Thesis*, University of Southampton, Southampton, 342 pp.

Ke, X., Collins, M.B. and Poulos, S. 1994. Velocity structures and sea bed roughness associated with intertidal (sand and mud) flats and saltmarshes of the Wash, UK. *Journal of Coastal Research*, 10: 702-715.

Ke, X., Evans, G. and Collins, M.B. 1996. Hydrodynamics and sediment dynamics of the Wash embayment, Eastern England. *Sedimentology*, 43: 157-174.

Ke, X. and Collins, M.B. 2000. Tidal characteristics of an accretional tidal flat (The Wash, U.K.). In: *Muddy Coast Dynamics and Resource Management* (Ed B.W. Flemming), Elsevier Science, Amsterdam. pp. 13-38.

Kelley, J.T., Gehrels, W.R. and Belknap, D.F. 1995. Late Holocene sea-level rise and the geological development of tidal marshes at Wells, Maine, U.S.A. *Journal of Coastal Research*, 11: 136-153.

Kestner, F.J.T. 1975. The loose-boundary regime of the Wash. *The Geographical Journal*, 141: 388-410.

Kirby, R. 1987. Sediment exchanges across the coastal margins of NW Europe. *Journal of Geological Society*, 144: 121-126.

Kirby, R. 2000. Practical implications of tidal flat shape. *Continental Shelf Research*, 20: 1061-1077.

Kirby, R., Bleakley, R.J., Weatherup, S.T.C., Raven, P.J. and Donaldson, N.D. 1993. Effect of episodic events on tidal mud flat stability, Ardmillan Bay, Strangford Lough, Northern Ireland. In: *Nearshore and estuarine cohesive sediment transport* (Ed A.J. Mehta), American Geophysical Union, Washington DC. pp. 378-392.

Knighton, A.D., Woodroffe, C.D. and Mills, K. 1992. The evolution of tidal creek networks, Mary River, northern Australia. *Earth Surface Processes and Landforms*, 17: 167-190.

Kornman, B.A. and De Deckere, E.M.G.T. 1998. Temporal variation in sediment erodibility and suspended sediment dynamics in the Dollard estuary. In: *Sedimentary processes in the intertidal zone* (Eds K.S. Black, D.M. Paterson and A. Cramp), Geological Society Special Publication 139, London. pp. 231-241.

Lawrence, D.S.L., Allen, J.R.L. and Havelock, G.M. 2004. Salt marsh morphodynamics: an investigation of tidal flows and marsh channel equilibrium. *Journal of Coastal Research*, 20: 301-316.

Le Hir, P., Roberts, W., Cazaillet, O., Christie, M., Bassoullet, P. and Bacher, C. 2000. Characterisation of intertidal flat hydrodynamics. *Continental Shelf Research*, 20: 1433-1459.

Lees, B.J. 1983. The relationship of sediment transport rates and paths to sandbanks in a tidally dominated area off the coast of East Anglia, UK. *Sedimentology*, 30: 461-483.

Leonard, L.A., Hine, A.C. and Luther, M.E. 1995. Surficial sediment transport and deposition processes in *Juncus roemerianus* marsh, west-central Florida. *Journal of Coastal Research*, 11: 322-336.

Leopold, L.B. 1973. River channel changes with time - an example. *Geological Society of America Bulletin*, 84: 1845-1860.

Leopold, L.B., Wolman, M.G. and Miller, J.P. 1964. Fluvial processes in geomorphology. W.H.Freeman and Co., San Francisco, 522 pp.

Letsch, S.W. and Frey, R.W. 1980. Deposition and erosion in a Holocene salt marsh, Sapelo Island, Georgia. *Journal of Sedimentary Petrology*, 50: 529-542.

Luternauer, J.L., Atkins, R.J., Moody, A.I., Williams, H.F.L. and Gibson, J.W. 1995. Salt marshes. In: *Geomorphology and Sedimentology of Estuaries. Developments in Sedimentology, 53* (Ed G.M.E. Perillo), Elsevier, Amsterdam. pp. 307-332.

Maa, P.-Y. and Mehta, A.J. 1987. Mud erosion by waves: a laboratory study. *Continental Shelf Research*, 7: 1269-1284.

Macleod, C.L., Scrimshaw, M.D., Emmerson, R.H.C., Chang, Y.-H. and Lester, J.N. 1999. Geochemical changes in metal and nutrient loading at Orplands Farm managed retreat site, Essex, UK (April 1995-1997). *Marine Pollution Bulletin*, 38: 1115-1125.

Madsen, O.S. and Grant, W.D. 1976. Quantitative description of sediment transport by waves. In: *15th Coastal Engineering Conference*, 2, ASCE, Honolulu, Hawaii. pp. 1093-1112.

Manning, A.J. 2004. Observations of the properties of flocculated cohesive sediment in three western European estuaries. In: Sediment Transport in European Estuaries (Eds P. Ciavola and M.B. Collins), *Journal of Coastal Research*, SI 41, 70-81.

Martin, Y. and Ham, D. 2005. Testing bedload transport formulae using morphologic transport estimates and field data: lower Fraser River, British Columbia. *Earth Surface Processes and Landforms*, 30(10): 1265-1282.

McCave, I.N. 1971. Wave effectiveness at the sea bed and its relationship to bed-forms and deposition of mud. *Journal of Sedimentary Petrology*, 41: 89-96.

McCave, I.N. 1979. Suspended sediment. In: *Estuarine hydrography and sedimentation* (Ed K.R. Dyer), Cambridge University Press, Cambridge. pp. 131-185.

McCave, I.N. 1987. Fine sediment sources and sinks around the East Anglian coast (UK). *Journal of the Geological Society*, 144: 149-152.

Meadows, A., Meadows, P.S. and McLaughlin, P. 1998a. Spatial heterogeneity in an intertidal sedimentary environment and its macrobenthic community. In: *Sedimentary processes in the intertidal zone* (Eds K.S. Black, D.M. Paterson and A. Cramp), Geological Society Special Publication 139, London. pp. 367-388.

Meadows, P.S., Meadows, A., West, F.J.C., Shand, P.S. and Shaikh, M.A. 1998b. Mussels and mussel beds (*Mytilus edulis*) as stabilisers of sedimentary environments in the intertidal zone. In: *Sedimentary processes in the intertidal zone* (Eds K.S. Black, D.M. Paterson and A. Cramp), Geological Society Special Publication 139, London. pp. 331-347.

Mehta, A.J. and Partheniades, E. 1975. An investigation of the depositional properties of flocculated fine sediments. *Journal of Hydraulic Research*, 12: 361-609.

Mehta, A.J. 1989. On estuarine cohesive sediment suspension behaviour. *Journal of Geophysical Research*, 94 C10: 14303-14314.

Mehta, A.J., Hayter, E.J., Parker, W.R., Krone, R.B. and Teeter, A.M. 1989. Cohesive sediment transport. 1: process description. *Journal of Hydraulic Engineering*, 115: 1076-1093.

Midgley, S. and McGlashan, D.J. 2004. Planning and management of a proposed managed realignment project: Bothkennar, Forth Estuary, Scotland. *Marine Policy*, 28: 429-435.

Mikkelsen, O. and Pejrup, M. 1998. Comparison of flocculated and dispersed suspended sediment in the Dollard estuary. In: *Sedimentary processes in the intertidal zone* (Eds K.S. Black, D.M. Paterson and A. Cramp), Geological Society Special Publication 139, London. pp. 199-209.

Möller, I., Spencer, T. and French, J.R. 1996. Wind wave attenuation over saltmarsh surfaces: Preliminary results from Norfolk, England. *Journal of Coastal Research*, 12: 1009-1016.

Möller, I., Spencer, T., French, J.R., Leggett, D.J. and Dixon M. 1999. Wave transformation over salt marshes: a field and numerical modelling study from north Norfolk, England. *Estuarine, Coastal and Shelf Science*, 49: 411-426.

Möller, I. and Spencer, T. 2003. Wave transformations over mudflat and saltmarsh surfaces on the UK east coast - implications for marsh evolution. *Proceedings of the International Conference on Coastal Sediments '03*, Florida, USA. 14 pp.

Mwamba, M.J. and Torres, R. 2002. Rainfall effects on marsh sediment redistribution, North Inlet, South Carolina, USA. *Marine Geology*, 189: 267-287.

Neumeier, U. and Ciavola, P. 2004. Flow resistance and associated sedimentary processes in a *Spartina maritima* salt-marsh. *Journal of Coastal Research*, 20: 435-447.

Nielsen, N. and Nielsen, J. 2002. Vertical growth of a young back barrier salt marsh, Skallingen, SW Denmark. *Journal of Coastal Research*, 18: 287-299.

Novak, P. 1959. Study of the performance and efficiency of bed-load meters, Hydraulics Research Institute, Prague. 99 pp.

O'Brien, M.P. 1931. Estuary tidal prism related to entrance areas. *Civil Engineering*, 1: 738.

O'Brien, D.J., Whitehouse, R.J.S. and Cramp, A. 2000. The cyclic development of a macrotidal mudflat on varying timescales. *Continental Shelf Research*, 20: 1593-1619.

Odum, P., Fisher, J.S. and Pickral, J.C. 1979. Factors controlling the flux of particulate organic carbon from estuarine wetlands. In: *Ecological Processes in Coastal and marine Systems* (Ed R.J. Livingstone), Plenum, New York. pp. 69-80.

Orson, R.A., Warren, R.S. and Niering, W.A. 1998. Intertreting sea level rise and rates of vertical marsh accretion in a southern New England tidal salt marsh. *Estuarine, Coastal and Shelf Science*, 47: 419-429.

Panagiotopoulos, I., Voulgaris, G. and Collins, M.B. 1997. The influence of clay on the threshold of movement of fine sandy beds. *Coastal Engineering*, 32: 19-43.

Paphitis, D. and Collins, M.B. 2005. Sand grain threshold, in relation to bed 'stress history': and experimental study. *Sedimentology*, 52: 827.

Park, C.C. 1977. Man-induced changes in stream channel capacity. In: *River Channel Changes* (Ed K.J. Gregory), John Wiley & Sons, Chichester. pp. 121-144.

Paterson, D.M., Tolhurst, T.J., Kelly, J.A., Honeywill, C., de Deckere, E.M.G.T., Huet, V., Shayler, S.A., Black, K.S., de Brouwer, J. and Davidson, I. 2000. Variations in sediment properties, Skeffling mudflat, Humber Estuary, UK. *Continental Shelf Research*, 20: 1373-1396.

Pattiaratchi, C.B. and Collins, M.B. 1985. Sand transport under the combined influence of waves and tidal currents: an assessment of available formulae. *Marine Geology*, 67: 83-100.

Perillo, G.M.E. 2003. New mechanisms studied for creek formation in tidal flats: From crabs to tidal channels. *EOS, Transactions, American Geophysical Union*, 84: 1 & 5.

Perillo, G.M.E. and Iribarne, O.O. 2003. Processes of tidal channel development in salt and freshwater marshes. *Earth Surface Processes and Landforms*, 28: 1473-1482.

Pethick, J. 1984. An introduction to coastal geomorphology. Edward Arnold Ltd, London, 260 pp.

Pethick, J.S. 1980. Velocity surges and asymmetry in tidal channels. *Estuarine and Coastal Marine Science*, 11: 331-345.

Pethick, J.S. 1992. Saltmarsh geomorphology. In: *Saltmarshes: Morphodynamics, Conservation and Engineering Significance* (Eds J.R.L. Allen and K. Pye), Cambridge University Press, Cambridge. pp. 41-62.

Pethick, J.S. 1996. The geomorphology of mudflats. In: *Estuarine Shores: Evolution, Environments and Human Alterations* (Eds K.F. Nordstrom and C.T. Roman), John Wiley & Sons, Chichester. pp. 185-211.

Pethick, J. 2001. Coastal management and sea-level rise. *Catena*, 42: 307-322.

Petts, G.E. 1977. Channel response to flow regulation: The case of the River Derwent, Derbyshire. In: *River Channel Changes* (Ed K.J. Gregory), John Wiley & Sons, Chichester. pp. 145-164.

Pickup, G. 1977. Simulation modelling of river channel erosion. In: *River Channel Changes* (Ed K.J. Gregory), John Wiley & Sons, Chichester. pp. 47-60.

Pielou, E.C. and Routledge, R.D. 1976. Salt marsh vegetation: latitudinal gradients in the zonation patterns. *Oecologia*, 24: 311-321.

Poppe, L.J., Eliason, A.H., Redericks, J.J., Rendigs, R.R., Blackwood, D. and Polloni, C.F. 2000. USGS East-coast sediment analysis: procedures, database, and georeferenced displays, US Geological Survey Open-File report 00-358. CD-ROM.

Postma, H. 1967. Sediment transport and sedimentation in the estuarine environment. In: *Estuaries* (Ed G.M. Lauff), AAAS, New York. pp. 158-179.

Postma, H. 1988. Tidal flat areas. In: *Lecture Notes on Coastal and Estuarine Studies* (Ed B.-O. Jansson), 22, Springer-Verlag, Berlin. pp. 102-121.

Pringle, A.W. 1995. Erosion of a cyclic salt marsh in Morecambe Bay, north-west England. *Earth Surface Processes and Landforms*, 20: 387-405.

Pugh, D.T. 1987. Tides, surges and mean sea level. John Wiley & Sons, Chichester. 472 pp.

Pye, K. 1992. Saltmarshes on the barrier coastline of North Norfolk, eastern England. In: *Saltmarshes: Morphodynamics, Conservation and Engineering Significance* (Eds J.R.L. Allen and K. Pye), Cambridge University Press, Cambridge. pp. 148-178.

Pye, K. 1996. Evolution of the shoreline of the Dee estuary, United Kingdom. In: *Estuarine Shores: Evolution, Environments and Human Alterations* (Eds K.F. Nordstrom and C.T. Roman), John Wiley & Sons, Chichester. pp. 15-37.

Pye, K. 1995. Controls on long-term saltmarsh accretion and erosion in the wash, eastern England. *Journal of Coastal Research*, 11: 337-356.

Pye, K. 2000. Satmarsh erosion in southeast England: mechanisms, causes and implications. In: *British Saltmarshes* (Eds B.R. Sherwood, B.G. Gardiner and T. Harris), Forrest Text, Ceredigion. pp. 359-396.

Pye, K. and French, P.W. 1993. Erosion and accretion processes on British saltmarshes. Vol. 1, Introduction: saltmarsh processes and morphology, final report for MAFF Flood & Coastal Defence, Cambridge Environmental Research Consultants Limited, Cambridge.

Ranwell, D.S. 1972. Ecology of saltmarsh and sand dunes. Chapman and Hall, London. 258 pp.

Reed, D.J. 1987. Temporal sampling and discharge asymmetry in salt marsh creeks. *Estuarine, Coastal and Shelf Science*, 25: 459-466.

Reed, D.J. 1988. Sediment dynamics and deposition in a retreating coastal salt marsh. *Estuarine, Coastal and Shelf Science*, 26: 67-79.

Reed, D.J. 1990. The impact of sea-level rise on coastal saltmarshes. *Progress in Physical Geography*, 14: 465-481.

Reineck, H.-E. 1975. German North Sea tidal flats. In: *Tidal Deposits* (Ed R.N. Ginsburg), Springer-Verlag, New York. pp. 5-12.

Reineck, H.-E. and Singh, I.B. 1980. Depositional sedimentary environments: with reference to terrigenous clastics. Springer-Verlag, Berlin, 549 pp.

Ribberink, J.S. 1998. Bed-load transport for steady flows and unsteady oscillatory flows. *Coastal Engineering*, 34: 59-82.

Richards, K.S. and Lane, S.N. 1997. Prediction of morphological changes in unstable channels. In: *Applied Fluvial Geomorphology for River Engineering and Management* (Eds C.R. Thorne, R.D. Hey and M.D. Newson), John Wiley & Sons, Chichester. pp. 269-292.

Ridderinkhof, H., van der Ham, R. and van der Lee, W. 2000. Temporal variations in concentration and transport of suspended sediments in a channel-flat system in the Ems-Dollard estuary. *Continental Shelf Research*, 20: 1479-1493.

Riethmuller, R., Hakvoort, J.H.M., Heineke, M., Heymann, K., Kuhl, H. and Witte, G. 1998. Relating erosion shear stress to tidal flat surface colour. In: *Sedimentary processes in the intertidal zone* (Eds K.S. Black, D.M. Paterson and A. Cramp), Geological Society Special Publication 139, London. pp. 283-293.

Rigler, J.K., Collins, M.B. and Williams, S.J. 1981. A high precision digital-recording sedimentation tower for sands. *Journal of Sedimentary Petrology*, 51: 642-644.

Roberts, W., Le Hir, P. and Whitehouse, R.J.S. 2000. Investigation using simple mathematical models of the effect of tidal currents and waves on the profile shape of intertidal mudflats. *Continental Shelf Research*, 20: 1079-1097.

Roman, C.T. 1984. Estimating water volume discharge through salt-marsh tidal channels: an aspect of material exchange. *Estuaries*, 7: 259-264.

Roman, C.T. and Nordstrom, K.F. 1996. Environments, processes and interactions of estuarine shores. In: *Evolution, Environments and Human Alterations* (Eds K.F. Nordstrom and C.T. Roman), John Wiley & Sons, Chichester. pp. 1-12.

Roman, C.T., Peck, J.A., Allen, J.R.L., King, J.W. and Appleby, P.G. 1997. Accretion of a New England (U.S.A.) salt marsh in response to inlet migration, storms and sea-level rise. *Estuarine, Coastal and Shelf Science*, 45: 717-727.

Ryan, N.M. and Cooper, J.A.G. 1998. Spatial variability of tidal flats in response to wave exposure: examples from Strangford Lough, Co. Down, Northern Ireland. In: *Sedimentary processes in the intertidal zone* (Eds K.S. Black, D.M. Paterson and A. Cramp), Geological Society Special Publication 139, London. pp. 221-230.

Schostak, L.E., Davidson-Arnott, R.G.D., Ollerhead, J. and Kostaschuk, R.A. 2000. Patterns of flow and suspended sediment concentration in a macrotidal salt marsh creek, Bay of Fundy, Canada. In: *Coastal and Estuarine Environments: Sedimentology, Geomorphology and Geoarchaeology* (Eds K. Pye and J.R.L. Allen), Geological Society Special Publications 175, London. pp. 59-73.

Schumm, S.A. 1985. Patterns of alluvial rivers. *Annual Review of Earth and Planetary Sciences*, 13: 5-27.

Schumm, S.A., Mosley, M.P. and Weaver, W.E. 1987. Experimental fluvial geomorphology. John Wiley & Sons, New York. 402 pp.

Schumm, S.A., Dumont, J.F. and Holbrook, J.M. 2000. Active tectonics and alluvial rivers. Cambridge University Press, Cambridge. 276 pp.

Shaw, H.F. 1973. Clay mineralogy of Quaternary sediments in The Wash embayment, Eastern England. *Marine Geology*, 14: 29-45.

Shennan, I. and Woodworth, P.L. 1992. A comparison of late Holocene and twentieth-century sea-level trends from the UK and North Sea region. *International Journal of Geophysics*, 109: 96-105.

Shi, Z. 1995. The Morphology evolution of saltmarsh tidal creek networks in the Dyfi Estuary, Wales. *Proceedings of International Conference on Coastal Change '95,* 448-450.

Shimizu, Y. 1991. A study on prediction of flows and bed deformation in alluvial streams, *PhD Thesis*, Hokkaido University.

Soulsby, R. 1997. Dynamics of marine sands: a manual for practical applications. Thomas Telford, London, 249 pp.

Steers, J.A. 1939. Scolt Head report. Transactions of the Norfolk and Norwich Naturalists Society 15, 41-46

Steers, J.A. 1946. The coastline of England and Wales. Cambridge University Press, Cambridge, 644 pp.

Steers, J.A. 1977. Physiography. In: *Wet Coastal Ecosystems* (Ed V.J. Chapman), Elsevier, Amsterdam. pp. 31-60.

Sternberg, R.W. 1972. Predicting initial motion and bedload transport of sediment particles in the shallow marine environment. In: *Shelf Sediment Transport: Process and Pattern* (Eds D.J.P. Swift, D.B. Duane and O.H. Pilkey), Dowden, Hutchinson and Ross, Inc., Stroudsberg, pp. 61-82.

Stevenson, J.C. and Kearney, M.S. 1996. Shoreline dynamics on the windward and leeward shores of a large temperate estuary. In: *Estuarine Shores: Evolution, Environments and Human Alterations* (Eds K.F. Nordstrom and C.T. Roman), John Wiley & Sons, Chichester. pp. 233-259.

Stevenson, J.C., Ward, L.G. and Kearney, M.S. 1988. Sediment transport and trapping in marsh systems: implications of tidal flux studies. *Marine Geology*, 80: 37-59.

Stumpf, R.P. 1983. The process of sedimentation on the surfaces of a salt marsh. *Estuarine, Coastal and Shelf Science*, 17: 495-508.

Suk, N.S., Guo, Q. and Psuty, N.P. 1999. Suspended solids flux between salt marsh and adjacent bay: a long-term continuous measurement. *Estuarine, Coastal and Shelf Science*, 49: 61-81.

Symonds, A.M. and Collins, M.B. 2005. Sediment dynamics associated with managed realignment; Freiston Shore, The Wash, UK. *Coastal Engineering 2004, Lisbon, Vol 3,* pp. 3173-3185.

Tolhurst, T.J., Black, K.S., Paterson, D.M., Mitchener, H.J., Termaat, G.R. and Shayler, S.A. 2000a. A comparison and measurement standardisation of four in situ devices for determining the erosion shear stress of intertidal sediments. *Continental Shelf Research*, 20: 1397-1418.

Tolhurst, T.J., Riethmuller, R. and Paterson, D.M. 2000b. In situ versus laboratory analysis of sediment stability from intertidal mudflats. *Continental Shelf Research*, 20: 1317-1334.

Townend, I. and Pethick, J.S. 2002. Estuarine flooding and managed retreat. *Philosophical Transactions of the Royal Society of London,* A. 360: 1477-1495.

Townend, I. 2005. An examination of empirical stability relationships for UK estuaries. *Journal of Coastal Research*, 21: 1042-1053.

Townend, I. in press-a. Breach design for managed realignment sites. *Proceedings of ICE, Maritime Engineering*, 22 pp.

Townend, I. in press-b. An examinitation of the hypsometry of estuaries, inlets and breached sea wall sites. *Proceedings of ICE, Maritime Engineering*, 19 pp.

Tsompanoglou, K. 2003. Geochemical and radiochemical investigation of recent saltmarsh sediments from The Wash, UK. *MSc Thesis*, University of Southampton, Southampton. 65 pp.

Underwood, G.J.C. 2000. Changes in microalgal species composition, biostabilisation potential and succession during saltmarsh restoration. In: *British Saltmarshes* (Eds B.R. Sherwood, B.G. Gardiner and T. Harris), Forrest Text, Ceredigion. pp. 143-154.

Van der Lee, W.T.B. 1998. The impact of fluid shear and the suspended sediment concentration on the mud floc size variation in the Dollard estuary, The Netherlands. In: *Sedimentary processes in the intertidal zone* (Eds K.S. Black, D.M. Paterson and A. Cramp), Geological Society Special Publication 139, London. pp. 187-198.

Van der Lee, W.T.B. 2000. Temporal variation of floc size and settling velocity in the Dollard estuary. *Continental Shelf Research*, 20: 1495-1511.

Van Duyl, F.C., de Winder, B., Kop, A.J. and Wollenzien, U. 2000. Consequences of diatom mat erosion for carbohydrate concentrations and heterotrophic bacterial activities in intertidal sediments of the Ems-Dollard estuary. *Continental Shelf Research*, 20: 1335-1349.

Van Proosdij, D., Ollerhead, J. and Davidson-Arnott, R.G.D. 2000. Controls on suspended sediment deposition over single tidal cycles in a macrotidal salt marsh, Bay of Fundy, Canada. In: *Coastal and Estuarine Environments: Sedimentology, Geomorphology and Geoarchaeology* (Eds K. Pye and J.R.L. Allen), Geological Society Special Publication 175, London. pp. 43-57.

Van Smirren, J. and Collins, M.B. 1982. Short-term changes in sedimentological and hydrographic characteristics over a sandy intertidal zone, The Wash, U.K. *Geo-marine letters*, 2: 55-60.

Van Straaten, L.M.J.U. and Kuenen, P.H. 1958. Tidal action as a cause of clay accumulation. *Journal of Sedimentary Petrology*, 28: 406-413.

Vinther, N., Christiansen, C., Bartholdy, J., Sorensen, C. and Lund-Hansen, L.C. 2004. Sediment transport across a tidal divide in the Danish Wadden Sea. *Danish Journal of Geography*, 104: 71-86.

Vos, P.C. and van Kesteren, W.P. 2000. The long-term evolution of intertidal mudflats in the northern Netherlands during the Holocene; natural and anthropogenic processes. *Continental Shelf Research*, 20: 1687-1710.

Wang, B.-C. and Eisma, D. 1988. Mudflat deposition along the Wenzhou coastal plain in Southern Zhejiang, China. In: *Tide-influenced sedimentary environments and facies* (Eds P.L. de Boer, A. van Gelder and S.D. Nio), D.Reidel, Dordrecht. pp. 265-274.

Ward, L.G. 1979. Hydrodynamics and sediment transport in a salt marsh tidal channel. In: *Proceedings of 16th Conference on Coastal Engineering*, ASCE, New York. pp. 1953-1970.

Ward, L.G. 1981. Suspended-material transport in marsh tidal channels, Kiawah Island, South Carolina. *Marine Geology*, 40: 139-154.

Watts, C.W., Tolhurst, T.J., Black, K.S. and Whitmore, A.P. 2003. In situ measurements of erosion shear stress and geotechnical shear strength of the intertidal sediments of the experimental managed realignment scheme at Tollesbury, Essex, UK. *Estuarine, Coastal and Shelf Science*, 58: 611-620.

Werritty, A. 1997. Short-term changes in the channel stability. In: *Applied Fluvial Geomorphology for River Engineering and Management* (Eds C.R. Thorne, R.D. Hey and M.D. Newson), John Wiley & Sons, Chichester. pp. 47-65.

Wheeler, W.H. 1876. Fascine work at the outfalls of the Fen rivers. *Minutes of Proceedings of the Institution of Civil Engineers.* 61-80.

Whitehouse, R.J.S., Bassoullet, P., Dyer, K.R., Mitchener, H.J. and Roberts, W. 2000. The influence of bedforms on flow and sediment transport over intertidal mudflats. *Continental Shelf Research*, 20: 1099-1124.

Whitehouse, R.J.S. and Mitchener, H.J. 1998. Observations of the morphodynamic behaviour of an intertidal mudflat at different timescales. In: *Sedimentary Processes in the Intertidal Zone* (Eds K.S. Black, D.M. Paterson and A. Cramp), Geological Society Special Publication 139, London. pp. 255-271.

Widdows, J., Brinsley, M. and Elliott, M. 1998. Use of *in situ* flume to quantify particle flux (biodeposition rates and sediment erosion) for an intertidal mudflat in relation to changes in current velocity and benthic macrofauna. In: *Sedimentary Processes in the Intertidal Zone* (Eds K.S. Black, D.M. Paterson and A. Cramp), Geological Society Special Publication 139, London. pp. 85-97.

Widdows, J., Brown, S., Brinsley, M.D., Salkeld, P.N. and Elliott, M. 2000. Temporal changes in intertidal sediment erodability: influence of biological and climatic factors. *Continental Shelf Research*, 20: 1275-1289.

Wilmot, R.D. and Collins, M.B. 1981. Contemporary fluvial sediment supply to the Wash. *Spec. Pub. Int. Ass. Sediment*, 5: 99-110.

Winterwerp, J.C. 2002. On the flocculation and settling velocity of estuarine mud. *Continental Shelf Research*, 22: 1339-1360.

Winterwerp, J.C., Bale, A.J., Christie, M.C., Dyer, K.R., Jones, S., Lintern, D.G., Manning, A.J. and Roberts, W. 2002. Flocculation and settling velocity of fine sediment. In: *Fine Sediment Dynamics in the Marine Environment* (Eds J.C. Winterwerp and C. Kranenburg), Proceedings in Marine Science 5, Elsevier, Amsterdam. pp. 25-40.

Wolaver, T.G., Dame, R.F., Spurrier, J.D. and Miller, A.B. 1988. Sediment exchange between a euhaline salt marsh in South Carolina and the adjacent tidal creek. *Journal of Coastal Research*, 4. 17-26.

Wolman, M.G. and Gerson, R. 1978. Relative scales of time and effectiveness in watershed geomorphology. *Earth Surface Processes*, 3: 189-208.

Wood, R.G., Black, K.S. and Jago, C.F. 1998. Measurements and preliminary modelling of current velocity over an intertidal mudflat, Humber estuary, UK. In: *Sedimentary processes in the intertidal zone* (Eds K.S. Black, D.M. Paterson and A. Cramp), Geological Society Special Publication 139, London. pp. 167-175.

Wood, R. and Widdows, J. 2002. A model of sediment transport over an intertidal transect, comparing the influences of biological and physical factors. *Limnology and Oceanography*, 47: 848-855.

Woolnough, S.J., Allen, J.R.L. and Wood, W.L. 1995. An exploratory numerical model of sediment deposition over tidal salt marshes. *Estuarine, Coastal and Shelf Science*, 41: 515-543.

Yalin, M.S. and Ferreira da Silva, A.M. 2001. *Fluvial Processes*. IAHR, Delft, 197 pp.

Zeff, M.L. 1988. Sedimentation in a salt marsh-tidal channel system, southern New Jersey. *Marine Geology*, 82: 33-48.

Zhang, R.S. 1992. Suspended sediment transport processes on tidal mud flats in Jiangsu Province. *Estuarine, Coastal and Shelf Science*, 35: 225-233.